Synthesis, characterization and antimicrobial evaluation of piperazinyl-quinolinyl-α-aminophosphonates

Thesis submitted in fulfilment for the Degree of Master of Applied Science in Chemistry in the Faculty of Applied Sciences at the Durban University of Technology, Durban, South Africa

by

NIKISHA RAJKOOMAR

Under the guidance of

Professor R. M. Gengan

2019

Declaration

I, Nikisha Rajkoomar, hereby declare that this thesis entitled **"Synthesis, characterization and antimicrobial evaluation of piperazinyl-quinolinyl-α-aminophosphonates"**, handed in for the Master of Applied Science in Chemistry degree at the Durban University of Technology has not been submitted in any form to any other academic institution. This study presents original work by the author and all sources used or quoted have been duly acknowledged in the text. The research described in this thesis was carried out in the Department of Chemistry, Faculty of Applied Sciences, Durban University of Technology, South Africa, under the supervision of Professor Robert Moonsamy Gengan.

[redacted] __ **16 August 2019**

Nikisha Rajkoomar **Date**

Student number: 21337285

The final submission of the thesis is hereby approved by:

[redacted] **16 August 2019**

Professor R. M. Gengan **Date**

Dedication

I am dedicating this thesis to all beloved members of my family who mean so much to me. First and foremost, to my parents **Suresh Rajkoomar and Shanti Rajkoomar** who raised me with unconditional love, support and taught me the value of education. Next, my siblings **Natasha Rajkoomar** and **Erasha Rajkoomar** who have been my lifelong best friends. Thank you both for being the strong and influential women that you are to me. Lastly, my niece **Liya Singh** who brings out my inner child. I thank you for the joyfulness you bring to my life. I am grateful to each and every one of you.

Acknowledgements

There were a great number of people who helped make this journey possible. Foremost, I would like to express my sincere gratitude to supervisor, **Professor R. M. Gengan** of the Department of Chemistry, Durban University of Technology, for his relentless encouragement, constructive guidance and words of motivation throughout the duration of this research study and moreover for the inspiration he provided to ensure the completion of this work. His expertise, availability to discuss ideas and willingness to share his knowledge were instrumental. For this, I will be eternally grateful.

I would like to express my deepest appreciation to my colleague, **Dr Arul Murugesan**, who has the attitude and substance of a genius: he continually conveyed a spirit of adventure in regard to research. Without his guidance and persistent help this thesis would not have been possible.

My earnest thanks goes out to another colleague, **Dr Charlette Tiloke**, who has taken time out of her busy schedule to proof read my work without hesitation.

My special thanks extends to my other colleagues **Muthu Thangaraj**, **Talent Makhanya** and **Thabisile Kaunda** of the Department of Chemistry, Durban University of Technology for their moral support throughout the course of this study.

My appreciation goes to **Dilip Jagjivan** from the University of KwaZulu-Natal for his helpful advice and assistance provided on the power of characterization equipment. I would like to thank **Kabange Kasumbwe** of the Department of Biotechnology and Food Technology**,** Durban University of Technology for his guidance and all the work put into the biological testing techniques used in this study.

I would also like to acknowledge the National Research Foundation (NRF) for the financial support received and the tertiary institution, Durban University of Technology.

Last but most important thanks goes to my family, I would never have been able to do this you. You all have given me unconditional love and solid support. Above all else, I need to thank my father **Suresh Rajkoomar**, I owe everything to you and love you more than you can possibly know.

Abstract

α-Aminophosphonates (α-APs) is an important motif among heterocycles particularly in medicinal chemistry due to their reduced levels of cytotoxicity and structural resemblance to the corresponding α-amino acids. They are useful intermediates in synthetic organic processes and present with a broad spectrum of biological activities. Hence, there is an ongoing interest in the development of improved synthetic methods for the preparation of these α-APs. The complex molecules were initially synthesized in a step-wise reaction but this method suffered several drawbacks such as long reaction times and resulted in low yields. However, since the development of multi-component reactions (MCRs), three or more substrates can undergo an efficient one-pot reaction which results in higher product yields.

The first step in the synthetic aspect of this study involved the preparation of a novel palladium supported strontium titanate (Pd-$SrTiO_3$) material. Herein, an aqueous solution of strontium (II) nitrate was mixed with citric acid followed by reflux in an ethanolic solution of titanium (IV) butoxide. Thereafter, the dried solid was mixed with palladium (II) nitrate and this solution mixture was refluxed, filtered, calcined and subsequently dried. The characterization of Pd-$SrTiO_3$ was undertaken with FT-IR, P-XRD, SEM, BET, SEM-EDX and Raman spectroscopic techniques. The synthesis of a series of novel α-APs in a MCR system comprising an aldehyde, diethyl phosphate and selected aniline derivatives via the Kabachnik Fields reaction approach in the presence of catalytic amounts of Pd-$SrTiO_3$ was investigated Twenty methyl piperazinyl-quinolinyl α-aminophosphonates (MPQ-α-APs) (**4a-4t)** were synthesized, purified and characterized by FT-IR, ^{1}H-NMR, ^{13}C-NMR, ^{31}P-NMR, 2D-NMR and high resolution mass spectroscopic techniques. Valuable features of this routine included high yields, extensive substrate range, straight forward procedures and excellent catalytic properties.

The cytotoxicity of **4d**, **4e**, **4f**, **4m**, **4q**, **4r** and **4s** was evaluated using the Brine shrimp lethality assay. These compounds showed *Artemia salina* death < 50 % thereby suggesting their potential for other biological evaluation.

The antimicrobial evaluation was conducted using the agar disc diffusion assay. The twenty MPQ-α-APs were assessed against *Bacillus cereus , Staphylococcus aureus , Klebsiella pneumonia* and *Micrococcus luteus* ; and three yeast cultures *Candida albicans*, *Caraipa utilis* and *Saccharomyces cerevisiae*. Compound **4m** showed slight bacterial growth inhibition for the test species *Bacillus cereus* and *Micrococcus luteus* while compound **4r** was marginally inhibitory to the growth of *Staphylococcus aureus*.

Finally, the MPQ-α-APs were screened for their antioxidant activity by the DPPH assay. Compounds **4f** and **4r** demonstrated significant free radical scavenging potential of 94.24 % and 67.32 %, respectively. The remaining compounds showed low antioxidant activity within the range of 21 – 42 %.

Table of Contents

Title: Enhancing the effect of microwave irradiation with Pd-$SrTiO_3$ catalyst for the synthesis of methyl piperazinyl-quinolinyl α-aminophosphonates and their antibacterial and antioxidant activities

Journal: Journal of Molecular Structure

Reference Number: MOLSTRUC-D-19-00870

List of Figures

List of Schemes

List of Tables

Abbreviations

%	-percentage
^{13}C	- carbon 13
BSL	- Brine Shrimp Lethality
$CDCl_3$	- deuterated chloroform
DBT	- Durban University of Technology Culture collection reference based at the department of Biotechnology and Food Technology
DNA	- Deoxyribonucleic Acid
DSC-TGA	- Differential Scanning Calorimetry-Thermogravimetric Analysis
EtOH	- ethanol
g	- grams
HIV	- Human Immunodeficiency Virus
IC_{50}	- Concentration of inhibitor necessary for 50% inhibition
KF	- Kabachnik Fields
m.p	- melting point
MCR	- Multi-Component Reactions
mg	- milligram
min	- minute
mol	- mole
MS	- mass spectrometer
NMR	- Nuclear Magnetic Resonance
ROS	- Reactive Oxygen Species
SEM	- scanning electron microscope
TLC	- Thin- layer chromatography
UV/Vis	- ultraviolet visible spectroscopy
W	- watts
α-AP	- α-Aminophosphonate
˚C	- degrees celsius
^{1}H	- proton
dm	- decimeter
DMSO	- dimethyl sulphoxide
DPPH	-2,2-diphenyl-1-picrylhydrazyl
EDX	- Energy Dispersive X-ray spectroscopy
Hz	- Hertz
IR	- Infra-Red

KOH	- potassium hydroxide
MAOS	- Microwave Assisted Organic Synthesis
MeOH	- methanol
MIC	- Minimum Inhibition Concentration
mL	- millilitre
MPQ-α-AP	- methyl piperazinyl-quinolinyl-α-aminophosphonate
MW	- microwave
nm	- nanometre
OEt	- ethoxy
Pd-$SrTiO_3$	- Palladium-doped Strontium Titanate Oxide
ppm	- parts per million
s	- second
$SrTiO_3$	- Strontium Titanate Oxide
TOFES-MS	- Time-of-Flight Electron Spectroscopy - Mass Spectrometry
UV	- Ultraviolet
WHO	- World Health Organization

Chapter One: Introduction

Chemistry is the science that focuses on the study of matter which plays an integral part in our comprehension of the universe [Pauling, 1960]. It incorporates various branches of science such as physics, geology and biology therefore being central to all aspects of life. One major sub-group of chemistry is organic chemistry, from which a wealth of information is attained regarding carbon-containing molecules that are present in living organisms [Benner *et al.,* 2004] and in nature. Organic chemistry is broadly categorised into natural product chemistry and organic synthesis, the latter arose due to the high demand of pharmaceutical drugs and other industrial applications which could not be adequately obtained from natural sources [Houghton, 2001]. Over the years, the synthesis of new organic molecules has become more efficient and viable in providing new functionalized biologically active compounds [Wuts *et al.,* 2006]. Although there are thousands of known reactions and reaction schemes, many of which use linear or convergent synthesis, the most important strategy to synthesize new organic molecules is via the multi-component reaction (MCR) route. This is a method in which three or more reactants join to form a new product [Ganem, 2009] in a few *in-situ* reaction steps. It is an appealing synthetic route often used in organic chemistry. MCR encompasses features that contribute to an ideal synthesis including quick and simple implementation, high atom efficiency, time and energy saving, environmental consideration, high product yield and it also generates structural complexity to organic molecules [Weber, 2002]. The pharmaceutical industry has benefitted greatly because it utilizes MCRs to access a wide variety of drug-like chemical molecules as either new derivatives or new molecules [Schreiber, 2000]. However, the application of MCRs remains limited by the relatively small number of reactions that can be applied in the preparation of biologically relevant frameworks. Consequently, the development of new MCRs is critical for the synthesis of new pharmaceuticals for biological applications [Shestopalov Evans, 2002].

The search for novel molecules that can treat and cure disease dates back to the early days of human civilization when plant and animal extracts provided the necessary remedies [Gurib-Fakim, 2006]. The discovery of these treatments was acquired empirically through observations of human and animal reactions to ingesting plant and animal concoctions. These were the only remedies available until drug discovery and development started to follow scientific techniques in the late 1800s [Dias *et al.,* 2012]. From then onwards, drugs were synthesized, tested and manufactured by the pharmaceutical industry. Initially, drug discovery focused on the extraction of bioactive components from natural products that

displayed a desired pharmaceutical and biological effect but nowadays synthetic products have flooded the market with diverse applications.

One of the major threat to human health is antibiotic resistance amongst pathogenic bacteria, more specifically, multi-drug resistant pathogens [Antunes *et al.,* 2014]. Over decades, bacteria that caused disease have mutated their DNA sequences resulting in the development of antibiotic resistance genes protecting the bacteria from therapeutic drugs. Hence, these pathogens have become increasingly difficult to eradicate using commercially available known drugs. Thus, the continuous discovery and development of new antibacterial agents for effective treatment of infectious and life-threatening diseases is an urgent biomedical necessity [Banerjee, 2017]. Although, several classes of organic molecules can be exploited, an important class is the α-aminophosphonates (α-APs) which are known for their antibacterial properties [Krishna *et al.,* 2010] along with therapeutic properties that extend to a multitude of branches in medicinal chemistry [Karimi-Jaberi Amiri, 2010]. The medicinal properties of α-APs are attributable to their reduced levels of toxicity and their structural resemblance to corresponding α-amino acids [Oniţa *et al.,* 2010]. Hence, this study investigated the synthesis of novel α-APs and the evaluation of their potential application in biological systems.

The aim of this study was to prepare a recyclable novel Palladium-doped Strontium Titanium oxide (Pd-$SrTiO_3$) material to catalyze the synthesis of a new series of methyl piperazinyl-quinolinyl-α-aminophosphonates (MPQ-α-APs) and evaluate their cytotoxicity, antibacterial and antioxidant properties.

The objectives of this study were to:

1. Synthesize a novel Pd-$SrTiO_3$ catalyst material and fully characterize it by analytical techniques.
2. Synthesize the starting material 2-(4-methylpiperazin-1-yl) quinoline-3-carbaldehyde.
3. Assess the potential of the Pd-$SrTiO_3$ material as a new catalyst to synthesize novel MPQ-α-APs from readily available, simple and cost effective reactants.
4. Purify the MPQ-α-APs by chromatographic techniques and characterize these novel compounds by spectroscopic techniques.
5. Evaluate the cytotoxicity of MPQ-α-APs using the Brine shrimp assay.
6. Determine the antimicrobial and antioxidant properties of MPQ-α-APs.

The outcome of this research investigation is outlined in the chapters presented below:

Chapter 1 provides a brief introduction to the importance of organic compounds and outlined the aims and objectives of the study.

Chapter 2 presents a comprehensive literature review outlining heterocyclic chemistry, quinoline, α-APs, quinoline related α-APs, multi-component reaction processes, metal-doped $SrTiO_3$ catalysts and microwave assisted organic synthesis. Furthermore, a brief overview on structural elucidation by spectroscopic techniques is highlighted. Finally, this chapter concludes with a review of the biologically important α-APs with an emphasis on their cytotoxicity, antibacterial and antioxidant activities.

Chapter 3 details the research design and methodology of the study. This chapter includes the detailed description of the synthesis of the following compounds:
1) The novel Pd-$SrTiO_3$ catalyst followed by its characterization via FT-IR, P-XRD, SEM, BET, SEM-EDX and Raman spectroscopy
2) a novel series of MPQ-APs viz., **4a-4t** via the Kabachnik-Field reaction. The structure elucidation by FT-IR, ^{1}H-NMR, ^{13}C-NMR, ^{31}P-NMR, 2D-NMR and high resolution mass spectroscopic techniques is also presented.

Chapter 4 discusses the synthesis and characterization of Pd-$SrTiO_3$ and MPQ-APs followed by their cytotoxicity, antimicrobial and antioxidant evaluation. A conclusion is also presented.

Chapter Two: Literature Review

2.1. General Introduction

Organic chemistry is the science of the rules on how to design, synthesize, characterize and develop applications of molecules, containing carbon, based on their chemical and physical properties [Winter, 2005]. In the early 1800s, all organic compounds were obtained from living organisms or their decomposed bodies. This 'Vitalism' theory stated that a vital force from living organisms was necessary to make an organic compound [Benton, 1974]. However, in 1828, Frederich Wöhler synthesized the organic compound urea, a constituent of urine, from an inorganic compound ammonium cyanate (Scheme 1) thereby disproving the vitalism theory. This was recorded as a breakthrough in the history of science [Ramberg, 2000].

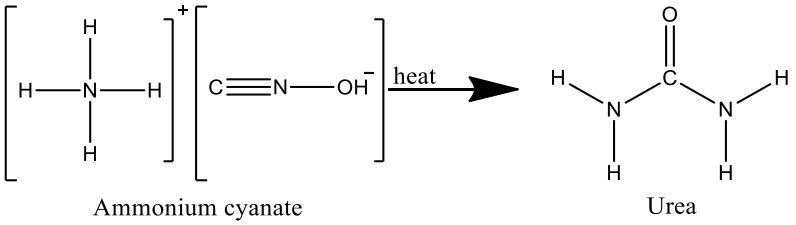

Scheme 1: Synthesis of urea from ammonium cyanate [Lipman, 1964]

The modification of existing procedures and the development of new ones for the synthesis of novel heterocyclic compounds are highly sought-after due to their wide applications in the fields of agriculture, industry and medicine. One such class of biologically active heterocyclic compounds are α-APs [Ramana *et al.,* 2012]. Several classical synthetic routes for the synthesis of α-APs face the drawbacks of harsh reaction conditions such as high temperatures, slow reactions and the generation of large amounts of waste which are not environmentally friendly [Sonawane, 2014]. Hence in recent years, a variety of α-APs have been synthesized by MCRs. Their popularity has grown, since they provide the platform for continuous and varied advancements in new organic synthetic approaches; in that way producing effective compounds with desired applications.

Research in synthetic organic chemistry has grown rapidly because of the great demand for new and improved pharmaceuticals, foods, dyes, fertilizers, cosmetics and other allied commodities by the world's rapidly growing population. This inevitably led to the development of several sub-disciplines such as photo-chemical, sono-chemical, microwave organic synthesis and MCRs [Seneci *et al.,* 2014].

2.2. Heterocyclic Chemistry

Heterocycles are a class of organic compounds which contains one or more rings of atoms with no less than one atom being an element other than carbon [Chinchilla *et al.,* 2004]. Typical heteroatoms include nitrogen, oxygen and sulphur [Adrian Suflita, 1994]. Heterocyclic compounds can be classified according to the size of the ring such as five-membered and six-membered. For example, furan, thiophene and pyrrole are all five-membered heterocyclic compounds while pyridine, pyrimidine and quinoline are all six-membered heterocyclic compounds.

Many natural heterocyclic compounds in plants and animals are responsible for important physiological roles: chlorophyll in plants are responsible for photosynthesis, haemoglobin in animal blood is required for oxygen delivery whilst antibiotics and vitamins are generally required to maintain good health [Soetan *et al.,* 2010]. However, approximately 50% of existing medicines are synthetic heterocyclic compounds. Thus, heterocycles are an important class for investigations by organic synthetic chemists [Wilkens, 1963]. Some examples of biologically active heterocycles include Cinchonine (1) which is a quinolone alkaloid with antimalarial activity [Wesełucha-Birczyńska Nakamoto, 1996], Anastrozole (2) is an aromatase-inhibiting drug used to treat post-menopausal breast cancer [Pfaller *et al.,* 2002] and Oseltamivir (3) is used as an antiviral drug to treat influenza infections [Ward *et al*., 2005].

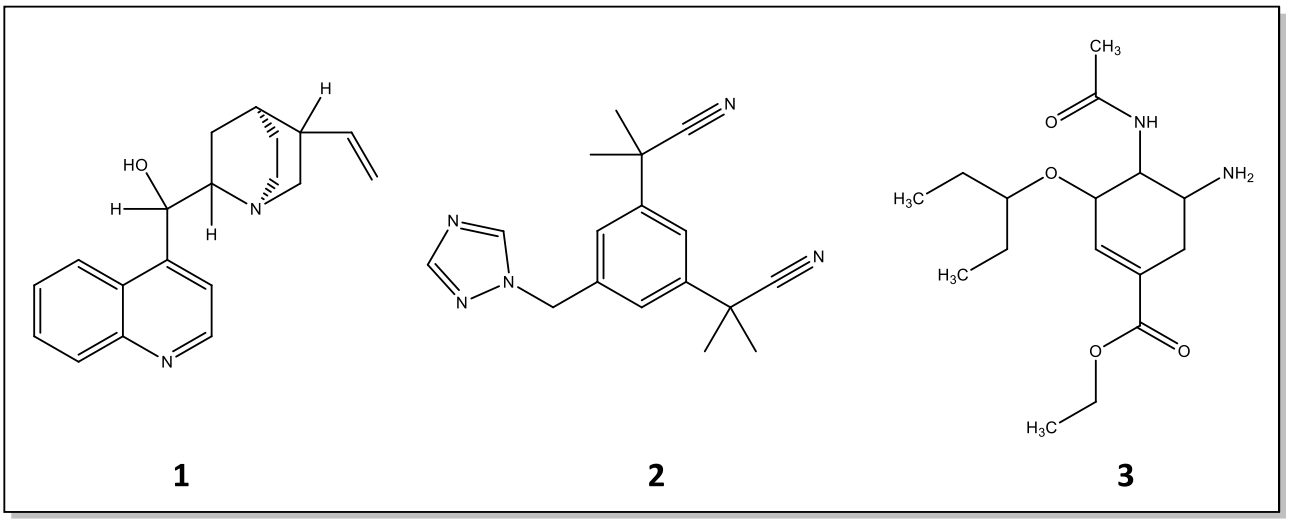

Figure 1: Some selected biologically active heterocyclic members

Since heterocyclic compounds find useful applications in the fields of biochemistry, polymers, photographic science, dyestuff, adhesives and molecular engineering; their discovery and desirable applications, especially in drug discovery, remains an active area of research interest for modern organic and medicinal chemists [Kale Patwardhan, 2013].

2.2.1. Quinoline

Quinoline is a major class of nitrogen heterocycles that is characterized by a two ring structure composed of benzene and pyridine fused at two adjacent carbon atoms. The quinoline skeleton structure is presented below:

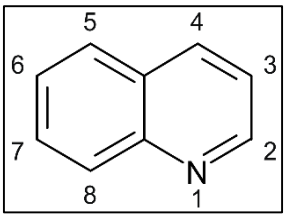

The quinoline ring system is an essential core structure of several natural heterocyclic compounds and exists in a diverse array of natural products that include tecleabine, tecleoxine, plakinidine and quinine [Ulaczyk-Lesanko Hall, 2005]. Quinolines have various pharmacological properties [Michael, 1999] such as arechloroquine which is used to prevent and treat malaria (4)**,** dibucaine hydrochloride is used for surface anaesthesia (5) and amodiaquine is an orally active anti-inflammatory drug (6) (Figure 2).

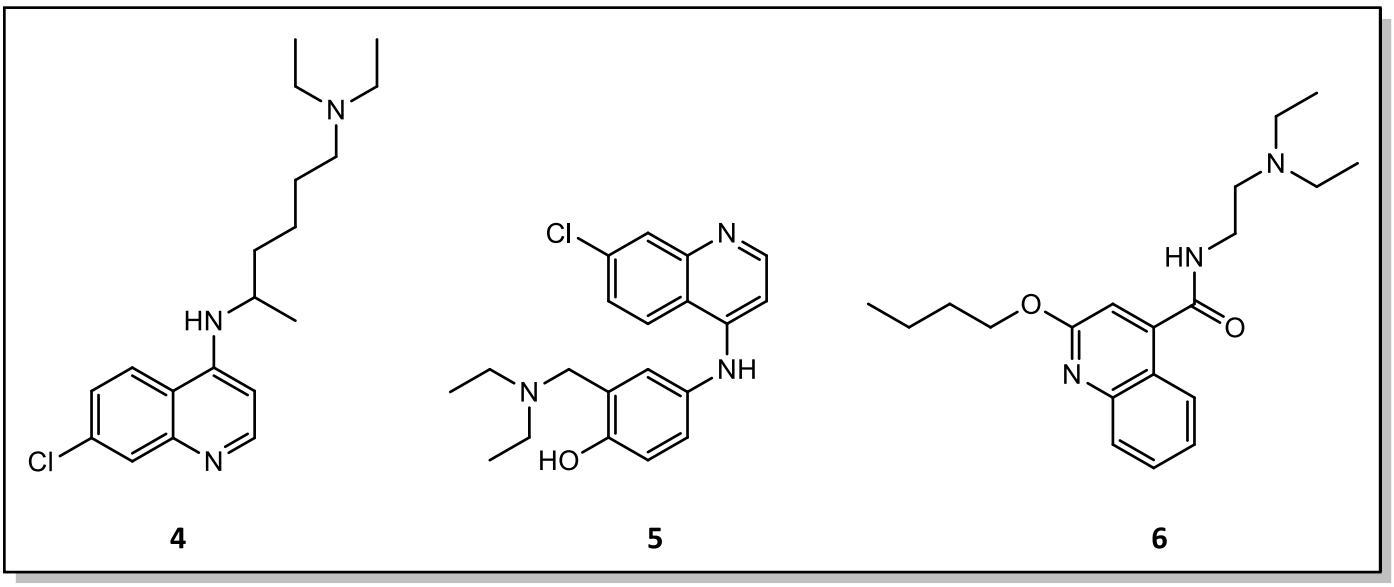

Figure 2: Important synthetic quinolines [Peters, 1965; Lin *et al*., 1987; Kotecka *et al*., 1997]

2.2.2. The α-Aminophosphonates and Phosphonic Acids

α-APs and α-aminophosphonic acids are important classes of organophosphorus compounds containing the P-C bond and an amino N-H group [Sankar *et al.,* 2007]. They are structural analogues of naturally occurring α-amino acids [Bera Namboothiri, 2014], where the carboxyl group on an α-amino acid (7) is replaced with a phosphoric acid group yielding

the corresponding α-AP (8) (Figure 3). They are classified according to the position of the amino group in relation to the phosphonate or alkyl side chain as amino phosphonates, α-amino phosphonates or β-amino phosphonates [Naydenova *et al.,* 2006].

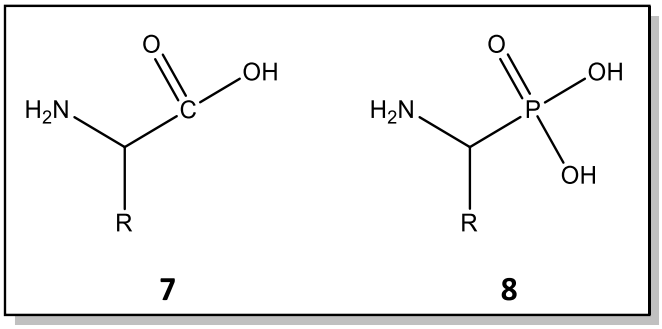

Figure 3: Structure of α-amino acid (7) and its corresponding α-aminophosphonate (8)

Aminophosphonic acids were unknown until 1959 when Horiguchi and Kandatsu isolated the naturally occurring 2-aminoethylphosphonic acid (AEP) (9) from protozoa that lived in ciliated sheep rumen [Akkada *et al.,* 1968]. The curiosity for these compounds led to the isolation of other naturally occurring aminophosphonic acids from a number of organic sources. These included 1-hydroxy-2-aminoethylphosphonic acid (10) present in bacteria, protozoa, insects, vertebrates and human tissue [Snyder Law, 1970]; Fosmidomycin (11) and Fosfomycin (12) found in *Streptomyces*. These compounds have been reported to exhibit remarkable antibacterial activity [Shigi, 1989].

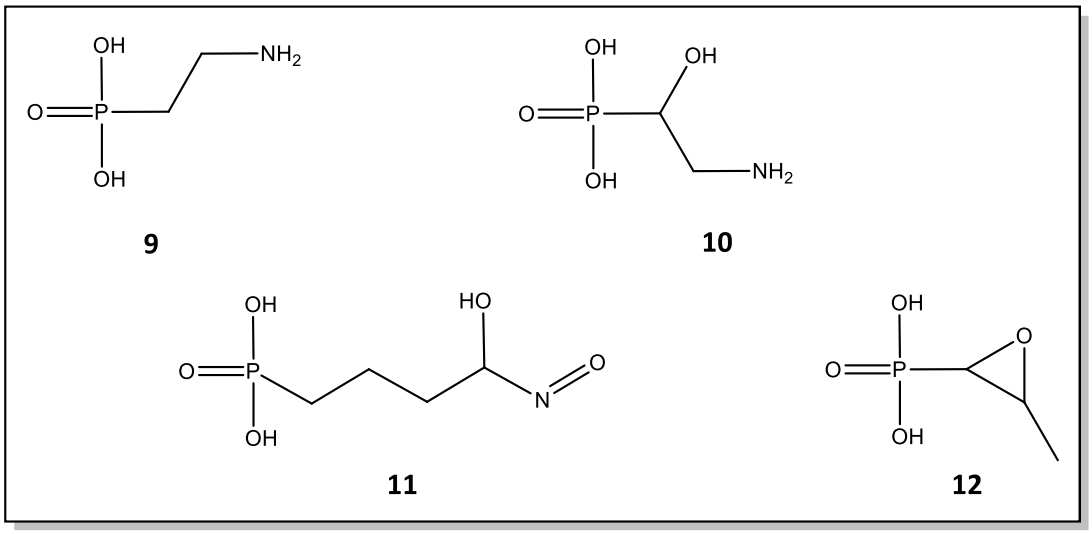

Figure 4: Naturally occurring α-aminophosphonates [Shigi, 1989]

Numerous synthetic methods have been developed for α-APs since they display intriguing biological applications in medicinal chemistry especially as effective antibiotics [Atherton *et al.,* 1986], antiviral drugs [Huang Chen, 2000] including HIV protease antagonists [Mucha *et*

al., 2011], peptide mimics [Mutihac, 2008], antitumor agents [Lavielle *et al.,* 1991] and antioxidants [Rao *et al.,* 2015]. Other examples of biologically active α-APs are presented in Figure 5.

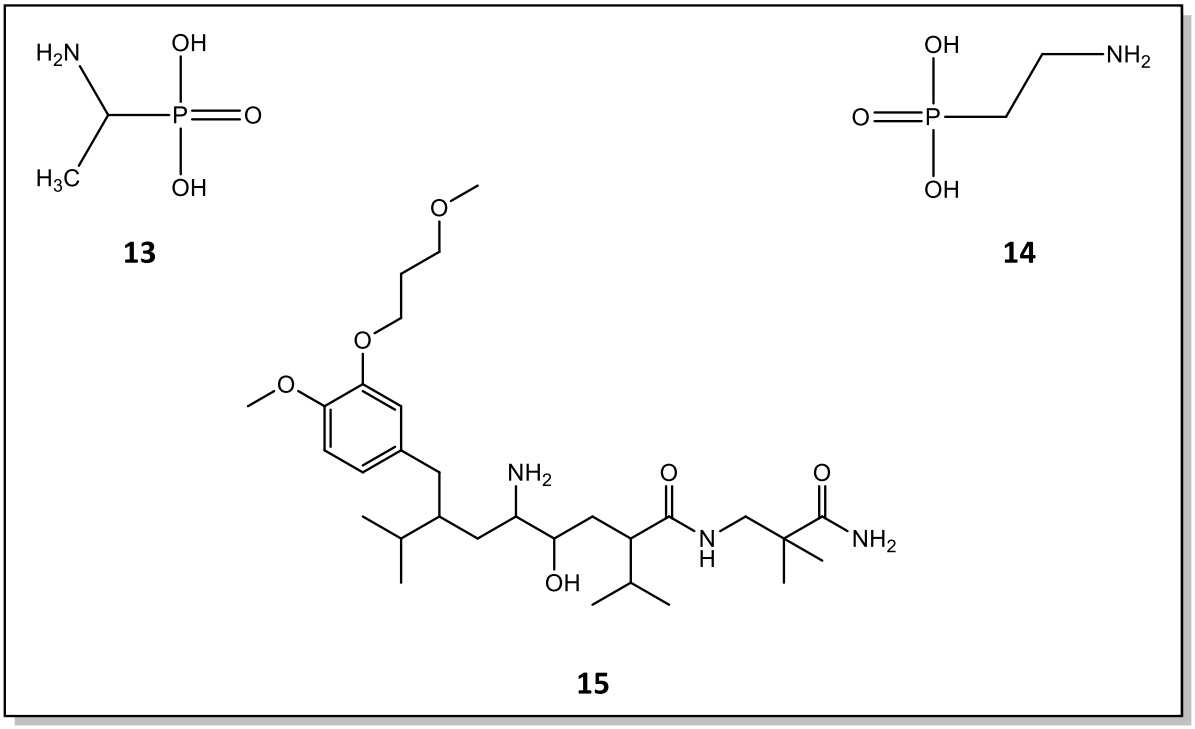

Figure 5: Biologically active α-aminophosphonate compounds [Brzezińska-Rodak *et al*., 2011; Yamauchi *et a*l., 1884; Hill *et al*., 1974]

α-APs are also important in agriculture where they are used as pesticides, fungicides and herbicides and plant growth regulators [Li *et al.,* 2018; Kudzin *et al.,* 2011].

2.2.3. α-Aminophosphonates Bearing a Quinoline Moiety

A major challenge in modern drug discovery is the use of highly efficient chemical reaction sequences to design new molecules with interesting bioactivity [Hopkins, 2008]. One approach uses a 'supporting' moiety which modifies the new molecule [Cavallini Massarani, 2002]. Since all moieties of the overall molecule have their own definite biological activity, it can therefore lead to compounds pre-determined to display interesting novel biological activity [Singh Barrett, 2006].

The therapeutic potential of α-APs with effective pharmacokinetic properties and reduced side-effects has encouraged scientists to modify synthetic schemes to yield new quinoline α-aminophosphonate conjugates (Figure 6) [Tusek-Bozic, 2013]. The main reason for the focus

on quinolines as a supporting moiety is their good pharmacological potential [Michael, 2008] especially as antibacterial [Chu, 1988], antimalarial [Kaur *et al.,* 2010] and anticancer [Kumar *et al.,* 2009] agents.

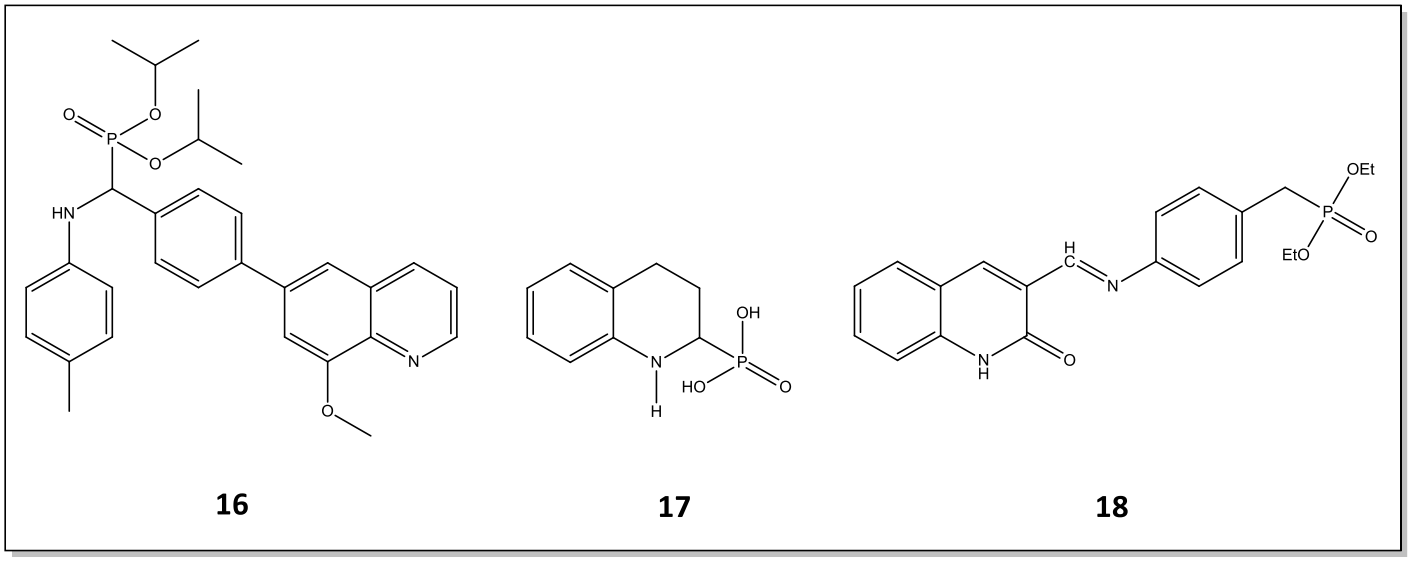

Figure 6: Selected quinoline-based α-aminophosphonates [Zhu *et al.,* 2017; Ordóñez *et al.,* 2016; Yu *et al.,* 2017]

2.3. Multi-component Reactions

MCRs are a synthetic methodology in which three or more substrates react in a single reaction vessel to form a new product. It is a convergent reaction in contrast to the multi-step synthesis. There have been remarkable discoveries of MCRs in the past decades but scientists still invest enormous efforts to develop novel MCRs due to their unique applications. Hence, MCRs is an active area of research in modern organic synthesis [Indu Kaliappan, 2018]. The main characteristic of MCRs is that the newly formed product contains essentially all of the atoms of the various reactants with the exception of condensation products such as H_2O, HCl, or EtOH. They frequently occur with superior regio-, diastereo- and even enantio-selectivity proceeding either jointly or step by step as depicted in Figure 7 below:

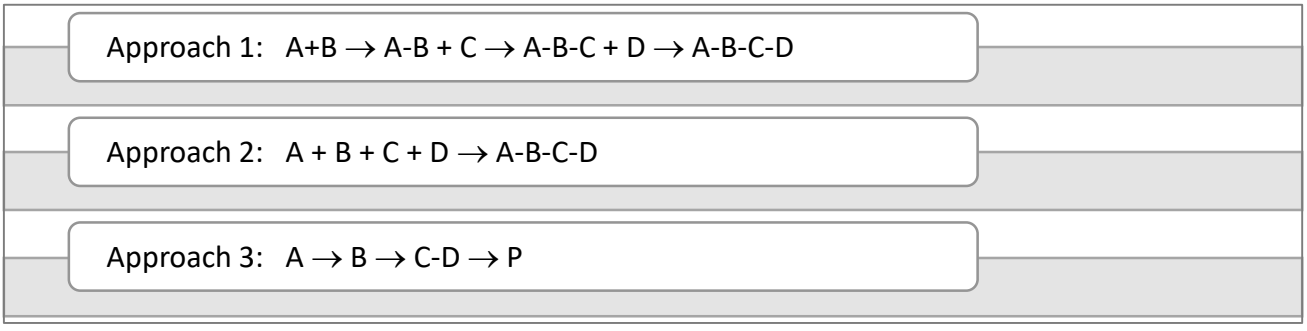

Figure 7: A general multi-component reaction strategy

The advantages of MCRs include minimal by-products, environmentally friendly, simple procedures, lower costs, time and energy saving, use of readily available starting materials, superior atom economy, atom utilization and selectivity [Ganem, 2009] . A selected few of the first MCRs and their reaction schemes are described below:

2.3.1. The Strecker Reaction

Named after Adolph Strecker in 1850, the Strecker reaction was the world's first MCR synthesis of α-amino acids. It was produced from three components viz. aldehyde, potassium cyanide and ammonium [Heydari *et al.,* 2007].

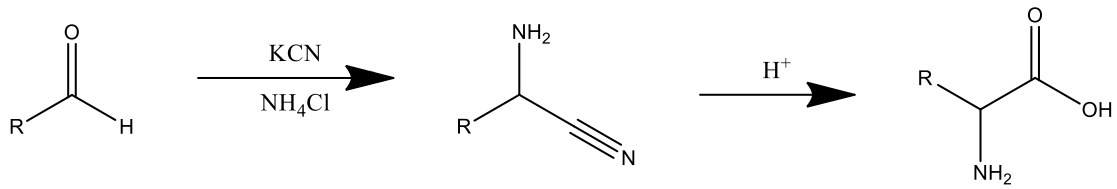

Scheme 2: The Strecker synthesis of α-amino acids [Iyer *et al.,* 1996]

2.3.2. The Biginelli Reaction

An elegant and useful three component cyclo-condensation reaction of an aldehyde, β-keto ester and urea was discovered by Pietro Biginelli in 1981. The reaction produced functionalized dihydropyrimidinones (DHPMs) [Kappe, 1993] that were especially important as calcium channel modulators, adrenergic receptor antagonists and antibacterial agents [Kumar Sandhu, 2010].

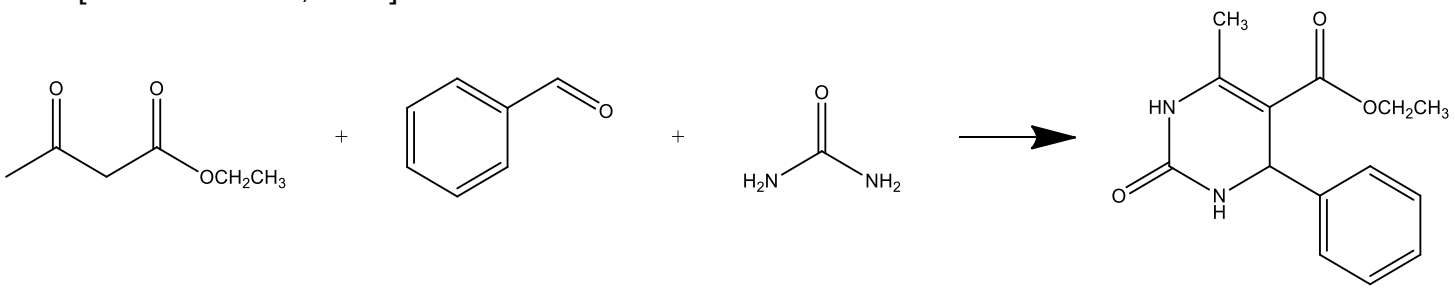

Scheme 3: The Biginelli reaction for the synthesis of pyrimidinones [Sweet Fissekis, 1973]**.**

2.3.3. The Hantzsch Reaction

In 1882, Arthur Hantzsch reported the MCR between an aldehyde, β-keto ester and ammonia for the direct synthesis of dihydropyridine (DHPs) [Nash, 1953]. Several DHPs are commonly known for their biological activities such as calcium channel blockers, neurotropic agents, antidiabetic agents and HIV protease inhibitors [Roy *et al.,* 2011].

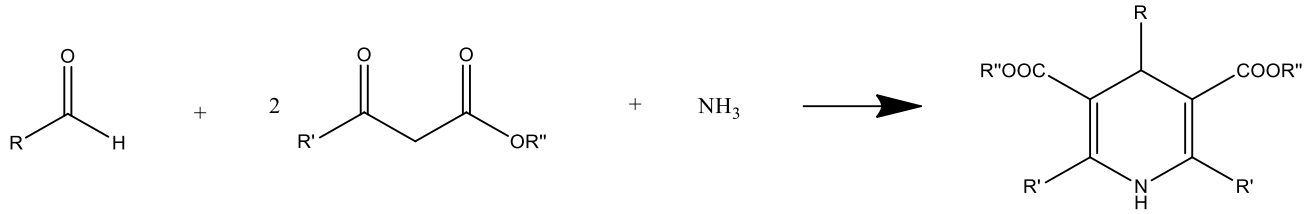

Scheme 4: The Hantzsch reaction for the synthesis of dihydropyridines [Nash, 1953]

2.3.4. The Mannich Reaction

The Mannich reaction discovered in 1912 is a useful tool for the synthesis of β-amino carbonyl compounds [Arend *et al.,* 1998]. This involved the amino alkylation of a carbonyl compound with formaldehyde and a primary or secondary amine or ammonia.

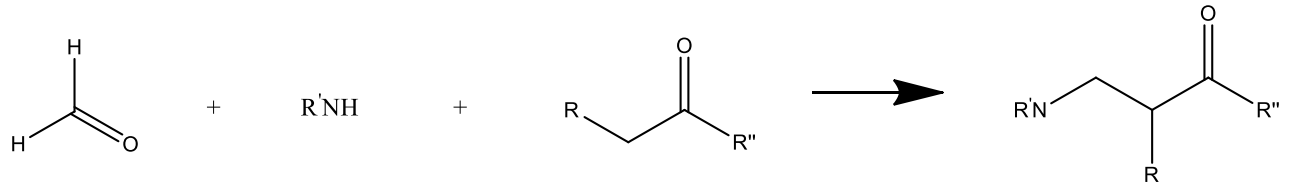

Scheme 5: The Mannich reaction for the synthesis of β-amino carbonyl compounds [Sahoo *et al.,* 2006]

2.3.5. The Kabachnik Fields Reaction

The Kabachnik Fields reaction was discovered and subsequently named after Martin Izrailevich Kabachnik in 1952. The reaction involves a three component condensation of a primary or secondary amine, aldehyde or ketone and a dialkyl phosphite [Bhagat Chakraborti, 2007]. This is a good MCR route for the synthesis of α-APs.

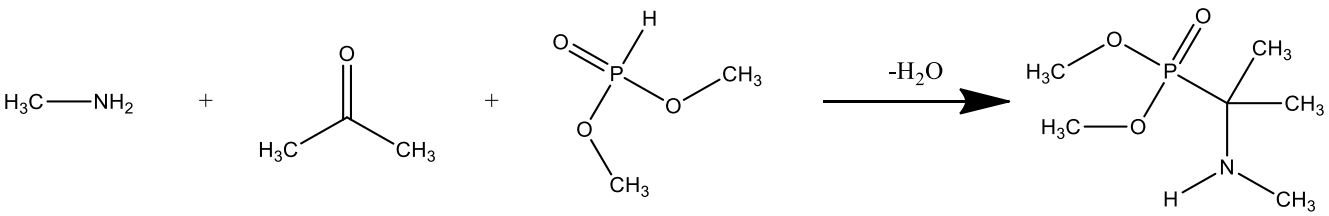

Scheme 6: The Kabachnik Fields reaction for the synthesis of α-aminophosphonates [Bhagat Chakraborti, 2007]

2.3.6. The Ugi Reaction

In 1959, Ugi reported the four-component condensation of a carboxylic acid, amine, ketone or aldehyde and isocyanide [Hulme Dietrich, 2009] as the most versatile MCR for the synthesis of bisamides [Tempest, 2005].

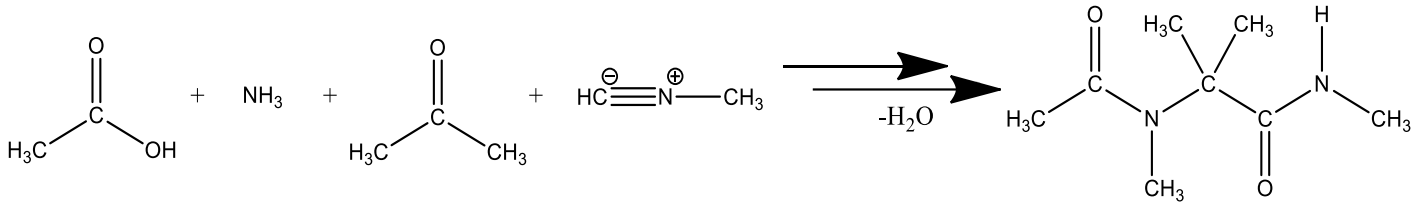

Scheme 7: The Ugi reaction for the synthesis of bisamides [Akbarzadeh *et al.,* 2010]

2.4. The Synthesis of α-Aminophosphonates

2.4.1. The Amidoalkylation of Trivalent Phosphorus Compounds

In 1940, Pikl Engelmann [Popat *et al.,* 1994] synthesized aminomethylphosphonic acid for the first time. In this reaction scheme, an amide reacted with formaldehyde to form N-hydroxymethyl amide, then a successive reaction with phosphorus trichloride provided the aminomethylphosphonic acid derivative.

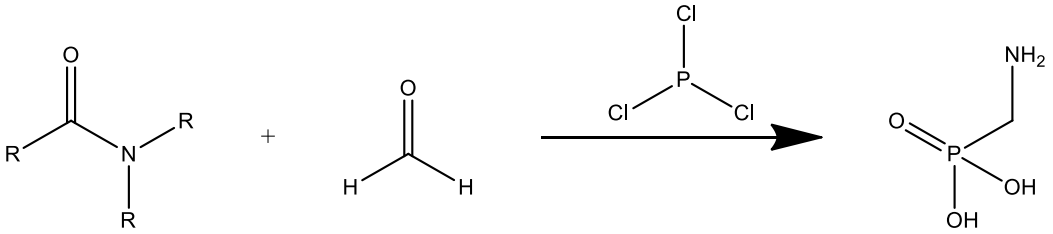

Scheme 8: The synthesis of aminomethylphosphonic acid [Popat *et al.,* 1994]

2.4.2. The Synthesis of α-Aminophosphonates from an Amine and Phosphorus acid

This reliable reaction approach uses an amine with an easily removable protecting group, such as benzyl or phosphorus acid, to synthesize α-APs derivatives [Wuts Greene, 2006].

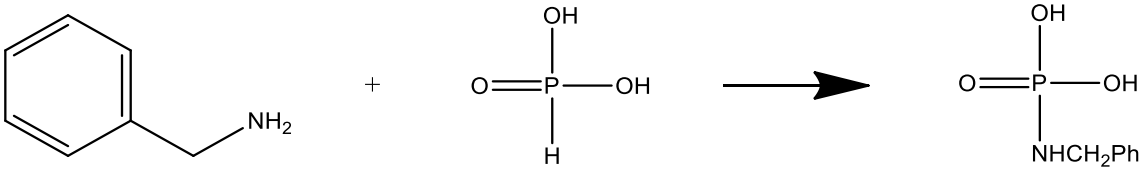

Scheme 9: The synthesis of aminomethylphosphonic acid derivatives

2.4.3. The Michaelis-Arbuzov reaction

The Michaelis-Arbuzov rearrangement reaction is a versatile method used to form the C-P bond [Bhattacharya Thyagarajan,1981]; an alkyl halide and trialkylphosphite yields the corresponding phosphonate. This widely investigated method is extensively used to prepare phosphinates and phosphine oxide.

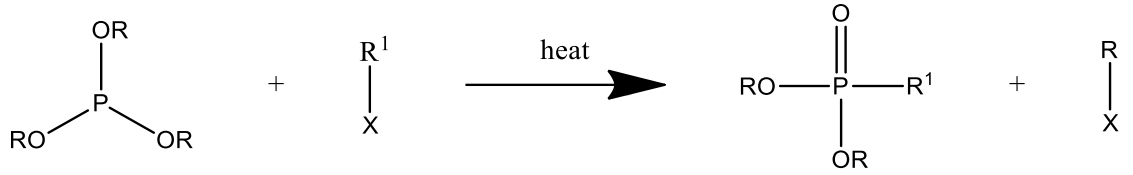

Scheme 10: The Michaelis-Arbuzov reaction for the synthesis of phosphonates, phosphinates or phosphine oxides [Bhattacharya Thyagarajan, 1981]

2.4.4. The Chambers and Isbell Reaction

This synthetic reaction subjects the starting material, 1-bromoalkanecarboxylates, to a series of rearrangement steps to produce α-APs [Chambers and Isbell, 1964].

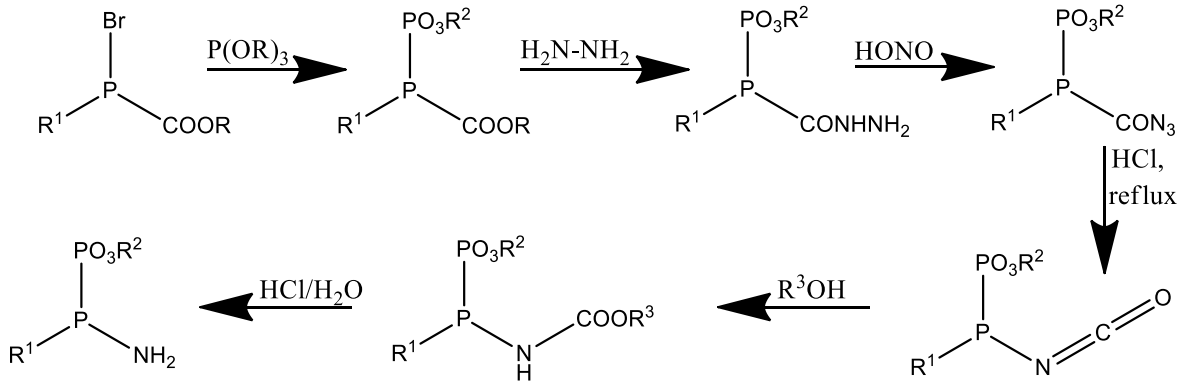

Scheme 11: The Chambers and Isbell reaction for the synthesis of α-aminophosphonates [Chambers and Isbell, 1964]

2.4.5. The synthesis of α-Aminophosphonates from a Nitrile and Grignard Reagent

Addition of a Grignard reagent to benzonitrile forms an imine which is further acylated to the corresponding phosphonate compound [Cristau *et al.,* 1998].

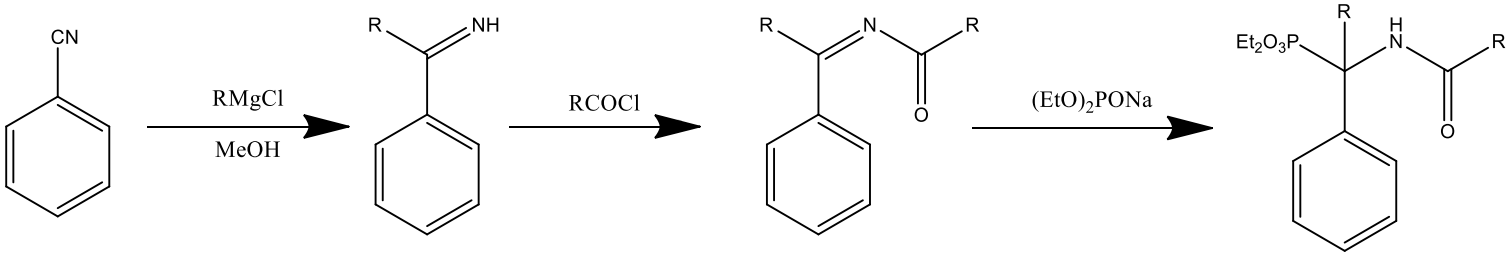

Scheme 12: The synthesis of α-aminophosphonates using the Grignard reagent [Davis *et al.,* 2001]

2.4.6. The Pudovik Reaction

This method involves the hydrophosphonylation of an aldehyde with dialkyl phosphite under basic conditions to obtain the corresponding α-hydroxyl phosphonate [Bera Namboothiri, 2012].

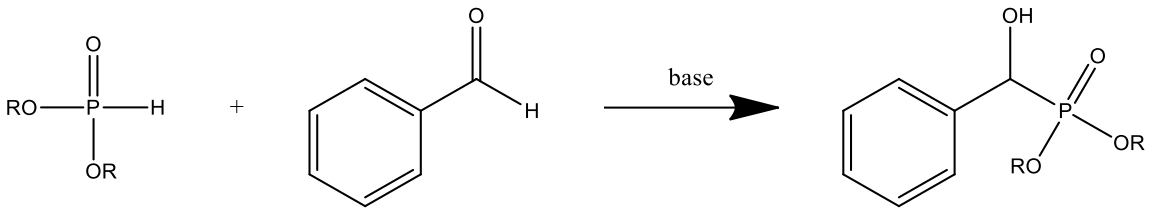

Scheme 13: The Pudovik reaction for the synthesis of α-hydroxyl phosphonates [Pawar *et al.,* 2006]

2.5. The Kabachnik Fields Reaction

The Kabachnik Fields reaction is an important synthetic method for functionally substituted α-APs [Keglevich Bálint, 2012]. It involves an *in situ* three component reaction of an aldehyde, amine and dialkyl phosphite [Simoni *et al.,* 1998] in the presence of an acid catalyst i.e. Brønsted or Lewis acids such as $ZnCl_2$, $MgBr_2$, $BF_3.OEt_2$ [Disale *et al.,* 2012].

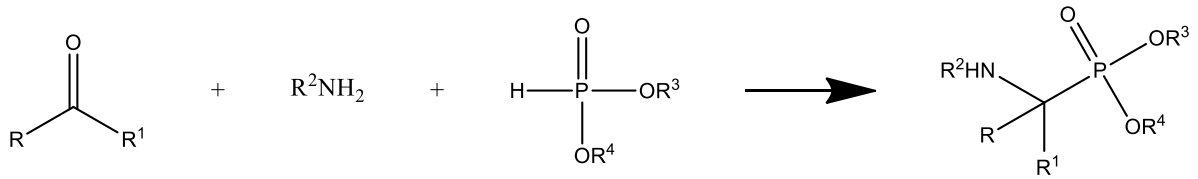

Scheme 14: An efficient three component Kabachnik Fields reaction for the synthesis of α-aminophosphonates [Bhagat Chakraborti, 2007]

Typical reaction schemes of important α-APs are presented below:

The $FeCl_3$ catalyzed reaction of benzaldehyde, aniline and diethyl phosphate in a one-pot three component reaction successfully produced α-APs after 90 minutes with a 73% yield [Rezaei *et al.,* 2011].

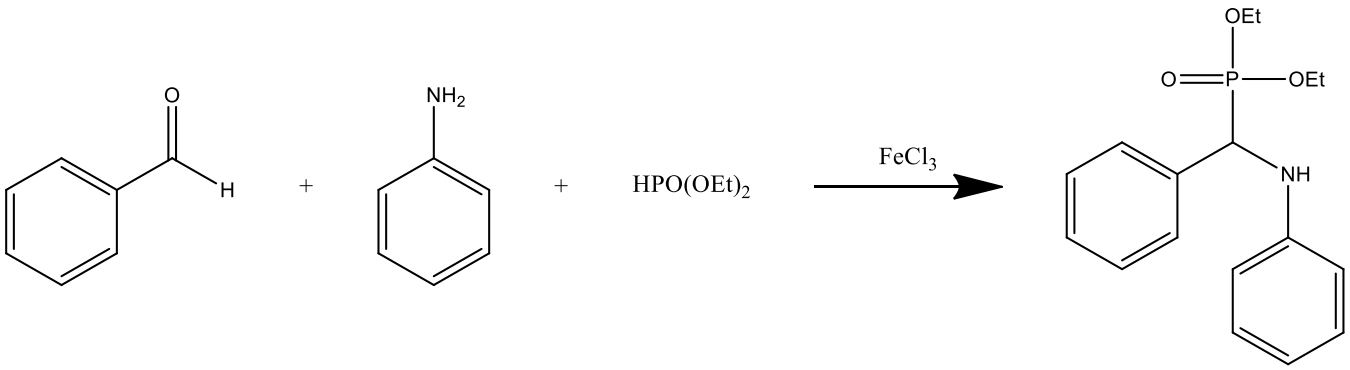

Scheme 15: The synthesis of α-aminophosphonates by the Kabachnik Fields reaction [Keglevich Bálint, 2012]

Keglevich Szekrenyi reported an eco-friendly accomplishment from the basic principles of the Kabachnik Fields reaction. The microwave assisted, solvent and catalyst free synthesis with an amine, ketone and dialkyl phosphite produced α-APs [Keglevich Szekrenyi, 2008].

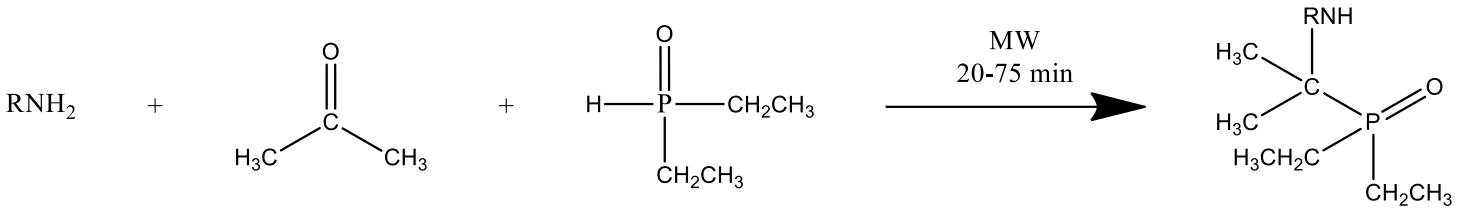

Scheme 16: The Kabachnik Fields reaction for the synthesis of α-aminophosphonates [Keglevich Szekrenyi, 2008]

2.6. Microwave Assisted Organic Synthesis

Organic reactions require an extensive amount of time to achieve a noticeable effect therefore heat is applied to a reaction mixture to speed up the process. Conventional heating methods provide an external heat source transferring energy to the reaction mixture by conductance. Hence, the amount of heat in the reaction mixture depends on the thermal conductivity of various materials that must first be penetrated [Berlan, 1995]. There are several drawbacks for these heating systems which include uneven heat source, require a long time to heat/cool the reaction mixture and tedious apparatus setup that often result in processes of higher costs. Microwave irradiation is an alternative heating approach to conventional heating [Stuerga *et al.,* 1995]. The basic principle of a microwave reaction is the interaction of charged particles in the reaction material with electromagnetic wavelength of a particular frequency i.e. microwaves. These charged ions lose electromagnetic energy in the form of heat by collisions, conduction or both thus results in the mixture being heated [Kappe 2004]. It allows direct coupling with reaction molecules leading to a rapid rise in temperature.

Microwave assisted organic synthesis (MAOS) [Tierney Lidström *et al.,* 2009] has gained popularity in the synthesis of new organic molecules, especially in the development of lead compounds for improved drug development and pharmaceuticals [Kappe *et al.,* 2012]. The advantages of MAOS are lowered energy costs, increased product yields, reduction in waste production, clean and efficient reactions and decreased side reactions that enhance product purity. It is for these reasons that microwave irradiation definitely gained popularity in modern synthetic transformations. Include

2.7. Catalysis

Catalysis is a term used to describe the process of modifying the rate of a chemical reaction with the addition of a catalyst [Lafaye Liang, 2017]. This chemical substance alters the reaction kinetics affording an alternative reaction pathway with a lower activation energy for the breaking and reformation of bonds; temporary bonds formed with reacting molecules result in an intermediate product which in turn reacts with the other starting molecules to yield the same amount of a specific product in a shorter time while remaining chemically unchanged at the end of the process [Inderwildi *et al.,* 2007]. Catalyzed reactions require less energy (Figure 8) and time so they contribute to an economical and environmental benign process for chemical transformation [Daştan *et al.,* 2012]. The two main types of catalysts are homogeneous and heterogeneous.

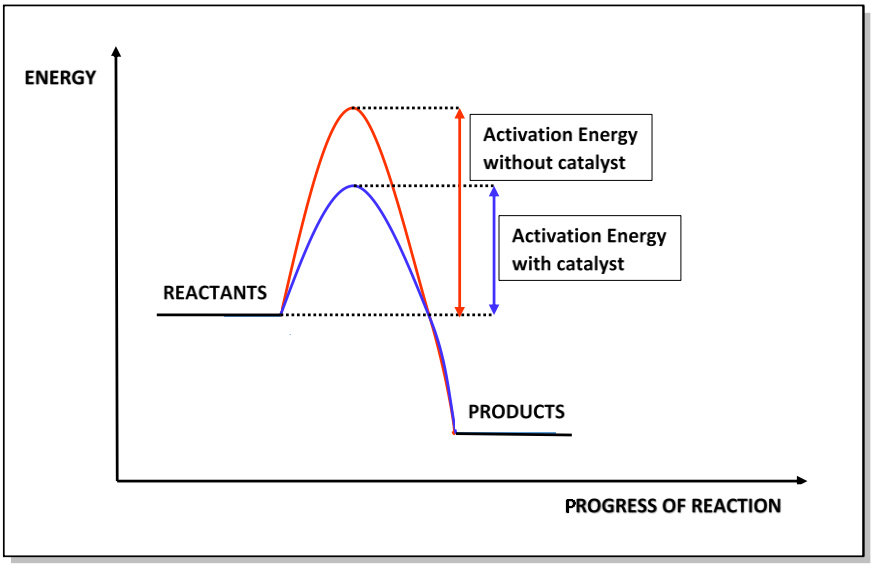

Figure 8: Energy profile diagram showing the effect on activation energy of a catalysed and uncatalysed reaction [Frost Pearson, 1961]

2.7.1. Homogenous Catalysis

Homogenous catalysis is a system in which the catalyst and reaction substrates are brought together in the same phase, most often the liquid phase. A few examples include acid, organometallic and enzymatic catalysis. The key advantage of this approach is that the catalyst combines with the reaction mixture allowing a high degree of interaction between reactants and catalyst thereby resulting in an active and selective catalytic process. The fundamental drawback of homogenous catalysis is that the catalyst is unrecoverable from the reaction mixtures after completion of the reaction [Hartley, 2012].

2.7.2. Heterogenous Catalysis

Heterogeneous catalysis is the type of catalysis where the physical phase of the catalyst differs from the physical phase of the reactants: substrates that are brought together in a chemical reaction. A typical example is the use of clay or silica based [Sheldon Van Bekkum, 2008] solid catalysts which are placed in a liquid reaction mixture. They play an important role as sustainable alternatives to classical homogeneous catalysts. The benefits displayed by heterogeneous catalysts include recyclability, good thermal stability, simple to handle, reasonably inexpensive and ease of separation from the reaction mixture [Thomas *et al.,* 1967]. The Lewis acids such as $SnCl_4$ [Laschat Kunz, 1992], $BF_3.OEt_2$ [Ha Nam, 1992], $ZrCl_4$ [Yadav *et al.,* 2001], $InCl_3$ [Ranu *et al.,* 1999], DTP/SiO_2 [Mirzaei *et al.,* 2015] and $LiClO_4$ [Sobhani Vafaee, 2010] have been applied to the Kabachnik Fields reaction as heterogeneous catalysts for the synthesis of α-APs.

Heterogeneous catalysts entail precise proportions of several elements to optimize their catalytic activity that leads to optimal selectivity, making this process a central focus area for green chemistry research and a crucial part of several industrial activities such as oil refining, pollution control, lead compound development and organic synthesis.

2.7.3. Metal Strontium Titanate

Alkaline earth metals with perovskite-type oxides have generated tremendous interests in science over the last fifty years [Khine *et al.,* 2013] due to their applications as advanced catalytic materials [Tejuca Fierro, 1992]. Strontium titanate ($SrTiO_3$) is arguably one of the most interesting multifunctional alkaline earth metal perovskite oxides in this structural family since its physical properties can be tailored by changing its oxygen stoichiometry [Nikodemski, 2016]. $SrTiO_3$ is a crystalline solid (Figure 9) under ambient conditions. The hybridization of the O-2p states with the Ti-3d states within the TiO^6 octahedra lead to pronounced covalent bonding but Sr^{2+} and O^{2-} ions exhibit ionic bonding characteristic [Kawasaki *et al.,* 1994] resulting in mixed ionic-covalent bonding properties [Chang *et al.,* 1997]. Characterized by high thermal stability, oxidative properties and low cost [Joshi Krupanidhi, 1993] makes it a promising catalyst support for all applications that call for stability as a key point.

Pt/$SrTiO_3$ has shown to be a promising low temperature hydrocarbon combustion catalyst in the automotive industry [Manginell *et al.,* 1997]. This important green chemical process [Farruto Heck, 2000] uses a catalyst to prompt desired oxidation reactions during fuel

combustion so to reduce the formation of pollutants, especially nitrogen oxide gases [Farruto Heck, 1999]. The high catalyst activity is accredited to the stabilized core structure of Pt/PtO by the strong epitaxy between Pt and $SrTiO_3$ support during the reaction process [Han *et al.,* 2007; Feng *et al.,* 2011]. Furthermore, Pd/$SrTiO_3$ can be used as a catalyst for electroless deposition in the Hybrid Sulphur cycle to split water and produce hydrogen [Kawamura *et al.,* 2009].

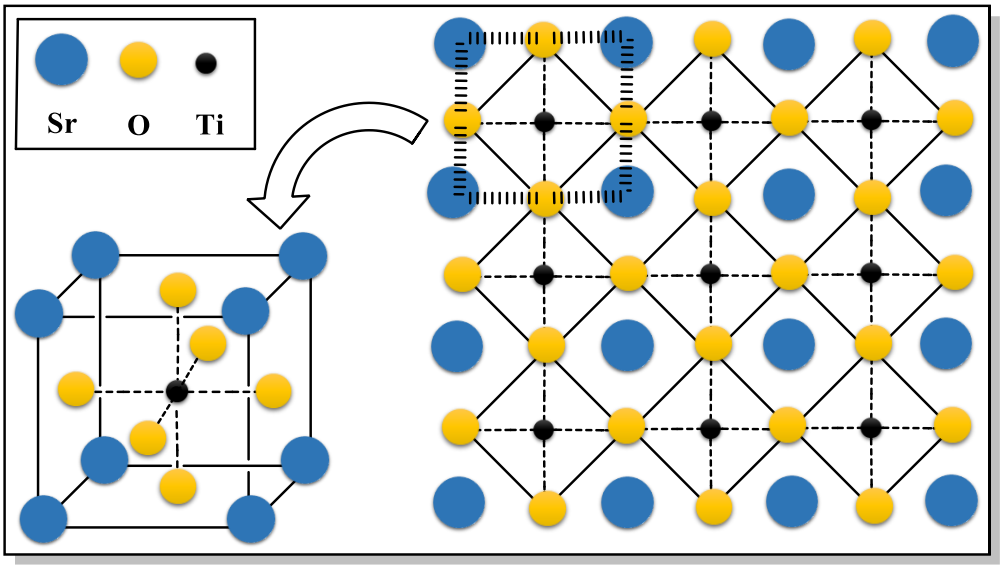

Figure 9: The cubic crystalline perovskite structure of Strontium Titanate at room temperature [Nilsen Skinner, 1968]

Figure 9 shows the Sr-type atoms located on the corners of the cell, single Ti-type atoms sit at the centre of the cell and oxygen atoms are at the centre of each face (size of the spheres representing each atom are arbitrary and are not related to atomic radii).

2.8. Structure Elucidation

Structure elucidation is a method used to determine the chemical structure of a compound; essentially the end result of such a process is to attain the coordinates of the atoms in a molecule [Kwan Huang, 2008]. Spectroscopic techniques are an especially important requirement for structure elucidation of organic compounds. These techniques include Infrared (IR) spectroscopy, Mass Spectrometry (MS) and Nuclear Magnetic Resonance (NMR) Spectroscopy.

- Infrared (IR) spectroscopy is an IR spectrometer that passes infrared radiation, over a range of different frequencies through a sample and measures the absorptions made by each type of bond in the compound [Vollhardt Schore, 2007].

- Mass Spectrometry (MS) is an analytical technique used to identify the amount and type of chemicals present in a sample by measuring the mass-to-charge ratio and abundance of gas-phase ions of a molecule [Sparkman, 2000].
- Nuclear Magnetic Resonance (NMR) Spectroscopy is a physical phenomenon based on the ability of atomic nuclei to receive electromagnetic energy at a characteristic frequency supplied by radio frequency pulses in a static magnetic field and thereby attain a higher resonance state. The detection of the resonance frequency of the nucleus and a standard compound is called chemical shift (δ/ppm); this is used to acquire the NMR spectrum of a test compound. Positions, intensities and fine arrangements of resonance peaks make it possible for scientists to study the constitution structures of test compounds [Fuloria Fuloria, 2013]. ^{1}H-NMR is the application of NMR with respect to hydrogen-1 nuclei within the molecules of a substance [Chen *et al.,* 2007]. ^{13}C-NMR is the application of NMR to carbon; the main carbon isotope (^{12}C) is not detectable by NMR since it has zero net spin and so it detects only the ^{13}C isotope of carbon making it an important chemical structure elucidation tool in organic chemistry [Fuloria Fuloria, 2013].
- Two dimensional nuclear magnetic resonance (2D NMR) is widely used in chemical analyses to interpret the structure of complex molecules that is otherwise difficult to work with using 1D NMR. This NMR technique provides data plotted in a space defined by two frequency axes originating from nuclei that exchange magnetization during the frequency of the first and second nucleus in each dimension respectively. This indicates the interaction concerning these two nuclei. As a result, the cross signals contain important information about the 2D NMR spectra. Types of 2D NMR include correlation spectroscopy (COSY), J-spectroscopy, exchange spectroscopy (EXSY), nuclear Overhauser effect spectroscopy (NOESY) and Heteronuclear Multi-Bond Connectivity (HMBC).

2.8.1. Structure Elucidation of Chromone Bearing α-Aminophosphonates

Jaiyeola *et al.,* (2017) reported the synthesis of chromone bearing α-aminophosphonates (4a-4m) catalyzed by rhodium boron nitride (RhBNT) [Jaiyeola *et al.,* 2017]. The structures were confirmed by elemental analysis, IR and NMR.

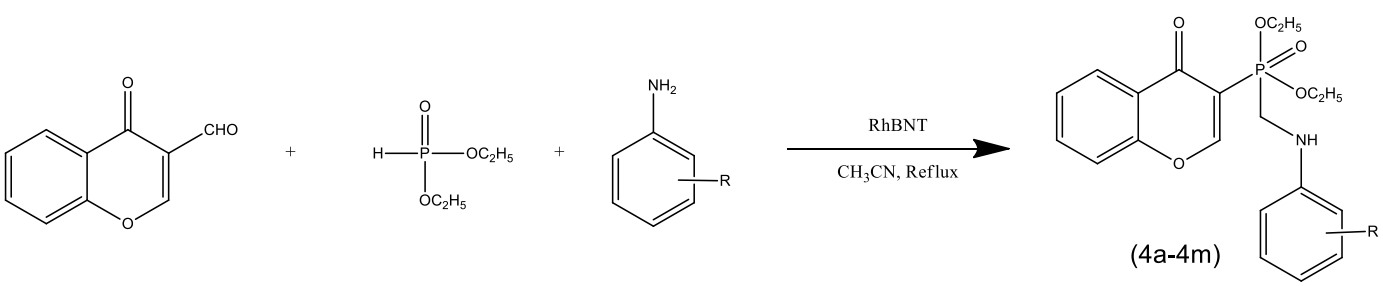

Scheme 17: Synthesis of α-aminophosphonate derivatives [Jaiyeola *et al.,* 2017]

Compound 4g is used as a typical example to elaborate on the method of characterization described by Jaiyeola *et al*., (2017). The same methodology was carried through to the structural elucidation of novel compounds synthesized and described in this thesis. Interpretation of spectroscopic data is presented below:

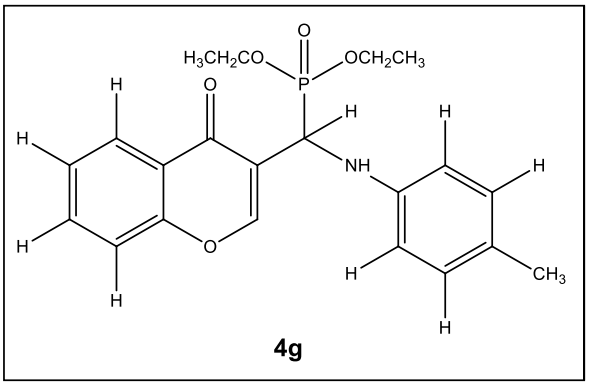

4g

The IR spectrum of 4g (Figure 10) showed absorption bands at 1637.52 cm^{-1} (C=O stretching vibrations), 3279.33 cm^{-1} (N-H stretching vibrations), 1221.79 cm^{-1} (P=O stretching vibrations), 2983.17 cm^{-1} (C-H aliphatic stretching), 1015.64 cm^{-1} (P-C-O bending), 766.19 cm^{-1} (P-C aliphatic stretching) and 1515.0 cm^{-1} (C=C stretch in ring).

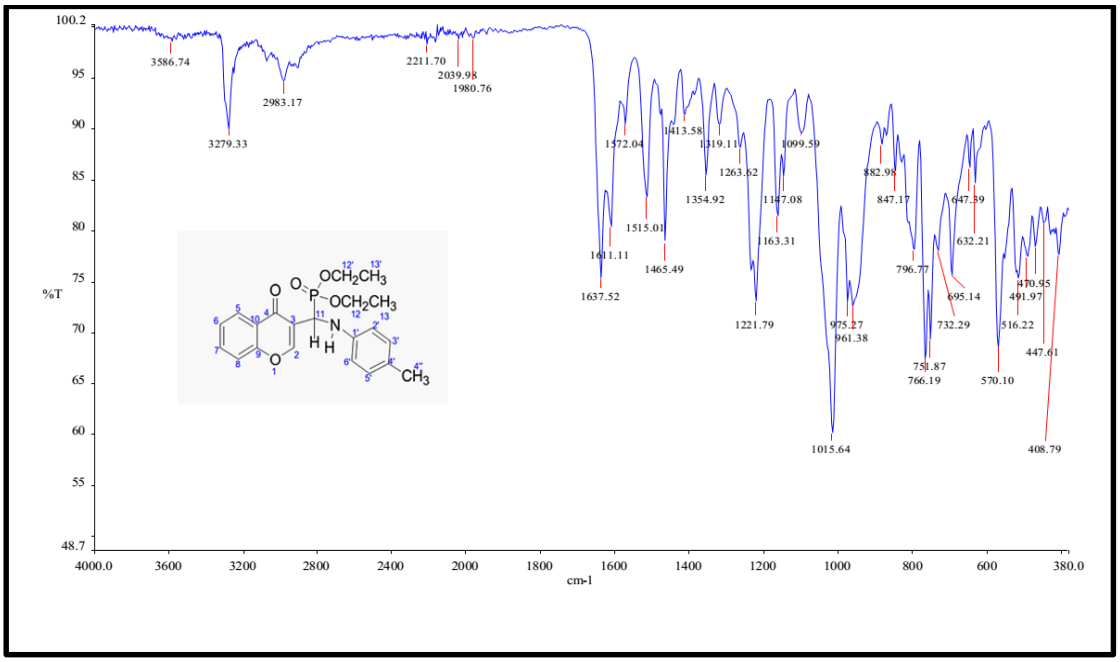

Figure 10: The IR spectrum of compound 4g [Jaiyeola *et al.,* 2017]

The ^{1}H-NMR spectrum of 4g (Figure 11) showed triplets at δ 1.16 and 1.30 for two aliphatic methyl protons and δ 2.16 for methyl protons attached to the aromatic portion. The multiplets at δ 4.01 and 4.11 appeared for methyl protons (H-12, H-12'), doublet at δ 5.29 appeared for the P-C-H proton (H-11) due to its coupling with the neighbouring N-H proton and phosphorus while a broad signal at δ 3.50 was assigned to the N-H proton.

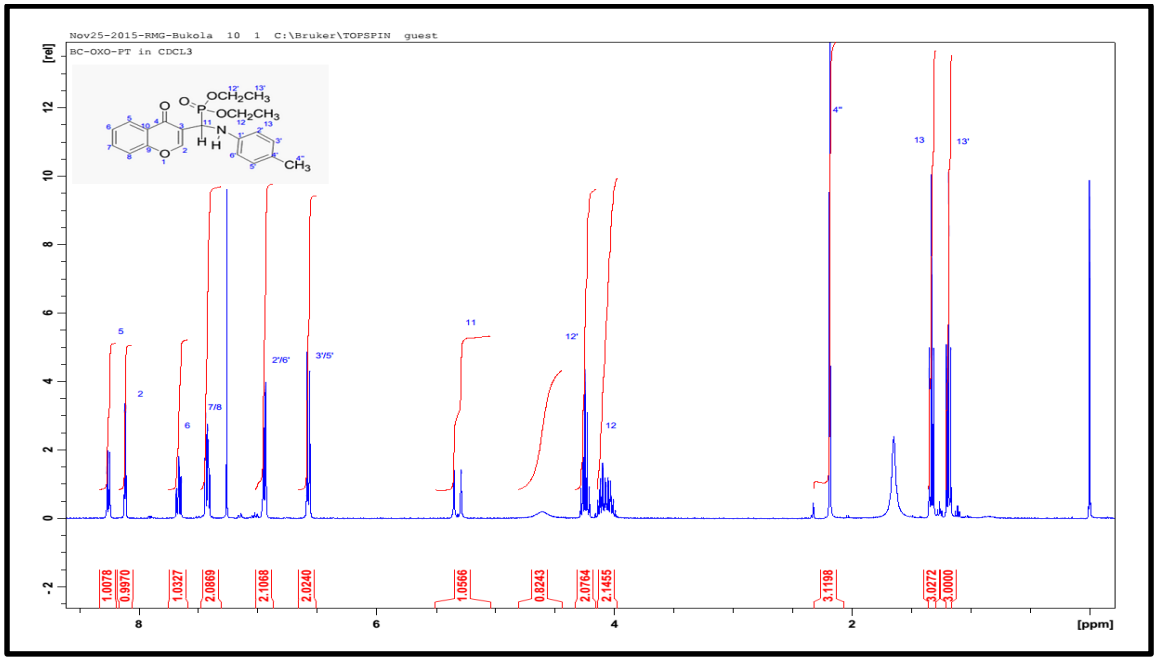

Figure 11: The ^{13}C-NMR spectrum of compound 4g [Jaiyeola *et al.,* 2017]

The ^{13}C-NMR spectrum of 4g (Figure 12) was in good agreement with the assigned structure. The peaks at δ 16.40 and δ 16.26 were assigned to two methyl carbons (C-13, C-13'), peaks at δ 63.40 and 63.81 were assigned to C-12 and C-12' respectively while peaks appeared at δ 113.86 for carbon 3'/5' and δ 128.20 for carbon 2'/6'. The peak at δ 20.35 was assigned to methyl carbon of the aromatic ring (C4''), the peak at δ 176.30 was assigned to the carbonyl carbon (C-4) whilst C-11 was attributed to δ 46.27. The remaining aromatic carbons appeared as: C-1' at δ 133.82, C-2 at δ 156.18, C-4' at δ 120.22, C-5 at δ 125.94, C-6 at δ 125.39, C-7 at δ 129.86, C-8 at δ 118.25, C-9 at δ 156.26 and C-10 at δ 123.44.

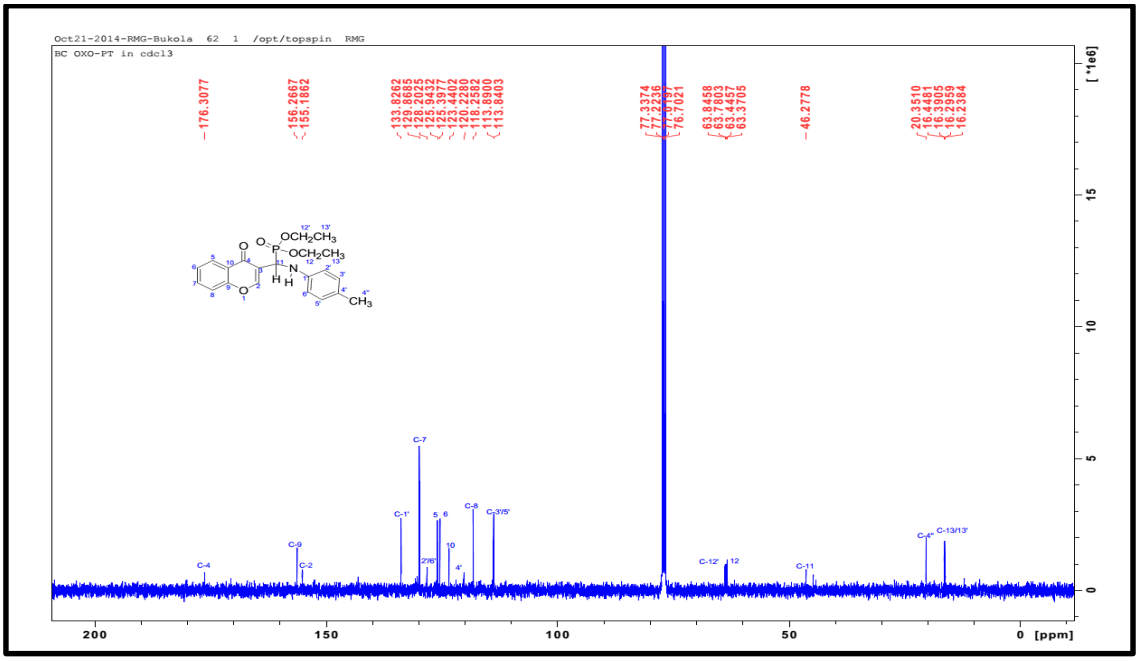

Figure 12: The ^{13}C-NMR spectrum of compound 4g [Jaiyeola *et al.,* 2017]

The ^{31}P-NMR signal of 4g (Figure 13) appeared as a singlet at δ 22.57.

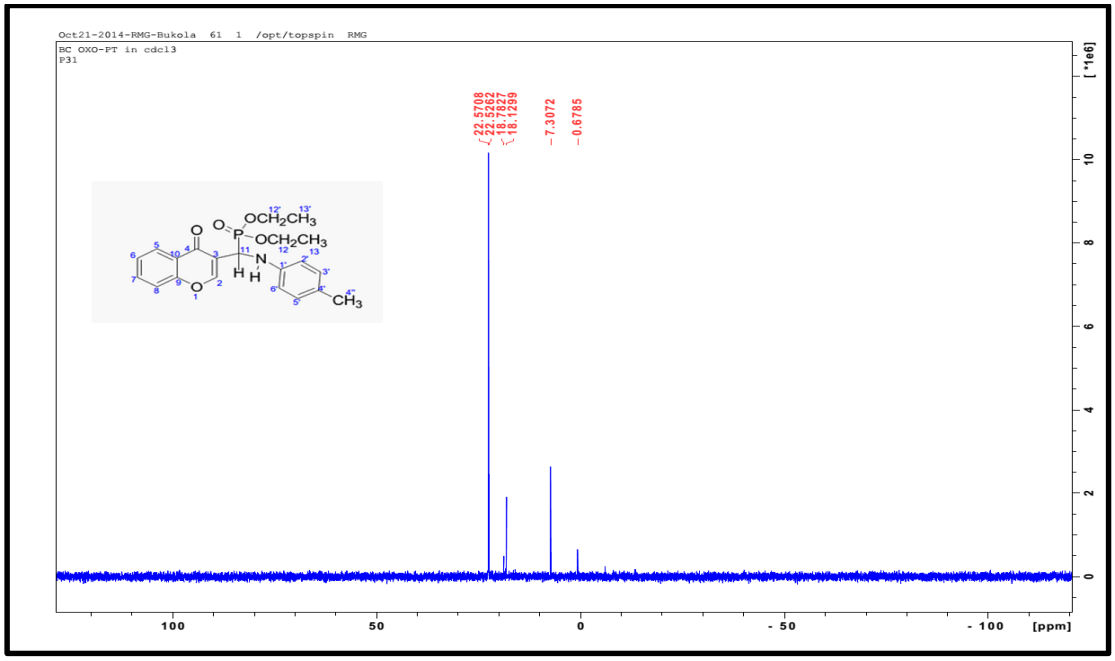

Figure 13: The ^{31}P-NMR of compound 4g [Jaiyeola *et al.,* 2017]

Table 1: ^{1}H and ^{13}C NMR structural elucidation of compound 4g [Jaiyeola *et al.,* 2017]

Compound 4g	No.	^{1}H NMR	^{13}C NMR
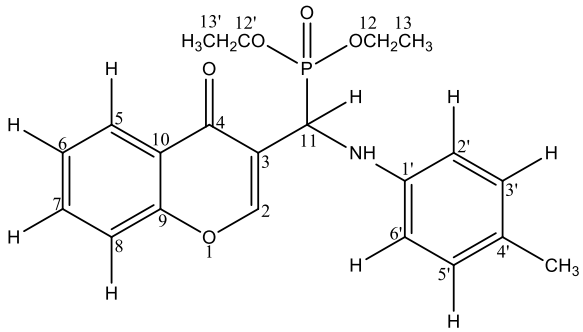	NH	4.60	-
	CH	5.32	-
	1’	-	133.82
	2	8.11	155.18
	5	8.23	125.94
	6	7.64	125.39
	7	-	129.86
	7/8	7.40	-
	2’/6’	6.92	128.20
	3’/5’	6.57	113.86
	4	-	176.30
	4’	-	120.22
	4’’	2.17	20.35
	8	-	118.25
	9	-	156.26
	10	-	123.44
	11	-	46.27
	12’	4.25	63.84
	12	4.07	63.40
	13’	1.30	16.26
	13	1.16	16.40

The HMBC spectrum of 4g showed H-2'/6' correlations with C-3'/5' at δ 118.36 and C-4' at δ 120.22. H-5 was correlated to C-4 at δ 176.30, C-7 at δ 129.86 and C-9 at δ 156.26. H-6 showed correlations with C-5 at δ 125.94 and C-9 at δ 156.26. H-7 was correlated with C9 and C-4 at δ 156.26 and δ 176.30. H-8 showed correlations with C-4 and C-2, C-10, C-11 at δ 176.30, δ 155.18, δ 123.44 and δ 46.27. H-11 was correlated with C-2, C-10 and C-4 at δ 155.18, δ 123.44 and δ 176.30.

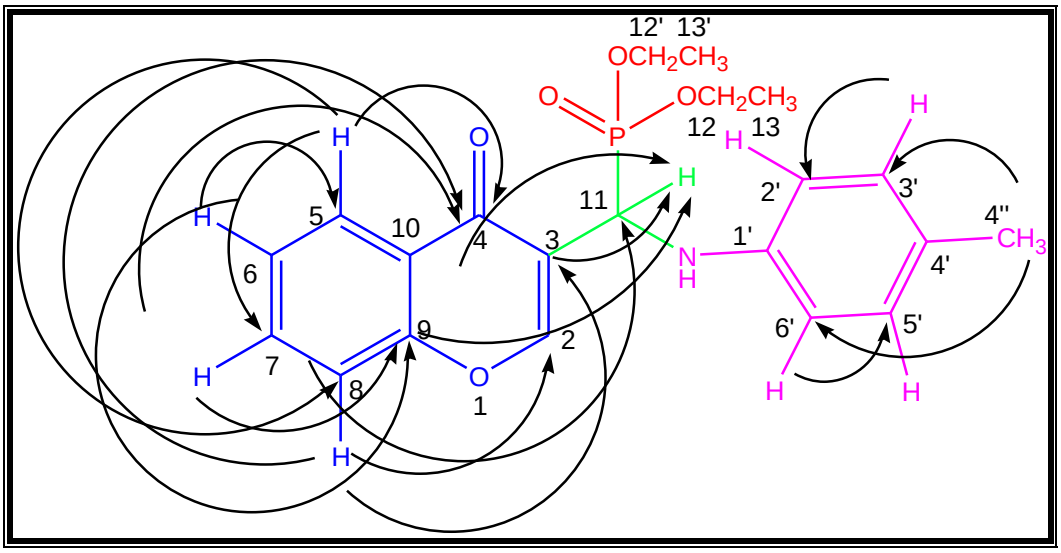

Figure 14: Selected HMBC correlations for compound 4g [Jaiyeola *et al.,* 2017]

2.9. Bacterial Studies

2.9.1. History of Bacteria

The oldest fossils known are bacteria-like organisms which date back nearly 3.5 billion years ago [Taylor Krings 2005]. Bacteria are existent in most habitats on the planet including the soil, water and acidic hot springs [Fisher *et al.,* 2007]. These microorganisms are essential to life on earth and are needed for the production of antibiotics, converting nitrogen into a usable form, make up the base of the food web, break down dead organic matter [Stackebrandt *et al.,* 2002] among other imperative processes. However, certain pathogenic bacteria gain access into the body and cause human and animal disease. Figure 15 provides an overview of bacterial infections in the human body.

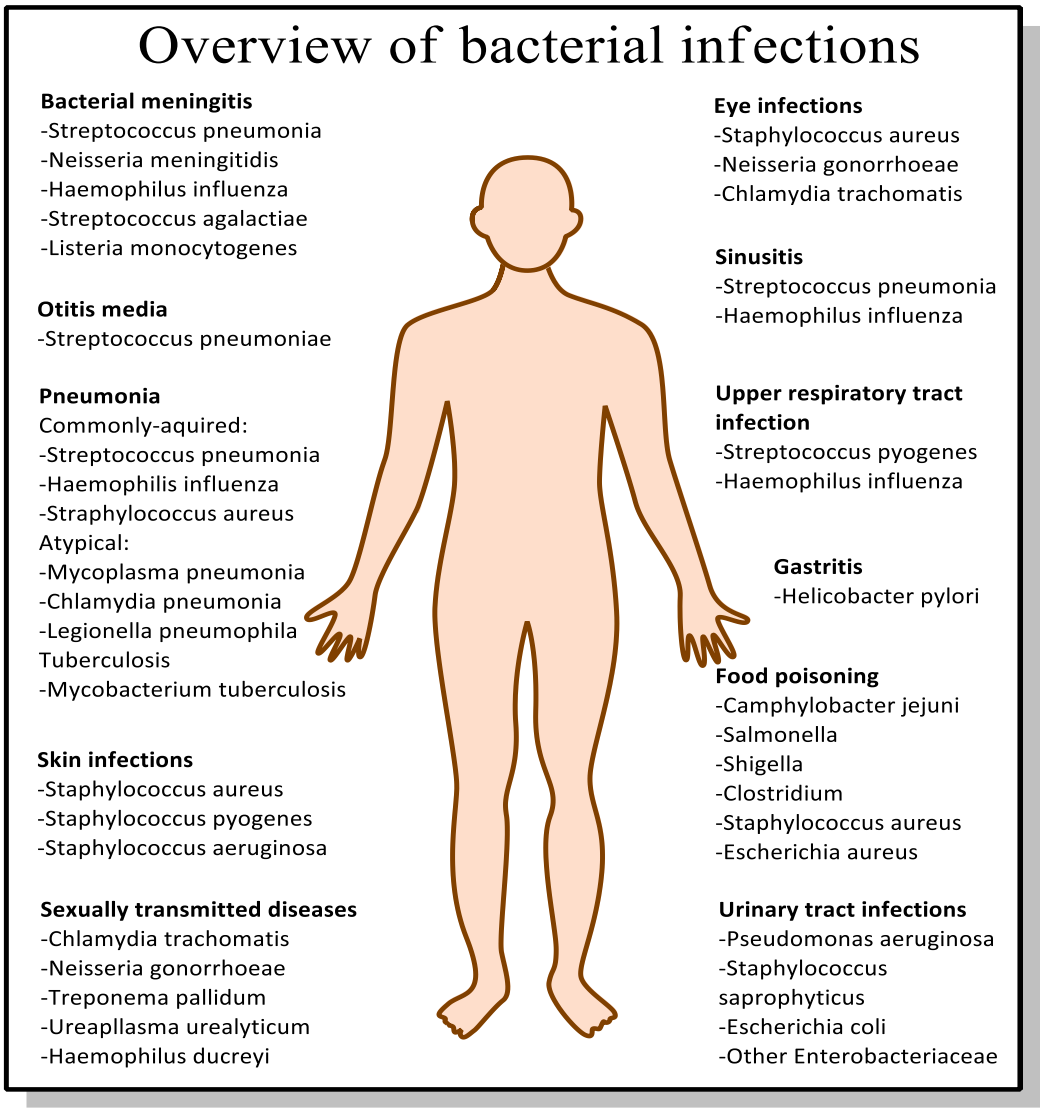

Figure 15: An overview of bacterial infections that can occur in the human body [Stackebrandt *et al.,* 2002].

2.9.2. Biological Activities of α-Aminophosphonates

α-APs have been subjected to extensive studies and used as healing agents for various diseases because of their interesting biological activities including:

2.9.2.1. Cytotoxicity Activity

While synthetic compounds may depict a wide spectrum of pharmacological properties, they may still be toxic for human use. For instance, the structure of α-APs bear close resemblance to corresponding natural amino acids and are known for their interesting biological properties and reduced levels of toxicity [Oniţa *et al.,* 2010]; however it is vital that novel compounds belonging to this class undergo cytotoxicity screening for safety purposes.

The Brine shrimp lethality bioassay is a simple, inexpensive yet high throughput method used to test the cytotoxicity of bioactive compounds [Krishnaraju *et al.,* 2005]. It is based on the ability of a test compound to kill a simple zoological organism viz., Brine shrimp (*Artemia salina*). This assay is a functional prelude evaluation of cytotoxicity for further experiments.

2.9.2.2. Antimicrobial Activity

For many years, α-APs have been reported to exhibit significant antimicrobial activity against a wide spectrum of bacteria [Abdel-Megeed *et al.,* 2012]. Typical α-APs 19, 20 and 21 (Figure 16) were synthesized via the three component condensation of an aromatic aldehyde, amines and diethyl phosphite with catalytic amounts of ethyl ammonium nitrate ionic liquid. These compounds were reported to have shown high antibacterial activity against pathogenic bacteria such as *Escherichia coli*, *Staphylococcus aureus*, *Salmonella typhi*, *Pseudomonas putida* and *Proteus vulgaris* [Dake *et al.,* 2011].

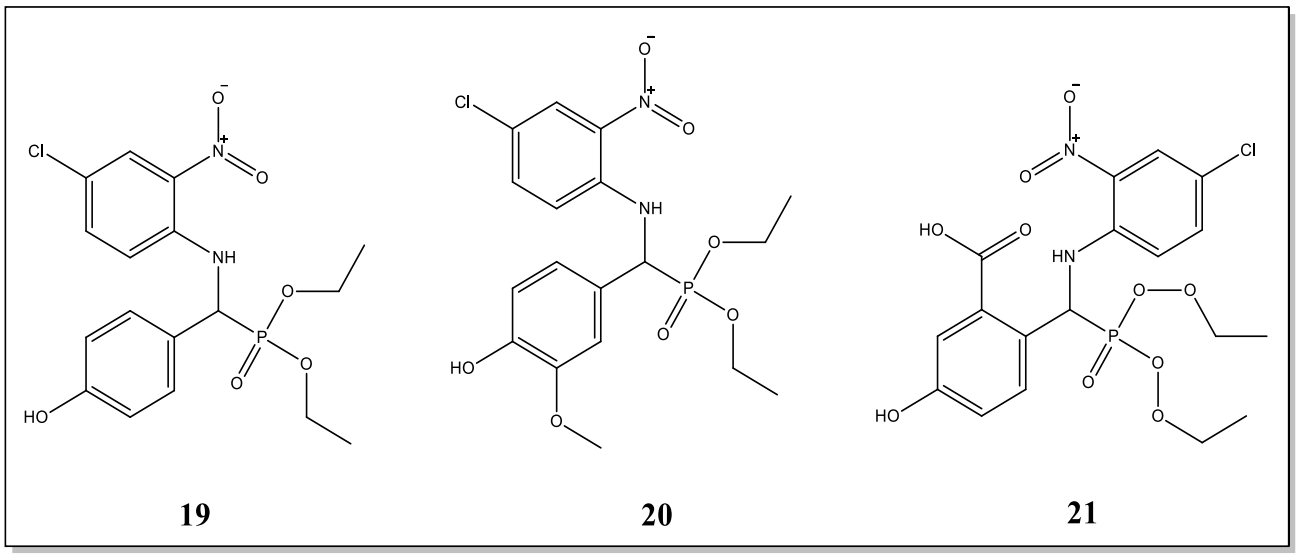

Figure 16: α-Aminophosphonates that exhibit antimicrobial activity [Dake *et al.,* 2011]

A series of α-AP compounds viz., 22, 23, 24 and 25 (Figure 17) were synthesized from chitosan, triphenylphosphite and an aromatic aldehyde catalyzed by lithium perchlorate [Reddy *et al.,* 2008; Kenawy *et al.,* 2015]. It was reported that these compounds showed bacteria growth inhibition and results of antimicrobial assays showed high activities against bacteria and fungi [Kenawy *et al.,*2015]. These included *Escherichia coli*, *Serratia marcescens*, *Enterobacter cloacae*, *Shigella dysenteriae*, *Salmonella enterica* and *Proteus vulgaris* as Gram-negative bacteria, *Bacillus subtilis* and *Staphylococcus aureus* as Gram-positive bacteria and *Candida albicans* [Kenawy *et al.,* 2015].

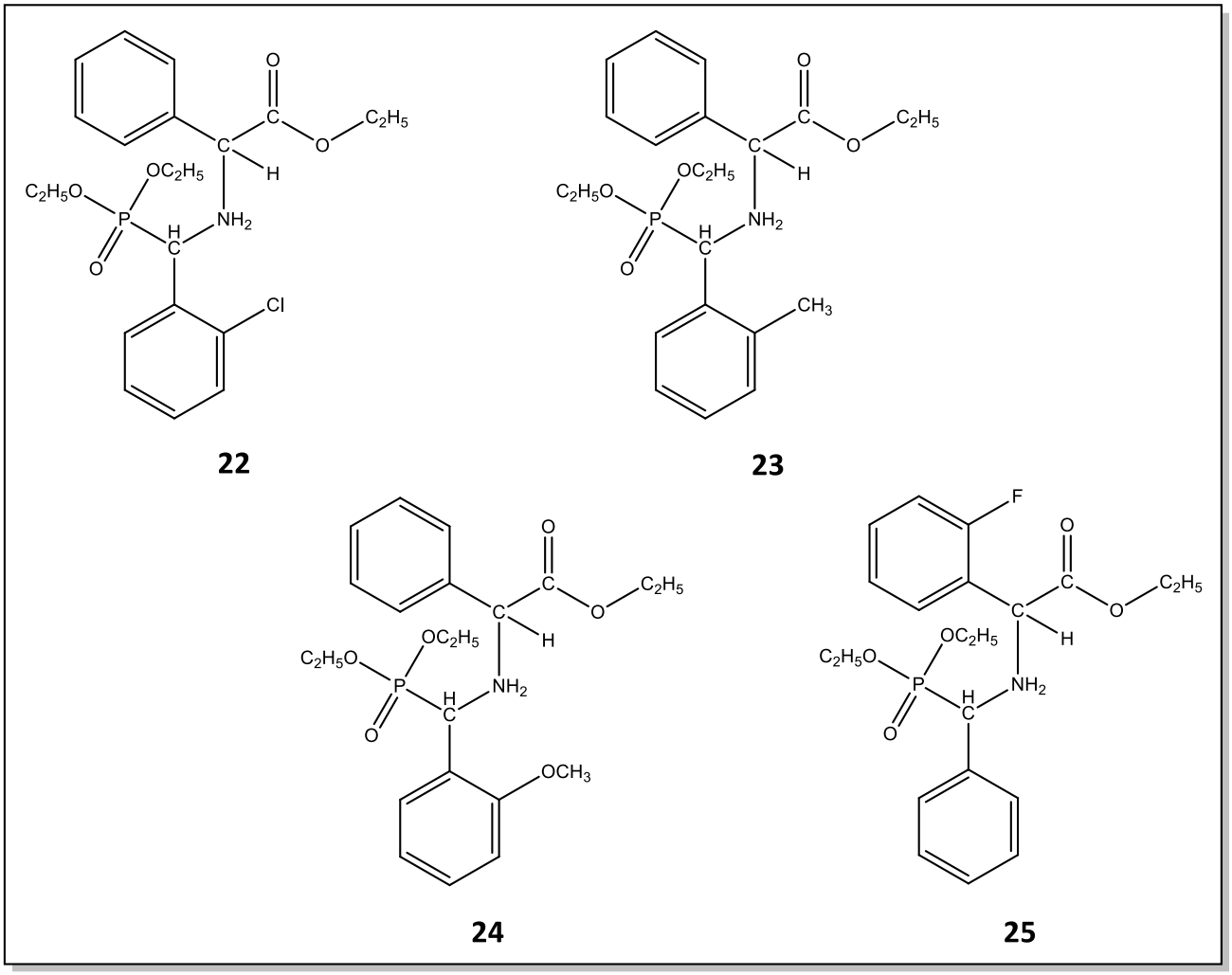

Figure 17: α-Aminophosphonates that exhibit antimicrobial activity [Reddy *et al.,* 2008; Kenawy *et al.,* 2015].

Some α-amnophosphonate antimicrobial drugs and their reaction schemes:

Nizamov *et al.,* (2013) synthesized O,O diethyl-(N-isobutylamino)-3,7-dimethylocta-2,6 dienylphosphonates (Scheme 18) via the Kabachnik Fields reaction using citral as a catalyst and diethyl phosphite in the presence of isobutylamine [Nizamov *et al.,* 2013]. These α-APs derivatives exhibited antimicrobial activity against *Staphylococcus aureus* and *Bacillus cereus*.

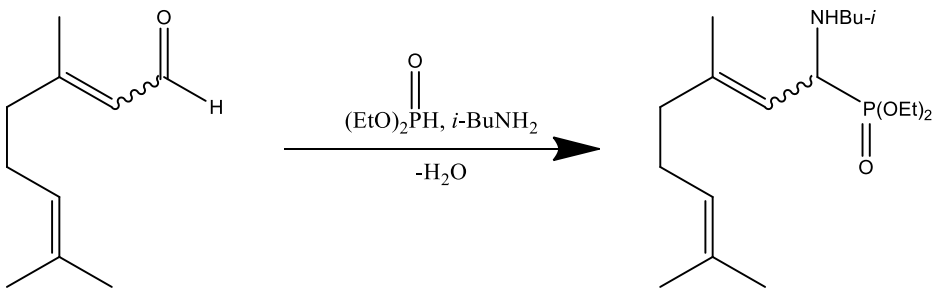

Scheme 18: The Kabachnik Fields reaction for the synthesis of O,O diethyl-(N-isobutylamino)-3,7-dimethylocta-2,6dienylphosphonates [Nizamov *et al.,* 2013]

Synthesis of novel α-APs by Badadhe *et al.,* (2011) was accomplished in two stages. Firstly, 1-phenyl-3-(pyridine-4-yl)-1Hpyrazole-4-carbaldehyde and different substituted anilines, in ethanol, with catalytic amounts of glacial acetic acid afforded the corresponding imine derivatives. This product was then treated with triethylphosphite in the presence of catalytic amounts of concentrated HCl, at room temperature, to produce α-APs [Badadhe *et al.,* 2011]. Selected compounds showed excellent antibacterial activity against both Gram-positive and Gram-negative bacterial strains

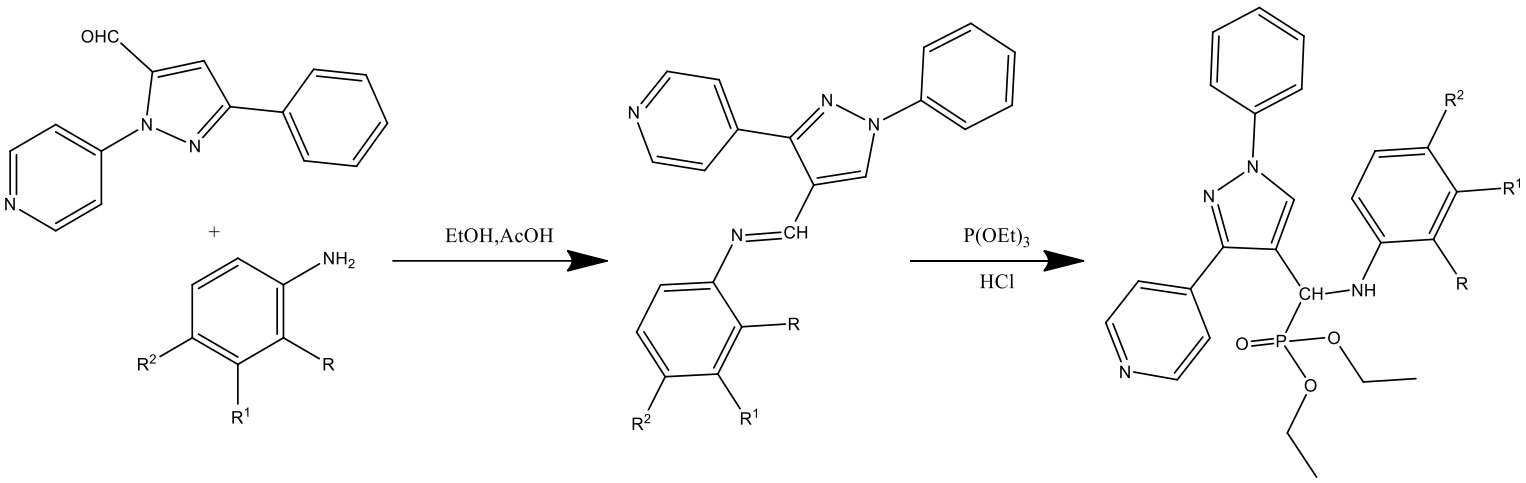

Scheme 19: The synthesis of thiazolidin-4-one and α-aminophosphonates derivatives [Badadhe *et al.,* 2011]

The synthesis of novel α-APs by the reaction of 4-amino-6-methyl-3-thioxo-2,3-dihydro[1,2,4]triazin5(4H)-one with various aromatic aldehydes and triethylphosphite by El-Barbary *et al.,* (2014) showed good activity against *Bacillus subtilis* [El-Barbary *et al.,* 2014].

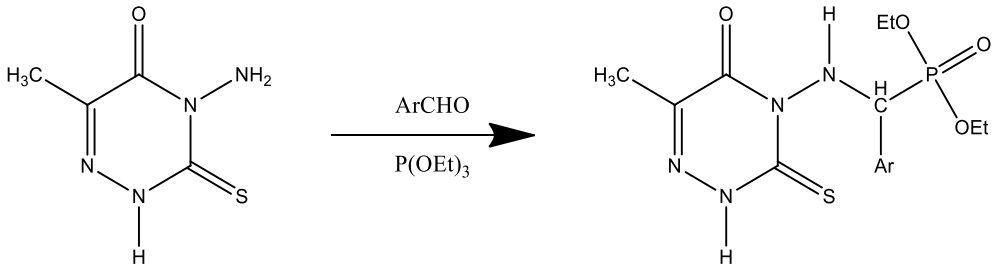

Scheme 20: The synthesis of α-aminophosphonate derivatives [El-Barbary *et al.,* 2014]

2.9.2.3. Antioxidant Activity

Oxygen is required for the essential biological process called ‘oxidation’ that produces natural antioxidants and highly reactive free radicals [Southorn Powis, 1988] within the body. These free radical molecules are important in the fight against infection causing pathogens but become problematic when their number supersedes that of natural antioxidants. Antioxidants introduced into the bodily system, generally orally from food sources or supplements, donate

electrons to neutralize these highly unstable free radicals forming a stable electron pair (Figure 18) before they attack cells causing disease and disorders. The antioxidant activity of a compound is owed to its ability to scavenge the stable free radical DPPH (2, 2 diphenyl-2-picryl hydrate) [Mossa Nawwar, 2011].

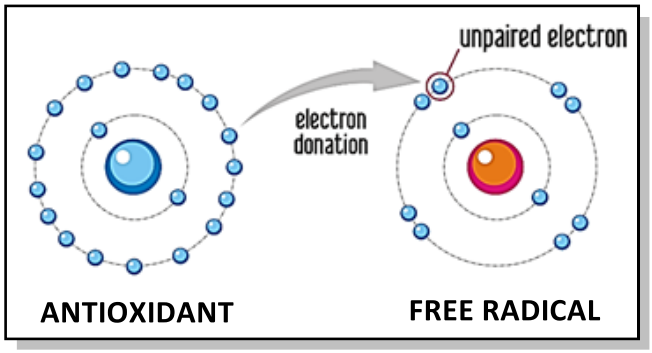

Figure 18: Antioxidant neutralizing an unstable free radical [Pham-Huy *et al.,* 2008]

A series of α-APs were synthesized by following a simple three component reaction of an amine, aldehyde and diethyl phosphite catalyzed by Amberlyst-15 [Reddy *et al.,* 2014]. Compounds 26, 27, 28 and 29 (Figure 19) demonstrated notable DPPH radical scavenging activity [Reddy *et al.,* 2014].

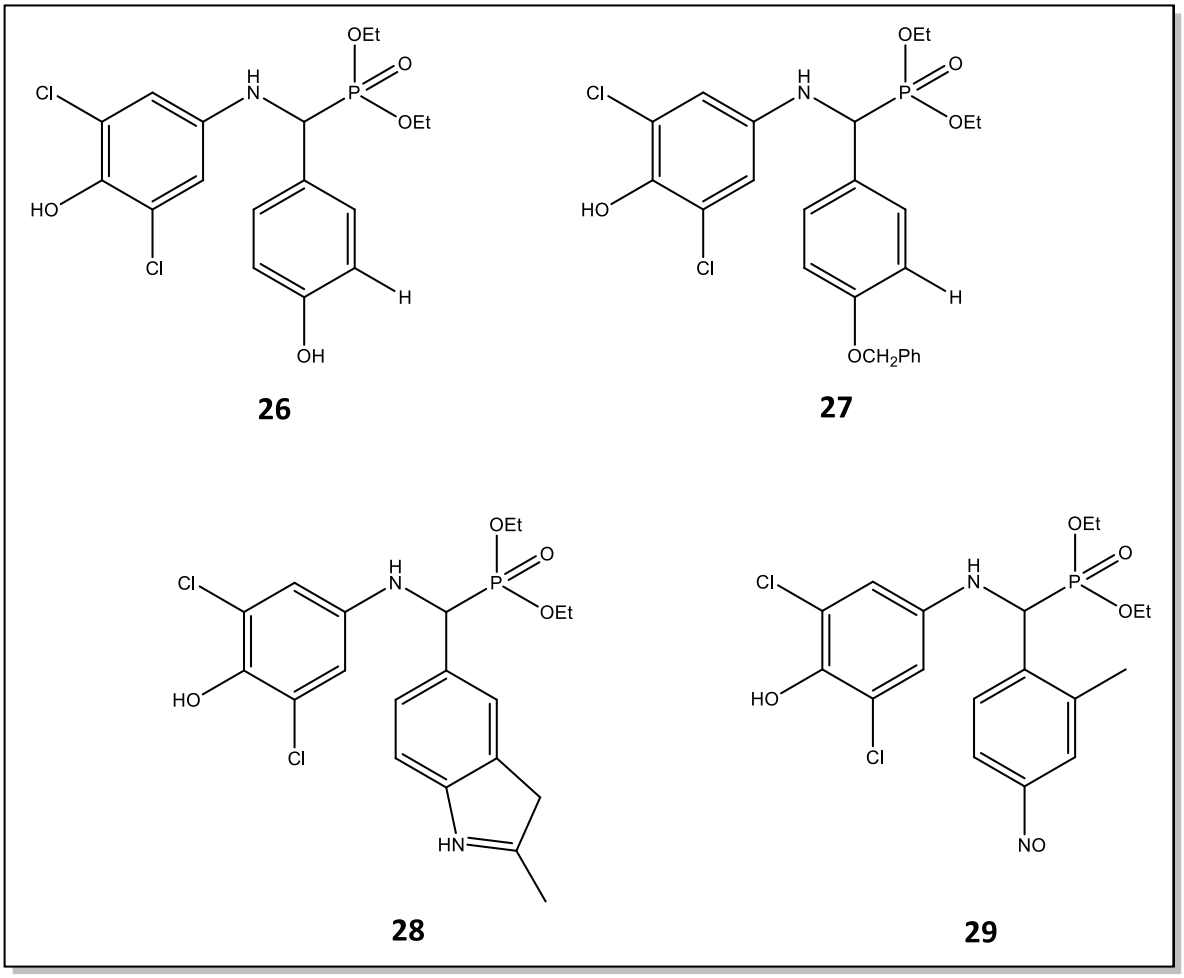

Figure 19: α-Aminophosphonates members that exhibit antioxidant activity [Reddy *et al.,* 2014]

The α-aminophosphonate antioxidant drugs and their reaction schemes are as follows:

The three component Kabachnik Fields reaction of 2-amino-6-methoxybenzothiazole, substituted aldehydes and diphenyl phosphite performed by Prasad Rao (2013) under microwave irradiation conditions produced active antimicrobial and antioxidant α-AP compounds [Prasad Rao, 2013].

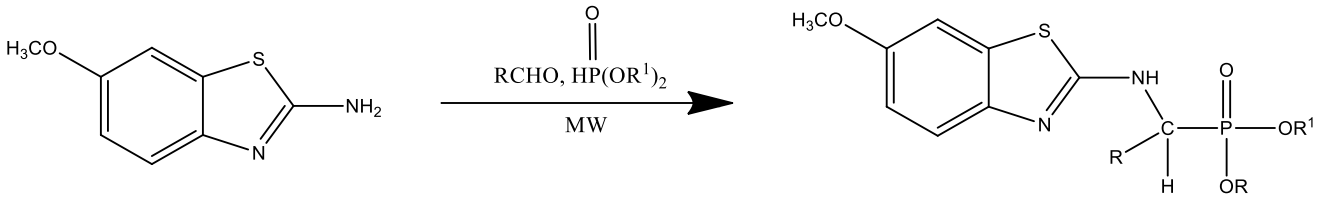

Scheme 21: The Kabachnik Fields reaction for the synthesis of α-aminophosphonate derivatives [Prasad Rao, 2013]

A new class of α-APs were synthesized from equimolar quantities of Schiff's bases with diphenyl phosphite and catalytic amounts of tetramethyl-guanidine (TMG) via the Pudovik reaction [Reddy *et al.,* 2011]. These compounds were found to be good antioxidants with more than 50% DPPH radical scavenging activity.

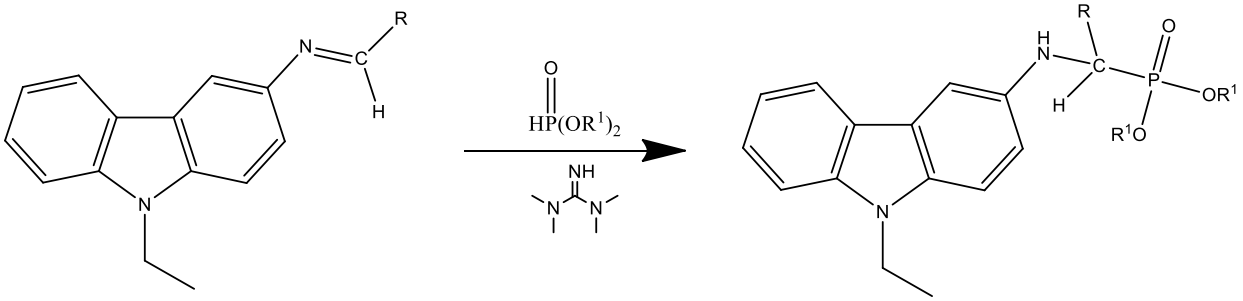

Scheme 22: The Pudovik reaction for the synthesis of α-aminophosphonate derivatives [Reddy *et al.,* 2011]

Selected tetraphenyl(phenylamino) bisphosphonate derivatives were synthesized by Balakrishna *et al.,* (2011) via a one pot reaction of an amine, triethyl orthoformate and diphenyl phosphite [Balakrishna *et al.,* 2011] showed high antioxidant activity with DPPH radical scavenging activities between 70-80%.

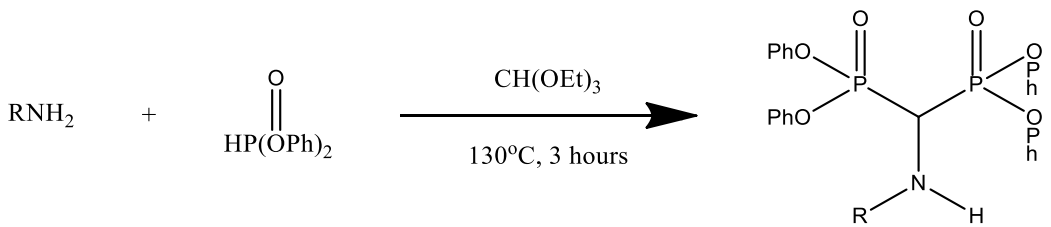

Scheme 23: The synthesis of tetraphenyl(phenylamino) bisphosphonate derivatives [Balakrishna *et al.,* 2011]

Chapter Three: Experimental

3.1. General

All chemicals were purchased from Merck and Sigma Aldrich. Both monitoring of progress of the reaction and product purity was accomplished by using TLC. The FTIR spectra were documented within the range of 4000-400 cm^{-1} using KBr pellets on a JASCO FT/IR-460 spectrophotometer. A Bruker D2 PHASER powder diffraction instrument, Cu Kα ray (wavelength λ = 0.154056 nm), was used to measure in a continuous step-scan mode. The minimum width of the stage 0.031°, equilibrium time of 256 seconds and the operating voltage to 30 kV with 10 mA was used. Characterization of the morphology was employed by scanning electron microscopy (SEM, Joel JSM 7600F). The Micromeritics Auto pore 9500 system was used for the BET gas sorption isotherms, measured at 77 K for N_2 and H_2, and 273 and 298 K for CO_2. The sample was dehydrated to begin with at 423 K for 24 hours under vacuum before gas sorption measurements were recorded.

The detector CCD (Triaxle) and the laser (He-Ne laser 632.8 nm) were used for the measurement of Raman Spectroscopy. All NMR spectra were recorded in a Bruker Avance 400 MHz instrument. Accurate (HRMS) was attained using a TOF-MS analyzer. A Buchi B-545 apparatus was used to record melting points (m.p) along with open capillary tubes.

3.2. Preparation of Palladium-doped Strontium Titanium Oxide (Pd-$SrTiO_3$) Catalyst

3.2.1. Preparation of Strontium Titanium Oxide

An accurate mass of Sr $(NO_3)_2$ (2.12 g) and citric acid (2.10 g) were dissolved in 40 mL of deionized H_2O. Thereafter, Titanium (IV) butoxide (TBT) (3.4 g), dissolved in 20 mL of ethanol, was added and the mixture stirred at 70 ˚C for 24 hours. This solid was washed with water and then air-dried to produce solid $SrTiO_3$.

3.2.2. Preparation of Palladium-doped Strontium Titanium Oxide

A total of 2.00 g of $SrTiO_3$ and 0.12 g of $PdCl_2$ were accurately weighed out then transferred to a beaker and heated on a water bath at 80 ˚C for 12 hours. Thereafter, the solid was transferred into a furnace set at 1000 ˚C for 2 hours. A 10 mL aliquot of ethanol was added to the cooled material, stirred and subsequently filtered. The solid was washed with acetone and water and then air-dried to produce Pd-$SrTiO_3$.

3.3. Synthesis of 2-(4-methylpiperazin-1-yl) quinoline-3-carbaldehyde

The starting material, 2-(4-methylpiperazin-1-yl) quinoline-3-carbaldehyde (1) was synthesized using 2-chloro-3-formyl quinoline (0.001 mol) and potassium carbonate (0.002 mol) followed by an excess amount 1-methylpiperazine. This mixture was then heated under reflux at 200˚C for 24 hours [Murugesan *et al.,* 2017].

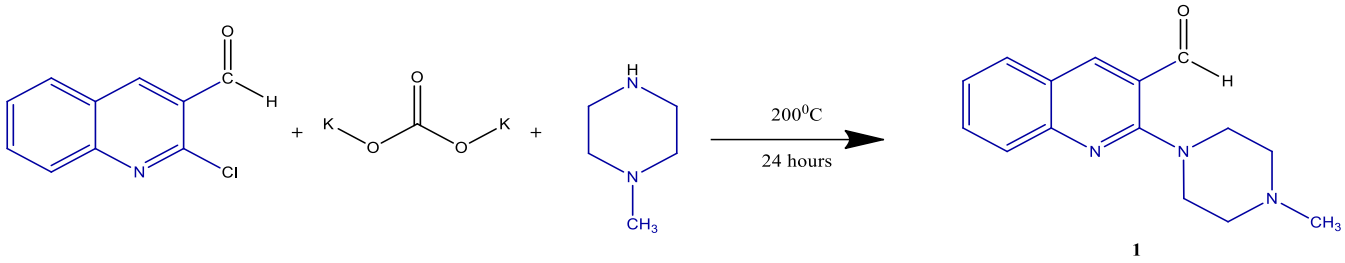

Scheme 24: The reaction scheme for the synthesis of 2-(4-methylpiperazin-1-yl) quinoline-3-carbaldehyde

3.4. Typical Procedure for the Synthesis of Quinoline Based α-Aminophosphonates (4a-4t)

In a 50 mL round bottom flask, a mixture containing 1 (1.0 mmol), diethyl phosphite (2) (1.0 mmol), aniline derivatives (3a-3t) (1.0 mmol) and Pd-$SrTiO_3$ (0.05 g), in THF (4 mL), was refluxed under microwave conditions at 140°C (Scheme 25). The progress of the reaction was monitored by TLC. Ethanol was added once the reaction reached completion. The crude product was cooled, filtered and purified by column chromatography using a silica gel and a mobile phase of acetone: hexane (80:20). The catalyst was recovered by washing with a dilute acid solution, distilled water and finally with acetone before being dried under vacuum and then reused.

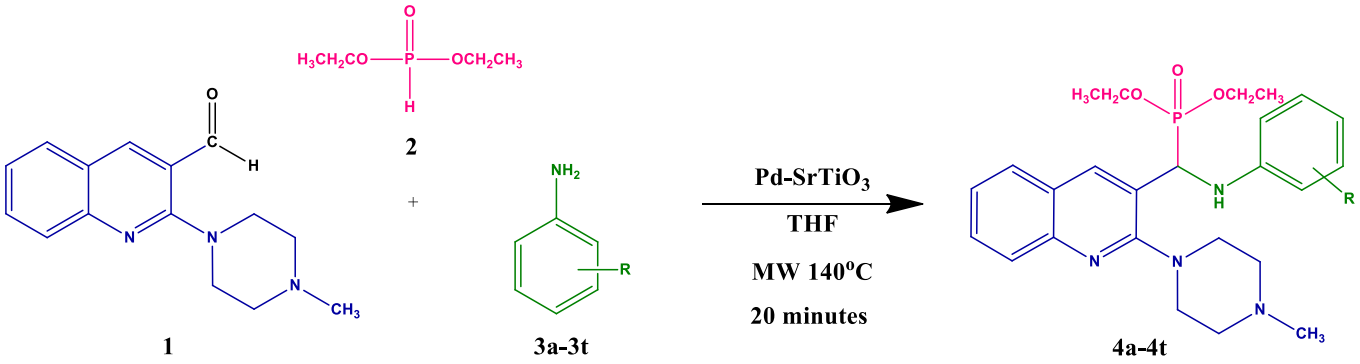

Scheme 25: The Kabachnik Fields reaction scheme for the synthesis of quinoline based α-aminophosphonates

3.5. The Spectroscopic Data (4a-4t)

4a:

diethyl ((2-(4-methylpiperazin-1-yl)quinolin-3-yl)(phenylamino)methyl)phosphonate

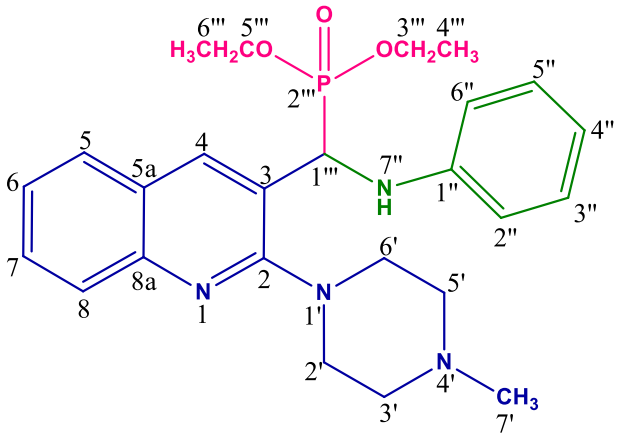

Yellow solid, 96 %, m.p. 133-135˚C, **IR (KBr):** 3320, 3058, 2940, 2842, 2789, 1588, 1426, 1368, 1285, 1243, 1137, 1010, 947, 742, 694, 576, 529 cm^{-1}. **TOFMS ES** *m/z* (rel. int.): 469.23 $[M]^+$. Anal Calculated for $C_{25}H_{33}N_4O_3P$: C, 64.09; H, 7.10; N, 11.96 %. Found: C, 64.11; H, 7.12; N, 11.98 %.

^{1}H-NMR ($CDCl_3$, 400 MHz): δ 8.74 (1H, s, N-H), 8.68 (1H, s, Ar-H), 8.44 (1H, d, *J* = 2.72 Hz, Ar-H), 7.88 (1H, d, *J* = 8.44 Hz, Ar-H), 7.82 (1H, d, *J* = 8 Hz, Ar-H), 7.64-7.68 (1H, m, Ar-H), 7.44-7.48 (1H, t, *J* = 7.48 Hz, Ar-H), 7.38-7.40 (1H, m, *J* = 2.52 Hz, Ar-H), 7.08-7.12 (1H, dd, *J* = 0.84 Hz, Ar-H), 6.81 (1H, d, *J* = 7.96 Hz, Ar-H), 6.66-6.70 (1H, dd, *J* = 2.5 Hz, Ar-H), 5.29-5.37 (1H, d, CH), 4.83-4.07 (1H, t, CH_2), 4.24-4.28 (1H, t, CH_2), 4.02-4.06 (1H, m, CH_2), 3.77-3.84 (1H, m, CH_2), 3.51-3.54 (4H, t, CH_2), 2.66-2.69 (4H, t, CH_2), 2.46 (3H, s, CH_3), 1.34-1.38 (3H, t, CH_3), 1.04-1.08 (3H, t, CH_3).

^{13}C-NMR ($CDCl_3$, 100 MHz): δ 160.63, 160.55, 159.84, 157.78, 148.11, 146.74, 145.84-145.97, 137.91, 129.36, 128.58, 127.60, 126.39, 124.64, 122.73, 121.02, 118.53, 113.80, 63.36-63.49, 54.94, 50.79, 50.05, 48.50, 46.10, 16.16-16.57.

^{31}P-NMR ($CDCl_3$, 400 MHz): δ 23.76.

4b:

diethyl((2-(4-methylpiperazin-1-yl)quinolin-3-yl)((2nitrophenyl)amino)methyl)phosphonate

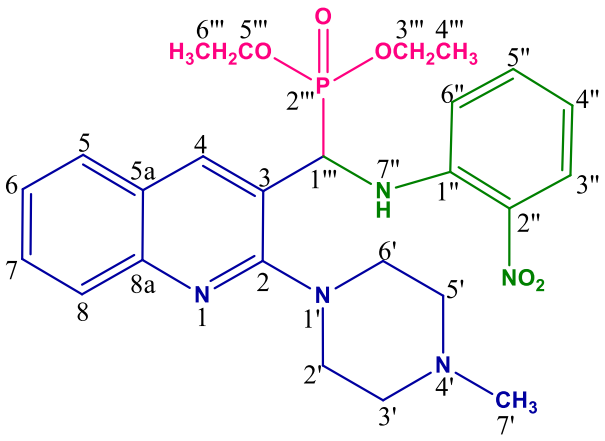

Yellow solid, 90 %, m.p. 114-116˚C, **IR (KBr):** 3471, 3378, 3190, 2982, 2839, 1736, 1625, 1503, 1427, 1343, 1239, 1014, 745 cm^{-1}. **TOFMS ES** *m/z* (rel. int.): 513.21 $[M]^+$. Anal Calculated for $C_{25}H_{22}N_5O_5P$: C, 58.47; H, 6.28; N, 13.64 %. Found: C, 58.49; H, 6.30; N, 13.66 %.

^{1}H-NMR ($CDCl_3$, 400 MHz): *δ* 8.38 (1H, s, Ar-H), 7.98-8.01 (1H, dd, *J* = 1.2 Hz, Ar-H), 7.73 (1H, d, *J* = 8.48 Hz, Ar-H), 7.70 (1H, d, *J* = 8.04 Hz, Ar-H), 7.60 (1H, t, *J* = 8.24 Hz, Ar-H), 7.27 (1H, t, *J* = 7.36 Hz, Ar-H), 6.70 (2H, t, *J* = 0.76 Hz, Ar-H), 6.56-6.59 (1H, dd, *J* = 0.88 Hz, Ar-H), 6.10 (1H, s, C-H), 5.3 (1H, d, *J* = 12.48 Hz, N-H), 4.12-4.15 (2H, m, CH_2), 3.89-4.01 (2H, m, CH_2), 3.44 (4H, t, CH_2), 2.56 (4H, t, CH_2), 2.28 (3H, s, CH_3), 1.25 (3H, t, CH_3), 1.11 (3H, t, CH_3).

^{13}C-NMR ($CDCl_3$, 100 MHz): *δ* 160.37, 160.30, 158.91, 149.30, 144.02, 142.50, 135.60, 132.51, 129.25, 127.52, 126.14, 124.66, 124.01, 122.06, 118.77, 116.80, 63.28, 63.21, 63.97, 63, 58.09, 54.88, 51.14, 50.85, 46.03, 29.68, 29.35, 16.59, 16.81, 16.41, 16.36.

^{31}P-NMR ($CDCl_3$, 400 MHz): *δ* 21.95.

4c:

diethyl((2-(4-methylpiperazin-1-yl)quinolin-3-yl)((3-nitrophenyl)amino)methyl)phosphonate

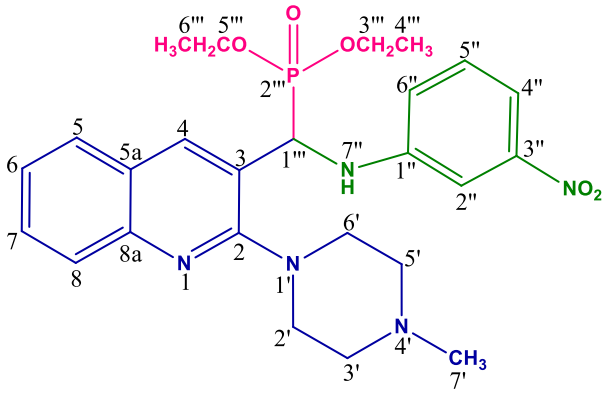

Yellow solid, 88 %, m.p. 125-127˚C, **IR (KBr):** 3406, 2937, 2844, 2794, 1549, 1521, 1420, 1349, 1139, 1008, 961, 733, 676 cm^{-1}. **TOFMS ES** *m/z* (rel. int.): 513.21 $[M]^+$. Anal Calculated for $C_{25}H_{32}N_5O_5P$: C, 58.47; H, 6.28; N, 13.64 %. Found: C, 58.48; H, 6.30; N, 13.67 %.

^{1}H-NMR ($CDCl_3$, 400 MHz): δ 8.75 (1H, s, N-H), 8.70 (1H, s, Ar-H), 8.13-8.15 (1H, dd, J = 1.64 Hz, Ar-H), 8.09 (1H, s, Ar-H), 7.90 (1H, d, J = 8.52 Hz, Ar-H), 7.84 (1H, d, J = 0.76 Hz, Ar-H), 7.67-7.71 (1H, m, Ar-H), 7.58-7.62 (1H, q, J = 1.56 Hz, Ar-H), 7.49 (1H, t, J = 2.28 Hz, Ar-H), 7.40-7.44 (1H, q, J = 0.8 Hz, Ar-H), 6.95 (1H, d, C-H), 4.02 (4H, s, CH_2), 3.51 (4H, t, CH_2), 2.68 (4H, t, CH_2), 2.40 (3H, s, CH_3), 1.37 (3H, t, CH_3), 1.23 (3H, t, CH_3).

^{13}C-NMR ($CDCl_3$, 100 MHz): δ 160.32, 160.05, 158.84, 149.25, 146.65, 146.63, 142.52, 138.74, 138.69, 132.48, 129.22, 127.85, 125.82, 124.63, 123.48, 122.02, 122.51, 110.87, 65.56, 63.18, 63.10, 63.07, 63, 54.80, 50.74, 45.96, 45.85, 34.46, 44.21, 30.32, 29.66, 16.55, 16.49, 16.39, 16.34.

^{31}P-NMR ($CDCl_3$, 400 MHz): δ 23.04.

4d:

diethyl(((2-fluorophenyl)amino)(2-(4-methylpiperazin-1-yl)quinolin-3-yl)methyl)phosphonate

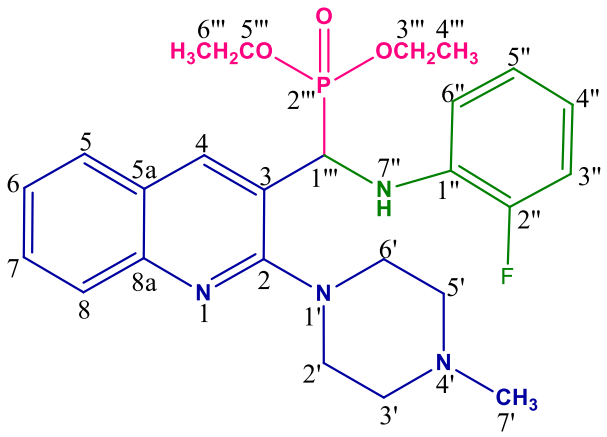

Yellow solid, 90 %, m.p. 149-151˚C, **IR (KBr):** 3055, 2934, 2849, 2788, 1691, 1588, 1495, 1419, 1372, 1241, 1144, 1008, 950, 745, 622 cm^{-1}. **TOFMS ES** *m/z* (rel. int.): 487.22 $[M]^+$. Anal Calculated for $C_{25}H_{32}FN_4O_3P$: C, 61.72; H, 6.63; N, 11.52 %. Found: C, 61.75; H, 6.62; N, 11.50 %.

^{1}H-NMR ($CDCl_3$, 400 MHz): *δ* 8.70 (1H, s, N-H), 8.61 (1H, s, Ar-H), 7.88 (1H, d, *J* = 8.44 Hz, Ar-H), 7.82 (1H, d, *J* = 7.96 Hz, Ar-H), 7.68-7.69 (1H, m, Ar-H), 7.42 (1H, t, *J* = 6.8 Hz, Ar-H), 7.36-7.38 (2H, dd, *J* = 8 Hz, Ar-H), 7.10-7.12 (2H, dd, *J* = 6 Hz, Ar-H), 6.51 (1H, s, C-H), 4.23-4.27 (2H, q, CH_2), 4.12 (1H, t, CH_2), 4.10 (1H, d, CH_2), 3.50 (4H, t, CH_2), 2.66 (4H, t, CH_2), 2.46 (3H, s, CH_3), 1.37 (3H, t, CH_3), 1.23 (3H, t, CH_3).

^{13}C-NMR ($CDCl_3$, 100 MHz): *δ* 160.37, 160.30, 158.91, 149.30, 146.67, 144.82, 142.50 138.53, 135.60, 132.51, 132.17, 129.80, 129.25, 127.99, 127.83, 127.59, 127.52, 126.14, 125.88, 125.30, 125.29, 124.66, 124.01, 122.06, 118.77, 116.80, 63.28, 63.21, 63.07, 63, 55.18, 55.09, 54.88, 53.94, 51.14, 50.85, 55.27, 46.04, 45.98, 29.68, 29.35, 16.57, 16.51, 16.41, 16.36.

^{31}P-NMR ($CDCl_3$, 400 MHz): *δ* 23.13, 21.76.

^{19}F-NMR ($CDCl_3$, 400 MHz): *δ* -127.26.

4e:

diethyl(((3-fluorophenyl)amino)(2-(4-methylpiperazin-1-yl)quinolin-3-yl)methyl)phosphonate

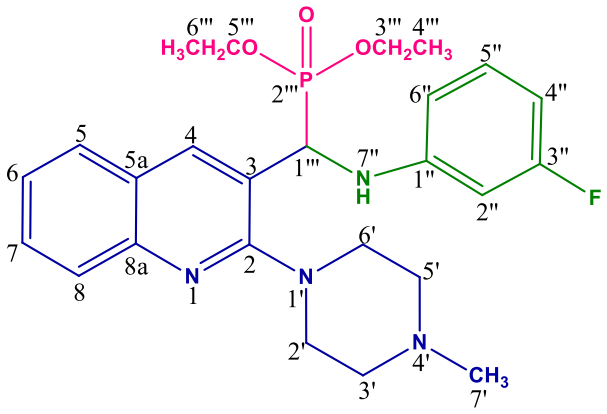

Yellow solid, 95 %, m.p. 128-130˚C, **IR (KBr):** 3458, 2974, 2947, 2844, 2797, 1737, 1579, 1419, 1373, 1230, 1138, 951, 877, 788, 755, 685, 624 cm^{-1}. **TOFMS ES** *m/z* (rel. int.): 487.22 $[M]^+$. Anal Calculated for $C_{25}H_{32}FN_4O_3P$: C, 61.72; H, 6.63; N, 11.52 %. Found: C, 61.74; H, 6.65; N, 11.55 %.

^{1}H-NMR ($CDCl_3$, 400 MHz): *δ* 8.72 (1H, s, N-H), 8.64 (1H, s, Ar-H), 7.88 (1H, d, *J* = 8.44 Hz, Ar-H), 7.81 (1H, d, *J* = 7.96 Hz, Ar-H), 7.62-7.64 (1H, m, Ar-H), 7.39 (2H, t, *J* = 7.64 Hz, Ar-H), 7.05 (1H, d, *J* = 7.48 Hz, Ar-H), 7 (2H, t, *J* = 9.44 Hz, Ar-H), 5.35 (1H, d, C-H), 4.23-4.27 (2H, q, CH_2), 4.03-4.08 (1H, q, CH_2), 3.78 (1H, t, CH_2), 3.50 (4H, t, CH_2), 2.68 (4H, t, CH_2), 2.40 (3H, s, CH_3), 1.42 (3H, t, CH_3), 1.24 (3H, t, CH_3).

^{13}C-NMR ($CDCl_3$, 100 MHz): *δ* 160.32, 160.25, 158.84, 149.25, 146.65, 146.63, 142.52, 138.74, 138.69, 132.48, 129.79, 129.22, 127.85, 127.64, 127.49, 125.82, 125.29, 124.63, 123.98, 122.02, 120.99, 112.37, 67.20, 65.56, 63.18, 63.10, 63.07, 63, 54.80, 50.74, 45.96, 45.85, 30.32, 29.66, 29.43, 16.55, 16.49, 16.39, 16.

^{31}P-NMR ($CDCl_3$, 400 MHz): *δ* 23.37, 21.87.

^{19}F-NMR ($CDCl_3$, 400 MHz): *δ* -112.13.

4f:

diethyl(((4-fluorophenyl)amino)(2-(4-methylpiperazin-1-yl)quinolin-3-yl)methyl)phosphonate

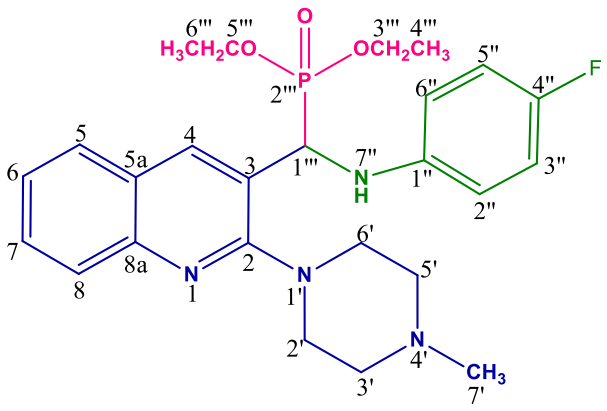

Yellow solid, 88 %, m.p. 127-129˚C, **IR (KBr):** 3378, 2975, 2853, 2394, 1748, 1643, 1504, 1428, 1210, 1129, 939, 810, 765 cm^{-1}. **TOFMS ES** *m/z* (rel. int.): 487.22 $[M]^+$. Anal Calculated for $C_{25}H_{32}FN_4O_3P$: C, 61.72; H, 6.63; N, 11.52 %. Found: C, 61.75; H, 6.65; N, 11.55 %.

^{1}H-NMR ($DMSOd_6$, 400 MHz): *δ* 8.19 (1H, s, Ar-H), 7.94 (1H, d, N-H), 7.76-7.78 (1H, t, *J* = 3.2 Hz, Ar-H), 7.46-7.52 (1H, t, *J* = 7.72 Hz, Ar-H), 7.40 (1H, d, *J* = 7.24 Hz, Ar-H), 7.25 (1H, d, *J* = 8.12 Hz, Ar-H), 7.08-7.11 (1H, t, *J* = 7.4 Hz, Ar-H), 6.80-6.89 (2H, dd, *J* = 8.56 Hz, Ar-H), 6.61 (1H, d, *J* = 4.4 Hz, Ar-H), 5.90 (1H, s, C-H), 5.01 (1H, d, CH_2), 3.76-3.80 (1H, m, CH_2), 3.40-3.44 (2H, t, CH_2), 3.29 (4H, d, CH_2), 2.84 (4H, d, CH_2), 2.61 (3H, s, CH_3), 1.13-1.17 (3H, t, CH_3), 1.02-1.06 (3H, m, CH_3).

^{13}C-NMR ($DMSOd_6$, 100 MHz): *δ* 161.77, 158.83, 158.76, 158.52, 155.71, 153.41, 145.15, 144.88, 144.22, 144.08, 137.87, 136.36, 135.47, 131.97, 129.61, 129.15, 127.38, 127.05, 125.42, 124.79, 123.20, 123.11, 121.79, 119.36, 114.84-115.23, 112.92-113.48, 62.03, 56, 52.43, 49.66, 48.44, 46.89, 42.99, 42.25, 28.92, 25.37, 18.45.

^{31}P-NMR ($DMSOd_6$, 400 MHz): *δ* 15.95.

^{19}F-NMR ($DMSOd_6$, 400 MHz): *δ* -129.13, -128.89.

4g:

diethyl(((4-chlorophenyl)amino)(2-(4-methylpiperazin-1-yl)quinolin-3-yl)methyl)phosphonate

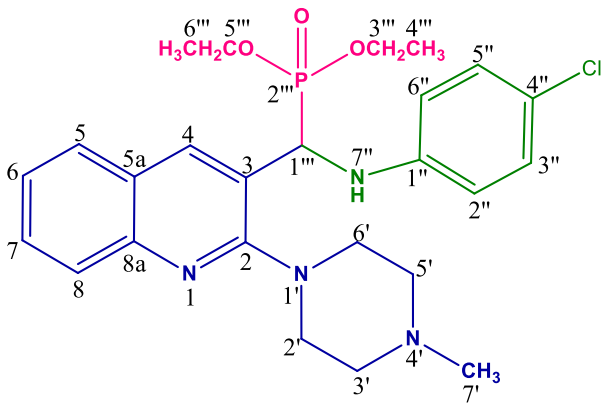

Yellow solid, 91 %, m.p. 181-183˚C, **IR (KBr):** 3059, 2933, 2984, 2849, 2792, 1736, 1597, 1424, 1373, 1220, 1148, 1018, 998, 949, 858, 736, 534 cm^{-1}. **TOFMS ES** *m/z* (rel. int.): 503.19 $[M]^+$. Anal Calculated for $C_{25}H_{32}ClN_4O_3P$: C, 59.70; H, 6.41; N, 11.14 %. Found: C, 59.72; H, 6.43; N, 11.16 %.

^{1}H-NMR ($CDCl_3$, 400 MHz): *δ* 8.72 (1H, s, N-H), 8.62 (1H, s, Ar-H), 7.87 (1H, d, *J* = 8.4 Hz, Ar-H), 7.82 (1H, d, *J* = 7.92 Hz, Ar-H), 7.74 (1H, t, *J* = 8.5 Hz, Ar-H), 7.65-7.69 (1H, m, Ar-H), 7.40-7.42 (2H, dd, *J* = 1.96 Hz, Ar-H), 7.19-7.21 (2H, dd, *J* = 1.92 Hz, Ar-H), 6.61 (1H, d, C-H), 4.22 (1H, t, CH_2), 3.95 (3H, t, CH_2), 3.62 (4H, s, CH_2), 2.87 (4H, d, CH_2), 2.59 (3H, d, CH_3), 1.20-1.36 (6H, m, CH_3).

^{13}C-NMR ($CDCl_3$, 100 MHz): *δ* 159.22, 157.85, 150.22, 148.03, 138.43, 132.78, 132.09, 131.06, 129.49, 129.18, 129.09, 129, 128,.60, 127.99, 127.65, 125.06, 124.96, 122.34, 122.31, 121.97, 116.21, 114.87, 63.07, 54.41, 54.17, 54.02, 49.85, 45.39, 29.69, 29.35, 16.52, 16.36.

^{31}P-NMR ($CDCl_3$, 400 MHz): *δ* 23.27.

4h:

diethyl(((3,4-dichlorophenyl)amino)(2-(4-methylpiperazin-1-yl)quinolin-3-yl)methyl) phosphonate

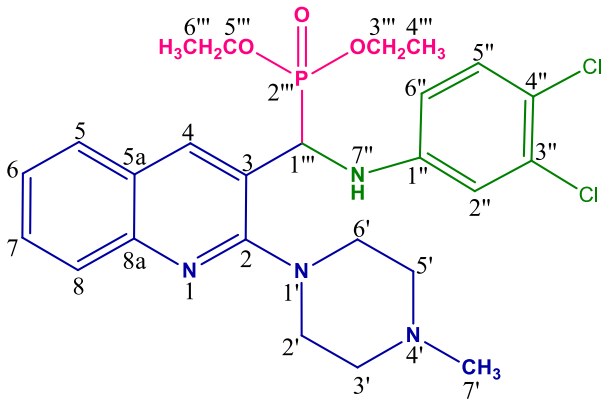

Yellow solid, 94 %, m.p. 188-190˚C, **IR (KBr):** 3421, 3067, 2984, 2941, 2843, 2800, 1598, 1417, 1373, 1240, 1134, 1003, 858, 734, 685, 594 cm^{-1}. **TOFMS ES** *m/z* (rel. int.): 536.15 $[M]^+$. Anal Calculated for $C_{25}H_{32}Cl_2N_4O_3P$: C, 55.87; H, 5.81; N, 10.43 %. Found: C, 55.89; H, 5.83; N, 10.45 %.

^{1}H-NMR ($CDCl_3$, 400 MHz): *δ* 8.70 (1H, s, N-H), 8.61 (1H, s, Ar-H), 7.88 (1H, d, *J* = 8.48 Hz, Ar-H), 7.82 (1H, d, *J* = 8.04 Hz, Ar-H), 7.65-7.69 (1H, m, Ar-H), 7.51 (1H, d, *J* = 8.52 Hz, Ar-H), 7.38-7.42 (1H, m, Ar-H), 7.16 (1H, d, *J* = 2.32 Hz, Ar-H), 7.12 (1H, d, *J* = 2.48 Hz, Ar-H), 7.10 (1H, d, *J* = 2.48 Hz, C-H), 4.23-4.27 (2H, q, CH_2), 4.10-4.14 (1H, q, CH_2), 3.98-4 (1H, q, CH_2), 3.49 (4H, t, CH_2), 2.66 (4H, t, CH_2), 2.40 (3H, s, CH_3), 1.37 (3H, t, CH_3), 1.23 (3H, t, CH_3).

^{13}C-NMR ($CDCl_3$, 100 MHz): *δ* 160.77, 160.69, 159.88, 151.90, 148.09, 146.39, 139.19, 137.39, 137.35, 130.72, 129.19, 128.57, 127.58, 127.17, 125.04, 124.61, 122.80, 122.04, 119.41, 117.79, 115.91, 114.20, 112.25, 111.27, 63.52, 63.46, 63.39, 55.42, 54.98, 51.17, 50.95, 50.54, 48.39, 46.15, 21.49, 16.59, 16.54, 16.23, 16.17.

^{31}P-NMR ($CDCl_3$, 400 MHz): *δ* 21.81.

4i:

diethyl(((4-bromophenyl)amino)(2-(4-methylpiperazin-1-yl)quinolin-3-yl)methyl)phosphonate

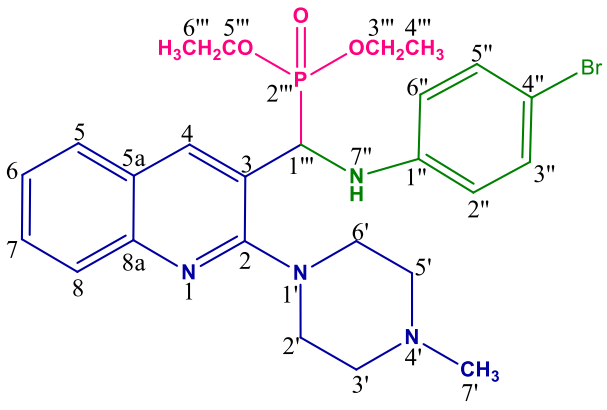

Yellow solid, 88 %, m.p. 194-196˚C, **IR (KBr):** 3411, 3055, 2973, 2941, 2843, 2796, 1596, 1482, 1423, 1372, 1242, 1148, 1064, 998, 948, 733, 539 cm^{-1}. **TOFMS ES** *m/z* (rel. int.): 546.14 $[M]^+$. Anal Calculated for $C_{25}H_{32}BrN_4O_3P$: C, 54.85; H, 5.89; N, 10.23 %. Found: C, 54.87; H, 5.91; N, 10.25 %.

^{1}H-NMR ($CDCl_3$, 400 MHz): *δ* 8.72 (1H, s, N-H), 8.62 (1H, s, Ar-H), 7.87 (1H, d, *J* = 8.4 Hz, Ar-H), 7.82 (1H, d, *J* = 7.92 Hz, Ar-H), 7.74 (1H, t, *J* = 8.8 Hz, Ar-H), 7.65-7.69 (1H, m, Ar-H), 7.40-7.42 (2H, dd, *J* = 2.16 Hz, Ar-H), 7.19-7.21 (2H, dd, *J* = 1.96 Hz, Ar-H), 6.61 (1H, d, *J* = 8.8 Hz, C-H), 4.22 (1H, t, CH_2), 4.07 (1H, t, CH_2), 3.95 (2H, t, CH_2), 3.62 (4H, s, CH_2), 2.87 (4H, d, CH_2), 2.53 (3H, s, CH_3), 1.34 (3H, t, CH_3), 1.21 (3H, t, CH_3).

^{13}C-NMR ($CDCl_3$, 100 MHz): *δ* 160.09, 160.01, 157.94, 156.74, 146.53, 145.17, 138.93, 138.87, 138.63, 137.32, 129.63, 129.49, 127.68, 127.49, 125.82, 125.79, 125.05, 125, 113.82, 112.08, 109.78, 108.87, 63.16, 63.07, 63.06, 59.62, 54.93, 54.52, 50.15, 45.30, 30.29, 16.35, 16.48, 16.43,16.36, 16.31.

^{31}P-NMR ($CDCl_3$, 400 MHz): *δ* 21.76.

4j:

diethyl ((2-(4-methylpiperazin-1-yl)quinolin-3-yl)(o-tolylamino)methyl)phosphonate

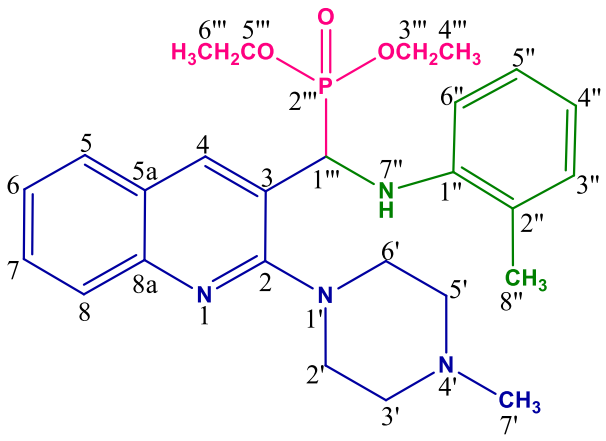

Yellow solid, 92 %, m.p. 140-142˚C, **IR (KBr):** 3415, 2975, 2928, 2863, 1735, 1606, 1513, 1457, 1420, 1364, 1045, 943, 743, 567 cm^{-1}. **TOFMS ES** *m/z* (rel. int.): 483.25 $[M]^+$. Anal Calculated for $C_{26}H_{35}N_4O_3P$: C, 64.71; H, 7.31; N, 11.61 %. Found: C, 64.73; H, 7.32; N, 11.63 %.

^{1}H-NMR ($CDCl_3$, 400 MHz): δ 8.34 (1H, s, Ar-H), 7.80 (1H, d, J = 8.44 Hz, Ar-H), 7.63 (1H, d, J = 8.04 Hz, Ar-H), 7.48 (1H, t, J = 7.72 Hz, Ar-H), 7.27 (1H, t, J = 7.32 Hz, Ar-H), 6.89 (2H, t, J = 7.32 Hz, Ar-H), 6.82 (1H, d, J = 7.11 Hz, Ar-H), 6.53 (1H, t, J = 7.44 Hz, Ar-H), 5.27 (1H, d, N-H), 4.65 (1H, t, C-H), 4.12-4.18 (2H, m, CH_2), 3.96 (1H, t, CH_2), 3.70-3.74 (1H, m, CH_2), 3.49 (2H, q, CH_2), 3.18 (2H, t, CH_2), 2.63 (4H, q, CH_2), 2.32 (3H, s, CH_3), 2.13 (3H, s, CH_3), 1.26 (3H, t, CH_3), 0.95 (3H, t, CH_3).

^{13}C-NMR ($CDCl_3$, 100 MHz): δ 160.69, 160.61, 146.81, 144.08, 143.95, 137.27, 137.22, 130.24, 129.57, 127.91, 127.54, 126.90, 125.07, 122.76, 118.29, 114.91, 111.49, 63.54, 63.49, 63.47, 63.43, 55.33, 51.07, 50.15, 48.61, 46.19, 29.71, 17.62, 16.60, 16.54, 16.24, 16.18.

^{31}P-NMR ($CDCl_3$, 400 MHz): δ 23.96.

4k:

diethyl ((2-(4-methylpiperazin-1-yl)quinolin-3-yl)(m-tolylamino)methyl)phosphonate

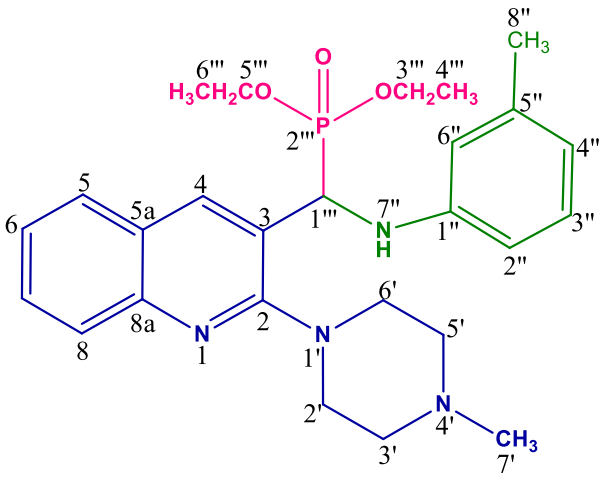

Yellow solid, 87 %, m.p. 137-139˚C, **IR (KBr):** 3365, 2943, 2834, 2786, 1735, 1593, 1423, 1369, 1219, 1148, 1043, 940, 764, 695 cm^{-1}. **TOFMS ES** *m/z* (rel. int.): 483.25 $[M]^+$. Anal Calculated for $C_{26}H_{35}N_4O_3P$: C, 64.71; H, 7.31; N, 11.61 %. Found: C, 64.73; H, 7.34; N, 11.63 %.

^{1}H-NMR ($CDCl_3$, 400 MHz): *δ* 8.73 (1H, s, N-H), 8.66 (1H, s, Ar-H), 8.45 (1H, d, *J* = 2.72 Hz, Ar-H), 7.90 (1H, d, *J* = 8.4 Hz, Ar-H), 7.80 (1H, d, *J* = 0.52 Hz, Ar-H), 7.64-7.66 (1H, dd, *J* = 1.32 Hz, Ar-H), 7.36 (1H, t, *J* = 7.88 Hz, Ar-H), 7.11 (1H, t, *J* = 3.64 Hz, Ar-H), 6.60 (1H, t, *J* = 7.52 Hz, Ar-H), 6.55 (1H, d, *J* = 8.08 Hz, Ar-H), 5.31-5.39 (1H, dd, *J* = 9.48 Hz, C-H), 4.86 (1H, t, CH_2), 4.24-4.29 (1H, q, CH_2), 4.03-4.07 (1H, q, CH_2), 3.78-3.83 (1H, q, CH_2), 3.51 (4H, t, CH_2), 2.66 (4H, t, CH_2), 2.27 (3H, s, CH_3), 2.22 (3H, s, CH_3), 1.37 (3H, t, CH_3), 1.06 (3H, t, CH_3).

^{13}C-NMR ($CDCl_3$, 100 MHz): *δ* 160.77, 160.69, 159.88, 151.58, 151.91, 148.09, 146.39, 139.19, 137.39, 137.35, 130.72, 129.19, 128.57, 127.58, 127.17, 125.04, 124.61, 122.80, 122.04, 119.41, 117.79, 115.91, 114.20, 112.25, 111.27, 63.52, 63.46, 63.39, 55.42, 54.98, 51.17, 50.95, 50.84, 48.39, 46.15, 21.49, 16.59, 16.54, 16.23, 16.17.

^{31}P-NMR ($CDCl_3$, 400 MHz): *δ* 23.86.

4l:

diethyl ((2-(4-methylpiperazin-1-yl)quinolin-3-yl)(p-tolylamino)methyl)phosphonate

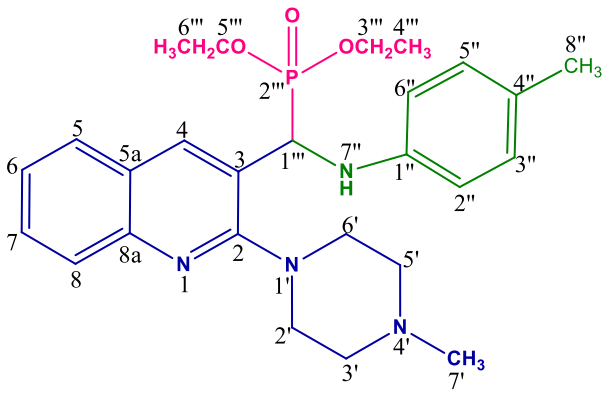

Yellow solid, 85 %, m.p. 150-152˚C, **IR (KBr):** 3393, 2973, 2917, 2850, 2805, 1743, 1691, 1592, 1425, 1373, 1218, 1148, 1015, 952, 789, 620 cm^{-1}. **TOFMS ES** *m/z* (rel. int.): 483.25 $[M]^+$. Anal Calculated for $C_{26}H_{35}N_4O_3P$: C, 64.71; H, 7.31; N, 11.61 %. Found: C, 64.73; H, 7.33; N, 11.63 %.

^{1}H-NMR ($CDCl_3$, 400 MHz): *δ* 8.38 (1H, d, *J* = 2.56 Hz, N-H), 8.35 (1H, s, Ar-H), 7.77 (1H, d, *J* = 8.36 Hz, Ar-H), 7.72 (1H, d, *J* = 8.44 Hz, Ar-H), 7.64 (2H, t, *J* = 8.6 Hz, Ar-H), 7.55-7.59 (1H, m, Ar-H), 7.50 (1H, t, *J* = 7.48 Hz, Ar-H), 7.26 (2H, dd, *J* = 0.76 Hz, Ar-H), 5.30 (1H, d, C-H), 4.08-4.12 (2H, q, CH_2), 3.94-3.99 (1H, q, CH_2), 3.86-3.91 (1H, q, CH_2), 3.41 (4H, t, CH_2), 2.53 (4H, t, CH_2), 2.21-2.24 (6H, s, CH_3), 1.22 (3H, s, CH_3), 1.07 (3H, t, CH_3).

^{13}C-NMR ($CDCl_3$, 100 MHz): *δ* 160.32, 160.24, 158.83, 149.24, 146.64, 146.62, 142.51, 138.74, 138.68, 132.47, 129.70, 127.84, 127.63, 127.49, 125.81, 125.19, 124.62, 123.97, 122.02, 120.99, 112.37, 67.19, 65.56, 63.17, 63.10, 63.06, 62.99, 54.79, 50.74, 45.95, 44.84, 30.31, 29.66, 29.43, 16.54, 16.49, 16.39, 16.33.

^{31}P-NMR ($CDCl_3$, 400 MHz): *δ* 22.16.

4m:

diethyl(((2,5-dimethylphenyl)amino)(2-(4-methylpiperazin-1-yl)quinolin-3-yl)methyl) phosphornate

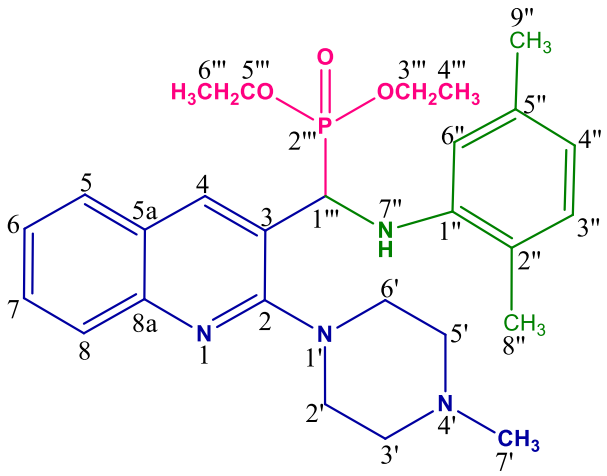

Yellow solid, 90 %, m.p. 147-149˚C, **IR (KBr):** 3320, 3058, 2940, 2842, 2789, 1588, 1426, 1368, 1285, 1243, 1137, 1010, 947, 742, 694, 576, 529 cm^{-1}. **TOFMS ES** *m/z* (rel. int.): 496.24 $[M]^+$. Anal Calculated for $C_{27}H_{37}N_4O_3P$: C, 65.30; H, 7.51; N, 11.28 %. Found: C, 65.32; H, 7.53; N, 11.30 %.

^{1}H-NMR ($CDCl_3$, 400 MHz): *δ* 8.64 (1H, s, N-H), 8.47 (1H, s, Ar-H), 8.33 (1H, d, *J* = 2.76 Hz, Ar-H), 7.78 (1H, d, *J* = 8.44 Hz, Ar-H), 7.72 (1H, d, *J* = 7.76 Hz, Ar-H), 7.48-7.54 (1H, m, Ar-H), 7.26-7.28 (1H, dd, *J* = 1.32 Hz, Ar-H), 6.98 (1H, t, *J* = 6.12 Hz, Ar-H), 6.71-6.78 (1H, m, Ar-H), 5.18-5.26 (1H, dd, *J* = 9.2 Hz, C-H), 4.53 (1H, t, Ar-H), 4.17 (1H, t, CH_2), 3.94-3.96 (1H, q, CH_2), 3.70-3.73 (1H, m, CH_2), 3.40 (1H, t, CH_2), 2.56 (1H, d, CH_2), 2.26 (3H, t, CH_2), 2.13 (3H, s, CH_2), 2.05 (3H, s, CH_3), 1.26 (3H, t, CH_3), 0.96 (3H, t, CH_3).

^{13}C-NMR ($CDCl_3$, 100 MHz): *δ* 160.66, 159.94, 156.34, 148.56, 148.02, 146.82, 146.80, 141.72, 141.59, 137.63, 137.21, 137.16, 135.76, 132.23, 131.31, 131.07, 130.55, 129.49, 128.53, 127.89, 127.60, 127.54, 127.48, 127.39, 127.13, 126.03, 125.12, 124.97, 124.55, 123.15, 122.89, 117.27, 111.74, 63.54, 63.48, 63.40, 63.33, 55.42, 55.04, 51.14, 50.85, 50.32, 48.77, 46.29, 46.18, 20.98, 20.26, 17.94, 17.58, 16.61, 16.56, 16.24, 16.18.

^{31}P-NMR ($CDCl_3$, 400 MHz): *δ* 24.03.

4n:

diethyl(((2-methoxyphenyl)amino)(2-(4-methylpiperazin-1-yl)quinolin-3-yl)methyl) phosphonate

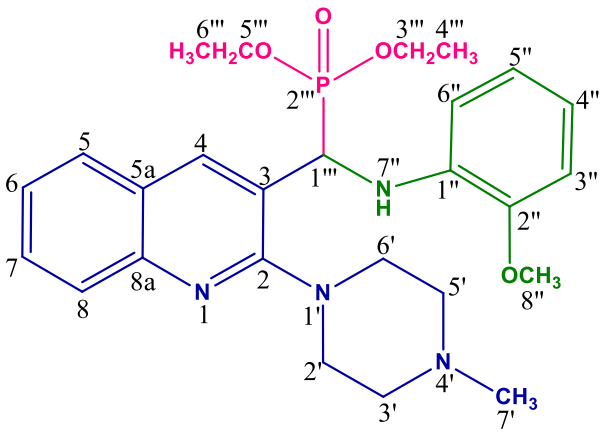

Yellow solid, 85 %, m.p. 130-132˚C, **IR (KBr):** 3420, 2928, 2833, 2788, 1735, 1583, 1494, 1429, 1373, 1230, 1139, 1026, 955, 740 cm^{-1}. **TOFMS ES** *m/z* (rel. int.): 521 $[M]^+$. Anal Calculated. for $C_{26}H_{35}N_4O_4P$: C, 62.64; H, 7.08; N, 11.24 %. Found: C, 62.66; H, 7.10; N, 11.26 %.

^{1}H-NMR ($CDCl_3$, 400 MHz): *δ* 8.76 (1H, s, N-H), 8.65 (1H, s, Ar-H), 7.85 (1H, d, *J* = 8.4 Hz, Ar-H), 7.76 (1H, d, *J* = 8 Hz, Ar-H), 7.57-7.61 (1H, q, *J* = 7.12 Hz, Ar-H), 7.32 (1H, t, *J* = 7.48 Hz, Ar-H), 7.05 (1H, t, *J* = 1.52 Hz, Ar-H), 7.01 (1H, d, *J* = 7.48 Hz, Ar-H), 6.96 (1H, d, *J* = 8.96 Hz, Ar-H), 6.67-6.75 (1H, m, *J* = 1.68 Hz, Ar-H), 5.22 (1H, s, C-H), 4.22-4.26 (2H, q, CH_2), 4.04-4.06 (2H, q, CH_2), 3.87 (3H, s, OCH_3), 3.78 (3H, s, CH_3), 3.50 (4H, s, CH_2), 2..59 (4H, s, CH_2), 1.31-1.42 (3H, s, CH_3), 1.06-1.26 (3H, t, CH_3).

^{13}C-NMR ($CDCl_3$, 100 MHz): *δ* 160.83, 160.75, 159.85, 158.93, 152.31, 149.30, 148.07, 147.27, 142.39, 141.57, 138.01, 136.22, 132.45, 130.63, 129.25, 128.59, 127.54, 126.93, 125.01, 124.51, 122.92, 121.13, 121.07, 121.69. 118.37, 114.97, 111.66, 110.41, 63.47, 63.40, 63.30, 63.23, 55.85, 55.02, 50.80, 46.15, 29.71, 16.58, 16.52, 16.26, 16.21.

^{31}P-NMR ($CDCl_3$, 400 MHz): *δ* 23.75.

4o:

diethyl(((4-methoxyphenyl)amino)(2-(4-methylpiperazin-1-yl)quinolin-3-yl)methyl) phosphonate

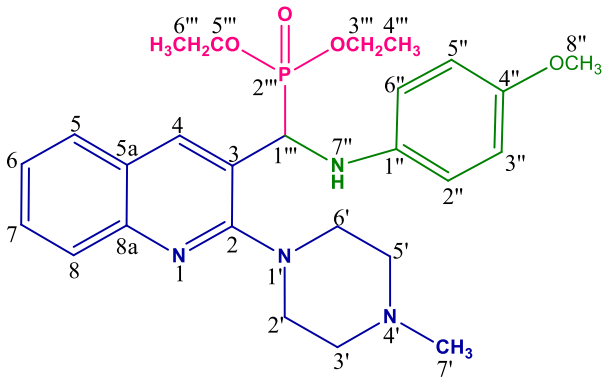

Yellow solid, 89 %, m.p. 119-121˚C, **IR (KBr):** 3441, 2926, 2843, 2785, 1745, 1594, 1502, 1420, 1372, 1231, 1148, 1042, 735 cm^{-1}. **TOFMS ES** *m/z* (rel. int.): 521 $[M]^+$. Anal Calculated for $C_{26}H_{35}N_4O_4P$: C, 62.64; H, 7.08; N, 11.24 %. Found: C, 62.66; H, 7.09; N, 11.26 %.

^{1}H-NMR ($CDCl_3$, 400 MHz): *δ* 8.70 (1H, s, N-H), 8.67 (1H, s, Ar-H), 7.87 (1H, d, *J* = 8.48 Hz, Ar-H), 7.78 (1H, d, *J* = 0.68 Hz, Ar-H), 7.61-7.65 (1H, m, Ar-H), 7.35-7.39 (1H, m, Ar-H), 7.29-7.31 (2H, dd, *J* = 2.16 Hz, Ar-H), 6.97-6.99 (2H, dd, *J* = 2.04 Hz, Ar-H), 5.28 (1H, t, C-H), 4.58 (1H, t, CH_2), 4.24-4.26 (2H, q, CH_2), 4.01-4.06 (1H, m, CH_2), 3.85 (3H, s, OCH_3), 3.67 (3H, s, CH_3), 3.49 (4H, t, CH_2), 2.65 (4H, t, CH_2), 1.36 (3H, t, CH_3), 1.06 (3H, t, CH_3).

^{13}C-NMR ($CDCl_3$, 100 MHz): *δ* 160.66, 159.94, 156.84, 148.56, 148.02, 146.82, 146.80, 141.72, 141.59, 137.63, 137.20, 137.18, 135.75, 132.22, 131.66, 130.55, 129.48, 128.53, 127.89, 127.61, 127.54, 127.49, 127.40, 127.14, 126.04, 125.12, 124.97, 124.56, 123.15, 122.89, 117.27, 111.75, 63.55, 63.48, 63.33, 55.42, 55.05, 51.14, 50.86, 50.32, 48.78, 46.30, 46.19, 20.29, 20.26, 17.94, 17.58, 16.61, 16.56.

^{31}P-NMR ($CDCl_3$, 400 MHz): *δ* 23.91.

4p: diethyl((2-(4-methylpiperazin-1-yl)quinolin-3-yl)(pyridin-2-ylamino)methyl) phosphonate

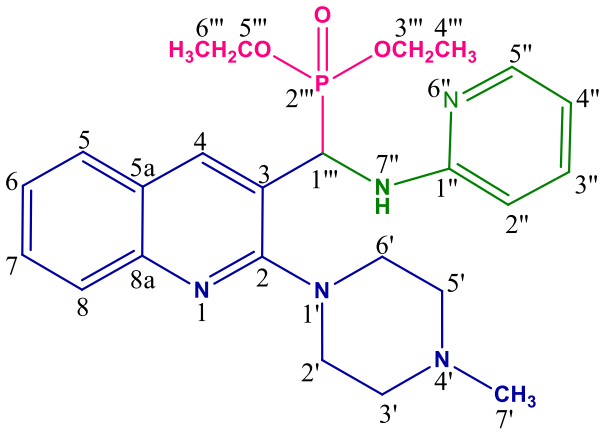

Yellow solid, 87 %, m.p. 145-147˚C, **IR (KBr):** 3397, 2984, 2937, 2857, 2784, 1748, 1588, 1495, 1424, 1373, 1240, 1190, 1045, 1008, 949, 755, 623 cm^{-1}. **TOFMS ES** *m/z* (rel. int.): 470.23 $[M]^+$. Anal Calculated for $C_{24}H_{32}N_5O_3P$: C, 61.39; H, 6.87; N, 14.92 %. Found: C, 61.41; H, 6.89; N, 14.95 %.

^{1}H-NMR ($CDCl_3$, 400 MHz): δ 8.43 (1H, s, Ar-H), 7.75-7.79 (2H, t, *J* = 6.36 Hz, Ar-H), 7.60 (1H, d, *J* = 7.96 Hz, Ar-H), 7.48 (1H, d, *J* = 7.48 Hz, Ar-H), 7.24-7.28 (2H, q, *J* = 0.92 Hz, Ar-H), 6.40-6.44 (2H, t, *J* = 3.76 Hz, Ar-H), 6.11 (1H, d, *J* = 7.88 Hz, N-H), 5.33 (1H, d, *J* = 12.44 Hz, C-H), 4-4.12 (1H, m, CH_2), 3.98 (1H, d, CH_2), 3.91 (1H, t, CH_2), 3.77-3.81 (1H, q, CH_2), 3.54-3.57 (1H, q, CH_2), 3.37 (1H, t, CH_2), 3.23 (4H, t, CH_2), 2.59 (4H, t, CH_2), 2.26 (3H, s, CH_3), 1.18-1.21 (3H, t, CH_3), 1.06-1.09 (3H, t, CH_3).

^{13}C-NMR ($CDCl_3$, 100 MHz): δ 160.55-160.61, 160.01-160.09, 157.94, 156.73, 146.52, 145.17, 138.92, 138.87, 138.63, 137.32, 129.65, 129.48, 127.68, 127.49, 125.81, 125.79, 125.05, 125, 113.82, 112.98, 109.77, 108.87, 63.06-63.08, 63.13, 63.16, 59.62, 59.58, 54.93, 5.51, 50.15, 45.30, 30.29, 16.54, 16.48, 16.42, 16.36, 16.30.

^{31}P-NMR ($CDCl_3$, 400 MHz): δ 23.49, 22.45.

4q:

diethyl((2-(4-methylpiperazin-1-yl)quinolin-3-yl)((4-methylpyridin-2-yl)amino)methyl) phosphonate

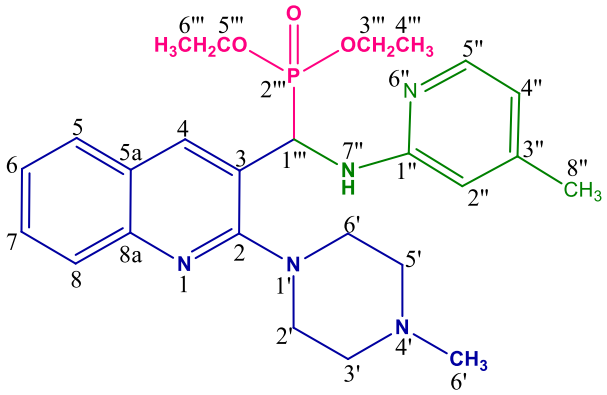

Yellow solid, 90 %, m.p. 144-146˚C, **IR (KBr):** 3288, 2956, 2915, 2842, 2806, 1746, 1615, 1485, 1424, 1367, 1232, 1017, 948, 742, 596, 528 cm^{-1}. **TOFMS ES** *m/z* (rel. int.): 484.24 $[M]^+$. Anal Calculated. for $C_{25}H_{34}N_5O_3P$: C, 62.10; H, 7.09; N, 14.48 %. Found: C, 62.12; H, 7.11; N, 14.46 %.

^{1}H-NMR ($CDCl_3$, 400 MHz): *δ* 8.29 (1H, d, *J* = 2.84 Hz, Ar-H), 7.80 (2H, t, *J* = 4.8 Hz, Ar-H), 7.62 (1H, d, *J* = 7.96 Hz, Ar-H), 7.52 (1H, t, *J* = 7.4 Hz, Ar-H), 7.27-7.31 (1H, q, *J* = 7.24 Hz, Ar-H), 6.37 (1H, s, Ar-H), 6.34 (1H, d, *J* = 5.24 Hz, Ar-H), 5.87 (1H, q, *J* = 9.28 Hz, N-H), 5.50 (1H, t, *J* = 8.6 Hz, C-H), 4.04-4.16 (2H, m, CH_2), 3.83-3.89 (1H, m, CH_2), 3.59-3.65 (1H, m, CH_2), 3.18-3.52 (4H, m, CH_2), 2.49-2.74 (4H, m, CH_2), 2.38 (3H, s, CH_3), 2.11 (3H, s, CH_3), 1.20-1.23 (3H, t, CH_3), 0.93-0.96 (3H, t, CH_3).

^{13}C-NMR ($CDCl_3$, 100 MHz): *δ* 160.78, 160.71, 157.05, 156.95, 148.51, 147.47, 146.63, 146.62, 137.18, 137.13, 129.43, 127.81, 127.50, 126.35, 125.90, 124.94, 115.66, 108.45, 63.29, 63.22, 63.17, 63.10, 55.24, 55.08, 50.50, 48.15, 46.63, 45.99, 30.32, 29.68, 21.10, 16.47, 16.41, 16.21, 16.15.

^{31}P-NMR ($CDCl_3$, 400 MHz): *δ* 23.43, 21.88.

4r:

diethyl((2-(4-methylpiperazin-1-yl)quinolin-3-yl)(naphthalen-1-ylamino)methyl) phosphonate

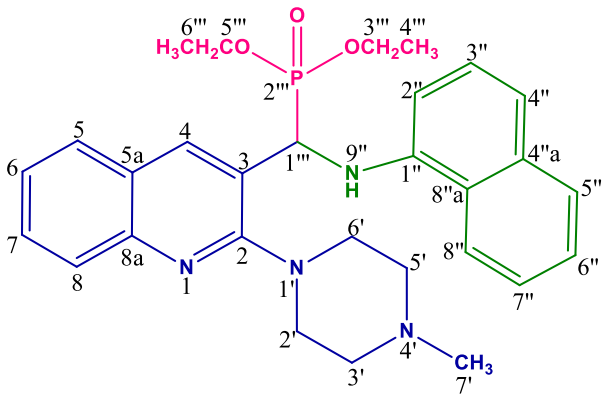

Yellow solid, 91 %, m.p. 131-133˚C, **IR (KBr):** 3457, 3356, 3227, 3046, 2975, 2785, 1748, 1593, 1415, 1369, 1285, 1218, 1142, 1007, 955, 782, 574 cm^{-1}. **TOFMS ES** *m/z* (rel. int.): 519.25 $[M]^+$. Anal Calculated. for $C_{29}H_{35}N_4O_3P$: C, 67.17; H, 6.80; N, 10.80 %. Found: C, 67.19; H, 6.83; N, 10.81 %.

^{1}H-NMR ($CDCl_3$, 400 MHz): *δ* 8.94 (1H, s, N-H), 8.77 (1H, s, Ar-H), 8.47 (1H, t, *J* = 3.32 Hz, Ar-H), 7.88-7.94 (2H, m, *J* = 3.84 Hz, Ar-H), 7.78-7.84 (1H, m, *J* = 4.12 Hz, Ar-H), 7.67-7.72 (1H, m, *J* = 1.24 Hz, Ar-H), 7.57-7.60 (1H, q, *J* = 2.52 Hz, Ar-H), 7.54 (1H, t, *J* = 7.4 Hz, Ar-H), 7.47 (1H, t, *J* = 4.36 Hz, Ar-H), 7.42 (1H, t, *J* = 0.8 Hz, Ar-H), 7.32 (1H, t, *J* = 3.24 Hz, Ar-H), 7.08 (1H, t, *J* = 0.6 Hz Ar-H), 6.80 (1H, d, *J* = 1.6 Hz Ar-H), 4.11-4.17 (4H, m, CH_2), 3.58 (4H, t, CH_2), 2.68 (4H, t, CH_2), 2.39 (1H, s, CH_3), 1.24-1.30 (6H, m, CH_3).

^{13}C-NMR ($CDCl_3$, 100 MHz): *δ* 160.37, 160.30, 158.91, 149.30, 144.02, 142.50, 135.60, 132.51, 129.25, 127.52, 126.14, 124.66, 124.01, 122.06, 118.77, 116.80, 63.28, 63.21, 63.97, 63, 58.09, 54.88, 51.14, 50.85, 46.03, 29.68, 29.35, 16.59, 16.81, 16.41, 16.36.

^{31}P-NMR ($CDCl_3$, 400 MHz): *δ* 23.80.

4s:

diethyl(((9-ethyl-9H-carbazol-3-yl)amino)(2-(4-methylpiperazin-1-yl)quinolin-3yl)methyl) phosphonate

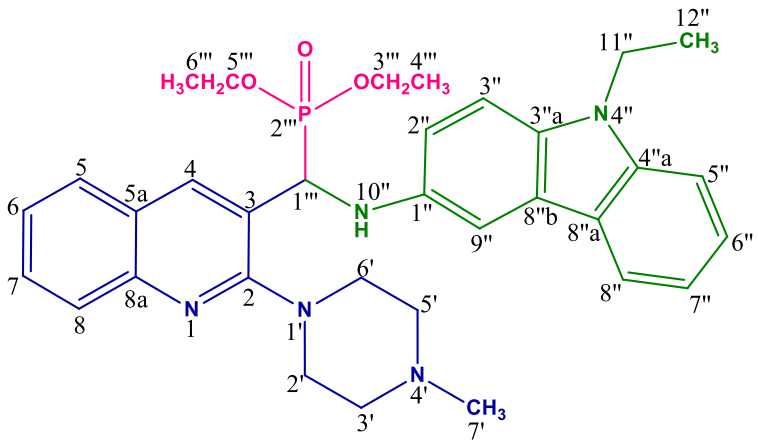

Yellow solid, 93 %, m.p. 109-111˚C, **IR (KBr):** 3320, 2975, 2917, 2853, 2786, 1738, 1598, 1456, 1364, 1232, 1045, 745, 548 cm^{-1}. **TOFMS ES** *m/z* (rel. int.): 608.27 $[M]^+$. Anal Calculated for $C_{33}H_{40}N_5O_3P$: C, 67.67; H, 6.88; N, 11.96 %. Found: C, 67.69; H, 6.70; N, 11.98 %.

^{1}H-NMR ($CDCl_3$, 400 MHz): *δ* 8.86 (1H, s, Ar-H), 8.80 (1H, s, Ar-H), 8.74 (1H, d, *J* = 2.72 Hz N-H), 8.11-8.17 (1H, dd, *J* = 1.88 Hz, Ar-H), 8.02 (1H, d, *J* = 7.72 Hz, Ar-H), 7.90-7.95 (1H, dd, *J* = 3.96 Hz, Ar-H), 7.87 (1H, t, *J* = 7.2 Hz, Ar-H), 7.74 (1H, d, *J* = 7.64 Hz, Ar-H), 7.55 (1H, t, *J* = 1.92 Hz, Ar-H), 7.36-7.49 (2H, m, *J* = 2.64 Hz, Ar-H), 7.17 (1H, t, *J* = 7.28 Hz, Ar-H), 6.99-7.02 (1H, dd, *J* = 2.16 Hz, Ar-H), 6.91-6.94 (1H, dd, *J* = 2.32 Hz, C-H), 4.40 (1H, q, CH_2), 4.23-4.30 (1H, m, CH_2), 4.14-4.17 (1H, m, CH_2), 3.84 (1H, t, CH_2), 3.58 (4H, t, CH_2), 2.72 (4H, t, CH_2), 2.41 (3H, s, CH_3), 1.40-1.50 (2H, m, CH_2), 1.38 (3H, m, CH_3), 1.29 (3H, t, CH_3), 1.10 (3H, t, CH_3).

^{13}C-NMR ($CDCl_3$, 100 MHz): *δ* 160.88, 160.80, 159.88, 155.12, 147.91, 143.73, 140.61, 139.05, 137.37, 134.54, 134.47, 130.48, 129.47, 128.53, 127.58, 126.09, 125.44, 124.98, 124.58, 122.46, 120.58, 120.40, 119.76, 119.07, 118.01, 115.57, 115.13, 113.07, 108.99, 108.35, 106.36, 104.65, 63.60, 63.53, 63.35, 63.28, 55.36, 54.97, 50.71, 46.15, 46.07, 37.76, 37.51, 37.44, 29.72, 22.72, 16.63, 16.57, 16.28, 16.22, 13.89, 13.82.

^{31}P-NMR ($CDCl_3$, 400 MHz): *δ* 24.16.

4t:

diethyl((2-(2-bromoacetamido)benzamido)(2-(4-methylpiperazin-1-yl)quinolin-3-yl) methyl)phosphonate

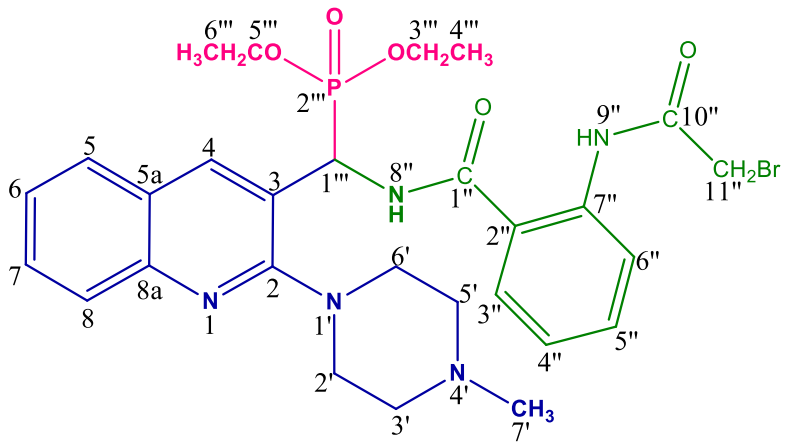

Yellow solid, 90 %, m.p. 120-122˚C, **IR (KBr):** 3404, 3196, 3028, 2944, 2842, 1736, 1677, 1594, 1523, 1364, 1220, 1026, 895, 765 cm^{-1}. **TOFMS ES** *m/z* (rel. int.): 570.20 $[M]^+$. Anal Calculated for $C_{28}H_{35}BrN_5O_5P$: C, 53.17; H, 5.58; N, 11.07 %. Found: C, 53.19; H, 5.60; N, 11.10 %.

^{1}H-NMR ($CDCl_3$, 400 MHz): *δ* 11.97 (1H, s, N-H), 10.08 (1H, s, N-H), 8.52 (1H, d, *J* = 8.44 Hz, Ar-H), 8.42 (1H, s, Ar-H), 7.74 (2H, t, *J* = 8.6 Hz, Ar-H), 7.61-7.65 (1H, q, *J* = 1.4 Hz, Ar-H), 7.52-7.54 (1H, dd, *J* = 0.96 Hz, Ar-H), 7.41 (1H, t, *J* = 7.28 Hz, Ar-H), 7.29-7.33 (1H, q, *J* = 0.8 Hz, Ar-H), 7.02-7.06 (1H, q, *J* = 0.68 Hz, Ar-H), 4.94 (1H, d, C-H), 4.08 (4H, s, CH_2), 3.51 (4H, t, CH_2), 2.69 (4H, t, CH_2), 1.35 (3H, s, CH_3), 1.14-1.25 (6H, q, CH_3), 0.82 (2H, t, CH_2).

^{13}C-NMR ($CDCl_3$, 100 MHz): *δ* 190.14, 176.93, 165.23, 149.23, 143.83, 139.14, 133.20, 132.76, 129.20, 127.61, 124.90, 124.09, 123.61, 121.96, 121.43, 119.40, 54.50, 49.86, 45.40, 43.28, 30.32, 29.69, 29.36, 14.12.

^{31}P-NMR ($CDCl_3$, 400 MHz): *δ* 21.75.

3.6. Biological Screening

An overview of the biological assays involved in this study is shown in Figure 20 below:

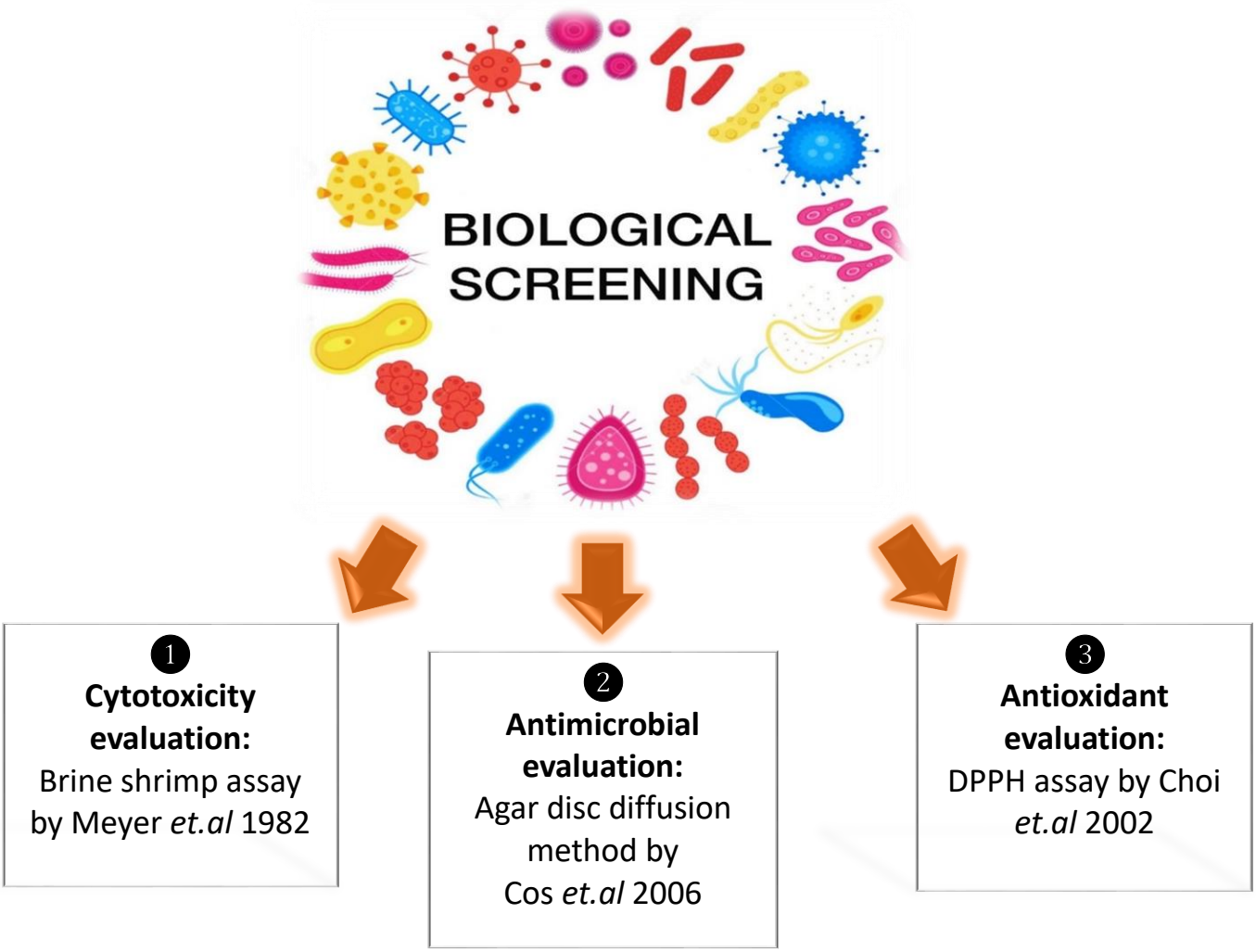

Figure 20: Schematic diagram of biological assays engaged in this study.

3.6.1. Cytotoxicity Activity of MPQ-α-APs (4a-4t)

3.6.1.1. Preparation of Artificial Seawater

An amount of 33 g of sea salt was dissolved in 1 L of water. The seawater was adjusted to a pH of 8.5 using a 1 N solution of NaOH.

3.6.1.2. Preparation of Brine Shrimp

The artificial seawater was transferred into a 1 L conical-shaped flask in which the Brine Shrimp eggs were allowed to hatch. This occurred under constant aeration for 48 hours, allowing adequate time for all the active nauplii to become free from their eggshells. The active nauplii were then collected from the brighter portion of the hatching chamber and used in the bioassay.

The Brine Shrimp toxicity test was carried out using the Brine Shrimp (*Artemia salina*) bioassay [Meyer *et al.,* 1982]. The procedure used a 6-well plate, where ten shrimps were drawn in through a glass capillary and placed in each well containing 4.95 mL of artificial seawater. Compounds **4d**, **4e**, **4f**, **4m**, **4q**, **4r** and **4s** were dissolved in 50 µL of DMSO and diluted to final concentrations of 10, 100 and 500 µg/mL. The Brine solution-containing wells were treated with the compound solution. The plate was retained under visible light at 37 ˚C for 24 hours. The number of dead Brine Shrimp was recorded and the percentage of death was determined.

The mortality endpoint of this bioassay was defined as the absence of controlled forward motion of the nauplii during a 30-second observation. The percent lethality of the nauplii was calculated using the formula below:

$$\%Death = \left[\frac{Number\ of\ dead\ nauplii}{(Number\ of\ dead\ nauplii + \ Number\ of\ live\ nauplii)}\right] x\ 100$$

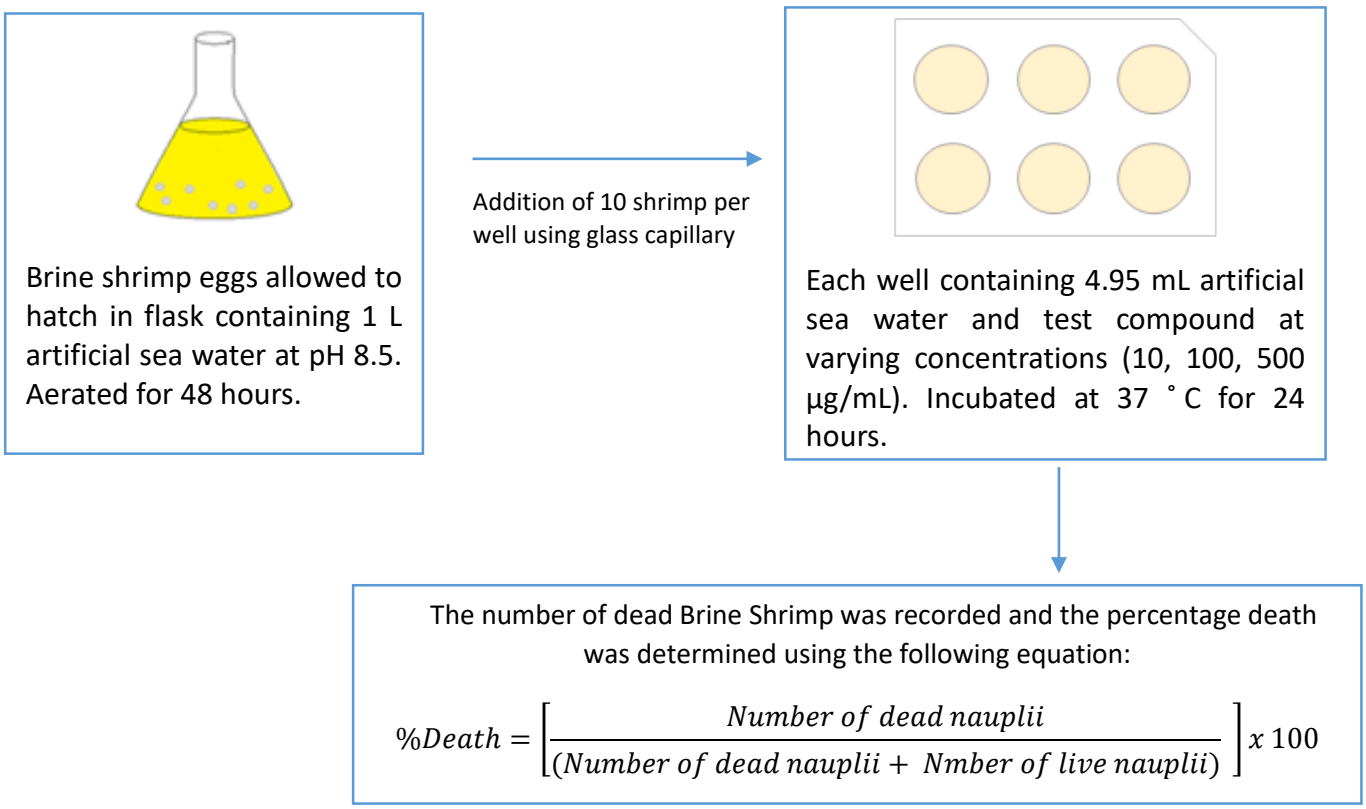

Figure 21: Graphical representation of Brine shrimp assay as described above [Meyer *et.al* 1982].

3.6.2. Antimicrobial Activity of MPQ-α-APs (4a-4t)

3.6.2.1. Preparation of Media

Fresh Nutrient Agar, Oxoid LTD (Hampshire, England) was prepared according to the manufacturer's instruction. A total of 28 g of the powder was added to 1 L of distilled water. The mixture was shaken until the powder completely dissolved. The bottles were sterilized by autoclaving at 121 °C for 15 minutes before the agar solution was poured into plates and left to solidify.

3.6.2.2. Preparation of Nutrient Broth

Nutrient Broth, Fresh Mueller Hinton Broth (Sigma-Aldrich) was prepared according to manufacturer's instruction. A total of 23 g of Nutrient Broth powder was added to 1 L of distilled water. The mixture was shaken until the powder completely dissolved. The solution was dispensed into bijou bottles and then sterilized by autoclaving at 121 °C for 15 minutes.

3.6.2.3. Microbial Cultures

The bacterial strains used in the study were collected from culture collection at the Department of Biotechnology and Food Technology, Durban University of Technology, South Africa (SA). The bacterial strains used included *Bacillus cereus* (B. *cereus*) (DBT*_F), *Staphylococcus aureus* (*S. aureus*) (DBT*_E), *Klebsiella pneumonia* (DBT*_AM) and *Micrococcus luteus* (DBT*_AR); and the three yeast cultures *Candida albicans* (*C. pneumonia*) (DBT*_AB), *Caraipa utilis* (*C. utilis*) (DBT*_AB) and *Saccharomyces cerevisiae* (*S. cerevisiae*) (DBT*_R) were selected.

DBT*: Durban University of Technology, reference based on bacterial culture strain as established at the department of Biotechnology and Food Technology.

The antibacterial activity of **4a**-**4t** was completed using the agar disc diffusion test [Cos *et al.,* 2006] by measuring the MIC of the compounds. MIC is defined as the lowest concentration of a compound that will inhibit the visible growth of bacteria.

Stock cultures were sub-cultured to assess their viability and stored using 50 % of glycerol in micro bank vials (Davies Diagnostics, SA). For the assay, cultures were plated on Nutrient Agar (Biolab) and incubated at 37 °C for 24 hours before growth in Nutrient Broth (Biolab) under the same conditions. A 10^8 cfu/mL of MacFarland standard with a 0.5 absorbance was used to standardize the bacterial cell concentration. A suspension (100 µL of 10^8 cfu/mL) of the test bacteria was plated on Mueller Hinton Agar plates (Fluka, Biochemika). The whatman

No. 1 filter paper was cut into 5 mm disks then dried in an open sterile petri dish biosafety chamber (LabtecBioflow II, SA). The disks were impregnated with 10 µL of each compound at the concentration of 3 mg/mL then placed onto the pre-inoculated bacterial agar plates and kept at 37 °C for 24 hours. The assay was carried out in triplicate. Ciprofloxacin (Fluka, Biochemika) (3 mg/mL) was used as the positive control and DMSO (100 %) as a negative control for the bacterial strains. Amphotericin B (Fluka, Biochemika) was used as the positive control and 10 µL DMSO (100 %) as negative control for the yeast cultures.

The MIC was determined by the broth micro dilution assay. The compounds (**4a-4t**) were tested at final concentrations of 0.09, 0.18, 0.35, 0.75, 1.5 and 3 mg/mL.

3.6.3. Antioxidant Activity of MPQ-α-APs (4a-4t)

The antioxidant activity of **4a-4t** was determined using the DPPH assay. This was conducted by measuring their radical scavenging capacity using the stable free radical scavenger, DPPH (2,2-diphenyl-1-picrylhydrazyl) [Choi *et al.,* 2002]. Stock solutions of **4a-4t** were diluted with methanol to final concentrations of 1, 20, 40, 60, 80, 100, 250, 500 and 1000 µg/mL. The radical scavenging capacity was measured spectrophotometrically at 517 nm as the decolouration percentage of the test sample following the formula below:

$$Scavenging\ capacity\ (\%) = 100 - \left[\frac{(\text{absorbance of sample} - \text{absorbance of blank})}{\text{absorbance of negative control}}\ x\ 100\right]$$

The effective antioxidant quercetin-3-rutinoside was used as a standard reference to compare the results obtained from this study.

In this study, palladium-doped strontium titanate oxide (Pd-$SrTiO_3$) was used to synthesize twenty novel methyl piperazinyl-quinolinyl-α-aminophosphonate (MPQ-α-AP) derivatives (**4a-4t**) followed by an evaluation of their biological potential.

The first step was to synthesize the novel catalyst, Pd-$SrTiO_3$. This occurred by a reaction of an aqueous mixture of Strontium (II) nitrate and citric acid under reflux in an ethanolic solution of Titanium (IV) butoxide. Thereafter, the dried solid was refluxed in a solution of Pd (II) nitrate after which the mixture was filtered, calcined, dried and the powder was collected. Several techniques were used for the characterization of Pd-$SrTiO_3$.

The FT-IR spectra of $SrTiO_3$ and Pd-$SrTiO_3$ were compared. The absorption spectrum of $SrTiO_3$ showed the Ti-O stretch at 1641 cm^{-1}, the Sr-Ti-O stretch at 1465 cm^{-1} and the Sr-Ti stretch at 555 cm^{-1}. The absorption spectrum of Pd-$SrTiO_3$ showed the Pd-Sr stretch at 2302 cm^{-1}, the Pd-Sr-Ti stretch at 1745 cm^{-1}, Pd-Sr-Ti-O stretch at 910 cm^{-1}, Sr-Ti-O stretch at 1448 cm^{-1} and Sr-Ti stretch at 574 cm^{-1} (Figure 22).

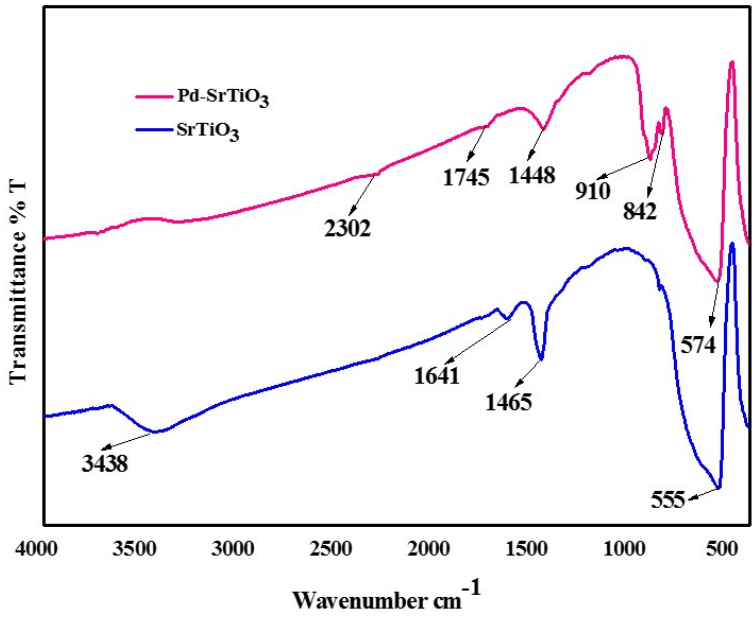

Figure 22: FT-IR spectrum of $SrTiO_3$ and Pd-$SrTiO_3$

Figure 23 shows the XRD pattern of $SrTiO_3$ and Pd-$SrTiO_3$. The diffraction peaks of pure $SrTiO_3$ were indexed to a crystalline phase and identical to the Pd-doped $SrTiO_3$ powder.

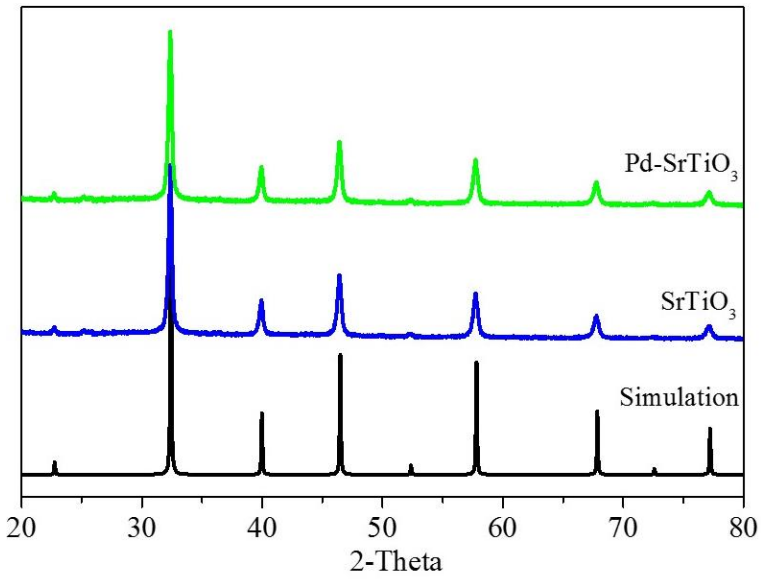

Figure 23: PXRD pattern of $SrTiO_3$ and Pd-$SrTiO_3$

SEM was used to determine the morphology and microstructure of $SrTiO_3$ and Pd-$SrTiO_3$ (Figure 24). Aggregates of these tightly packed spherically shaped particles were observed.

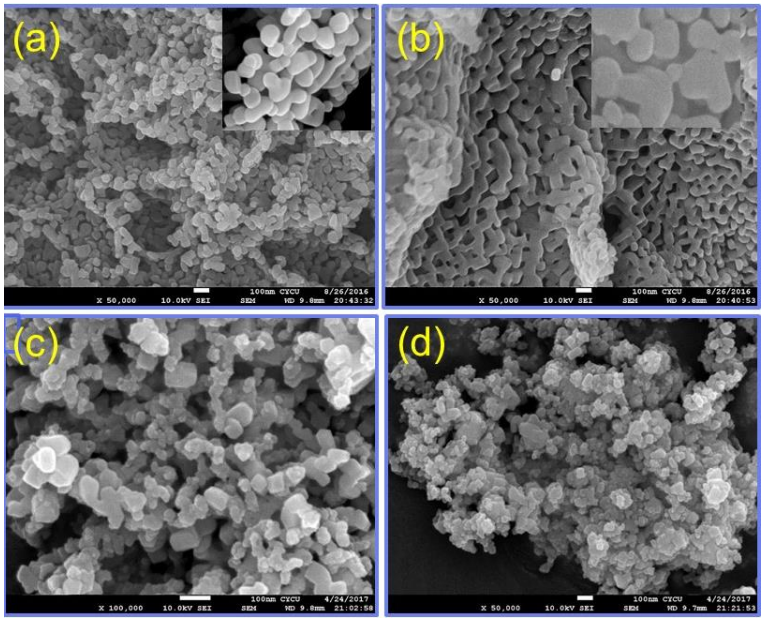

Figure 24: SEM image of $SrTiO_3$ (a and b) and Pd-$SrTiO_3$ (c and d)

The identity of $SrTiO_3$ and Pd-$SrTiO_3$ were confirmed by EDX analysis for C, O, Ti, Sr and Pd (Figure 25). The actual weight (%) in $SrTiO_3$ elements for C, O, Ti and Sr were 17.78, 30.55, 18.49 and 33.17 respectively whilst the atomic (%) were 35.63, 45.96, 9.29 and 9.11 respectively. The carbon content in $SrTiO_3$ may be due to the carbon tape that was used. The EDX of Pd-$SrTiO_3$ displayed elements C, O, Ti, Sr and Pd of weight (%) 0, 19.72, 19.84, 28.22 and 32.22 respectively whilst the atomic (%) were 0, 54.26, 18.23, 14.18 and 13.33 respectively (Table 2).

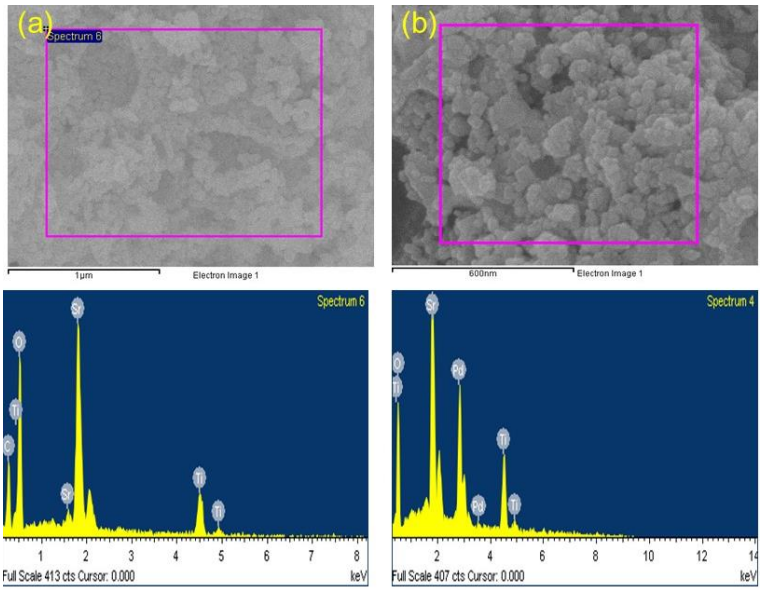

Figure 25: EDX analysis for $SrTiO_3$ (a) and Pd-$SrTiO_3$ (b)

Table 2: The weight (%) analysis for $SrTiO_3$ and Pd-$SrTiO_3$.

Element	$SrTiO_3$		Pd-$SrTiO_3$	
	Weight (%)	Atomic (%)	Weight (%)	Atomic (%)
C	17.78	35.63	-	-
O	30.55	45.96	19.72	54.26
Ti	18.49	9.29	19.84	18.23
Sr	33.17	9.11	28.22	14.18
Pd	-	-	32.22	13.33

The porosity of $SrTiO_3$ and Pd-$SrTiO_3$ is shown by N_2 gas adsorption measurements at 273 K (Figure 26). $SrTiO_3$ is a Type-I adsorption isotherm which is characteristic of microporous material and the BET and Langmuir surface area of $SrTiO_3$ were calculated as 89 m^2/g and 158 m^2/g respectively. The N_2 adsorption isotherm of Pd-$SrTiO_3$ also indicated a Type-I adsorption isotherm while the BET and Langmuir surface area were calculated as 127 m^2/g and 214 m^2/g respectively.

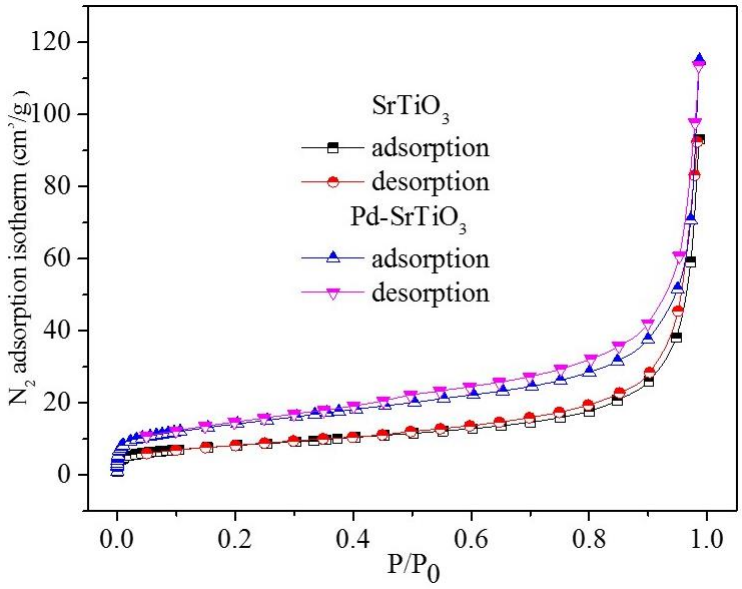

Figure 26: Adsorption and desorption isotherms of $SrTiO_3$ and Pd-$SrTiO_3$ at 273K.
$SrTiO_3$ BET and Langmuir Surface area = 89 m^2/g and 158 m^2/g;
Pd-$SrTiO_3$ BET and Langmuir Surface area = 127 m^2/g and 214 m^2/g

The structure of $SrTiO_3$ and Pd-$SrTiO_3$ were also studied by Raman spectroscopy (Figure 27). The adsorption signal of both $SrTiO_3$ and Pd-$SrTiO_3$ occurred at 529 cm^{-1} but the additional signal at 723 cm^{-1} is probably due to Pd.

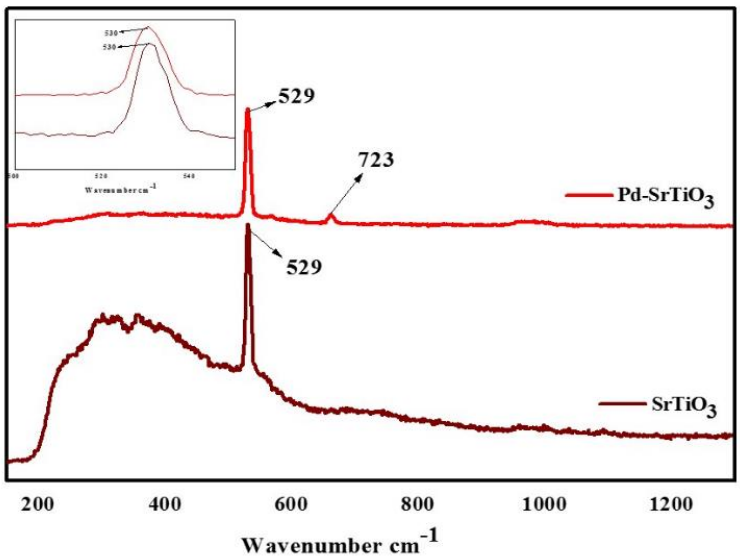

Figure 27: Raman Shift of $SrTiO_3$ and Pd-$SrTiO_3$

After synthesizing and identifying the structure of the catalyst, it was used with substrates 1, 2 and various amine derivatives (3a-3t) to synthesize twenty novel methyl-piperazinyl quinolinyl (diethyl ((2-(4-methylpiperazin-1-yl)quinolin-3-yl)(phenylamino)methyl)phosphonates (**4a-4t**) with catalytic amounts of Pd-$SrTiO_3$ (Scheme 26).

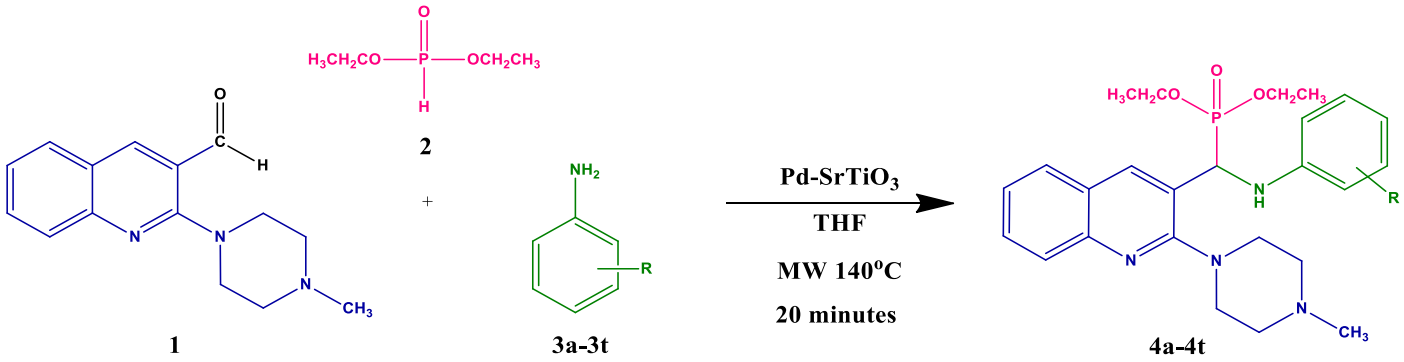

Scheme 26: The synthesis of (diethyl ((2-(4-methylpiperazin-1-yl)quinolin-3 yl)(phenylamino)methyl)phosphonates in the presence of the Pd-$SrTiO_3$ catalyst under microwave conditions.

In the initial study, Pd-$SrTiO_3$ was used in the Kabachnik Fields reaction in order to assess the catalytic potential. A model reaction was set up in order to synthesize novel methyl-piperazinyl quinolinyl α-aminophosphonates. An equimolar quantity of substrates 1, 2 and 3a catalyzed by Pd-$SrTiO_3$ was used to synthesize compound **4a** which was then characterized by FT-IR, ^{1}H-NMR, ^{13}C-NMR, 2D-NMR, ^{31}P-NMR, TOF-MS and elemental analysis. Thereafter the reaction was repeated to optimize the solvent system (Table 3).

Table 3: Solvent optimization for the synthesis of **4a** by the Kabachnik Fields reaction

Entry	Catalyst	Solvent	Temperature (˚C)	Time (hours/minutes)	Isolated Yield (%)
1	Pd-$SrTiO_3$	EtOH	r.t	24	60
2	Pd-$SrTiO_3$	MeOH	r.t	24	50
3	Pd-$SrTiO_3$	CH_3CN	r.t	24	75
4	Pd-$SrTiO_3$	Toluene	r.t	24	65
5	Pd-$SrTiO_3$	DMF	r.t	24	58
6	Pd-$SrTiO_3$	THF	r.t	24	70
7	Pd-$SrTiO_3$	EtOH	Reflux	12	65
8	Pd-$SrTiO_3$	MeOH	Reflux	10	53
9	Pd-$SrTiO_3$	CH_3CN	Reflux	6	78
10	Pd-$SrTiO_3$	Toluene	Reflux	14	60
11	Pd-$SrTiO_3$	DMF	Reflux	24	62
12	Pd-$SrTiO_3$	THF	Reflux	12	75
13	Pd-$SrTiO_3$	THF	MW	20 minutes	96

MW = Microwave

Several solvents including ethanol, methanol, acetonitrile, toluene, dimethylformamide and tetrahydrofuran were examined. Compound 4a was obtained in the highest yield of 96 % when the reaction was catalyzed with Pd-$SrTiO_3$ in THF under MW conditions at 20 minutes (Table 3, entry 13).

An extended amount of time was required to reach reaction completion when the solvents ethanol, methanol, acetonitrile, Toluene, DMF and THF were used at room temperature conditions for 24 hours resulting in moderate yields (%) of 4a as 60, 50, 75, 65, 58 and 70 respectively (Table 3, entries 1-6). Product yield saw a slight increase when the solvents ethanol, methanol, acetonitrile, Toluene, DMF and THF were used under reflux conditions: yield (%) of 4a was 65, 53, 78, 60, 62 and 75 % respectively (Table 3, entries 7-12). Hence, THF was used as a solvent in all subsequent reactions under MW irradiation for 20 minutes.

Table 4: Quantity of Pd-$SrTiO_3$ catalyst optimization for the synthesis of **4a** by the Kabachnik Fields reaction

Entry	Pd-$SrTiO_3$ (g)	Isolated Yield (%)
1	0.03	82
2	0.05	96
3	0.07	96

In order to determine the optimum amount of Pd-$SrTiO_3$, different amounts of catalyst viz., 0.03, 0.05 and 0.07 g, in THF, were used in the model reaction under MW conditions at 140 ºC for 20 minutes. It was found that 0.05 g of Pd-$SrTiO_3$ gave the highest product yield (96 %). Increasing the quantity of Pd-$SrTiO_3$ did not enhance the product yield of **4a** but rather increased the cost of the synthetic process and so 0.05 g of Pd-$SrTiO_3$ was used as an optimum mass of the catalyst in all subsequent reactions.

Furthermore, the model reaction was subjected to MW irradiation at different time intervals but twenty minutes was concluded ideal as the yield of **4a** was 96 %. Reaction times less than 20 minutes showed an incomplete reaction visualised by TLC whilst higher temperatures favoured side reactions that was seen by additional spots on the TLC plate.

The possible recyclability of Pd-$SrTiO_3$ was also explored in the model reaction **4a**; briefly the solid catalyst was washed with ethanol, heated at 100 °C then used for succeeding reactions. The outcome indicated that the catalyst may possibly be re-used five times over with only a 4 % loss of catalytic activity. This concluded the catalyst to be satisfactory which makes it applicable for commercial application if required.

Once the reaction conditions were optimized, products **4a-4t** were synthesized using the appropriate starting materials 1, 2 and various amine (3a-3t) in THF and catalyzed with Pd-$SrTiO_3$ via the Kabachnik Fields reaction under microwave conditions. The isolated yield of products **4a-4t** ranged from 85 to 96 % and were characterized by FT-IR, ^{1}H-NMR, ^{13}C-NMR, ^{19}F-NMR, ^{31}P-NMR and MS-TOF whilst **4a** included 2D-NMR, DEPT-90 and DEPT-135.

Table 5: The synthesis of methyl piperazinyl-quinolinyl α-aminophosphonate derivatives (**4a-4t**) in the presence of Pd-$SrTiO_3$

Compound	Substrate (3a-t)	Time (minutes)	Isolated Yield (%)	Melting Point (˚C)
4a	$C_6H_5NH_2$	20	96	133-135
4b	2-$O_2NC_6H_4NH_2$	20	90	114-116
4c	3-$O_2NC_6H_4NH_2$	20	88	125-127
4d	2-$FC_6H_4NH_2$	20	90	149-151
4e	3-$FC_6H_4NH_2$	20	95	128-130
4f	4-$FC_6H_4NH_2$	20	88	127-129
4g	4-$ClC_6H_4NH_2$	20	91	181-183
4h	$Cl_2C_6H_3NH_2$	20	94	188-190
4i	4-$BrC_6H_4NH_2$	20	88	194-196
4j	*o*-$CH_3C_6H_4NH_2$	20	92	140-142
4k	*m*-$CH_3C_6H_4NH_2$	20	87	137-139
4l	*p*-$CH_3C_6H_4NH_2$	20	85	150-152
4m	$(CH_3)_2C_6H_4NH_2$	20	90	147-149
4n	*o*-C_6H_9NO	20	85	130-132
4o	*p*-C_6H_9NO	20	89	119-121
4p	$C_6H_6N_2$	20	87	145-147
4q	$C_6H_8N_2$	20	90	144-146
4r	$C_{10}H_7NH_2$	25	91	131-133
4s	$C_{14}H_{14}N_2$	25	93	109-111
4t	C_9H_9Br-N_2O_2	25	90	120-122

Reaction recipe were as follows: 2-(4-methylpiperazin-1-yl) quinoline-3-carbaldehyde (1mmol), diethyl phosphite (1mmol), aniline (1mmol) and Pd-$SrTiO_3$ catalyst (0.05g) under MW at 140 ˚C

The proposed mechanism presented in Scheme 27 is based on the Kabachnik Fields reaction. Here, the Pd-$SrTiO_3$ catalyst acts as a Lewis acid by pulling the lone pair of electrons on the heteroatom to the carbonyl compound thereby prompting the reaction. Firstly, the condensation of 1 (carbonyl compound) and 3 (amines), with a loss of water molecule, gave the Schiff base intermediate I. This is followed by H-bond formation between the P=O function of the phosphite 2 and the HN unit of the amine to produce intermediate II. An intramolecular cyclisation and loss of catalyst finally produces the corresponding α-aminophosphonate.

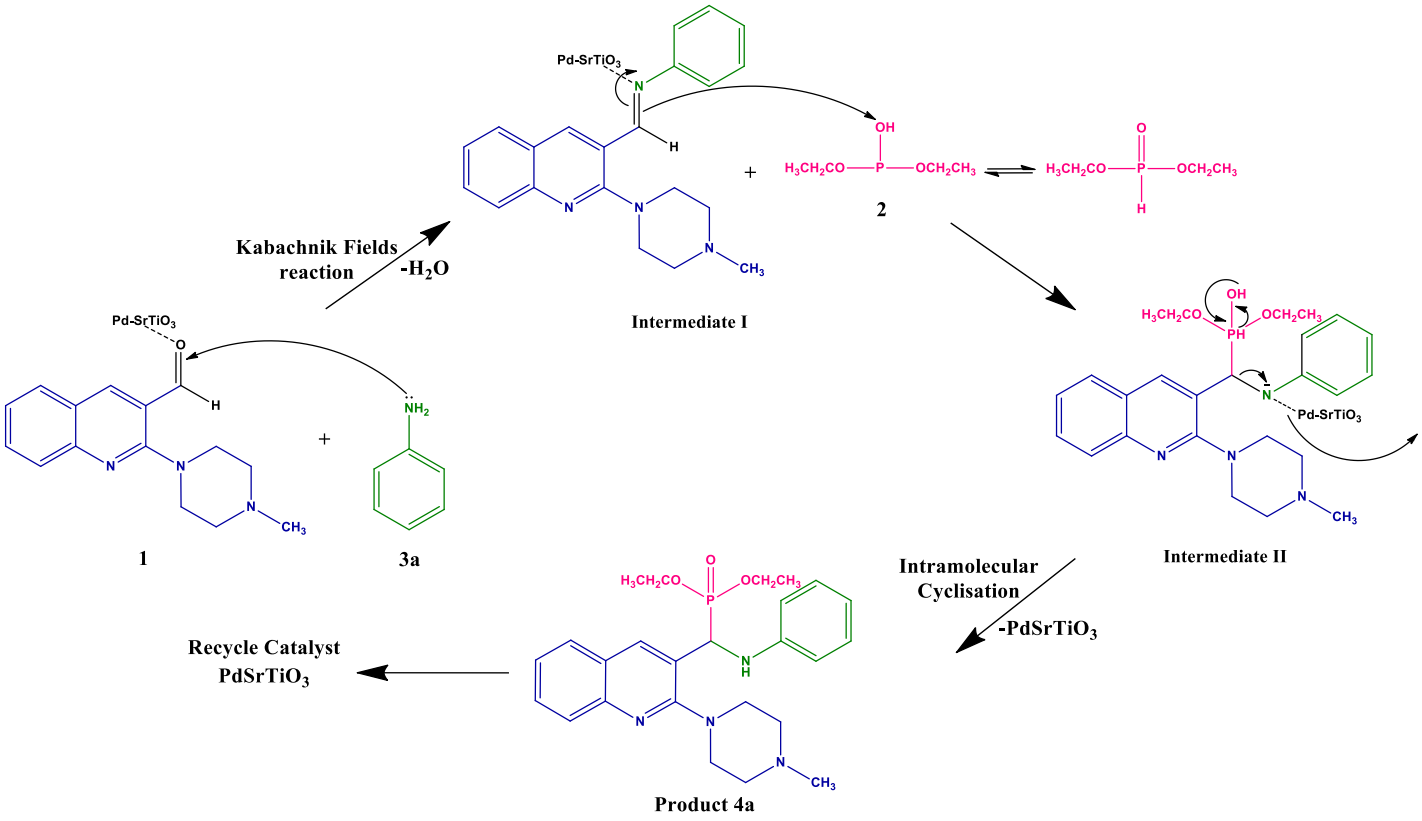

Scheme 27: The proposed mechanism for the synthesis of ((2-(4-methylpiperazin-1-yl)quinolin-3 yl)(phenylamino)methyl)phosphonates **4a-4t**

The identity of all synthesized compounds (**4a-4t**) was confirmed by spectral data obtained from FT-IR, ^{1}H-NMR, ^{13}C-NMR, 2D-NMR, ^{31}P-NMR, TOF-MS and elemental analysis; where all the spectra were well resolved. Compound **4a** was selected as the template and it was characterized fully with the aid of 2D NMR techniques especially HSQC, HMBC and COSY which led to the unambiguous assigning of all protons, carbons and nitrogen.

The FT-IR spectrum of **4a**, presented in Figure S1 (Appendix 1, page 101), showed stretching at 1588 and 3320 cm^{-1} for carbonyl and NH groups, respectively.

The ^{1}H-NMR spectrum of **4a**, presented in Figure S2 (Appendix 2), showed two singlets at δ 8.74, and 8.68 for N1"-H and C4-H, respectively. The C1'"-CH proton was assigned to δ 5.29-5.37 as a doublet.

The ^{13}C-NMR spectrum of **4a**, presented in Figure S3 (Appendix 3), showed the presence of two -OCH_2 carbonyl group at δ 63.36-63.49.

The ^{31}P-NMR spectrum of **4a**, presented in Figure S4 (Appendix 4), showed the presence of one phosphorus group at δ 23.76.

Table 6: Selected HMBC, ^{1}H-NMR and ^{13}C-NMR chemical shifts of **4a**

Shift Number	Proton	Correlated Carbons
1	$C_{1'''}$-H (d, 1H) at *δ.* 5.29-5.37	C_4 at *δ* (137.92), $C_{1''}$ at *δ* (145.97), $C_{3''}$ at *δ* (126.40), C_2 at *δ* (160.64),
2	$C_{7''}$-H (s, 1H, N-H) at *δ.* 8.74	$C_{1''}$ at *δ* (145.97), C_2 at *δ* (160.64) $C_{3''}$ at *δ* (126.40),
3	C_4-H (s, 1H) at *δ.* 8.68	C_{5a} at *δ* (151.87), C_{8a} at *δ* (148.12), C_3 at *δ* (121.03),
4	C_5-H (d, 1H, *J*= 8.44Hz) at *δ.* 7.88	C_6 at *δ* (129.36), C_8 at *δ* (128.58), C_4 at *δ* (137.92), C_{5a} at *δ* (151.87),
5	C_6-H (m, 1H) at *δ.* 7.64-7.68	C_7 at *δ* (124.64), C_{8a} at *δ* (148.12),
6	C_7-H (t, 1H, *J*= 7.48Hz) at *δ.* 7.44-7.48	C_{5a} at *δ* (151.87), C_8 at *δ* (128.58),
7	C_8-H (d, 1H, *J*= 8Hz) at *δ.* 7.82	C_{8a} at *δ* (148.12), C_6 at *δ* (129.36), C_{5a} at *δ* (151.87),
8	$C_{2''}$-H (d, 1H, *J*= 7.96Hz) at *δ.* 6.81	C_3 at *δ* (121.03),
9	$C_{3''}$-H (m, 1H, *J*= 2.52Hz) at *δ.* 7.38-7.40	$C_{1''}$ at *δ* (145.85), $C_{4''}$ at *δ* (118.54), $C_{5''}$ at *δ* (122.73),
10	$C_{4''}$-H (dd,1H, *J*= 2.5Hz) at *δ.* 6.66-6.70	$C_{2''}$ at *δ* (113.81),
11	$C_{5''}$-H (dd,1H, *J*= 0.84Hz) at *δ.* 7.08-7.12	$C_{1''}$ at *δ* (145.97), $C_{2''}$ at *δ* (113.81),
12	$C_{6''}$-H (d,1H, *J*= 2.72Hz) at *δ.* 8.44	$C_{1''}$ at *δ* (145.97), $C_{1'''}$ at *δ* (48.51), $C_{5''}$ at *δ* (122.73),

The structure was further confirmed on the basis of 2D-NMR spectral studies. The C, H-COSY (HSQC) spectrum of **4a**, presented in Figure S8 (Appendix 8), shows correlation at δ 16.16-16.57, 46.10, 48.51, 50.05, 50.79, 54.95, 63.37-63.49, 113.81, 118.54, 122.73, 124.64, 126.40, 127.60, 128.58, 129.36, 137.92 which were assigned to C4'", C6'", C7', C2', C6', C5', C3', C3'", C5'", C2",C6", C4", C7, C3", C5, C8, C6, and C4, respectively. The carbon signal at δ 137.92, was due to the quinolinyl C4-carbon. The H, H-COSY spectrum revealed the doublet at δ 5.29-5.37 which confirmed only one nearby hydrogen to C4.

The HMBC correlation of **4a** is presented in Figure 11 (Appendix 11). The C1'"-H proton correlated with quinolinyl and amine carbon C4 at 137.92, C2 at 160.64, C2" at 145.97, C4"

at 126.40, whilst the C1”-H (N-H) proton correlated with quinolinyl and amine carbon C2 at 160.64, C2” at 145.97, C4” at 126.40. The C4-H proton correlated with quinolinyl carbon C5a at 151.87, C8a at 148.12, C3 at 121.03, similarly, correlation of C5-H with quinolinyl carbon C6 was at 129.60, C8 at 128.58, C4 at 137.92, C5a at 151.87. The C6-H proton correlated with quinoline carbon C7 at 124.64, C8a at 148.12. The C7-H correlated with quinolinyl carbon C5a at 151.87, C8 at 128.58, whilst C8-H correlated with amine carbon C8a at 148.12, C6 at 129.36, C5a at 151.87. The C2”-H correlated with quinolinyl carbon C3 at 121.03, whilst C3”-H correlated with amine carbon C7” at 145.97, C3” at 118.54, C4” at 122.73. The C5”-H correlated with amine carbon C1” at 113.81, C4”-H correlated with amine carbon C7” at 145.97, C1” at 113.81, and C5”-H correlated with amine and -C-H carbon C7” at 145.97, C1’” at 48.51, C4” at 122.73 (Figure 28).

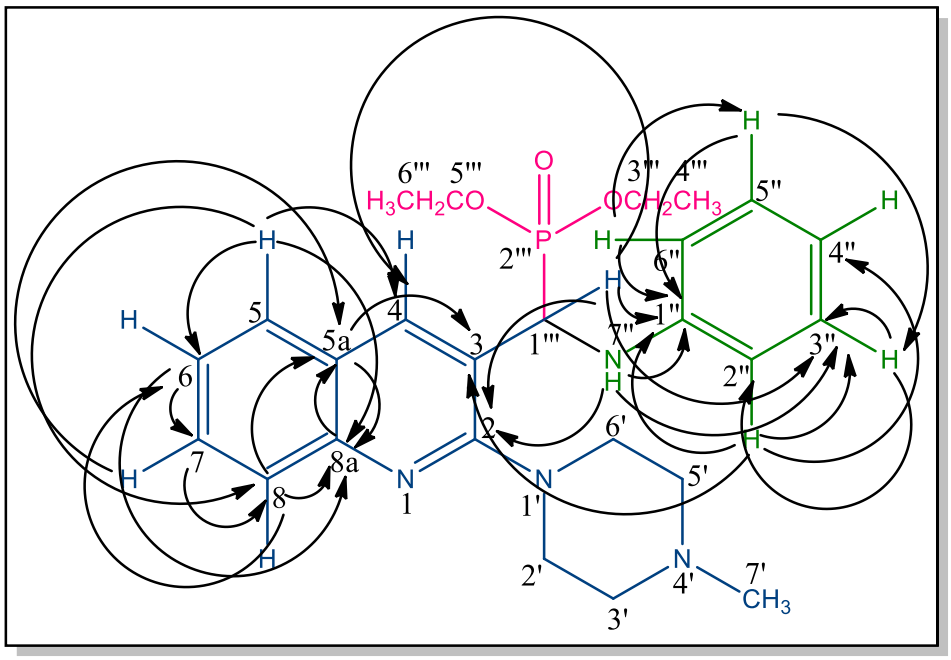

Figure 28: Selected HMBC correlations of compound **4a**.

The TOFMS ES spectrum of **4a** showed an m/z (rel. int.) of 469.23 $[M]^+$ as the molecular ion. Elemental analysis gave: Anal. Calc. for $C_{25}H_{33}N_4O_3P$: C, 64.09; H, 7.10; N, 11.96 %. Found: C, 64.11; H, 7.12; N, 11.98 % thereby confirming the structure of **4a** as diethyl ((2-(4-methylpiperazin-1-yl)quinolin-3 yl)(phenylamino)methyl)phosphonate. Scheme 28 shows the possible fragments of compound **4a** produced by the electron impact ionization technique.

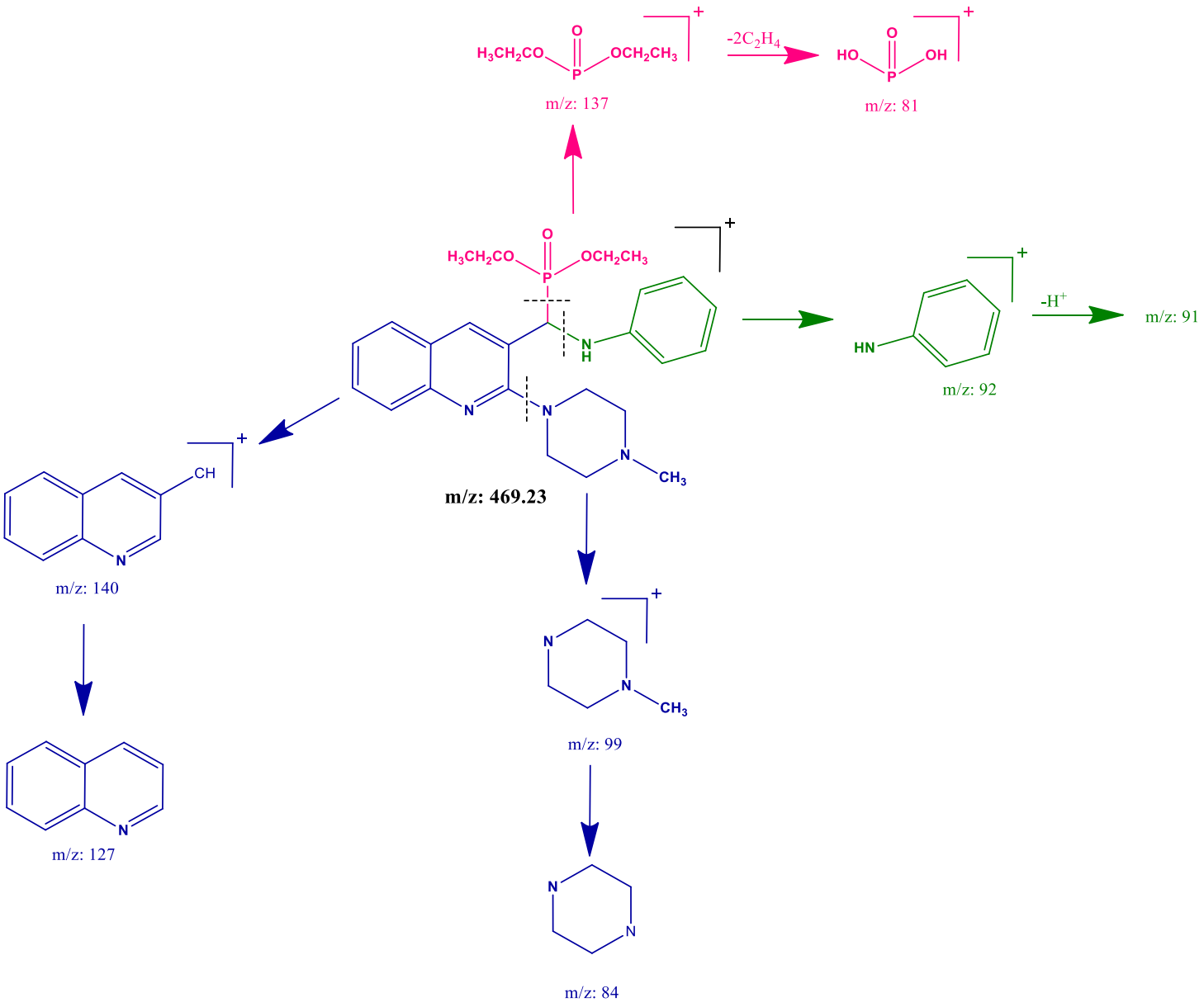

Scheme 28: Proposed fragments of **4a**

Table 7: ^{1}H NMR chemical shifts for compounds 4a-4e, δ of ^{1}H (*J*, Hz)

H	4a	4b	4c	4d	4e
NH	8.74 (s)	5.3 (d, *J* = 12.48)	8.75 (s)	8.70 (s)	8.72 (s)
4	8.68 (s)	8.38 (s)	8.70 (s)	8.61 (s)	8.64 (s)
5	7.88 (d, *J* = 8.44)	7.73 (d, *J* = 8.48)	7.90 (d, *J* = 8.52)	7.88 (d, *J* = 8.44)	7.88 (d, *J* = 8.44)
6	7.64-7.68 (m)	7.60 (t, *J* = 8.24)	7.67-7.71 (m)	7.68-7.69 (m)	7.62-7.64 (m)
7	7.44-7.48 (t, *J* = 7.48)	7.27 (t, *J* = 7.36)	7.49 (t, *J* = 2.28)	7.42 (t, *J* = 6.8)	7.39 (t, *J* = 7.64)
8	7.82 (d, *J* = 8)	7.70 (d, *J* = 8.04)	7.84 (d, *J* = 0.76)	7.82 (d, *J* = 7.96)	7.81 (d, *J* = 7.96)
2′	2.66-2.69 (t)	2.56 (t)	2.68 (t)	2.66 (t)	2.68 (t)
3′	3.51-3.54 (t)	3.44 (t)	3.51 (t)	3.50 (t)	3.50 (t)
5′	4.24-4.28 (t)	-	-	4.23-4.27 (q)	4.23-4.27 (q)
6′	4.83-4.07 (t)	-	-	4.12 (t)	-
7′	2.46 (s)	2.28 (s)	2.40 (s)	2.46 (s)	2.40 (s)
1″	-	-	-	-	-
2″	7.38-7.40 (m, *J* = 2.52)	-	7.58-7.62 (q, *J* = 1.56)	-	-
3″	6.66-6.70 (dd, *J* = 2.5)	6.56-6.59 (dd, *J* = 0.88)	-	7.10-7.12 (dd, *J* = 6)	-
4″	7.08-7.12 (dd, *J* = 0.84)	7.98-8.01 (dd, *J* = 1.2)	8.13-8.15 (dd, *J* = 1.64)	7.36-7.38 (dd, *J* = 8)	7 (t, *J* = 9.44)
5″	8.44 (d, *J* = 2.72)	-	8.09 (s)	-	-
6″	-	-	-	-	-
1‴	5.29-5.37 (d)	6.10 (s)	6.95 (d)	6.51 (s)	5.35 (d)
3‴	3.77-3.84 (m)	3.89-4.01 (m)	-	4.10 (d)	3.78 (t)
4‴	1.04-1.08 (t)	1.11 (t)	1.23 (t)	1.24 (t)	1.24 (t)
5‴	4.02-4.06 (m)	4.12-4.15 (m)	4.02 (s)	-	4.03-4.08 (q)
6‴	1.34-1.38 (t)	1.25 (t)	1.37 (t)	1.37 (t)	1.42 (t)

Table 8: ^{1}H NMR chemical shifts for compounds 4f-4j, δ of ^{1}H (*J*, Hz)

H	4f	4g	4h	4i	4j
NH	7.94 (d)	8.72 (s)	8.70 (s)	8.72 (s)	5.27 (d)
4	8.19 (s)	8.62 (s)	8.61 (s)	8.62 (s)	8.34 (s)
5	7.76-7.78 (t, *J* = 3.2)	7.82 (d, *J* = 7.92)	7.88 (d, *J* = 8.48)	7.87 (d, *J* = 8.4)	7.63 (d, *J* = 8.04)
6	7.08-7.11 (t, *J* = 7.4)	7.65-7.69 (m)	7.65-7.69 (m)	7.65-7.69 (m)	7.27 (t, *J* = 7.32)
7	7.46-7.52 (t, *J* = 7.72)	7.74 (t, *J* = 8.5)	7.38-7.42 (m)	7.74 (t, *J* = 8.8)	7.48 (t, *J* = 7.72)
8	7.25 (d, *J* = 8.12)	7.87 (d, *J* = 8.4)	7.82 (d, *J* = 8.04)	7.82 (d, *J* = 7.92)	7.80 (d, *J* = 8.44)
2′	2.84 (d)	2.87 (d)	2.66 (t)	2.87 (d)	2.63 (q)
3′	3.29 (d)	3.62 (s)	3.49 (t)	3.62 (s)	3.49 (q)
5′	3.40-3.44 (t)	4.22 (t)	4.23-4.27 (q)	4.07 (t)	3.18 (t)
6′	5.01 (d)	-	-	4.22 (t)	3.96 (t)
7′	2.61 (s)	2.59 (d)	2.40 (s)	2.53 (s)	2.32 (s)
1″	-	-	-	-	-
2″	7.40 (d, *J* = 7.24)	-	7.16 (d, *J* = 2.32)	7.40-7.42 (dd, *J* = 2.16)	-
3″	6.80-6.89 (dd, *J* = 8.56)	7.40-7.42 (dd, *J* = 1.96)	-	7.19-7.21 (dd, *J* = 1.96)	7.63 (d, *J* = 8.04)
4″	-	-	-	-	6.89 (t, *J* = 7.32)
5″	6.61 (d, *J* = 4.4 Hz)	7.19-7.21 (dd, *J* = 1.92)	7.12 (d, *J* = 2.48)	-	6.82 (d, *J* = 7.11)
6″	-	-	-	-	-
1‴	5.90 (s)	6.61 (d)	7.10 (d, *J* = 2.48)	6.61 (d, *J* = 8.8)	4.65 (t)
3‴	3.76-3.80 (m)	3.95 (t)	3.98-4 (q)	3.95 (t)	3.70-3.74 (m)
4‴	1.02-1.06 (m)	-	1.23 (t)	1.21 (t)	0.95 (t)
5‴	-	-	4.10-4.14 (q)	-	4.12-4.18 (m)
6‴	1.13-1.17 (t)	1.20-1.36 (m)	1.37 (t)	1.34 (t)	1.26 (t)

Table 9: ^{1}H NMR chemical shifts for compounds 4k-4o, δ of ^{1}H (*J*, Hz)

H	4k	4l	4m	4n	4o
NH	8.73 (s)	8.38 (d, *J* = 2.56)	8.64 (s)	8.76 (s)	8.70 (s)
4	8.66 (s)	8.35 (s)	8.47 (s)	8.65 (s)	8.67 (s)
5	7.90 (d, *J* = 8.4)	7.77 (d, *J* = 8.36)	7.78 (d, *J* = 8.44)	7.76 (d, *J* = 8)	7.87 (d, *J* = 8.48)
6	-	7.64 (t, *J* = 8.6)	7.48-7.54 (m)	6.67-6.75 (m, *J* = 1.68)	7.61-7.65 (m)
7	7.11 (t, *J* = 3.64)	7.50 (t, *J* = 7.48)	6.98 (t, *J* = 6.12)	7.32 (t, *J* = 7.48)	7.29-7.31 (dd, *J* = 2.16)
8	7.80 (d, *J* = 0.52)	7.72 (d, *J* = 8.44)	7.72 (d, *J* = 7.76)	7.85 (d, *J* = 8.4)	7.78 (d, *J* = 0.68)
2’	2.66 (t)	2.53 (t)	2.56 (d)	2.59 (s)	2.65 (t)
3’	3.51 (t)	3.41 (t)	3.40 (t)	3.50 (s)	3.49 (t)
5’	4.24-4.29 (q)	3.86-3.91 (q)	4.17 (t)	4.22-4.26 (q)	4.24-4.26 (q)
6’	4.86 (t)	3.94-3.99 (q)	4.53 (t)		4.58 (t)
7’	2.22 (s)	1.22 (s)	2.13 (s)	3.78 (s)	3.67 (s)
1’’	-	-	-	-	-
2’’	6.60 (t, *J* = 7.52)	7.55-7.59 (m)	-	-	
3’’	6.55 (d, *J* = 8.08)	7.26 (dd, *J* = 0.76)	6.71-6.78 (m)	6.96 (d, *J* = 8.96)	6.97-6.99 (dd, *J* = 2.04)
4’’	7.64-7.66 (dd, *J* = 1.32)	-	7.48-7.54 (m)	7.01 (d, *J* = 7.48)	-
5’’	-	-	-	7.57-7.61 (q, *J* = 7.12)	7.35-7.39 (m)
6’’	-	-	-	7.05 (t, *J* = 1.52)	-
1’’’	5.31-5.39 (dd, *J* = 9.48)	5.30 (d)	5.18-5.26 (dd, *J* = 9.2)	5.22 (s)	5.28 (t)
4’’’	1.06 (t)	1.07 (t)	0.96 (t)	1.06-1.26 (t)	1.06 (t)
5’’’	4.03-4.07 (q)	4.08-4.12 (q)	3.94-3.96 (q)	4.04-4.06 (q)	4.01-4.06 (m)
6’’’	1.37 (t)	-	1.26 (t)	1.31-1.42 (s)	1.36 (t)

Table 10: ^{1}H NMR chemical shifts for compounds 4p-4t, δ of ^{1}H (*J*, Hz)

H	4p	4q	4r	4s	4t
NH	6.11 (d, *J* = 7.88)	5.87 (q, *J* = 9.28)	8.94 (s)	8.74 (d, *J* = 2.72)	10.08 (s)
4	8.43 (s)	6.37 (s)	8.77 (s)	8.86 (s)	8.42 (s)
5	-	7.80 (t, *J* = 4.8)	7.88-7.94 (m, *J* = 3.84)	7.87 (t, *J* = 7.2)	-
6	7.24-7.28 (q, *J* = 0.92)	-	7.67-7.72 (m, *J* = 1.24)	7.74 (d, *J* = 7.64)	7.61-7.65 (q, *J* = 1.4)
7	7.75-7.79 (t, *J* = 6.36)	7.52 (t, *J* = 7.4)	7.42 (t, *J* = 0.8)	7.55 (t, *J* = 1.92)	7.74 (t, *J* = 8.6)
8	7.60 (d, *J* = 7.96)	7.62 (d, *J* = 7.96)	7.57-7.60 (q, *J* = 2.52)	7.90-7.95 (dd, *J* = 3.96 Hz)	7.52-7.54 (dd, *J* = 0.96)
2’	2.59 (t)	2.49-2.74 (m)	2.68 (t)	2.72 (t)	2.69 (t)
3’	3.23 (t)	3.18-3.52 (m)	3.58 (t)	3.58 (t)	3.51 (t)
5’	3.54-3.57 (q)	3.83-3.89 (m)	-	3.84 (t)	-
6’	3.77-3.81 (q)	-	-	4.40 (q)	-
7’	2.26 (s)	2.38 (s)	2.39 (s)	2.41 (s)	1.35 (s)
1’’	-	-	-	-	-
2’’	-	7.27-7.31 (q, *J* = 7.24)	-	6.99-7.02 (dd, *J* = 2.16)	-
3’’	6.40-6.44 (t, *J* = 3.76)	-	-	-	8.52 (d, *J* = 8.44)
4’’	-	2.11 (s)	7.78-7.84 (m, *J* = 4.12)	-	7.02-7.06 (q, *J* = 0.68)
5’’	7.48 (d, *J* = 7.48)	8.29 (d, *J* = 2.84)	8.47 (t, *J* = 3.32)	8.80 (s)	7.29-7.33 (q, *J* = 0.8 Hz)
6’’	-	-	7.08 (t, *J* = 0.6)	7.17 (t, *J* = 7.28)	7.41 (t, *J* = 7.28)
1’’’	5.33 (d, *J* = 12.44)	5.50-5.87 (t, *J* = 8.6)	-	6.91-6.94 (dd, *J* = 2.32)	4.94 (d)
4’’’	1.06-1.09 (t)	0.93-0.96 (t)	-	1.10 (t)	0.82 (t)
5’’’	4-4.12 (m)	4.04-4.16 (m)	4.11-4.17 (m)	4.23-4.30 (m)	-
6’’’	1.18-1.21 (t)	1.20-1.23 (t)	1.24-1.30 (m)	1.29 (t)	1.14-1.25 (q)

Table 11: ^{13}C NMR chemical shifts (δ in ppm) for compounds 4a-4j

C	4a	4b	4c	4d	4e	4f	4g	4h	4i	4j
2	160.63	160.37	160.32	160.30	160.32	161.77	159.22	160.77	160.09	160.69
3	121.02	124.01	124.63	124.01	123.98	123.20	124.96	124.61	125.79	126.90
4	137.91	135.60	138.69	138.53	138.74	137.87	138.43	137.39	138.93	137.27
5	127.60	127.52	127.85	127.83	127.85	127.38	127.65	127.58	127.68	127.54
5a	157.78	158.91	158.84	158.91	158.84	158.83	157.85	159.88	157.94	160.61
6	129.36	129.25	129.22	129.25	129.22	129.15	129.49	129.19	129.49	129.57
7	124.64	124.66	123.48	124.66	124.63	124.79	122.34	122.80	125.82	127.91
8	128.58	132.51	132.48	132.51	132.48	131.97	132.78	130.72	129.63	130.24
8a	148.11	149.30	149.25	149.30	149.25	145.15	148.03	148.09	146.53	146.81
2’	48.51	50.85	44.21	45.98	45.85	42.99	49.85	48.39	50.15	48.61
3’	54,95	63.21	63	55.09	63.07	52.43	63	55.42	63.06	63.43
5’	50.79	58.09	50.74	51.14	63	49.66	54.17	50.95	59.62	50.15
6’	50.05	51.14	45.85	50.85	50.74	48.44	54.02	50.54	54.52	51.07
7’	54.94	54.88	54.80	54.88	54.80	56	54.41	54.98	54.93	55.33
1’’	145.97	144.02	146.63	144.82	146.63	144.88	150.22	146.39	145.17	144.08
2’’	113.80	116.80	110.87	116.80	120.99	113.48	114.87	115.91	113.82	114.91
3’’	126.39	126.14	125.82	126.14	125.82	125.42	125.06	125.04	125.05	125.07
4’’	118.53	118.77	122.02	118.77	112.37	114.84	116.21	117.79	112.08	118.29
5’’	122.73	122.06	122.51	122.06	122.02	121.79	122.31	122.04	125	122.76
6’’	113.80	116.80	110.87	116.80	120.99	113.48	114.87	114.20	113.82	114.91
1’’’	48.50	46.03	45.96	46.04	45.96	46.89	45.39	46.15	45.30	46.19
3’’’	63.36	63.28	63.10	63.21	63.10	62.03	63.07	63.46	63.07	63.49
4’’’	16.16	16.36	16.49	16.51	16.49	-	16.36	16.54	16.48	16.54
5’’’	63.49	63.97	63.18	63.28	63.18	-	-	63.52	63.16	63.54
6’’’	16.57	16.59	16.55	16.57	16.55	-	16.52	16.59	16.35	16.60

Table 12: ^{13}C NMR chemical shifts (δ in ppm) for compounds 4k-4t

C	4k	4l	4m	4n	4o	4p	4q	4r	4s	4t
2	160.77	160.32	160.66	160.83	160.66	160.61	160.71	160.37	160.88	165.23
3	122.80	120.99	122.89	121.07	122.89	125.79	137.13	132.51	120.58	121.43
4	137.39	138.68	137.63	138.01	137.63	137.32	137.18	135.60	137.37	139.14
5	127.58	127.63	127.60	127.54	127.61	127.68	127.81	126.14	127.58	127.61
5a	159.88	158.83	156.34	158.93	156.84	157.94	157.05	158.91	159.88	176.93
6	129.19	129.70	129.49	129.25	129.48	129.48	129.43	129.25	129.47	129.20
7	124.61	124.62	124.55	124.51	124.97	125	124.94	124.66	124.58	124.90
8	128.57	127.84	128.53	128.59	128.53	127.49	127.50	127.52	128.53	132.76
8a	148.09	149.24	148.02	148.07	148.02	146.52	148.51	149.30	147.91	149.23
2’	46.15	44.84	46.29	50.80	46.30	45.30	46.63	46.03	46.15	43.28
3’	55.42	63.06	55.42	63.30	51.14	59.62	55.24	58.09	55.36	30.32
5’	50.95	62.99	50.85	63.23	50.86	59.58	50.50	63	63.28	-
6’	50.84	50.74	50.32	55.85	50.32	50.51	45.99	51.14	46.07	45.40
7’	54.98	54.79	55.04	55.02	55.05	54.93	55.08	54.88	54.97	54.50
1’’	146.39	146.64	146.80	147.27	146.80	145.17	146.62	144.02	143.73	143.83
2’’	111.27	112.37	111.74	111.66	111.75	113.82	108.45	116.80	113.07	123.61
3’’	125.04	125.81	126.03	126.93	126.04	125.81	126.35	124.01	126.09	124.09
4’’	117.79	123.97	117.27	118.37	117.27	112.98	115.66	118.77	118.01	119.40
5’’	122.04	122.02	123.15	122.92	123.15	125.05	125.90	122.06	122.46	121.96
6’’	111.27	112.37	111.74	114.97	111.75	113.82	108.45	116.80	113.07	123.61
1’’’	48.39	45.95	48.77	46.15	48.78	50.15	48.15	50.85	50.71	49.86
3’’’	63.46	63.10	63.48	63.40	63.33	63.16	63.22	63.28	63.53	-
4’’’	16.54	16.49	16.56	16.52	16.56	16.48	16.41	16.59	16.57	29.36
5’’’	63.52	63.17	63.54	63.47	63.48	63.08	63.29	63.97	63.60	-
6’’’	16.59	16.54	16.61	16.58	16.61	16.54	16.47	16.81	16.63	29.69

The Brine shrimp lethality assay was used to evaluate the toxicity of the selected compounds. Experiments were performed in triplicate at varying concentrations (10, 100 and 500 µg/mL) following 1, 2, 3, 4, 20 and 24 hour intervals. Mortality was recorded as mean percentage of the Brine shrimp death after 24 hours. All results are expressed as mean ± SD and presented in Table 13 below:

Table 13: Percentage death of Brine shrimp

Compound	Concentration(µg/mL)	%Death (hour)					
		1	2	3	4	20	24
4d	10	0	0	0	0	0	0
	100	0	0	0	0	0	8±1.17
	500	0	0	0	0	0	**35±1.53**
4e	10	0	0	0	0	0	0
	100	0	0	0	0	0	6±0.57
	500	0	0	0	0	0	**43±2.10**
4f	10	0	0	0	0	0	0
	100	0	0	0	0	0	5±0.57
	500	0	0	0	0	0	**45±0.3**
4m	10	0	0	0	0	0	0
	100	0	0	0	0	0	5±0.59
	500	0	0	0	0	0	**30±1.50**
4q	10	0	0	0	0	0	0
	100	0	0	0	0	0	1±0.55
	500	0	0	0	0	0	**16±1.54**
4r	10	0	0	0	0	0	0
	100	0	0	0	0	0	0
	500	0	0	0	0	0	**31±0.53**
4s	10	0	0	0	0	0	0
	100	0	0	0	0	0	0
	500	0	0	0	0	0	**21±0.54**

Values are expressed as mean (±SD), n=3

The study was based on the ability of the test compounds to kill active nauplii. Reported protocols [Meyer *et al.,* 1982] specify crude extracts and pure substances can be classified as toxic (Brine shrimp death > 50%) or non-toxic (Brine shrimp death < 50%). All test

compounds were completely devoid of cytotoxicity after 20 hours of exposure but compounds **4d, 4e, 4f, 4m** and **4q** showed minimal toxicity after 24 hours of exposure. The α-APs are known for their low levels of toxicity [Krishnaa *et al.,* 2010]. Therefore, minimal cytotoxicity of these compounds was anticipated.

The antimicrobial activity of **4a-4t** was screened using the agar disc diffusion method against four bacterial strains and three yeast cultures. The results are shown as zones of inhibition in Tables 14 and 15 respectively.

Table 14: Antibacterial activity of synthesized MPQ-α-APs (**4a-4t**)

Compound	Bacteria			
	B. cereus	*M. Luteus*	*S. aureus*	*K. pneumonia*
4a	0	0	0	0
4b	0	0	0	0
4c	0	0	0	0
4d	0	0	0	0
4e	0	0	0	0
4f	0	0	0	0
4g	0	0	0	0
4h	0	0	0	0
4i	0	0	0	0
4j	0	0	0	0
4k	0	0	0	0
4l	0	0	0	0
4m	9±0.5	9±0.8	0	0
4n	0	0	0	0
4o	0	0	0	0
4p	0	0	0	0
4q	0	0	0	0
4r	0	7±0.6	9±0.5	0
4s	0	0	0	0
4t	0	0	0	0
Control Ciprofloxacin	28±0.5	30±0.7	25±1	28±1.4

Values are mean ±SD, number of samples (n=3), 0= no activity

Table 15: Antifungal activity of synthesized MPQ-α-APs (**4a-4t**)

Compound	Yeast		
	C. albicans	*C. utilus*	*S. cerevisiae*
4a	0	0	0
4b	0	0	0
4c	0	0	0
4d	0	0	0
4e	0	0	0
4f	0	0	0
4g	0	0	0
4h	0	0	0
4i	0	0	0
4j	0	0	0
4k	0	0	0
4l	0	0	0
4m	0	0	0
4n	0	0	0
4o	0	0	0
4p	0	0	0
4q	0	0	0
4r	0	0	0
4s	0	0	0
4t	0	0	0
Control Amphotericin	31±0.2	28±0.6	26±0.0

Values are mean ±SD (n=3), 0= no activity

The MIC was determined by serial dilution of the test compounds to levels where the inhibition of bacterial growth could not be detected. The results are summarized in Table 16. The inhibitory zone of compounds: (A) **4m**, (B) **4r** and (C) Ciprofloxacin against *B. cereus, M. luteus and S. aureus* are also shown in Figures 29, 30 and 31.

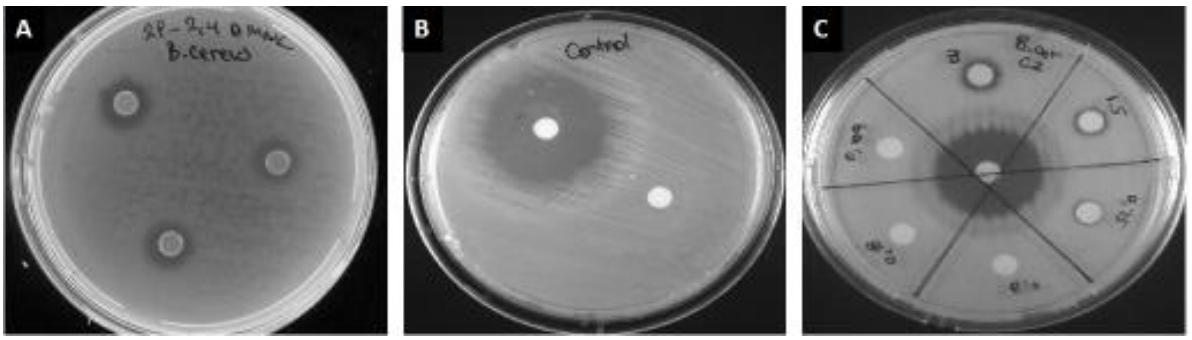

Figure 29: Antibacterial screening showing zones of inhibition produced by compounds: (A) **4m**, (B) Ciprofloxacin (positive control), (C) MIC, against *B. cereus*

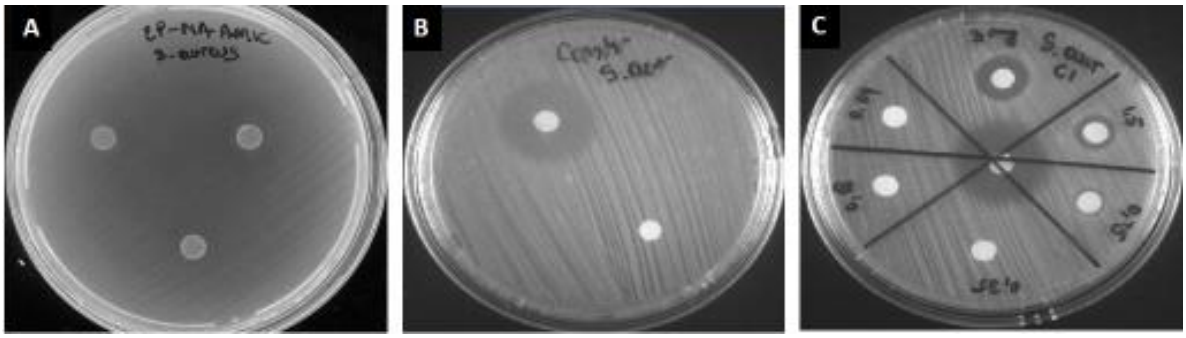

Figure 30: Antibacterial screening showing zones of inhibition produced by compounds: (A) **4r**, (B) Ciprofloxacin (positive control), (C) MIC, against *S. aureus*

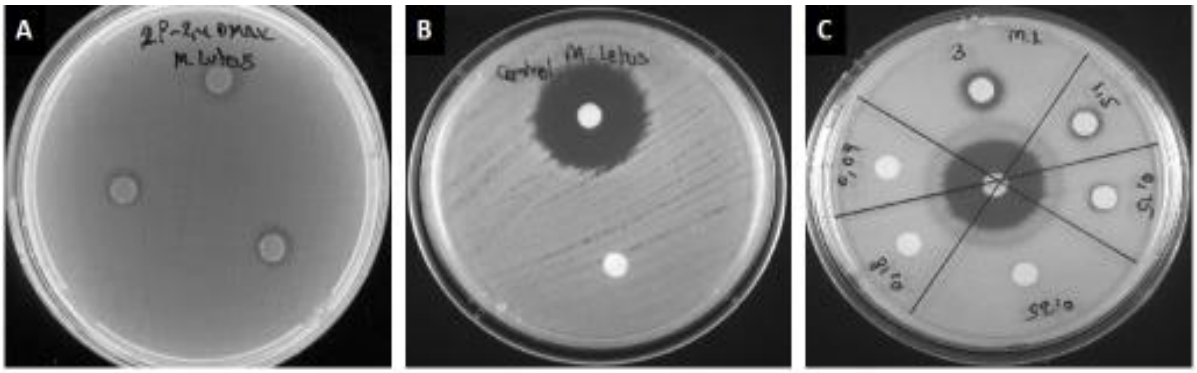

Figure 31: Antibacterial screening showing zones of inhibition produced by compounds: (A) **4m**, (B) Ciprofloxacin (positive control), (C) MIC, against *M. Luteus*

Compound **4m** displayed a MIC of 0.75 mg/mL and 0.35 mg/mL against *B. cereus* and M. *luteus,* respectively while compound **4r** revealed a MIC of 0.75 mg/mL against *S. aureus*. These results are summarized in Table 16.

Table 16: Minimum inhibition concentration (MIC) of synthesized MPQ-α-APs derivatives

Compound	MIC (mg/mL)		
	B. cereus	*M. luteus*	*S. aureus*
4m	0.75	0.35	na
4r	na	na	0.75

Values are mean ±SD (n=3), standard deviation = 0, number of samples (n=3), na: not applicable

It has been reported that the pharmacological effects of α-APs are stereoselective [Łyżwa Mikołajczyk, 2014]. Therefore the antibacterial effect of the compounds may be stereoselective and the antibacterial evaluation of each enantiomer is suggested to confirm this matter. Other reports propose that the presence of α-AP moiety at fourth position of the quinoline system significantly increases the antibacterial activity [Cai Li, 1999]. The agar disc diffusion assay is widely used for antimicrobial susceptibility testing and offers many advantages over other methods: simple execution, low cost, large scale sample testing and results are easily interpreted. However, there are limitations to this method; one should be mindful of the fact that the agar disc diffusion method is not applicable to some pathogenic microorganisms and can be problematic when testing certain antibiotics due to their specific physicochemical properties.

The antioxidant activity of **4a-4t** were screened using the DPPH assay. Results are shown as percentage (±SD) (Table 17). The results are also represented graphically in Figure 32.

Table 17: Percentage antioxidant activity of synthesized MPQ-α-APs (**4a-4t**)

Compounds	Concentration (µg/mL)								
	1 µg/mL	20 µg/mL	40 µg/mL	60 µg/mL	80 µg/mL	100 µg/mL	250 µg/mL	500 µg/mL	1000 µg/mL
4a	0,17 ± 0,02	0,72 ±0,01	3,44 ± 0,05	4,64 ± 0,06	5,19 ±0,02	8,21 ± 0,15	5,15 ± 0,01	9,97 ± 0,07	14,71 ± 0,01
4b	0	0	0	0	0	0	0	0	0
4c	7,2 ± 0,02	15,1 ± 0,01	21,1 ± 0,01	24,9 ± 0,02	27,7 ± 0,01	29,9 ± 0,01	33,6 ± 0,01	41,1 ± 0,02	42,0 ± 0.06
4d	0,82 ± 0,01	1,72 ± 0,03	4,30 ± 0,04	6,12 ± 0,06	9,76 ± 0,08	11,62 ± 0,11	14,19 ± 0,09	17,18 ± 0,03	21,17 ± 0,08
4e	0,55 ± 0,02	3, 64 ± 0,04	6,74 ± 0,12	8,38 ± 0,07	11,00 ± 0,08	12,03 ± 0,15	17,25 ± 0,05	28,63 ± 0,01	36,63 ± 0,01
4f	5,89 ±0,05	22,10 ± 0,05	38,99 ± 0,03	52,77 ± 0,03	63,12 ± 0,06	84,14 ± 0,05	90,93 ± 0,01	92,86 ± 0,00	94,24 ± 0,00
4g	0,52 ± 0,01	7,11 ± 0,06	9,28 ± 0,06	11,37 ± 0,09	12,82 ± 0,08	15,60 ± 0,08	16,98 ± 0,09	21,86 ± 0,11	30,52 ± 0,05
4h	7,56 ± 0,09	15,46 ± 0,11	17,18 ± 0,05	21,99 ± 0,06	24,05 ± 0,09	26,80 ± 0,04	29,21 ± 0,07	34,36 ± 0,05	38,49 ± 0,10
4i	11,5 ± 0,86	15,7 ± 0,82	19,1 ± 0,78	21,6 ± 0,76	24,1 ± 0,74	29,3 ± 0,69	33,7 ± 0,64	36,3 ± 0,62	40,4 ± 0,58
4j	0	0	0	0	0	0	0	0	0
4k	0,41 ± 0,03	3,47 ± 0,05	7,94 ± 0,10	10,82 ± 0,05	13,02 ± 0,03	15,98 ± 0,06	22,04 ± 0,06	27,53 ± 0,08	29, 66 ± 0,17
4l	0	0	0	0	0	0	0	0	0
4m	4,12 ± 0,05	6,36 ± 0,07	14,78 ± 0,13	15,46 ± 0,10	17,42 ± 0,09	21,48 ± 0,11	26,12 ± 0,09	34,64 ± 0,04	40,21 ± 0,01
4n	0,58 ± 0,02	2,99 ± 0,04	6,77 ± 0,07	9,90 ± 0,02	13,23 ± 0,04	16,94 ± 0,01	25,09 ± 0,06	30,65 ± 0,07	34,36 ± 0,00
4o	0	0	0	0	0	0	0	0	0
4p	0,79 ± 0,00	2,16 ±0,02	5,02 ± 0,03	8,04 ± 0,05	8,76 ± 0,07	10,62 ± 0,05	13,81 ± 0,11	18,28 ± 0,08	22,71 ± 0,01
4q	0	0	0	0	0	0	0	0	0
4r	0,65 ±0,01	8,49 ± 0,03	9,73 ± 0,01	15,46 ± 0,04	28,18 ± 0,06	32,30 ± 0,06	42,54 ± 0,04	56,74 ± 0,02	67,32 v 0,01
4s	0	0	0	0	0	0	0	0	0
4t	0	0	0	0	0	0	0	0	0
Methanol (-control)	-	-	-	-	-	-	-	-	0
Rutin (+control)	-	-	-	-	-	-	-	-	96.32

Values are mean ±SD (n=3), 0= no activity

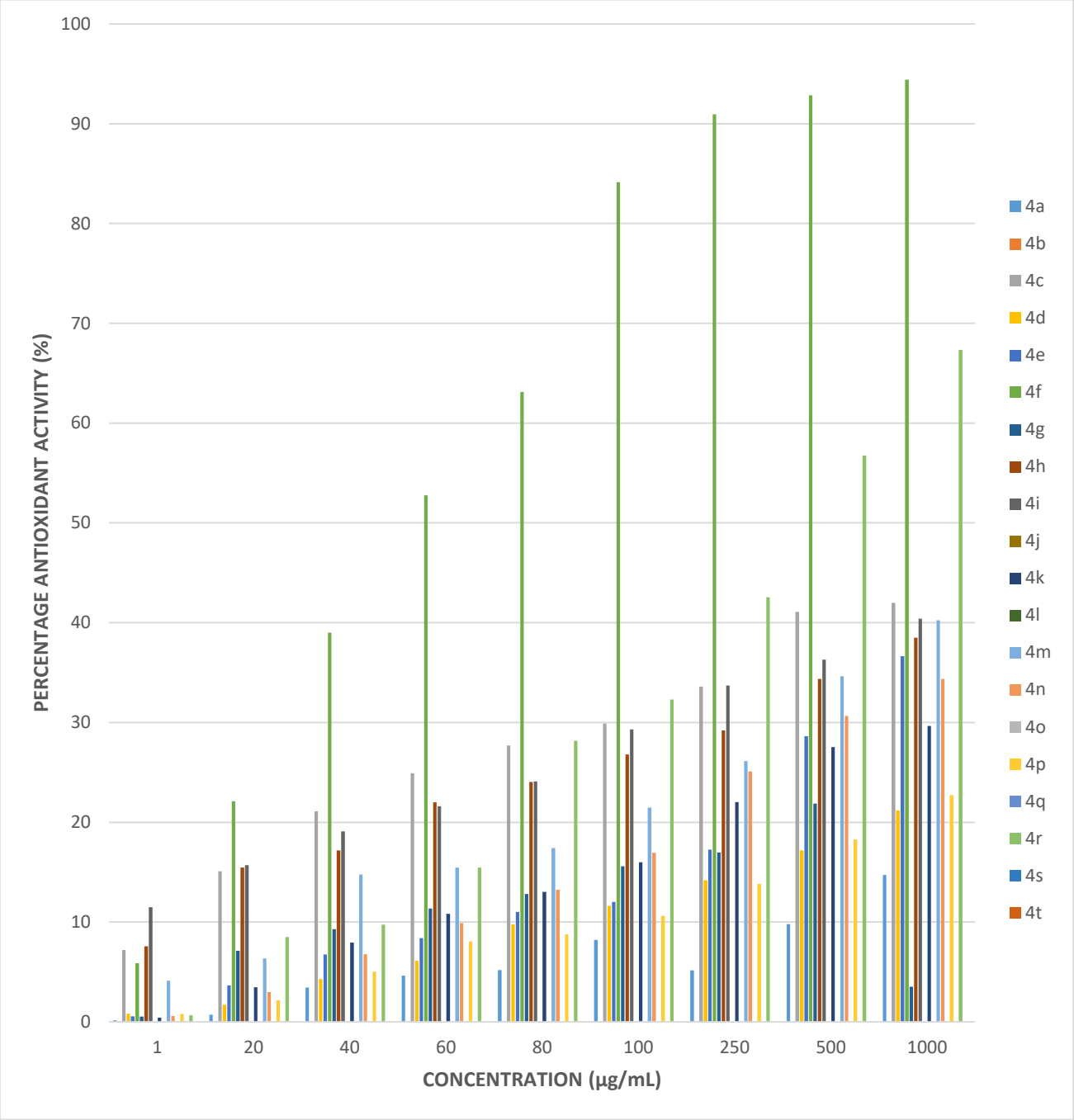

Figure 32: Percentage antioxidant activity of the synthesized MPQ-α-APs (**4a-4t**)

The DPPH assay is widely used to determine the radical scavenging capacity of various synthetic compounds. DPPH is a nitrogen cantered organic compound composed of stable free radicals [Eklund *et al.,* 2005]. The hydrogen donating ability of the test compounds have an effect on the scavenging DPPH i.e. on accepting hydrogen atoms, DPPH becomes a stable diamagnetic molecule. The initial deep purple colour of the DPPH solution turned to the pale yellow diphenylpicrylhydrazine (DPPH.H) solution. Discolouration occurred as a result of the decreasing quantity of DPPH radicals in the environment. The extent of discolouration of the DPPH therefore reflected the radical scavenging capacity of the test compounds. This colour change was observed spectrophotometrically at a maximum absorbance of 517 nm [Tirzitis Bartosz, 2010].

Results from this study showed the antioxidant activity of MPQ-α-AP derivatives tested by the DPPH assay. A few of the test compounds did not show antioxidant activity but compounds **4f** and **4r** exhibited the highest antioxidant activity with values of 94.24 % and 67.32 % respectively. It is interesting to note the chemical composition of these compounds. Compound **4f** has a fluoro group at position C5'' and **4r** displays the benzenoid ring naphthalene on its molecular system.

While the scavenging capacity of compounds **4f** and **4r** were lower than that of the standard positive control rutin, results served as evidence that these compounds are indeed hydrogen donating. The scavenging capacity of **4f** is almost as potent as the standard control rutin - **4f** at 94.24 % and rutin at 96.32 %. Therefore, it is suggested that further work on the synthesis, identification and antioxidant applications of this compound should be done. This could ultimately lead to its inclusion in pharmaceutical formulation developments. The scavenging capacity of **4r** at 67.32 % indicates noticeable antioxidant potential. This compound may possibly act as a primary antioxidant.

Although the DPPH assay is a widely used method, limitations remain as the centralized location of the nitrogen free radical in the DPPH molecular structure is freely accessible to small molecules. Larger molecules may have limited access to this radical portion due to steric hindrances and materials that have a strong absorbance at the same wavelength as DPPH will interfere with the assay.

Conclusion

α-AP compounds find applications in the fields of medicine, agriculture and industry. They are especially important in the field of medicine and display a vast spectrum of biological properties due to their structural similarities to natural α-amino acids. Many efforts have been made towards their synthesis however, conventional methods suffer drawbacks that include less accessibility of reagents and require a long reaction time. Hence the search for the development of a synthetic protocol for α-APs that is green, simple and efficient remains a continued and ever-challenging objective.

In continuation of scientists' endless development of novel organic synthetic methodologies, a novel heterogeneous palladium strontium titanate catalyst was prepared and characterized by several instrumental techniques. This material was then used to prepare and fully characterize a series of twenty novel MPQ-α-APs following the Kabachnik Fields reaction sequence under MW irradiation conditions. The catalyst was seen as stable and did not show any decrease in catalytic activity hence could be used five times over. This synthetic reaction proceeded with high efficiency to give corresponding α-aminophosphonate which are imperative for the construction of biologically important compounds. The methodology reported in this thesis offers significant advantages in terms of simple operation, cost effectiveness, cleaner conversion and excellent reusability of the catalyst while offering high product yields.

The toxicity of **4d**, **4e**, **4f**, **4m**, **4q**, **4r** and **4s** were evaluated using the Brine shrimp lethality assay. This study disclosed that the tested compounds did not show noteworthy toxicity against the Brine shrimp even at a concentration of up to 500 µg/mL after a 24 hour period. This illustrates the potential value of the compounds in medicinal and biological applications and should be investigated further.

Twenty novel MPQ-α-AP derivatives were assessed for their antibacterial activity. The results revealed that compounds **4m** and **4r** have slight activity compared to that of the standard ciprofloxacin. Compound **4m** showed antibacterial activity with MIC of 0,75 mg/mL for both *B. cereus* and *M. leteus*. Compound **4r** showed antibacterial activity with MIC of 0,75 mg/mL for *S. aureus*.

Twenty novel MPQ-α-AP derivatives were assessed for their antioxidant activity and compared to the standard control quercetin-3-rutinoside at 96.32 %. The results revealed that two of the compounds **4f** and **4r** have notable antioxidant activity of 94.24 % and 67.32 % respectively. The remaining compounds showed low antioxidant activity within a range of 21 – 42 % at 1 mg/mL.

Many challenges remain in this area of study, some known while many wait to be revealed by new discoveries or creative disruptions. No tool, instrument or researcher can understand catalysed organic synthesis entirely and so it remains an active, multifaceted and evolving field of study.

List of References

Abdel-Megeed, M. F., Badr, B. E., Azaam, M. M., El-Hiti, G. A. 2012. Synthesis and Antimicrobial Activities of a Novel Series of Heterocyclic α-Aminophosphonates. *Archiv der Pharmazie*, 10, 784-789.

Adrian, N. R., Suflita, J. M. 1994. Anaerobic biodegradation of halogenated and nonhalogenated N-, s-, and o-heterocyclic compounds in aquifer slurries. *Environmental Toxicology and Chemistry*, 13, 1551-1557.

Akbarzadeh, R., Mirzaei, P., Bazgir, A. 2010. A simple synthesis of ferrocenyl bis-amides by a Ugi four-component reaction. *Journal of Organometallic Chemistry*, 695, 2320-2324.

Akkada, A. A., Messmer, D. A., Fina, L. R., Bartley, E. E. 1968. Distribution of 2-Aminoethylphosphonic Acid in Some Rumen Microorganisms. *Journal of Dairy Science*, 51, 78-81.

Anand, S. P., Sati, N. 2013. Artificial preservatives and their harmful effects: looking toward nature for safer alternatives. *International Journal of Pharmaceutical Sciences and Research*, 7, 2496.

Antunes, L., Visca, P.,Towner, K. J. 2014. Acinetobacter baumannii: evolution of a global pathogen. *Pathogens and Disease*, 71, 292-301.

Arend, M., Westermann, B., Risch, N. 1998. Modern variants of the Mannich reaction. *Angewandte Chemie International Edition*, 37, 1044-1070.

Astruc, D. 2008. *Nanoparticles and catalysis*. John Wiley & Sons.

Atherton, F. R., Hassall, C. H., Lambert, R. W. 1986. Synthesis and structure-activity relationships of antibacterial phosphonopeptides incorporating (1-aminoethyl) phosphonic acid and (aminomethyl) phosphonic acid. *Journal of Medicinal Chemistry*, 29, 29-40.

Badadhe, P. V., Chavan, N. M., Ghotekar, D. S., Mandhane, P. G., Joshi, R. S., Gill, C. H. 2011. Synthesis, Characterization, and Biological Screening of Some Novel Thiazolidin-4-One and α-Aminophosphonate Derivatives. *Phosphorus, Sulfur, and Silicon and the Related Elements*, 10, 2021-2032.

Balakrishna, A., Reddy, M. V. N., Rao, P. V., Kumar, M. A., Kumar, B. S., Nayak, S. K., Banerjee, B. 2017. Recent developments on ultrasound assisted catalyst-free organic synthesis. *Ultrasonics Sonochemistry*, *35*, 1-14.

Barr, E. S. 1960. Historical survey of the early development of the infrared spectral region. *American Journal of Physics*, 1, 42-54.

Bax, A., Ikura, M., Kay, L. E., Torchia, D. A. Tschudin, R. 1990. Comparison of different modes of two-dimensional reverse-correlation NMR for the study of proteins. Journal of Magnetic Resonance (1969), 2, 04-318.

Benner, S. A., Ricardo, A., Carrigan, M. A. 2004. Is there a common chemical model for life in the universe?. *Current Opinion in Chemical Biology*, 8, 672-689.

Benton, E. 1974. Vitalism in nineteenth-century scientific thought: a typology and reassessment. *Studies in History and Philosophy of Science Part A*, *5*(1), 17-48.

Bera, K., Namboothiri, I. N. 2012. Enantioselective Synthesis of Quaternary α-Aminophosphonates via Conjugate Addition of α-Nitrophosphonates to Enones. *Organic Letters*, 14, 980-983.

Bera, K., Namboothiri, I. N. 2014. Asymmetric synthesis of quaternary α-amino acids and their phosphonate analogues. *Asian Journal of Organic Chemistry*, 3, 1234-1260.

Berlan, J. 1995. Microwaves in chemistry: another way of heating reaction mixtures. *Radiation Physics and Chemistry*, 45, 581-589.

Bernardi, L., Zhuang, W., Jørgensen, K. A. 2005. An easy approach to optically active α-Amino phosphonic acid derivatives by Chiral Zn (II)-Catalyzed enantioselective amination of phosphonates. *Journal of the American Chemical Society*, 127, 5772-5773.

Bhagat, S., Chakraborti, A. K. 2007. An extremely efficient three-component reaction of aldehydes/ketones, amines, and phosphites (Kabachnik− Fields reaction) for the synthesis of α-aminophosphonates catalyzed by magnesium perchlorate. *The Journal of Organic Chemistry*, 72, 1263-1270.

Bhagat, S., Chakraborti, A. K. 2007. An extremely efficient three-component reaction of aldehydes/ketones, amines, and phosphites (Kabachnik− Fields reaction) for the synthesis of α-aminophosphonates catalyzed by magnesium perchlorate. *The Journal of organic chemistry*, 72, 1263-1270.

Bhattacharya, A. K., Thyagarajan, G. 1981. Michaelis-arbuzov rearrangement. *Chemical Reviews*, 81, 415-430.

Bhattacharya, A. K., Thyagarajan, G. 1981. Michaelis-arbuzov rearrangement. *Chemical reviews*, 81, 415-430.

Boukallaba, K., Elachqar, A., El Hallaoui, A., Alami, A., El Hajji, S., Labriti, B., Rolland, V. 2006. Synthesis of new α-heterocyclic α-aminophosphonates. *Phosphorus, Sulfur, and Silicon*, 181, 819-823.

Brzezińska-Rodak, M., Klimek-Ochab, M., Żymańczyk-Duda, E., Kafarski, P. 2011. Biocatalytic resolution of enantiomeric mixtures of 1-aminoethanephosphonic acid. *Molecules*, 16, 5896-5904.

Cao, G., Alessio, H. M., Cutler, R. G. 1993. Oxygen-radical absorbance capacity assay for antioxidants. *Free Radical Biology and Medicine*, 14, 303-311.

Cavallini, G., Massarani, E. 2002. The concept of a supporting moiety as applied to the synthesis of anti-viral compounds. *Journal of Medicinal Chemistry*, 4, 365-370.

Chambers, J. R., Isbell, A. F. 1964. A New Synthesis of Amino Phosphonic Acids1. *The Journal of Organic Chemistry*, 29, 832-836.

Chang, H., Rodrigues, R. P., Xu, J. H., Ellis, D. E., Dravid, V. P. 1997. Electronic structure of grain boundaries in SrTiO3. *Ferroelectrics*, 194, 249-262.

Chen, Y., Zhang, F., Snyder, D., Gan, Z., Bruschweiler-Li, L., Brüschweiler, R. 2007. Quantitative covariance NMR by regularization. *Journal of Biomolecular NMR*, 3, 73-77.

Chinchilla, R., Nájera, C., Yus, M. 2004. Metalated heterocycles and their applications in synthetic organic chemistry. *Chemical reviews*, 104, 2667-2722.

Choi, C. W., Kim, S. C., Hwang, S. S., Choi, B. K., Ahn, H. J., Lee, M. Y., Park, S. H., Kim, S. K. 2002. Antioxidant activity and free radical scavenging capacity between Korean medicinal plants and flavonoids by assay-guided comparison. *Plant Science*, 163, 1161-1168.

Chu, D. T. 1988. *U.S. Patent No. 4,730,000*. Washington, DC: U.S. Patent and Trademark Office.

Colthup, N. 2012. *Introduction to Infrared and Raman Spectroscopy*. Elsevier.

Cos, P., Vlietinck, A. J., Berghe, D. V., Maes, L. 2006. Anti-infective potential of natural products: how to develop a stronger in vitro 'proof-of-concept'. *Journal of Ethnopharmacology*, 106, 290-302.

Cristau, H. J., Lambert, J. M., Pirat, J. L. 1998. Synthesis and Characterization of New Cα, α-Disubstituted (Diarylaminomethyl)-phosphonates. *Synthesis*, 8, 1167-1170.

Cronin, J. R., Pizzarello, S. 1983. Amino acids in meteorites. *Advances in Space Research*, 3, 5-18.

Dake, S. A., Raut, D. S., Kharat, K. R., Mhaske, R. S., Deshmukh, S. U., Pawar, R. P. 2011. Ionic liquid promoted synthesis, antibacterial and in vitro antiproliferative activity of novel α-aminophosphonate derivatives. *Bioorganic & Medicinal Chemistry Letters*, 21, 2527-2532.

Daştan, A., Kulkarni, A., Toeroek, B. 2012. Environmentally benign synthesis of heterocyclic compounds by combined microwave-assisted heterogeneous catalytic approaches. *Green Chemistry*, 14, 17-37.

Davis, F. A., Lee, S., Yan, H., Titus, D. D. 2001. Asymmetric synthesis of quaternary α-amino phosphonates using sulfinimines. *Organic letters*, 11, 1757-1760.

Dias, D. A., Urban, S., Roessner, U. 2012. A historical overview of natural products in drug discovery. *Metabolites*, 2, 303-336.

Disale, S. T., Kale, S. R., Kahandal, S. S., Srinivasan, T. G., Jayaram, R. V. 2012. Choline chloride· $2ZnCl_2$ ionic liquid: an efficient and reusable catalyst for the solvent free Kabachnik–Fields reaction. *Tetrahedron Letters*, 53, 2277-2279.

Eklund, P. C., Långvik, O. K., Wärnå, J. P., Salmi, T. O., Willför, S. M., Sjöholm, R. E. 2005. Chemical studies on antioxidant mechanisms and free radical scavenging properties of lignans. *Organic & biomolecular chemistry*, 18, 3336-3347.

El-Barbary, A. A., El-Shehawy, A. A., Abdo, N. I. 2014. Synthesis and antimicrobial activities of some 6-methyl-3-thioxo-2, 3-dihydro-1, 2, 4-triazine derivatives. *Phosphorus, Sulfur, and Silicon and the Related Elements*, 3, 400-409.

El-Magbri, M. 2014. The Synthesis and Analysis of Aspirin.

Enterkin, J. A., Setthapun, W., Elam, J. W., Christensen, S. T., Rabuffetti, F. A., Marks, L. D., Marshall, C. L. 2011. Propane oxidation over Pt/SrTiO3 nanocuboids. *Acs Catalysis*, 6, 629-635.

Farrauto, R. J., Heck, R. M. 1999. Catalytic converters: state of the art and perspectives. *Catalysis Today*, 51, 351-360.

Farrauto, R. J., Heck, R. M. 2000. Environmental catalysis into the 21st century. *Catalysis Today*, 55, 179-187.

Feng, Z., Kazimirov, A., Bedzyk, M. J. 2011. Atomic imaging of oxide-supported metallic nanocrystals. *Acs Nano*, 5, 9755-9760.

Firouzabadi, H., Iranpoor, N., Sobhani, S. 2004. Metal triflate-catalyzed one-pot synthesis of α-aminophosphonates from carbonyl compounds in the absence of solvent. *Synthesis*, 16, 2692-2696.

Fisher, B., Harvey, R. P., Champe, P. C. 2007. Lippicott's Illustrated Reviews: Microbiology. *Lippicott's Illustrated Reviews Series.* Lippictt Williams and Wilkins, Hagerstown, MD.

Frost, A., Pearson, R. 1961. Kinetics and mechanism. *The Journal of Physical Chemistry*, 65, 384-384.

Fuloria, N., Fuloria, S. 2013. Structural elucidation of small organic molecules by 1D, 2D and multi-dimensional-solution NMR spectroscopy. *J Anal Bioanal Techniques S*, *1*, 1-8.

Ganem, B. 2009. Strategies for innovation in multicomponent reaction design. *Accounts of Chemical Research*, 42, 463-472.

Gao, G. L., Niu, Y. N., Yan, Z. Y., Wang, H. L., Wang, G. W., Shaukat, A., Liang, Y. M. 2010. Unexpected domino reaction via Pd-catalyzed sonogashira coupling of benzimidoyl chlorides with 1, 6-enynes and cyclization to synthesize quinoline derivatives. *The Journal of Organic Chemistry*, 75, 1305-1308.

Geisler, E., Heller, O. 1998. The Rise of New Scientific Fields of Study from Established Disciplines. *Management of Medical Technology*, 259-272.

Gosset, G., Satre, M., Blaive, B., Clement, J. L., Martin, J. B., Culcasi, M., Pietri, S. 2008. Investigation of subcellular acidic compartments using α-aminophosphonate 31P nuclear magnetic resonance probes. *Analytical Biochemistry*, 2, 184-194.

Griesinger, C., Sørensen, O. W., Ernst, R. R. 1987. Practical aspects of the E. COSY technique. Measurement of scalar spin-spin coupling constants in peptides. *Journal of Magnetic Resonance* , 3, 474-492.

Gröger, H. 2003. Catalytic enantioselective Strecker reactions and analogous syntheses. *Chemical Reviews*, 103, 2795-2828.

Gurib-Fakim, A. 2006. Medicinal plants: traditions of yesterday and drugs of tomorrow. *Molecular Aspects of Medicine*, *27*, 1-93.

H Kudzin, Z., H Kudzin, M., Drabowicz, J., V Stevens, C. 2011. Aminophosphonic acids-phosphorus analogues of natural Amino Acids. Part 1: Syntheses of α-aminophosphonic acids. *Current Organic Chemistry*, 15, 2015-2071.

Ha, H. J., Nam, G. S. 1992. An efficient synthesis of anilinobenzylphosphonates. *Synthetic Communications*, 22, 1143-1148.

Han, S. H., Ahn, W. S., Lee, H. C., Choi, S. K. 2007. Ferroelectric properties of heteroepitaxial PbTiO 3 and PbZr 1–x Ti x O 3 films on Nb-doped SrTiO 3 fabricated by hydrothermal epitaxy below Curie temperature. *Journal of Materials Research*, 22, 1037-1042.

Hartley, F. R. 2012. *Supported metal complexes: a new generation of catalysts*, 6. Springer Science & Business Media.

Haslam, E. 1996. Natural polyphenols (vegetable tannins) as drugs: possible modes of action. *Journal of Natural Products*, 59, 205-215.

Heydari, A., Arefi, A., Khaksar, S., Shiroodi, R. K. 2007. Guanidine hydrochloride: An active and simple catalyst for Strecker type reaction. *Journal of Molecular Catalysis A: Chemical*, 271, 142-144.

Hikita, T., Hanada, T., Kudo, M., Kawai, M. 1993. Structure and electronic state of the TiO_2 and SrO terminated SrTiO3 (100) surfaces. *Surface Science*, 287, 377-381.

Hill, R. D., Lahav, E., Givol, D. 1974. A rennin-sensitive bond in α s1 B-casein. *Journal of Dairy Research*, 41, 147-153.

Hopkins, A. L. 2008. Network pharmacology: the next paradigm in drug discovery. *Nature Chemical Biology*, 4, 682.

Houghton, P. J. 2001. Old yet new-pharmaceuticals from plants. *Journal of Chemical Education*, 78, 175.

Huang, J., Chen, R. 2000. An overview of recent advances on the synthesis and biological activity of α-aminophosphonic acid derivatives. *Heteroatom Chemistry: An International Journal of Main Group Elements*, 11, 480-492.

Hulme, C., Dietrich, J. 2009. Emerging molecular diversity from the intra-molecular Ugi reaction: iterative efficiency in medicinal chemistry. *Molecular Diversity*, 13, 195.

Inderwildi, O. R., Starukhin, D., Volpp, H. R., Lebiedz, D., Deutschmann, O., Warnatz, J. 2007. Springer, Berlin, Heidelberg: Reaction processes on catalytically active surfaces. *In Reactive Flows, Diffusion and Transport*, 311-340.

Indu, S., Kaliappan, K. P. 2018. A new and informative [a, b, c, d] nomenclature for one-pot multistep transformations: a simple tool to measure synthetic efficiency. *RSC Advances*, 8, 21292-21305.

Iyer, M. S., Gigstad, K. M., Namdev, N. D., Lipton, M. 1996. Asymmetric catalysis of the Strecker amino acid synthesis by a cyclic dipeptide. *Journal of the American Chemical Society*, 118, 4910-4911.

Jaiyeola, A. O., Anand, K., Kasumbwe, K., Ramesh, M., Gengan, R. M. 2017. Catalytic synthesis of α-amino chromone phosphonates and their antimicrobial, toxicity and potential HIV-1 RT inhibitors based on silico screening. *Journal of Photochemistry and Photobiology B: Biology*, 166, 136-147.

Joshi, P. C., Krupanidhi, S. B. 1993. Structural and electrical characteristics of SrTiO3 thin films for dynamic random access memory applications. *Journal of Applied Physics*, 73, 7627-7634.

Kale, M., Patwardhan, K. 2013. Synthesis of heterocyclic scaffolds with anti-hyperlipidemic potential: a review. *Der Pharma Chemica*, 5, 213-22.

Kappe, C. O. 1993. 100 years of the Biginelli dihydropyrimidine synthesis. *Tetrahedron*, 49, 6937-6963.

Kappe, C. O. 2004. Controlled microwave heating in modern organic synthesis. *Angewandte Chemie International Edition*, 43, 6250-6284.

Kappe, C. O., Stadler, A., Dallinger, D. 2012. *Microwaves in organic and medicinal chemistry*. John Wiley & Sons.

Karimi-Jaberi, Z., Amiri, M. 2010. One-pot synthesis of α-aminophosphonates catalyzed by boric acid at room temperature. *Heteroatom Chemistry: An International Journal of Main Group Elements*, 21, 96-98.

Kaur, K., Jain, M., Reddy, R. P., Jain, R. 2010. Quinolines and structurally related heterocycles as antimalarials. *European Journal of Medicinal Chemistry*, 45, 3245-3264.

Kawamura, H., Mori, M., Hashimoto, S. I., Uotani, M. 2009. Development of Pd-coated ceramic electrodes in hybrid sulphur cycle. *International Journal of Nuclear Hydrogen Production and Applications*, 2, 29-41.

Kawasaki, M., Takahashi, K., Maeda, T., Tsuchiya, R., Shinohara, M., Ishiyama, O., Koinuma, H. 1994. Atomic control of the SrTiO3 crystal surface. *Science*, 266, 1540-1542.

Keglevich, G., Bálint, E. 2012. The Kabachnik–Fields reaction: Mechanism and synthetic use. *Molecules*, 17, 12821-12835.

Keglevich, G., Szekrenyi, A. 2008. Eco-Friendly Accomplishment of the Extended Kabachnik-Fields Reaction; a Solvent-and Catalyst-Free Microwave-Assisted Synthesis of α-Aminophosphonates and α-Aminophosphine Oxides. *Letters in Organic Chemistry*, 5, 616-622.

Keller, J., Bless, H. 2008. When positive and negative expectancies disrupt performance: Regulatory focus as a catalyst. *European Journal of Social Psychology*, 38, 187-212.

Kemp, W. 1991. *Infrared spectroscopy In Organic Spectroscopy*, 19-99. Palgrave, London.

Kenawy, E. R. S., Azaam, M. M., Saad-Allah, K. M. 2015. Synthesis and antimicrobial activity of α-aminophosphonates containing chitosan moiety. *Arabian Journal of Chemistry*, 8, 427-432.

Khine, M. S. S., Chen, L., Zhang, S., Lin, J., Jiang, S. P. 2013. Syngas production by catalytic partial oxidation of methane over (La0. 7A0. 3) BO3 (A= Ba, Ca, Mg, Sr, and B= Cr or Fe) perovskite oxides for portable fuel cell applications. *International Journal of Hydrogen Energy*, 38, 13300-13308.

Kostova, I. 2005. Synthetic and natural coumarins as cytotoxic agents. *Current Medicinal Chemistry-Anti-Cancer Agents*, 5, 29-46.

Kotecka, B. M., Barlin, G. B., Edstein, M. D., Rieckmann, K. H. 1997. New quinoline di-Mannich base compounds with greater antimalarial activity than chloroquine, amodiaquine, or pyronaridine. *Antimicrobial Agents and Chemotherapy*, 41, 1369-1374.

Krishnaa, A. B., Reddya, M. V. N., Reddya, G. C. S., Krishnaa, B. S., Nayakb, S. K., Reddy, C. S. 2010. Synthesis, anti-oxidant and antibacterial properties of diethyl (4-flouro-3-nitro phenylamino)(substituted phenyl) methyl phosphonates. *The International Journal of Applied Biology and Pharmaceutical Technology*, 1, 873-882.

Krishnaraju, A. V., Rao, T. V., Sundararaju, D., Vanisree, M., Tsay, H. S., Subbaraju, G. V. 2005. Assessment of bioactivity of Indian medicinal plants using brine shrimp (Artemia salina) lethality assay. *International Journal of Applied Science and Engineering*, 3, 125-34.

Kumar, D., Sandhu, J. S. 2010. Microwave enhanced, solvent free green protocol for the production of 3, 4-dihydropyrimidine-2-(1H)-ones using $AlCl_3$. $6H_2O$ as a catalyst.

Kumar, S., Bawa, S.,Gupta, H. 2009. Biological activities of quinoline derivatives. *Mini Reviews in Medicinal Chemistry*, 9, 1648-1654.

Kwan, E. E., Huang, S. G. 2008. Structural elucidation with NMR spectroscopy: practical strategies for organic chemists. *European journal of organic chemistry*, 16, 2671-2688.

Lafaye, G., Liang, C. 2017. Catalysis Science & Technology. *Catalysis*, 22, 5171-5468.

Laschat, S., Kunz, H. 1992. Carbohydrates as chiral templates: stereoselective synthesis of (R)-and (S)-α-aminophosphonic acid derivatives. *Synthesis*, 01/02, 90-95.

Lavielle, G., Hautefaye, P., Schaeffer, C., Boutin, J. A., Cudennec, C. A., Pierre, A. 1991. New. alpha.-amino phosphonic acid derivatives of vinblastine: chemistry and antitumor activity. *Journal of Medicinal Chemistry*, 34, 1998-2003.

Lemire, J. A., Harrison, J. J., Turner, R. J. 2013. Antimicrobial activity of metals: mechanisms, molecular targets and applications. *Nature Reviews Microbiology*, 11, 371.

Lerner, L. Bax, A. 1986. Sensitivity-enhanced two-dimensional heteronuclear relayed coherence transfer NMR spectroscopy. *Journal of Magnetic Resonance*, 2, 375-380.

Li, W., Wang, Y., Xu, D. 2018. Asymmetric Synthesis of α-Amino Phosphonates by Using Cinchona Alkaloid-Based Chiral Phase Transfer Catalyst. *European Journal of Organic Chemistry*, 39, 5422-5426.

Li, Y., Wang, A., Shen, L., Zhang, D., Zhu, T., Liu, S. 2010. Recent Progress in Synthesis and Biological Activity of the α-aminophosphonates [J]. *Journal of Hebei Normal University (Natural Science Edition)*, 2, 21.

Lima, L. M., Barreiro, E. J. 2005. Bioisosterism: a useful strategy for molecular modification and drug design. *Current Medicinal Chemistry*, 12, 23-49.

Lin, C. T., Malak, M., Vanderkooi, G., Mason, W. R. 1987. Solvent effects on the photophysical properties of dibucaine: a quinoline analogue. *Photochemistry and Photobiology*, 45, 749-755.

Lindström, B., Pettersson, L. J. 2003. A brief history of catalysis. *Cattech*, 7, 130-138.

Lipman, T. O. 1964. Wohler's preparation of urea and the fate of vitalism. *Journal of Chemical Education*, *41*(8), 452.

Lobo, V., Patil, A., Phatak, A., Chandra, N. 2010. Free radicals, antioxidants and functional foods: Impact on human health. *Pharmacognosy Reviews*, 8, 118.

Loupy, A. 2004. Solvent-free microwave organic synthesis as an efficient procedure for green chemistry. *Comptes Rendus Chimie*, 7, 103-112.

Ludwig, R., Dzung, N. 2002. Calixarene-based molecules for cation recognition. *Sensors*, 2, 397-416.

Manginell, R. P., Smith, J. H., Ricco, A. J. 1997. Overview of micromachined platforms for thermal sensing and gas detection. *Smart Structures and Materials 1997: Smart Electronics and MEMS*, 3046, 273-285.

Manske, R. H. 942. The Chemistry of Quinolines. *Chemical Reviews*, 30, 113-144.

McCarroll, A. J., Walton, J. C. 2001. Programming Organic Molecules: Design and Management of Organic Syntheses through Free-Radical Cascade Processes. *Angewandte Chemie International Edition*, 40, 2224-2248.

Meyer, B., Ferrigni, N., Putnam, J., Jacobsen, L., Nichols, D., Mclaughlin, J. 1982. Brine shrimp: a convenient general bioassay for active plant constituents. *Planta Medica*, 45, 31-34.

Michael, A. S., Thompson, C. G., Abramovitz, M. 1956. *Artemia salina as a Test Organism for Bioassay. Science* (New York, NY), 123, 464.

Michael, J. P. 1999. Quinoline, quinazoline and acridone alkaloids. *Natural Product Reports*, 16, 697-709.

Michael, J. P. 2008. Quinoline, quinazoline and acridone alkaloids. *Natural Product Reports*, 25, 166-187.

Mirzaei, M., Eshghi, H., Rahimizadeh, M., Bakavoli, M., Matin, M. M., Hosseinymehr, M., Bruno, G. 2015. An Eco-friendly Three Component Manifold for the Synthesis of α-Aminophosphonates under Catalyst and Solvent-free Conditions, X-ray Characterization and Their Evaluation as Anticancer Agents. *Journal of the Chinese Chemical Society*, 12, 1087-1096.

Mishra, A., Prasad, R. 2014. Preparation and application of perovskite catalysts for diesel soot emissions control: an overview. *Catalysis Reviews*, 56, 57-81.

Mossa, A. T. H., Nawwar, G. A. M. 2011. Free radical scavenging and antiacetylcholinesterase activities of Origanum majorana L. essential oil. *Human and Experimental Toxicology*, 10, 1501-1513.

Mucha, A., Kafarski, P., Berlicki, Ł. 2011. Remarkable potential of the α-aminophosphonate/phosphinate structural motif in medicinal chemistry. *Journal of Medicinal Chemistry*, 54, 5955-5980.

Murugesan, A., Gengan, R. M., Rajamanikandan, R., Ilanchelian, M. 2017. One-pot synthesis via 1, 3-dipolar cycloaddition reaction to piperazinyl-quinolinyl dispiro heterocyclic derivatives and spectrofluorometric and molecular docking studies on their binding with human serum albumin. *Journal of Molecular Structure*, 1149, 439-451.

Mutihac, L. 2008. Functionalized calix [n] arenes as membrane transporters for biological compounds. A minireview. *Current Drug Discovery Technologies*, 5, 98-104.

Nash, T. 1953. The colorimetric estimation of formaldehyde by means of the Hantzsch reaction. *Biochemical Journal*, 55, 416.

Naydenova, E., Topashka-Ancheva, M., Todorov, P., Yordanova, T., Troev, K. 2006. Novel α-aminophosphonic acids. Design, characterization, and biological activity. *Bioorganic and Medicinal Chemistry*, 14, 2190-2196.

Nikodemski, S. 2016. *Modification of electrical properties via interfacial manipulation in novel oxide heterostructures.* Doctoral dissertation, Colorado School of Mines. Arthur Lakes Library.

Nilsen, W. G., Skinner, J. G. 1968. Raman spectrum of strontium titanate. *The Journal of Chemical Physics*, 48, 2240-2248

Nizamov, I. S., Yambushev, F. D., Nizamov, I. D., Voloshina, A. D., Alfonsov, V. A. 2013. The Kabachnik–Fields and Pudovik Reactions on the Basis of E, Z-Citral and Its Imines and (R, S)-Citronellal. *Heteroatom Chemistry*, 24, 36-42.

Oniţa, N., Şişu, I., Penescu, M., Purcarea, V. L., Kurunczi, L. 2010. Synthesis, characterization and biological activity of some α-aminophosphonates. *Synthesis*, 58, 1-5.

Ordóñez, M., Arizpe, A., Sayago, F. J., Jiménez, A. I., Cativiela, C. 2016. Practical and efficient synthesis of α-aminophosphonic acids containing 1, 2, 3, 4-tetrahydroquinoline or 1, 2, 3, 4-tetrahydroisoquinoline heterocycles. *Molecules*, 21, 1140.

Paraskar, A. S., Sudalai, A. 2006. A novel $Cu(OTf)_2$ mediated three component high yield synthesis of α-aminophosphonates. *Arkivoc*, 10, 183-189.

Pasquini, C. 2003. Near infrared spectroscopy: fundamentals, practical aspects and analytical applications. *Journal of the Brazilian Chemical Society*, 2, 198-219.

Pauling, L. 1960. The Nature of the Chemical Bond. *Ithaca, NY: Cornell University Press*, 260, 3175-3187.

Pawar, V. D., Bettigeri, S., Weng, S. S., Kao, J. Q., Chen, C. T. 2006. Highly enantioselective aerobic oxidation of α-hydroxyphosphonates catalyzed by chiral vanadyl (V) methoxides bearing N-salicylidene-α-aminocarboxylates. *Journal of the American Chemical Society*, 128, 6308-6309.

Pawson, T. 1995. Protein modules and signalling networks. *Nature*, 373, 573.

Peters, W. 1965. Drug resistance in Plasmodium berghei. I. Chloroquine resistance. *Experimental Parasitology*, 17, 80-89.

Pfaller, M., Messer, S., Hollis, R. and Jones, R. 2002. Antifungal activities of posaconazole, ravuconazole, and voriconazole compared to those of itraconazole and amphotericin B against 239 clinical isolates of Aspergillus supplements and other filamentous fungi: report from sentry Antimicrobial Surveillance Program. *Antimicrobial Agents and Chemotherapy*, 46, 1032-1037.

Pham-Huy, L. A., He, H., Pham-Huy, C. 2008. Free radicals, antioxidants in disease and health. *International journal of biomedical science: IJBS*, 4, 89.

Popat, K. M., Anand, P. S., Dasare, B. D. 1994. Selective removal of fluoride ions from water by the aluminium form of the aminomethylphosphonic acid-type ion exchanger. *Reactive Polymers*, 23, 23-32.

Prasad, G. S., Rao, G. N. 2013. Synthesis of biologically active α-aminophosphonates. *Journal of Modern Medicinal Chemistry*, 1, 49-60.

Rafael'A, C., Galkin, V. I. 1998. The Kabachnik–Fields reaction: synthetic potential and the problem of the mechanism. *Russian Chemical Reviews*, 67, 857-882.

Ramana, K. V., Rasheed, S., Sekhar, K. C., Adam, S., Raju, C. N. 2012. One-pot and catalyst-free synthesis of novel α-aminophosphonates under microwave irradiation and their biological activity. *Der Pharmacia Lettre*, 456-463.

Ramberg, P. J. 2000. The death of vitalism and the birth of organic chemistry: Wohler's urea synthesis and the disciplinary identity of organic chemistry. *Ambix*, 47, 170-195.

Ranu, B. C., Hajra, A., Jana, U. 1999. General procedure for the synthesis of α-amino phosphonates from aldehydes and ketones using indium (III) chloride as a catalyst. *Organic Letters*, 8, 1141-1143.

Rao, K. U. M., Swapna, S., Manidhar, D. M., Reddy, K. M. K., Reddy, C. S. 2015. Efficient Synthesis of α-Aminophosphonates and Evaluation of Significance of P=O Group towards Antioxidant Activity. *Phosphorus, Sulfur, and Silicon and the Related Elements*, 190, 232-239.

Reddy, C. S. 2011. Synthesis and bio-activity evaluation of tetraphenyl (phenylamino) methylene bisphosphonates as antioxidant agents and as potent inhibitors of osteoclasts in vitro. *European Journal of Medicinal Chemistry*, 5, 1798-1802.

Reddy, G. S., Rao, K. U. M., Sundar, C. S., Sudha, S. S., Haritha, B., Swapna, S., Reddy, C. S. 2014. Neat synthesis and antioxidant activity of α-aminophosphonates. *Arabian Journal of Chemistry*, 7, 833-838.

Reddy, S. S., Rao, V. K., Krishna, B. S., Reddy, C. S., Rao, P. V., Raju, C. N. 2011. Synthesis, antimicrobial, and antioxidant activity of new α-aminophosphonates. *Phosphorus, Sulfur, and Silicon and the Related Elements*, 7, 1411-1421.

Reddy, S. S., Sankar, A. R., Raju, C. N., Rao, V. K. 2008. Synthesis and antimicrobial activity of new α-aminophosphonic acid esters. *South African Journal of Chemistry*, 61, 97-101.

Rezaei, Z., Khabnadideh, S., Zomorodian, K., Pakshir, K., Nadali, S., Mohtashami, N., Faghih Mirzaei, E. 2011. Design, Synthesis, and Antifungal Activity of New α-Aminophosphonates. *International Journal of Medicinal Chemistry*.

Roy, K. K., Singh, S., Sharma, S. K., Srivastava, R., Chaturvedi, V., Saxena, A. K. 2011. Synthesis and biological evaluation of substituted 4-arylthiazol-2-amino derivatives as potent growth inhibitors of replicating Mycobacterium tuberculosis H37RV. *Bioorganic & Medicinal Chemistry Letters*, 21, 5589-5593.

Sahoo, S., Joseph, T., Halligudi, S. B. 2006. Mannich reaction in Brönsted acidic ionic liquid: A facile synthesis of β-amino carbonyl compounds. *Journal of Molecular Catalysis A: Chemical*, 244, 179-182.

Sal'keeva, L. K., Nurmaganbetova, M. T., Kurmanaliev, O. S., Gazizov, T. K. 2002. Aminophosphonates in the synthesis of new radioprotecting agents. *Russian Journal of Organic Chemistry*, 38, 723-725.

Sankar, A. U. R., Kumar, B. S., Raju, C. N., Reddy, C. S. 2007. Tetramethylguanidine (TMG)-catalysed Synthesis of α-Aminophosphonates by a One-pot Reaction. *South African Journal of Chemistry*, 60, 125-128.

Schmink, J. R., Kormos, C. M., Devine, W. G., Leadbeater, N. E. 2010. Exploring the scope for scale-up of organic chemistry using a large batch microwave reactor. *Organic Process Research & Development*, 14, 205-214.

Schreiber, S. L. 2000. Target-oriented and diversity-oriented organic synthesis in drug discovery. *Science*, 287, 1964-1969.

Seneci, P., Fassina, G., Frecer, V., Miertus, S. 2014. The Effects of Combinatorial Chemistry and Technologies on Drug Discovery and Biotechnology–a Mini Review. *Nova Biotechnologica et Chimica,* 13*,* 87-108.

Sharma, S. 2010. *Interaction of metal ions with electron rich species* (Doctoral dissertation, Aligarh Muslim University).

Shashikumar, N. D. 2013. Preparation of New α-Aminophosphonate Derivatives by Kabachnik-Fields Reaction Using a Recyclable Catalyst. *Journal of Chemistry*, *2013*.

Sheldon, R. A., Van Bekkum, H. 2008. *Fine chemicals through heterogeneous catalysis*. John Wiley & Sons.

Shestopalov, A. M., Emeliyanova, Y. M., Shestopalov, A. A., Rodinovskaya, L. A., Niazimbetova, Z. I., Evans, D. H. 2002. One-Step Synthesis of Substituted 6-Amino-5-cyanospiro-4-(piperidine-4 ‘)-2 H, 4 H-dihydropyrazolo [3, 4-b] pyrans. *Organic Letters*, 4, 423-425.

Shigi, Y. 1989. Inhibition of bacterial isoprenoid synthesis by fosmidomycin, a phosphonic acid-containing antibiotic. *Journal of Antimicrobial Chemotherapy*, 24, 131-145.

Simoni, D., Invidiata, F. P., Manferdini, M., Lampronti, I., Rondanin, R., Roberti, M., Pollini, G. P. 1998. Tetramethylguanidine (TMG)-catalyzed addition of dialkyl phosphites to α, β-unsaturated carbonyl compounds, alkenenitriles, aldehydes, ketones and imines. Tetrahedron Letters, 39, 7615-7618.

Singh, S. B., Barrett, J. F. 2006. Empirical antibacterial drug discovery foundation in natural products. *Biochemical Pharmacology*, 7, 1006-1015.

Sleet, R. B., Brendel, K. 1983. Improved methods for harvesting and counting synchronous populations of Artemia nauplii for use in developmental toxicology. *Ecotoxicology and Environmental Safety*, 7, 435-446.

Snyder, W. R., Law, J. H. 1970. A quantitative determination of phosphonate phosphorus in naturally occurring aminophosphonates. *Lipids*, 5, 800-802.

Sobhani, S., Vafaee, A. 2010. Molecular iodine: An efficient catalyst for the one-pot synthesis of primary 1-aminophosphonates. *Journal of the Iranian Chemical Society*, 7, 227-236.

Soetan, K. O., Olaiya, C. O., Oyewole, O. E. 2010. The importance of mineral elements for humans, domestic animals and plants-A review. *African journal of food science*, 4, 200-222.

Sonawane, R. P. 2014. Comparative Study of Chemical Synthesis of Pyrimidine Derivatives by Using Grindstone Chemistry Technique and Conventional Metod. *International Letters of Chemistry, Physics and Astronomy*, 14.

Southorn, P. A., Powis, G. 1988. Free radicals in medicine. I. Chemical nature and biologic reactions. In *Mayo Clinic Proceedings*, 63, 381-389

Sparkman, O. D. 2000. Mass spectrometry desk reference 2. *Journal of the American Society for Mass Spectrometry*, 11, 1144.

Stackebrandt, E., Frederiksen, W., Garrity, G. M., Grimont, P. A., Kämpfer, P., Maiden, M. C., Vauterin, L. 2002. Report of the ad hoc committee for the re-evaluation of the species definition in bacteriology. *International Journal of Systematic and Evolutionary Microbiology*, 52, 1043-1047.

Stuerga, D., Gaillard, P., Lallemant, M. 1995. Microwave heating and chemistry: what can be expected of them?. *Canadian Conference on Electrical and Computer Engineering*, 1, 338-341

Sweet, F., Fissekis, J. D. 1973. Synthesis of 3, 4-dihydro-2 (1H)-pyrimidinones and the mechanism of the Biginelli reaction. *Journal of the American Chemical Society*, 26, 8741-8749.

Syono, Y., Akimoto, S. I., Kohn, K. 1969. Structure relations of hexagonal perovskite-like compounds ABX3 at high pressure. *Journal of the Physical Society of Japan*, 26, 993-999.

Takehira, K. 2002. Highly dispersed and stable supported metal catalysts prepared by solid phase crystallization method. *Catalysis Surveys from Asia*, 6, 19-32.

Taylor, T. N., Krings, M. 2005. Fossil microorganisms and land plants: associations and interactions. *Symbiosis*, 40, 119-135.

Tejuca, L. G., Fierro, J. L. 1992. *Properties and applications of perovskite-type oxides*. CRC Press.

Tempest, P. A. 2005. Recent advances in heterocycle generation using the efficient Ugi multiple-component condensation reaction. *Current Opinion in Drug Discovery & Development*, 8, 776-788.

Thomas, J. M., Thomas, W. J., Salzberg, H. W. 1967. Introduction to the principles of heterogeneous catalysis. *Journal of The Electrochemical Society*, 11, 279C.

Tian, T., Wang, W., Zhan, M., Chen, C. 2010. Catalytic partial oxidation of methane over SrTiO3 with oxygen-permeable membrane reactor. *Catalysis Communications*, 11, 624-628.

Tierney, J., Lidström, P. 2009. *Microwave assisted organic synthesis*. John Wiley & Sons.

Tillu, V. H., Dumbre, D. K., Wakharkar, R. D., Choudhary, V. R. 2011. One-pot three-component Kabachnik–Fields synthesis of α-aminophosphonates using H-beta zeolite catalyst. *Tetrahedron Letters*, 52, 863-866.

Tusek–Bozic, L. 2013. Aminophosphonate metal complexes of biomedical potential. *Current Medicinal Chemistry*, 20, 2096-2117.

Ulaczyk-Lesanko, A., Hall, D. G. 2005. Wanted: New multicomponent reactions for generating libraries of polycyclic natural products. *Current opinion in chemical biology*, 9, 266-276.

Valko, M., Leibfritz, D., Moncol, J., Cronin, M. T., Mazur, M., Telser, J. 2007. Free radicals and antioxidants in normal physiological functions and human disease. *The International Journal of Biochemistry & Cell Biology*, 39, 44-84.

Vollhardt, K. P. C., Schore, N. E. 2007. Omega: *Química Orgánica: Estructura y Función*, 547.

Ward, P., Small, I., Smith, J., Suter, P., Dutkowski, R. 2005. Oseltamivir (Tamiflu®) and its potential for use in the event of an influenza pandemic. *Journal of Antimicrobial Chemotherapy*, *55*, i5-i21.

Weber, L. 2002. Multi-component reactions and evolutionary chemistry. *Drug Discovery Today*, 7, 143-147.

Wesełucha-Birczyńska, A., Nakamoto, K. 1996. Study of the Interaction of the Antimalarial Drug Cinchonine with Nucleic Acids by Raman Spectroscopy. *Journal of Raman spectroscopy*, 27, 915-919.

Wilkins, M. H. 1963. Molecular configuration of nucleic acids. *Science*, 140, 941-950.

Winter, A. 2005. *Organic chemistry I for dummies*. John Wiley & Sons.

Wolf, G. 2005. The discovery of the antioxidant function of vitamin E: the contribution of Henry A. Mattill. *The Journal of Nutrition*, 135, 363-366.

Wuts, P. G., Greene, T. W. 2006. *Greene's protective groups in organic synthesis*. John Wiley & Sons.

Yadav, J. S., Reddy, B. V. S., Raj, K. S., Reddy, K. B., Prasad, A. R. 2001. Zr^{4+}-catalyzed efficient synthesis of α-aminophosphonates. *Synthesis*, 15, 2277-2280.

Yamauchi, K., Ohtsuki, S., Kinoshita, M. 1984. Synthesis of peptide analogs containing (2-aminoethyl) phosphonic acid (ciliatine). *The Journal of Organic Chemistry*, 49, 1158-1163.

Yu, Y. C., Kuang, W. B., Huang, R. Z., Fang, Y. L., Zhang, Y., Chen, Z. F., Ma, X. L. 2017. Design, synthesis and pharmacological evaluation of new 2-oxo-quinoline derivatives containing α-aminophosphonates as potential antitumor agents. *MedChemComm*, 8, 1158-1172.

Zhu, X. F., Zhang, J., Sun, S., Guo, Y. C., Cao, S. X., Zhao, Y. F. 2017. Synthesis and structure-activity relationships study of α-aminophosphonate derivatives containing a quinoline moiety. *Chinese Chemical Letters*, 28, 1514-151.

APPENDICES

Appendix 1

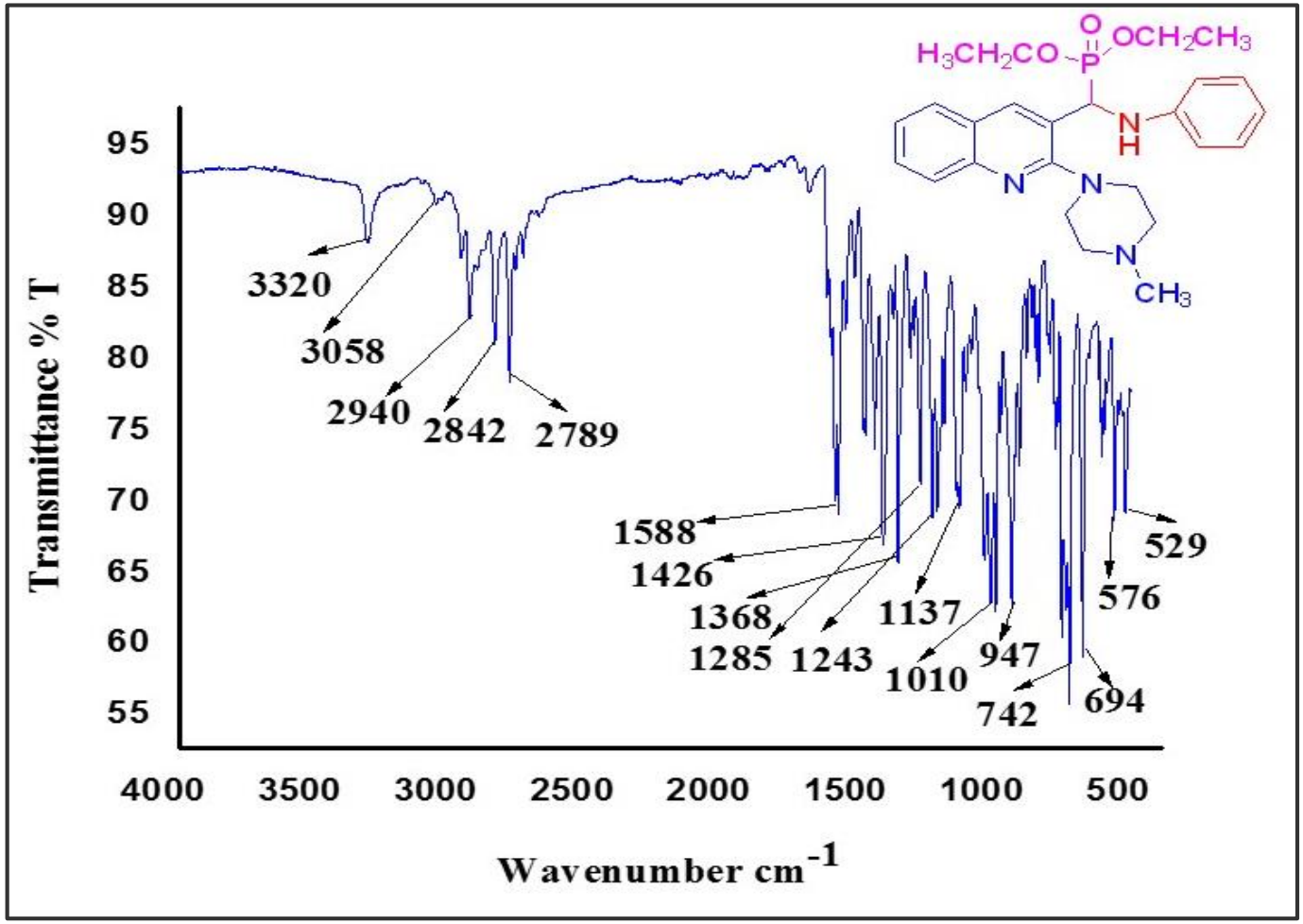

Figure S1: The IR Spectrum of 4a, diethyl ((2-(4-methylpiperazin-1-yl)quinolin-3-yl)(phenylamino)methyl)phosphonate

Appendix 2

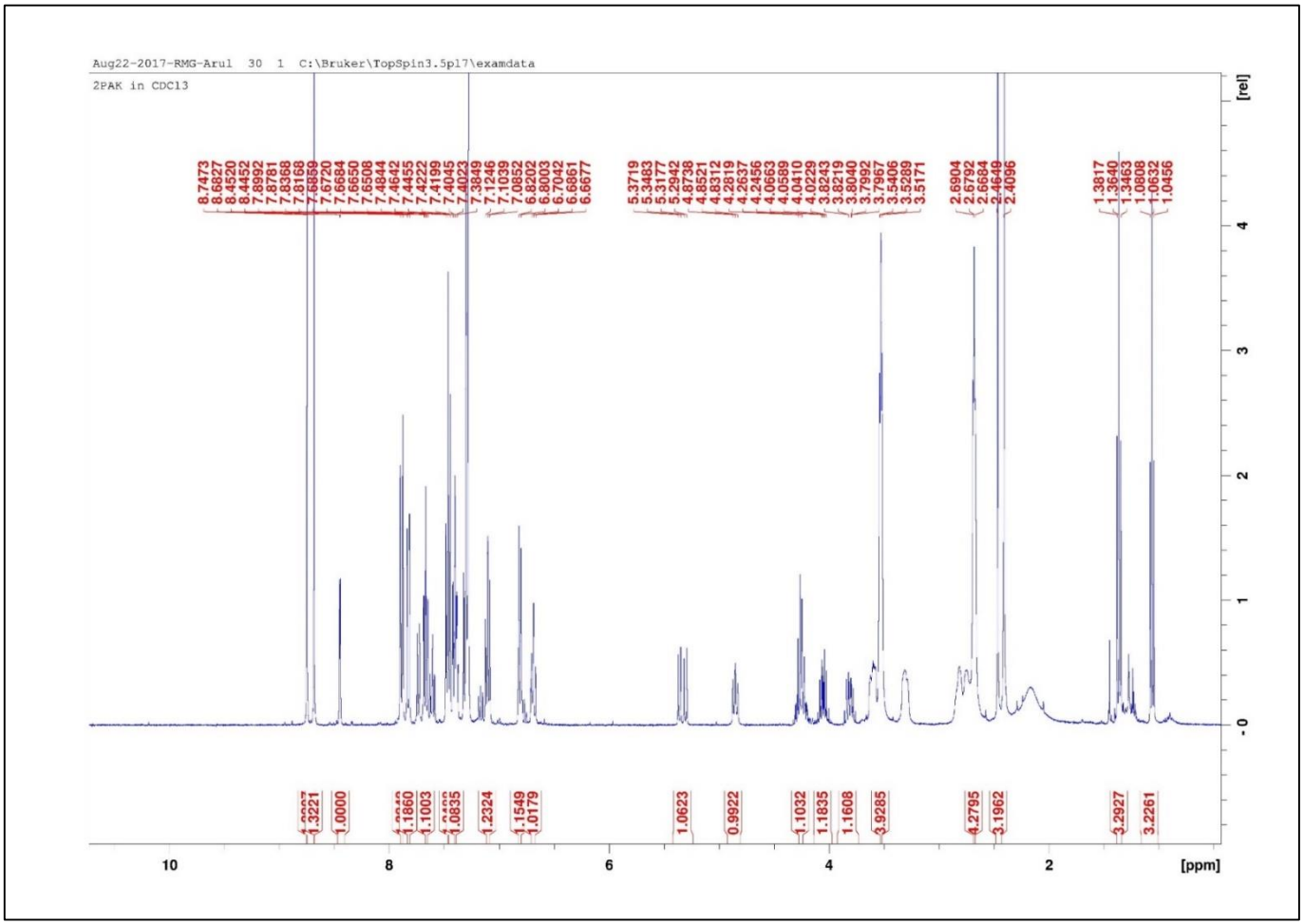

Figure S2: The ^{1}H NMR Spectrum of 4a, diethyl ((2-(4-methylpiperazin-1-yl)quinolin-3-yl)(phenylamino)methyl)phosphonate

Appendix 3

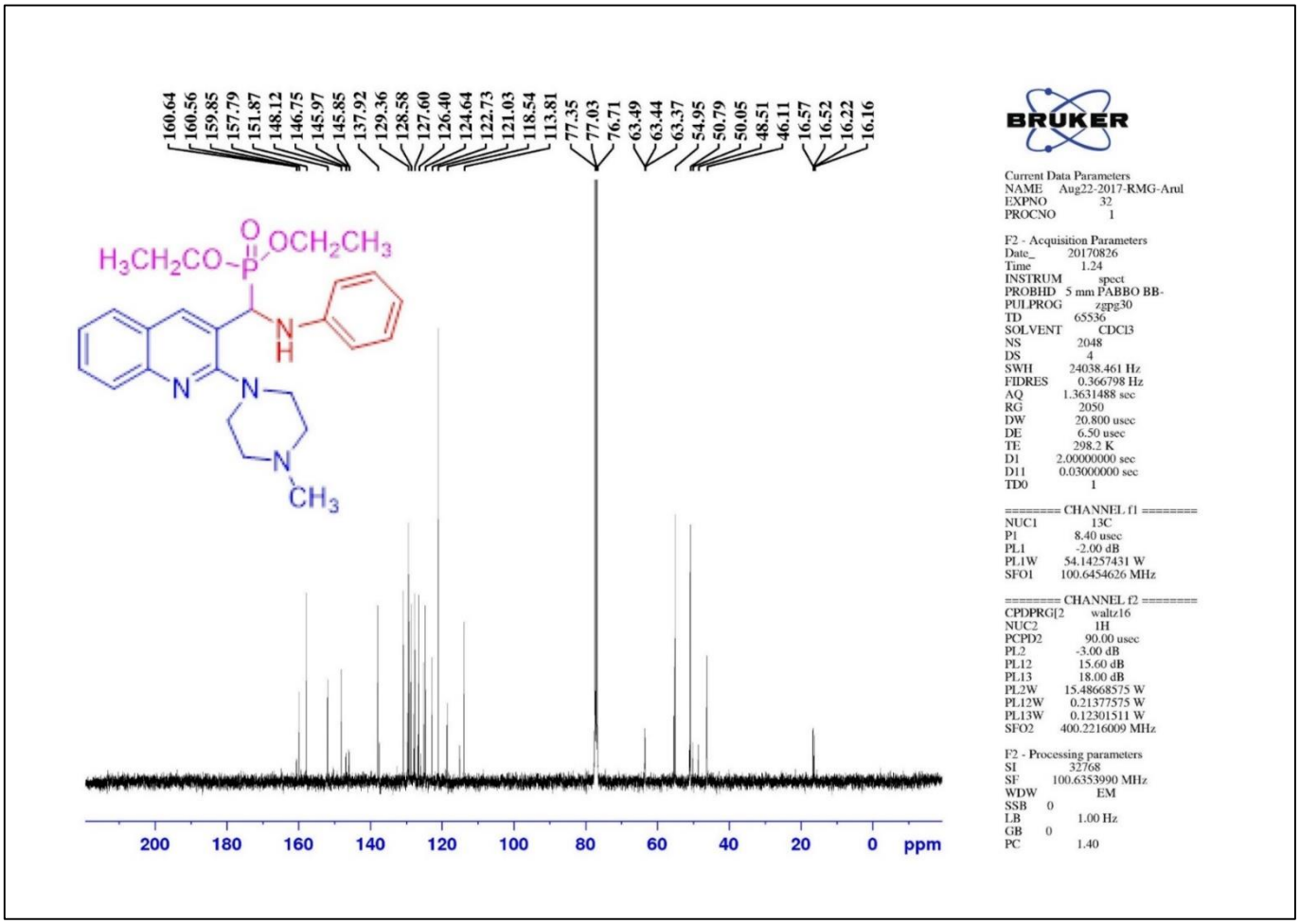

Figure S3: The ^{13}C NMR Spectrum of 4a, diethyl ((2-(4-methylpiperazin-1-yl)quinolin-3-yl)(phenylamino)methyl)phosphonate

Appendix 4

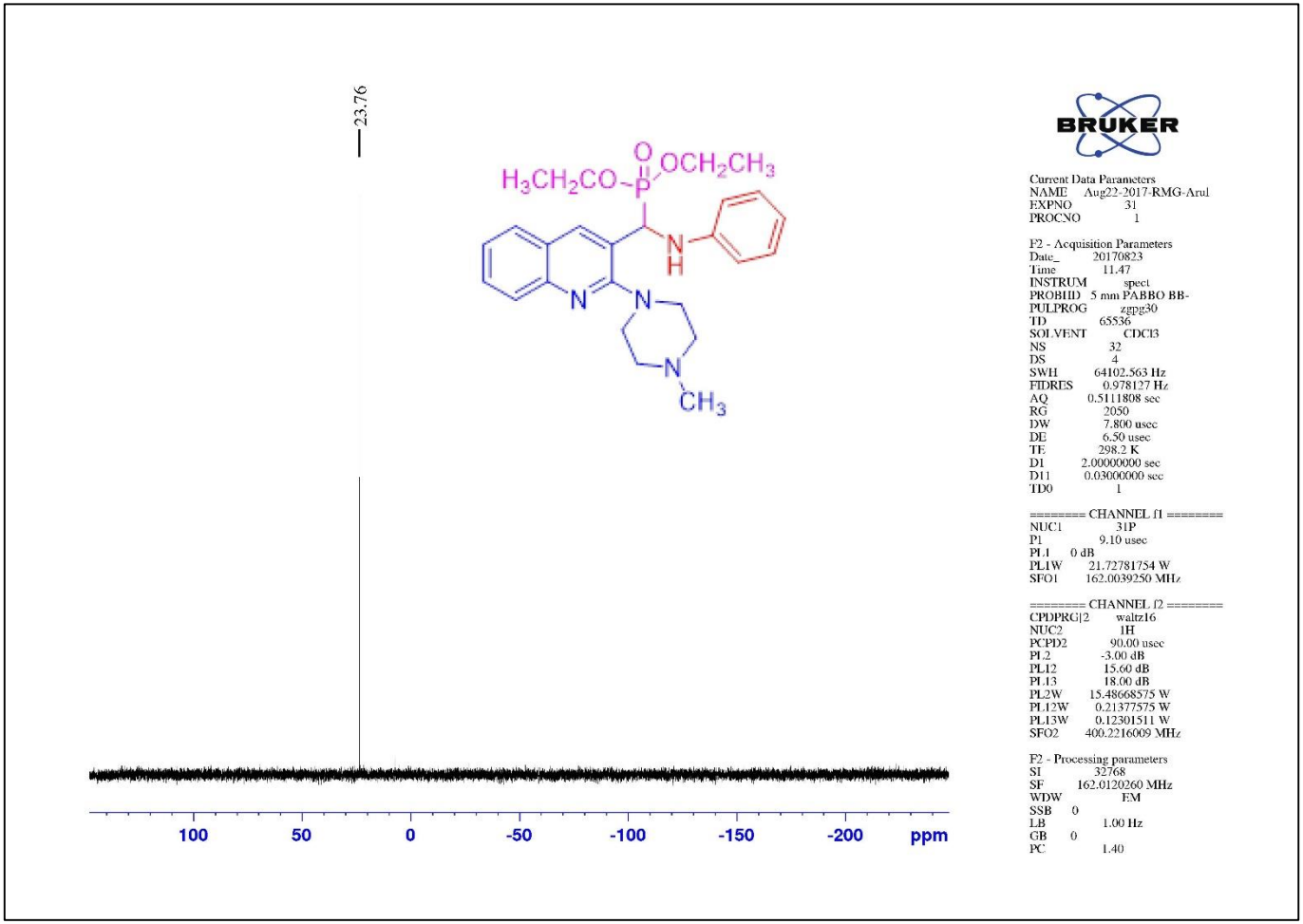

Figure S4: The ^{31}P NMR Spectrum of 4a, diethyl ((2-(4-methylpiperazin-1-yl)quinolin-3-yl)(phenylamino)methyl)phosphonate

Appendix 5

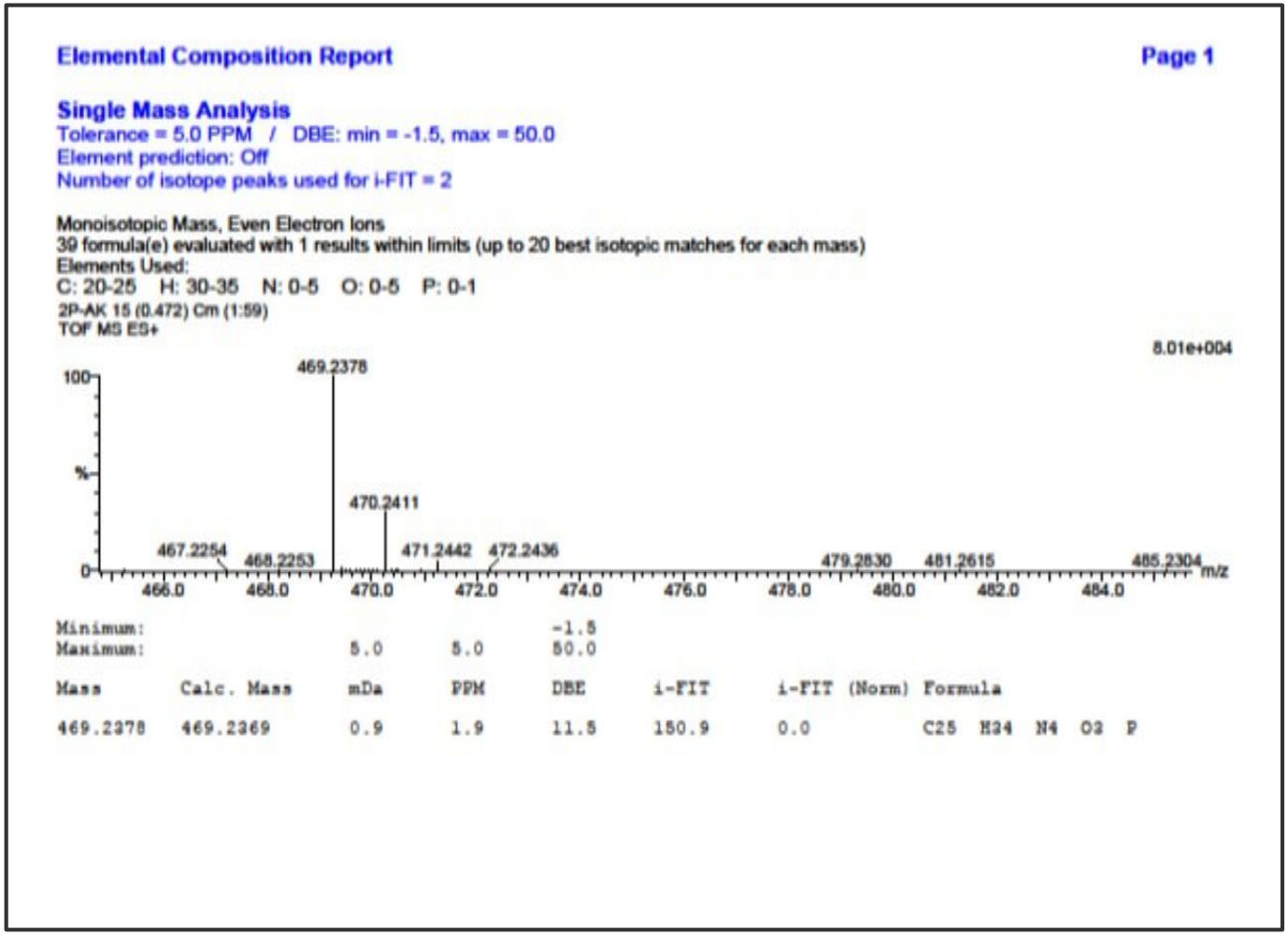

Elemental Composition Report **Page 1**

Single Mass Analysis
Tolerance = 5.0 PPM / DBE: min = -1.5, max = 50.0
Element prediction: Off
Number of isotope peaks used for i-FIT = 2

Monoisotopic Mass, Even Electron Ions
39 formula(e) evaluated with 1 results within limits (up to 20 best isotopic matches for each mass)
Elements Used:
C: 20-25 H: 30-35 N: 0-5 O: 0-5 P: 0-1
2P-AK 15 (0.472) Cm (1:59)
TOF MS ES+

Minimum:				-1.5			
Maximum:		5.0	5.0	50.0			
Mass	Calc. Mass	mDa	PPM	DBE	i-FIT	i-FIT (Norm)	Formula
469.2378	469.2369	0.9	1.9	11.5	150.9	0.0	C25 H34 N4 O3 P

Figure S5: The HRMS Spectrum of 4a, diethyl ((2-(4-methylpiperazin-1-yl)quinolin-3-yl)(phenylamino)methyl)phosphonate

Appendix 6

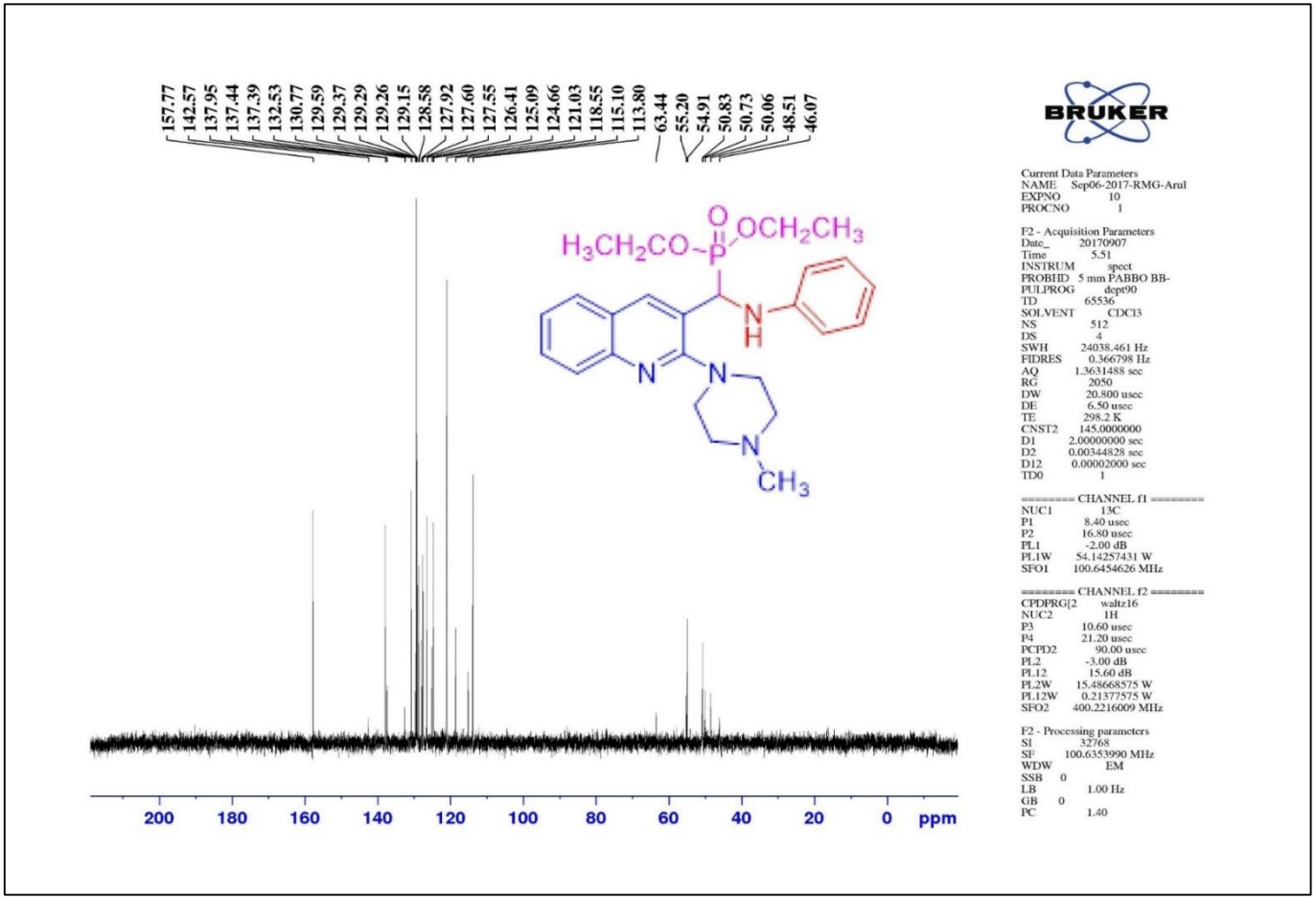

Figure S6: The DEPT-90 NMR Spectrum of 4a, diethyl((2-(4-methylpiperazin-1-yl)quinolin-3yl)(phenylamino)methyl)phosphonate

Appendix 7

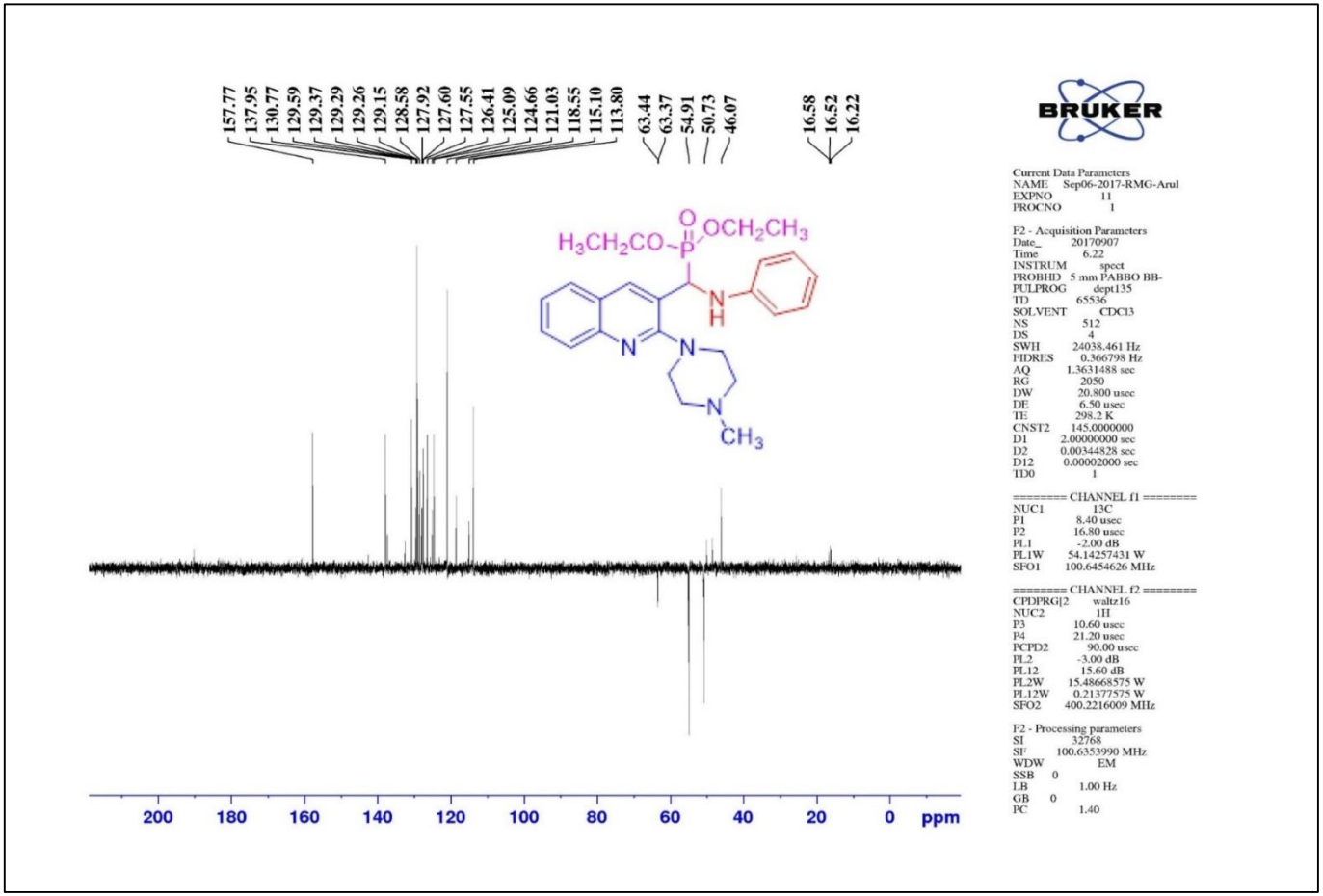

Figure S7: The DEPT-135 NMR Spectrum of 4a, diethyl ((2-(4-methylpiperazin-1-yl)quinolin-3-yl)(phenylamino)methyl)phosphonate

Appendix 8

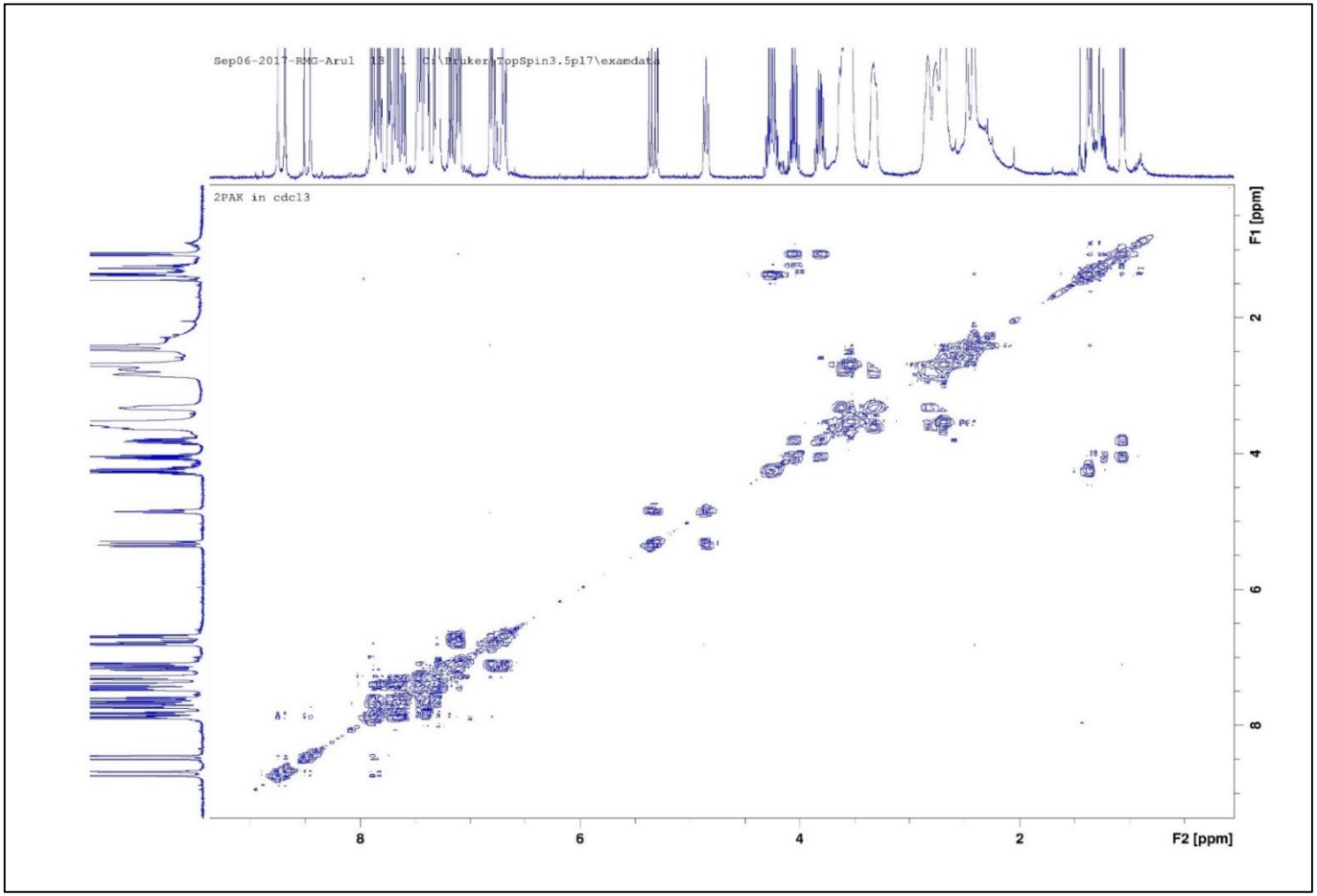

Figure S8: The COSY NMR Spectrum of 4a, diethyl ((2-(4-methylpiperazin-1-yl)quinolin-3-yl)(phenylamino)methyl)phosphonate

Appendix 9

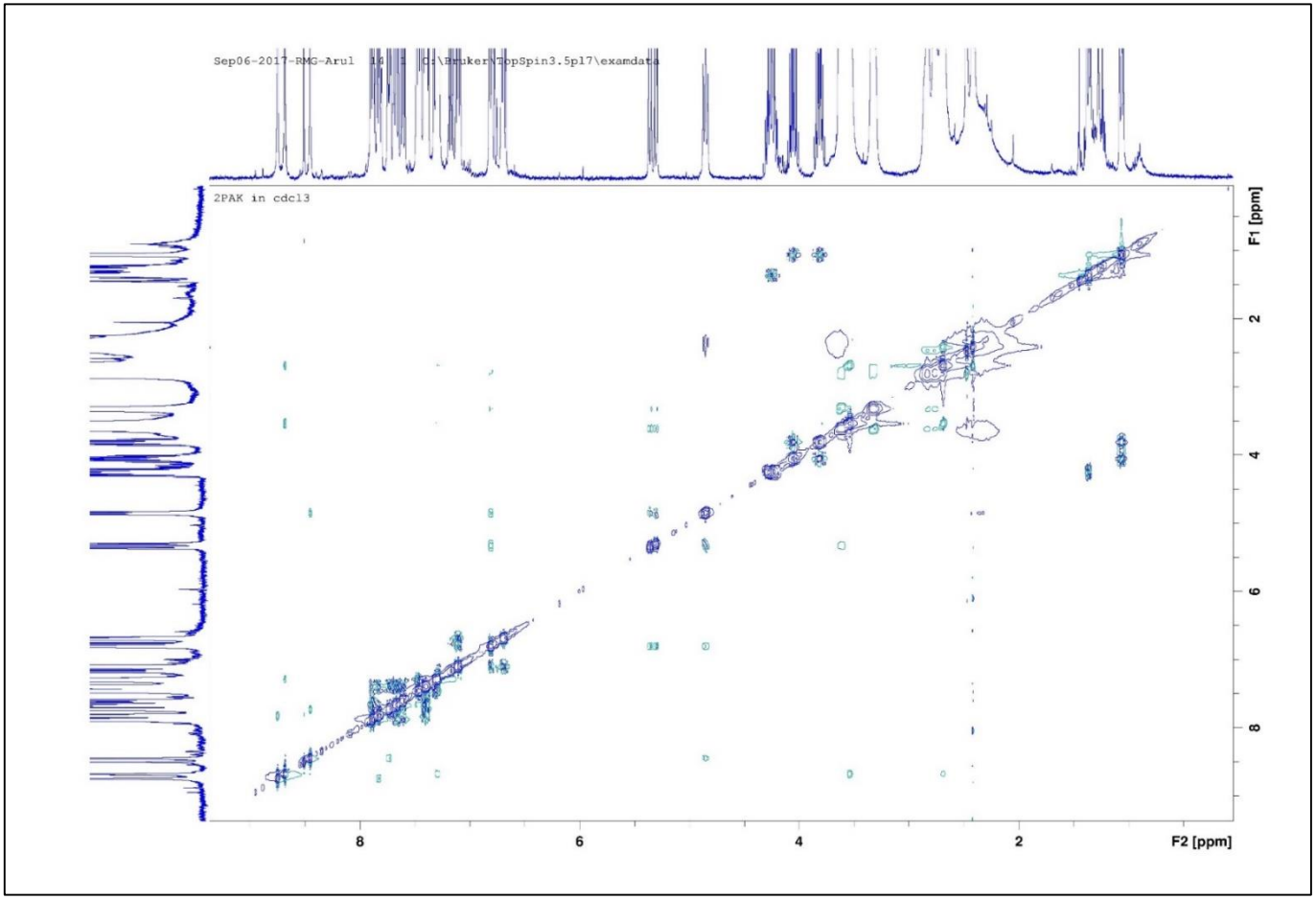

Figure S9: The NOESY NMR Spectrum of 4a, diethyl ((2-(4-methylpiperazin-1-yl)quinolin-3-yl)(phenylamino)methyl)phosphonate

Appendix 10

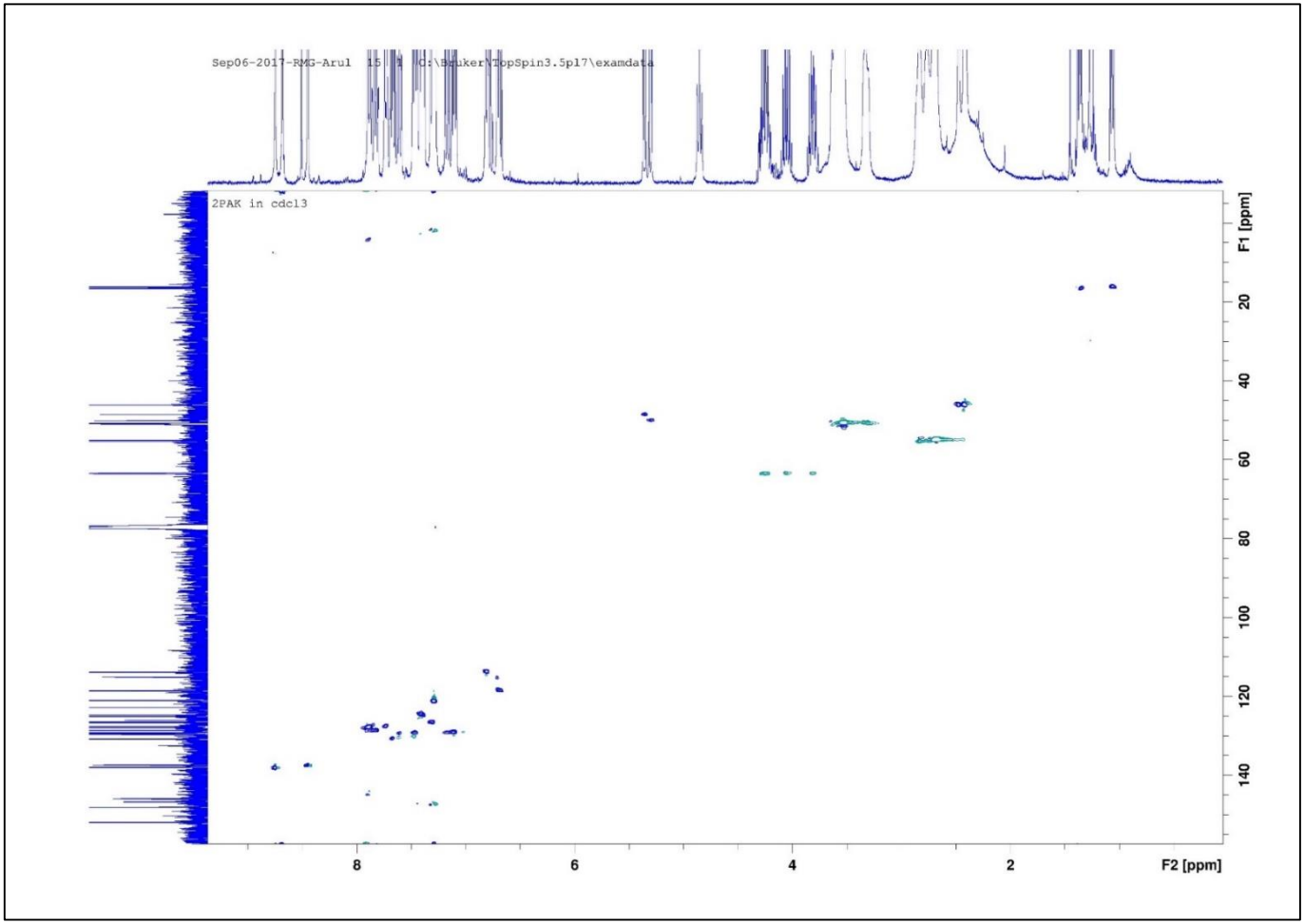

Figure S10: The HSQCE NMR Spectrum of 4a, diethyl ((2-(4-methylpiperazin-1-yl)quinolin-3-yl)(phenylamino)methyl)phosphonate

Appendix 11

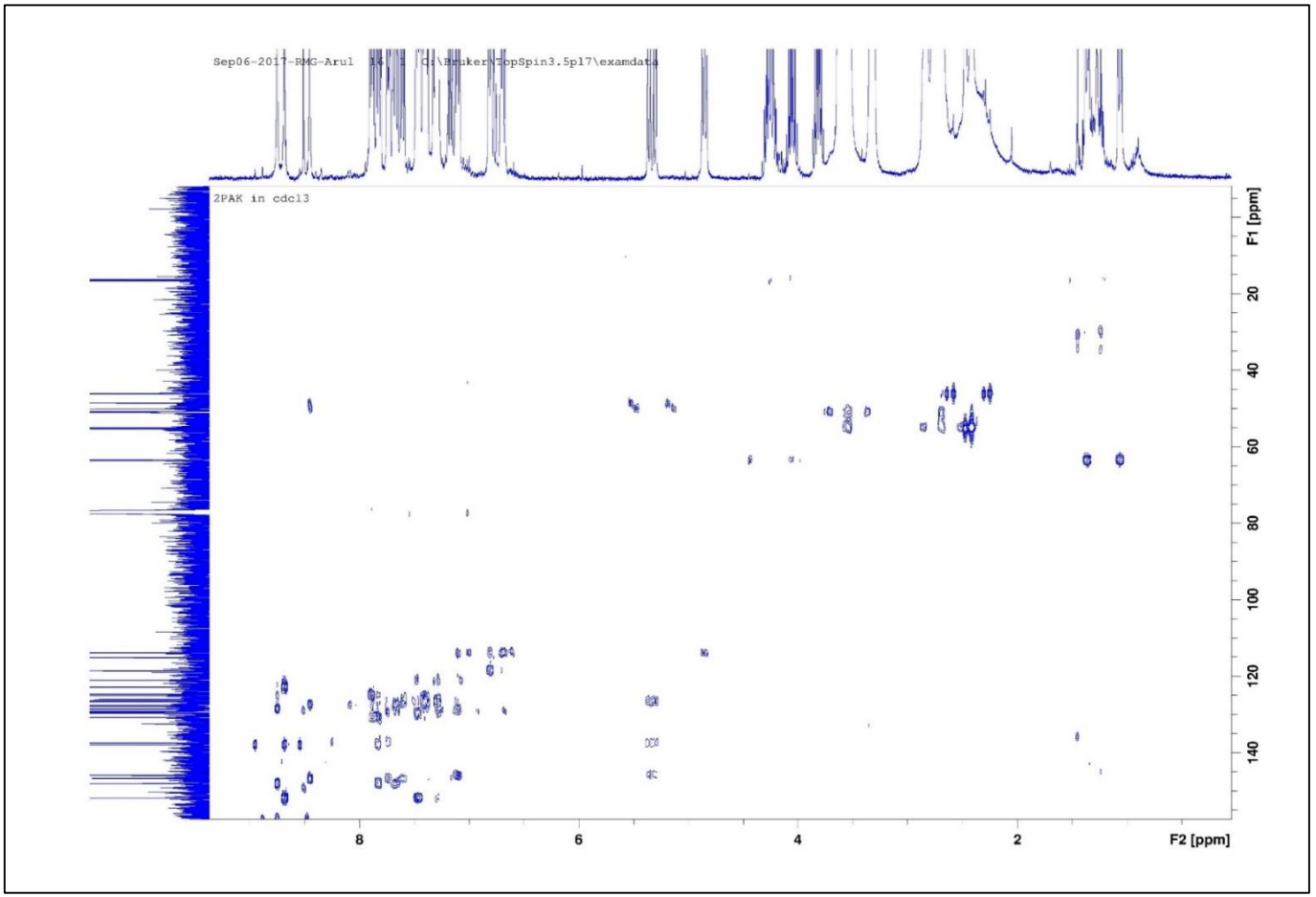

Figure S11: The HMBC NMR Spectrum of 4a, diethyl ((2-(4-methylpiperazin-1-yl)quinolin-3-yl)(phenylamino)methyl)phosphonate

Appendix 12

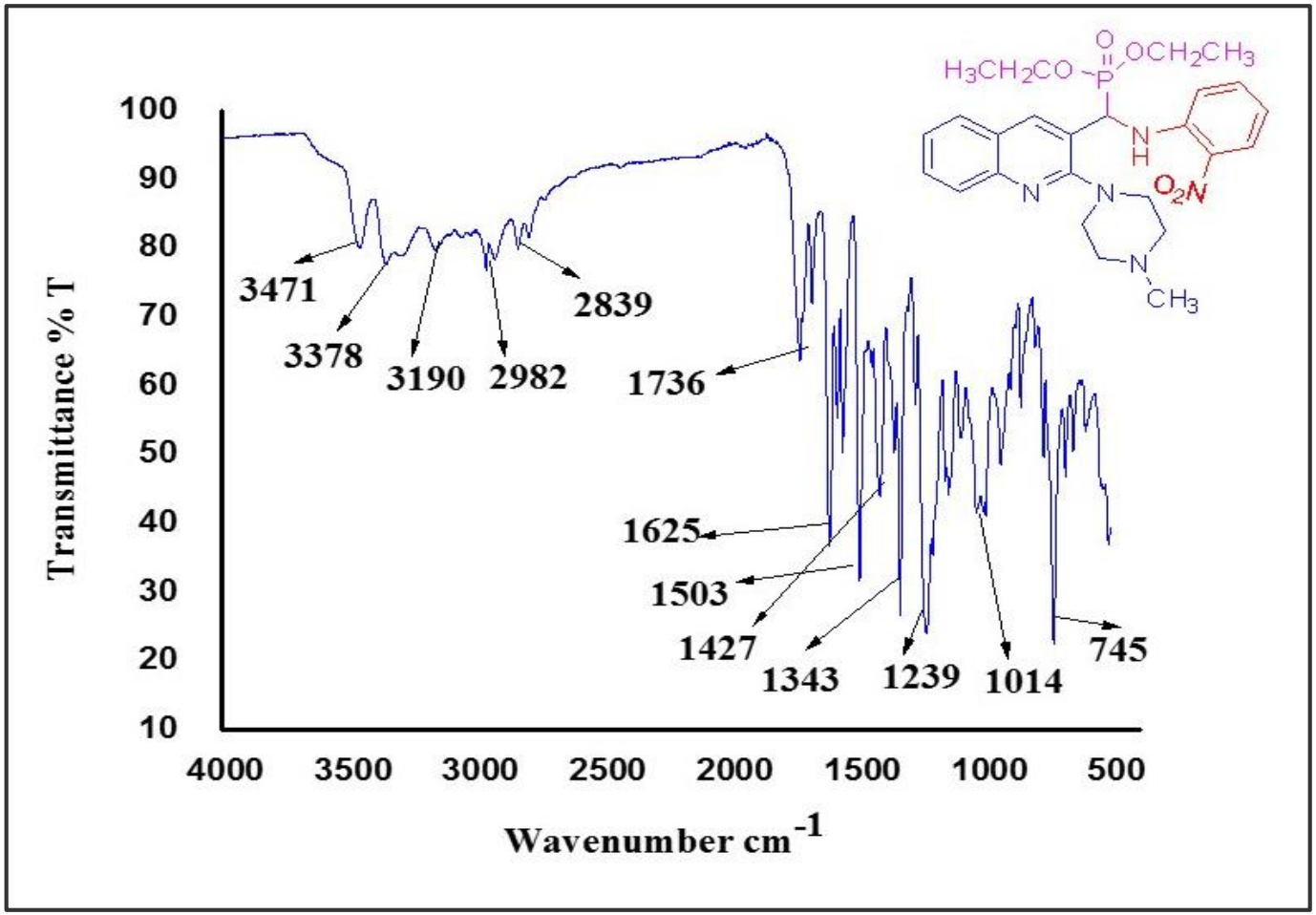

Figure S12: The IR Spectrum of 4b, diethyl ((2-(4-methylpiperazin-1-yl)quinolin-3-yl)((2-nitrophenyl)amino)methyl)phosphonate

Appendix 13

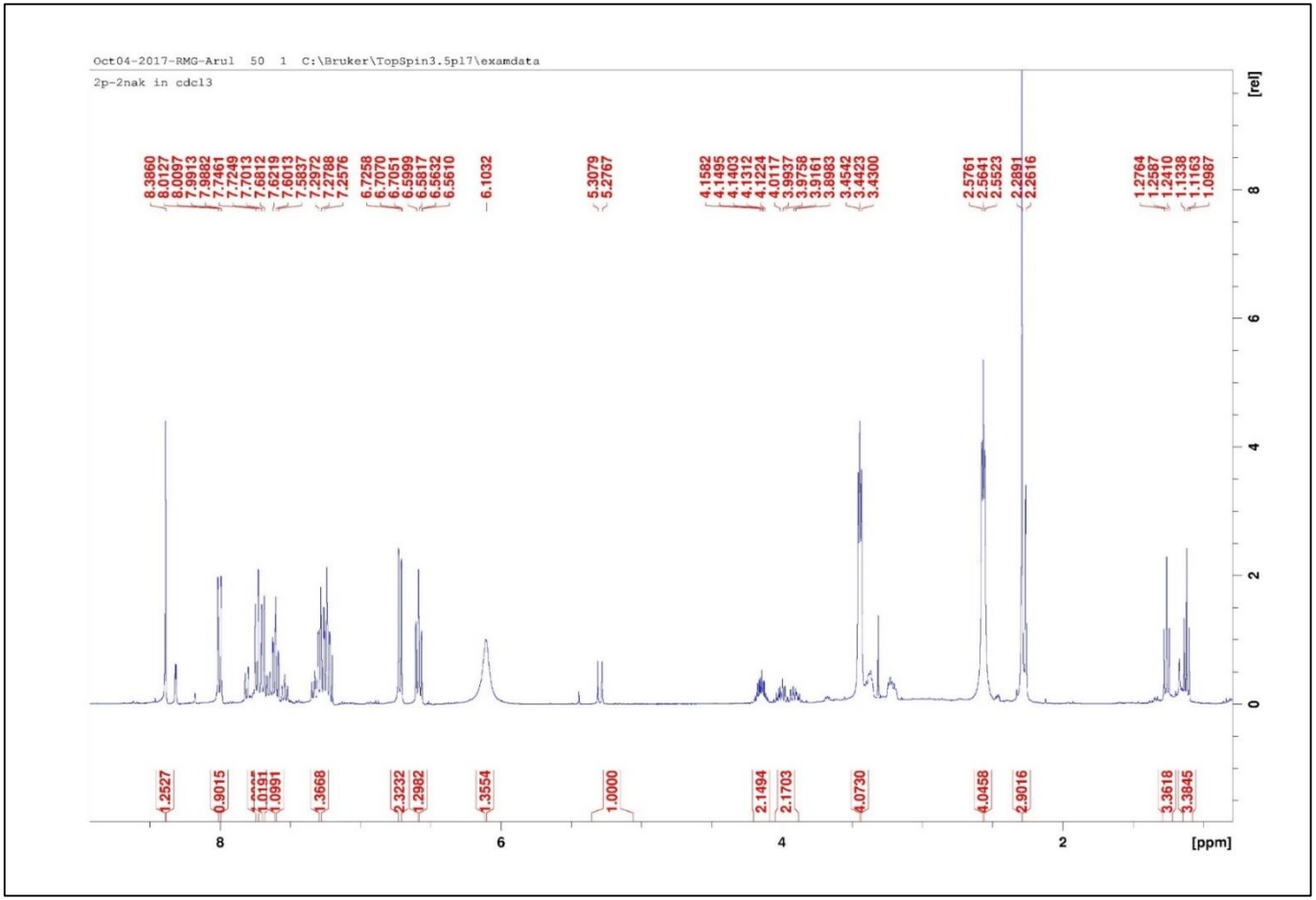

Figure S13: ^{1}H NMR Spectrum of 4b, diethyl ((2-(4-methylpiperazin-1-yl)quinolin-3-yl)((2-nitrophenyl)amino)methyl)phosphonate

Appendix 14

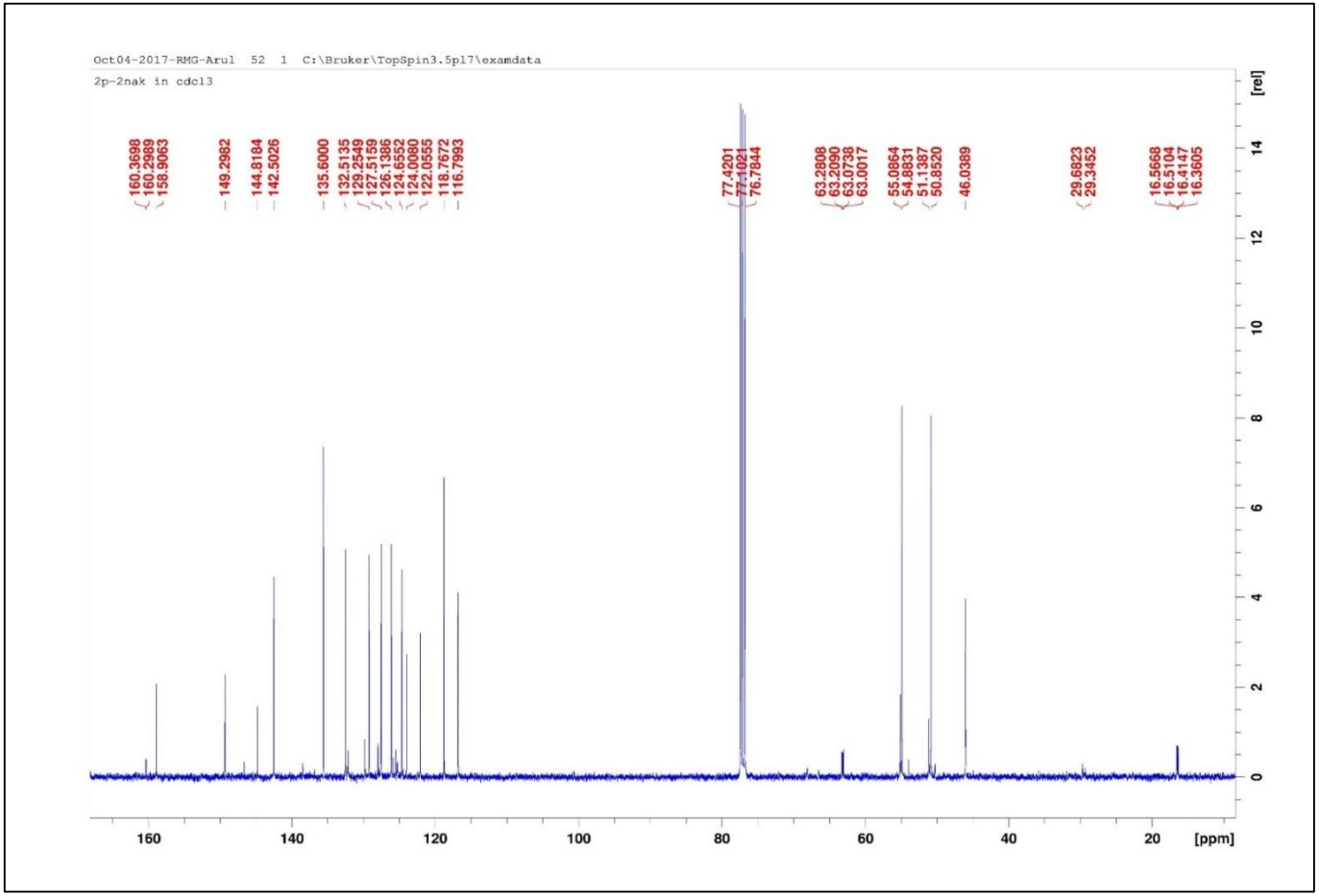

Figure S14: ^{13}C NMR Spectrum of 4b, diethyl ((2-(4-methylpiperazin-1-yl)quinolin-3-yl)((2-nitrophenyl)amino)methyl)phosphonate

Appendix 15

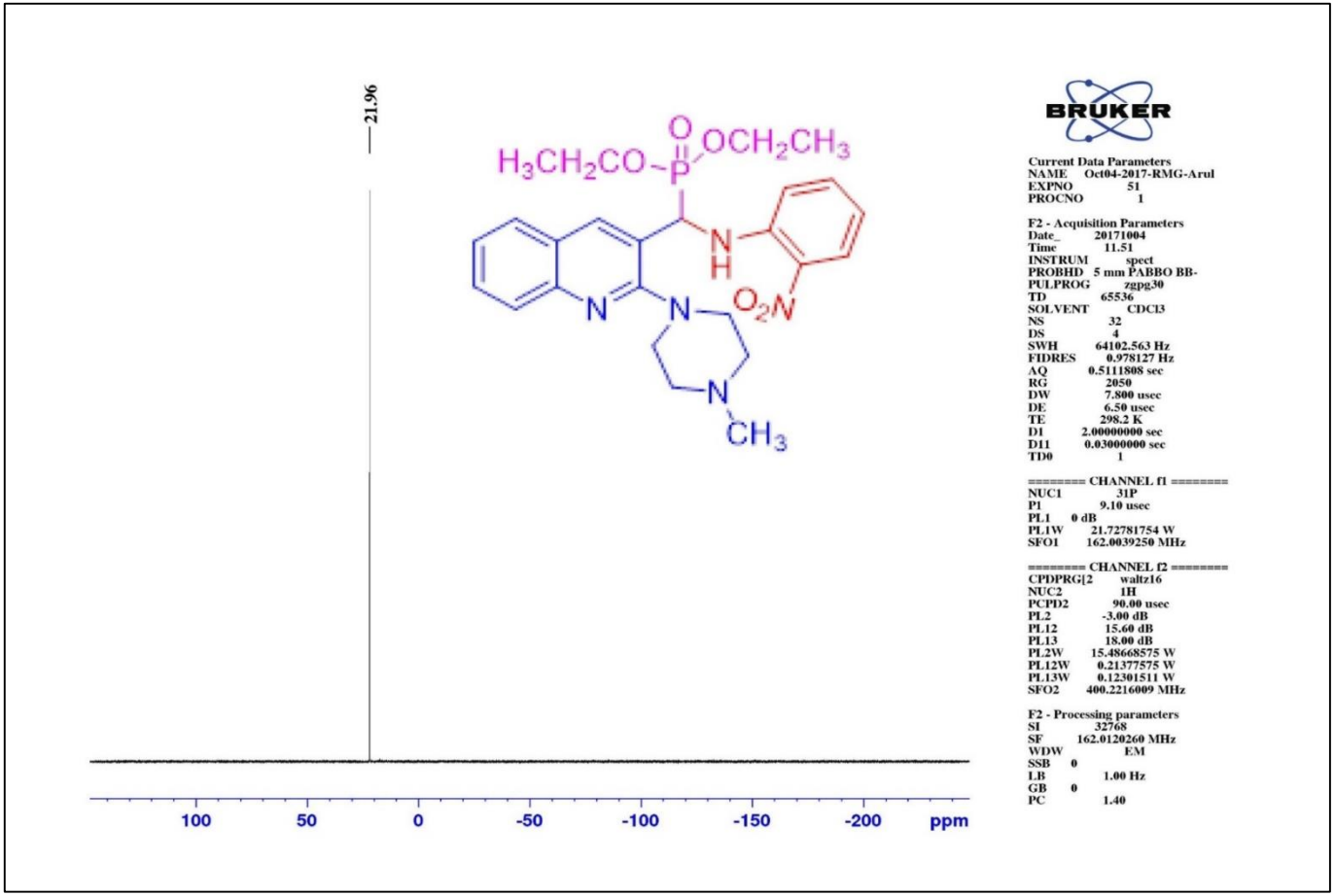

Figure S15: ^{31}P NMR Spectrum of 4b, diethyl ((2-(4-methylpiperazin-1-yl)quinolin-3-yl)((2-nitrophenyl)amino)methyl)phosphonate

Appendix 16

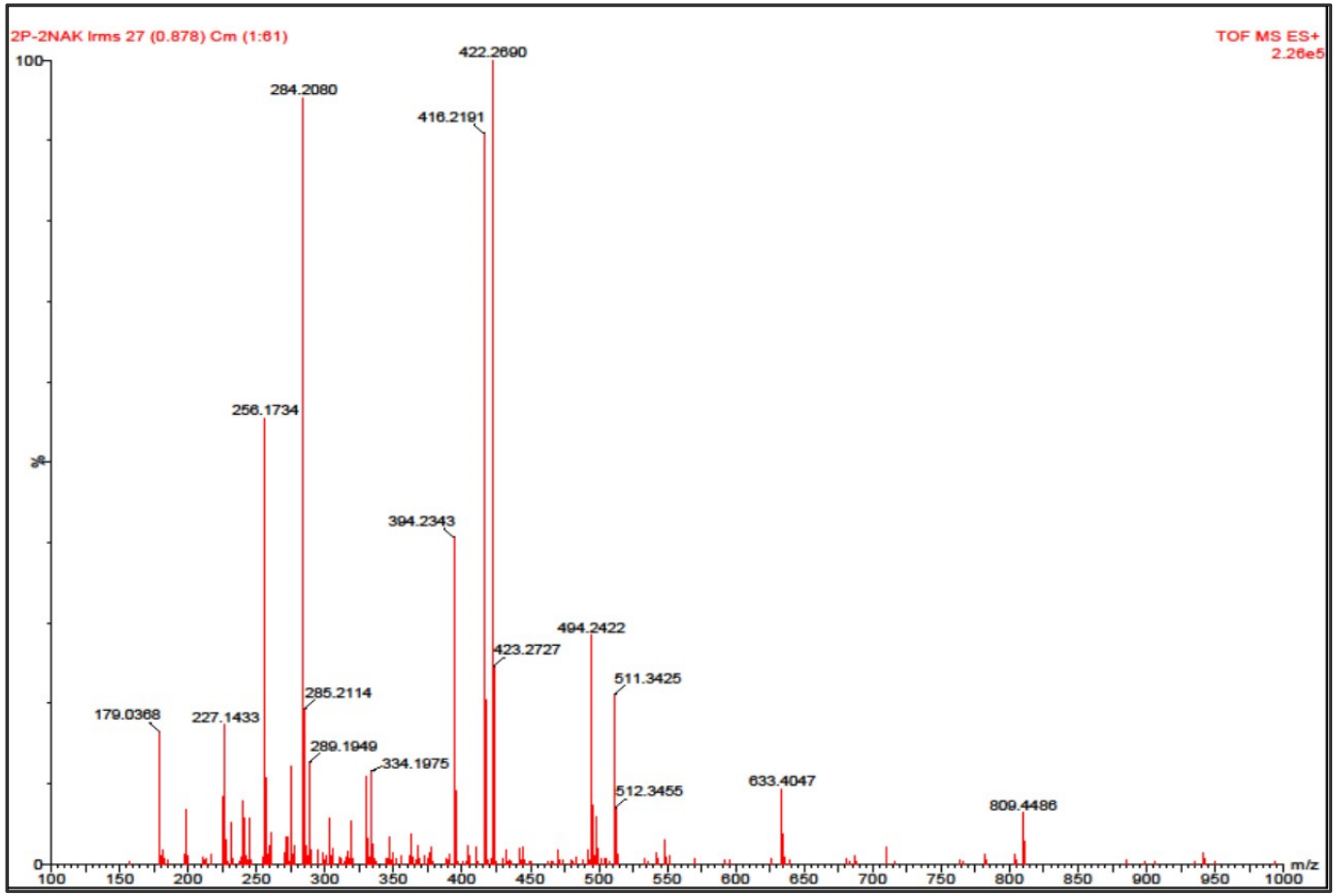

Figure S16: HRMS Spectrum of 4b, diethyl ((2-(4-methylpiperazin-1-yl)quinolin-3-yl)((2-nitrophenyl)amino)methyl)phosphonate

Appendix 17

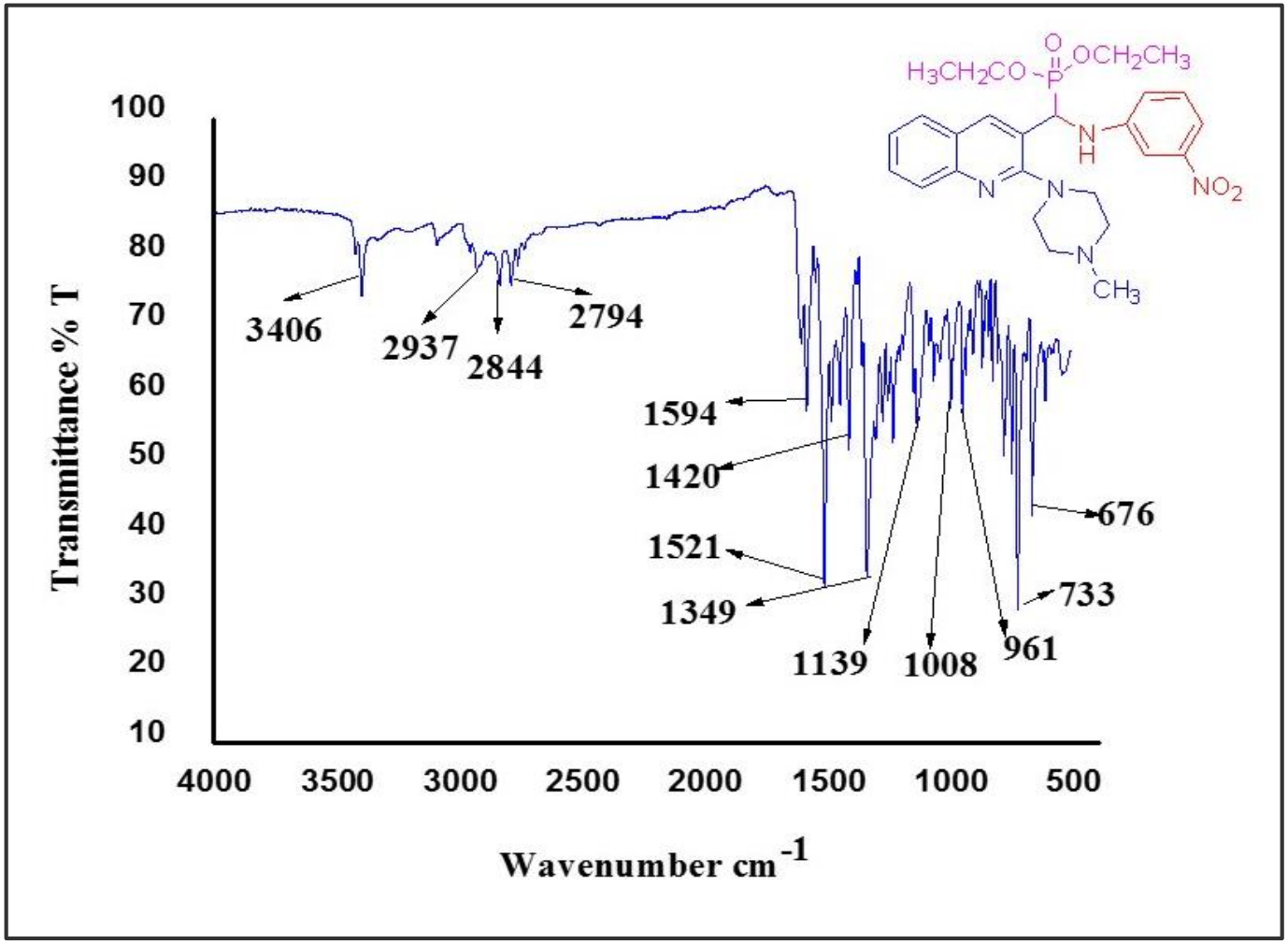

Figure S17: The IR Spectrum of 4c, diethyl ((2-(4-methylpiperazin-1-yl)quinolin-3-yl)((3-nitrophenyl)amino)methyl)phosphonate

Appendix 18

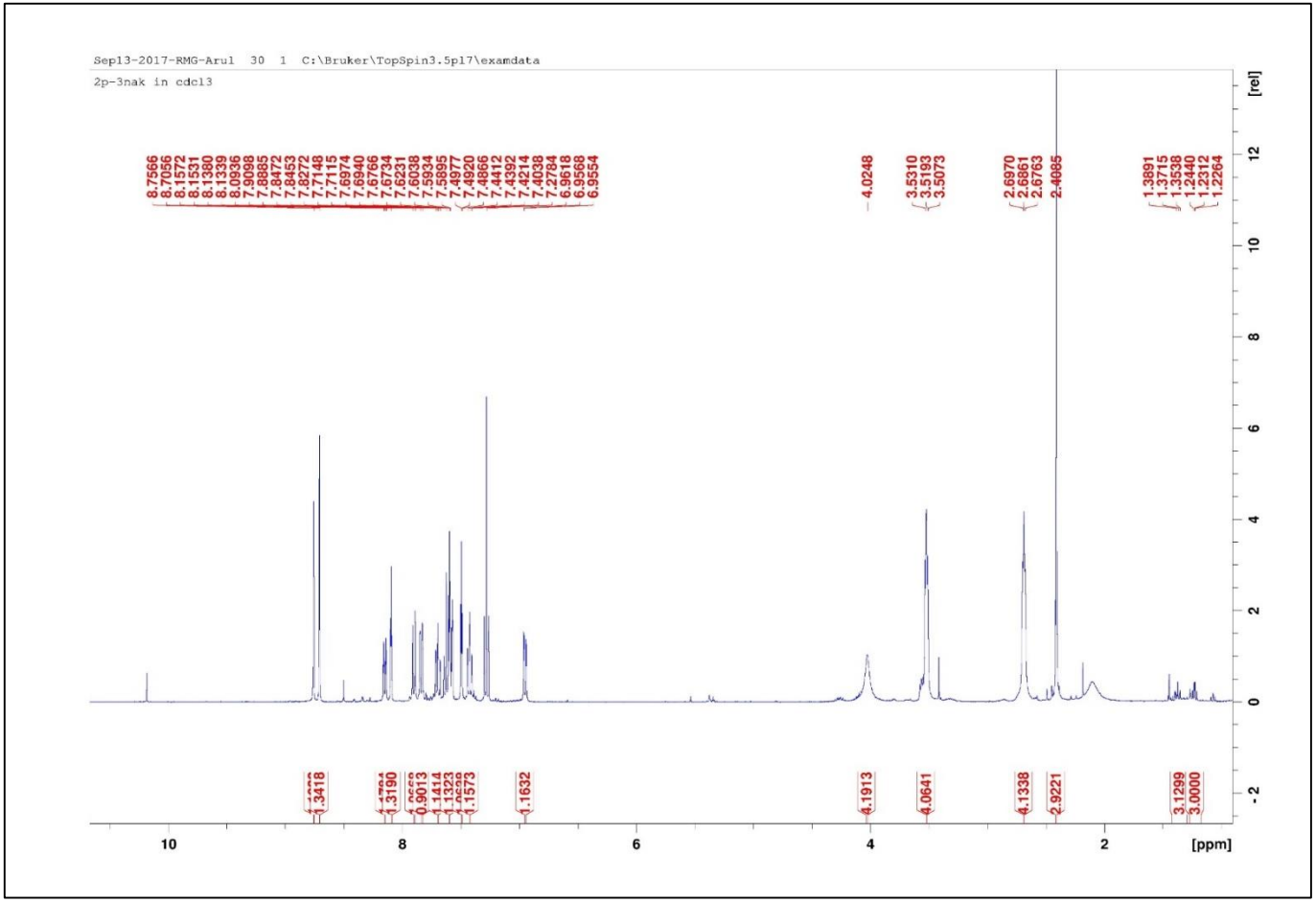

Figure S18: The ^{1}H NMR Spectrum of 4c, diethyl ((2-(4-methylpiperazin-1-yl)quinolin-3-yl)((3-nitrophenyl)amino)methyl)phosphonate

Appendix 19

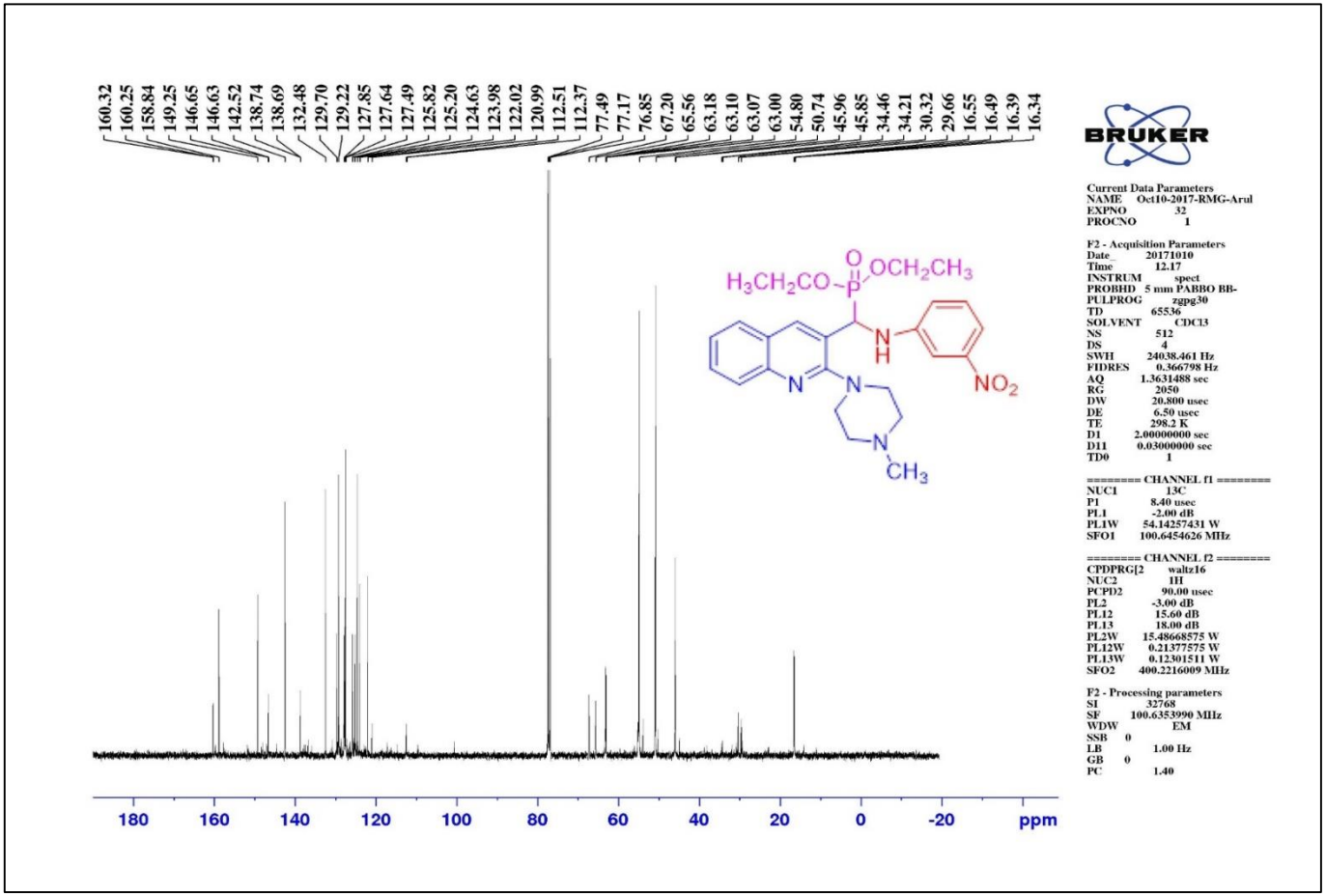

Figure S19: The ^{13}C NMR Spectrum of 4c, diethyl ((2-(4-methylpiperazin-1-yl)quinolin-3-yl)((3-nitrophenyl)amino)methyl)phosphonate

Appendix 20

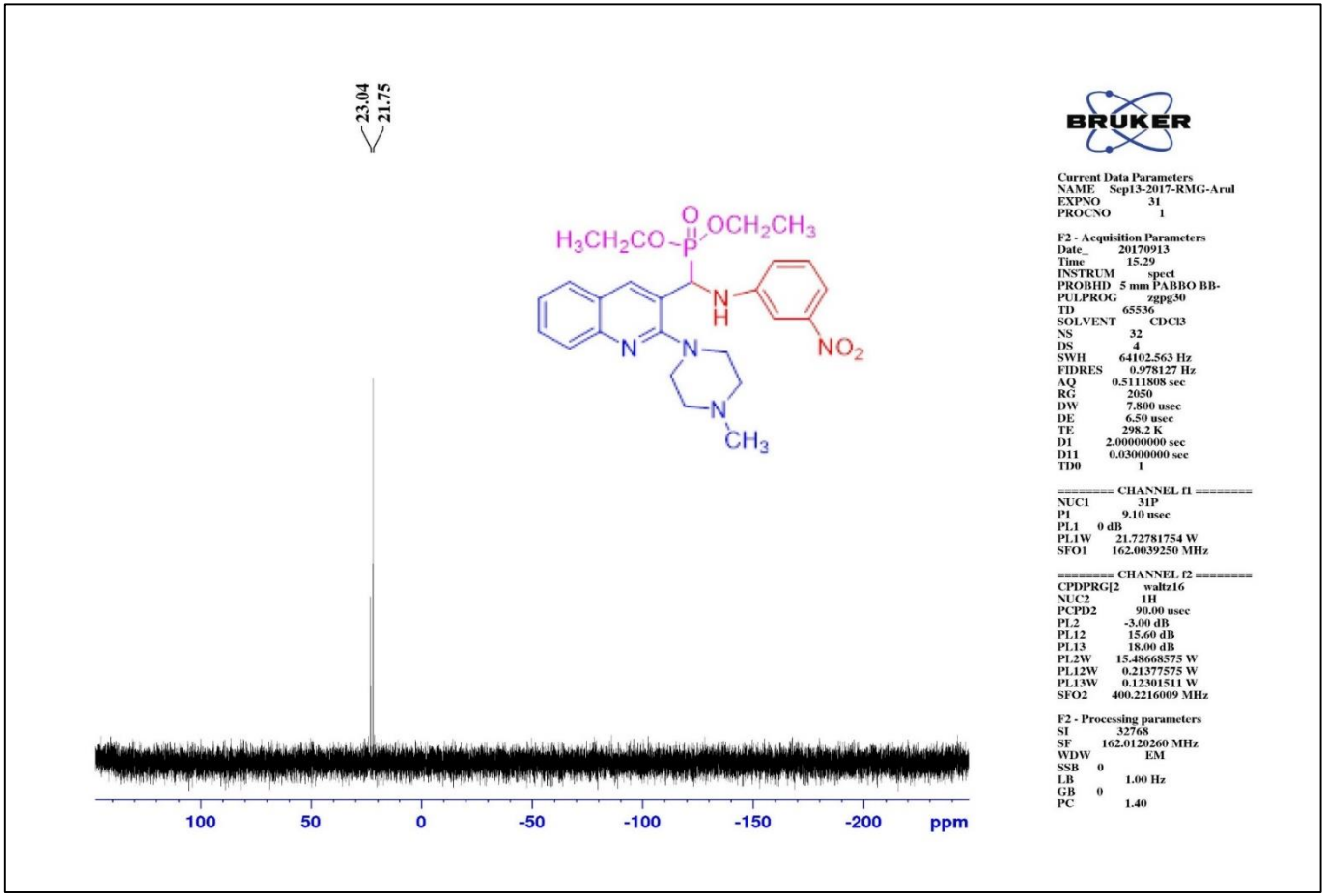

Figure S20: The ^{31}P NMR Spectrum of 4c, diethyl ((2-(4-methylpiperazin-1-yl)quinolin-3-yl)((3-nitrophenyl)amino)methyl)phosphonate

Appendix 21

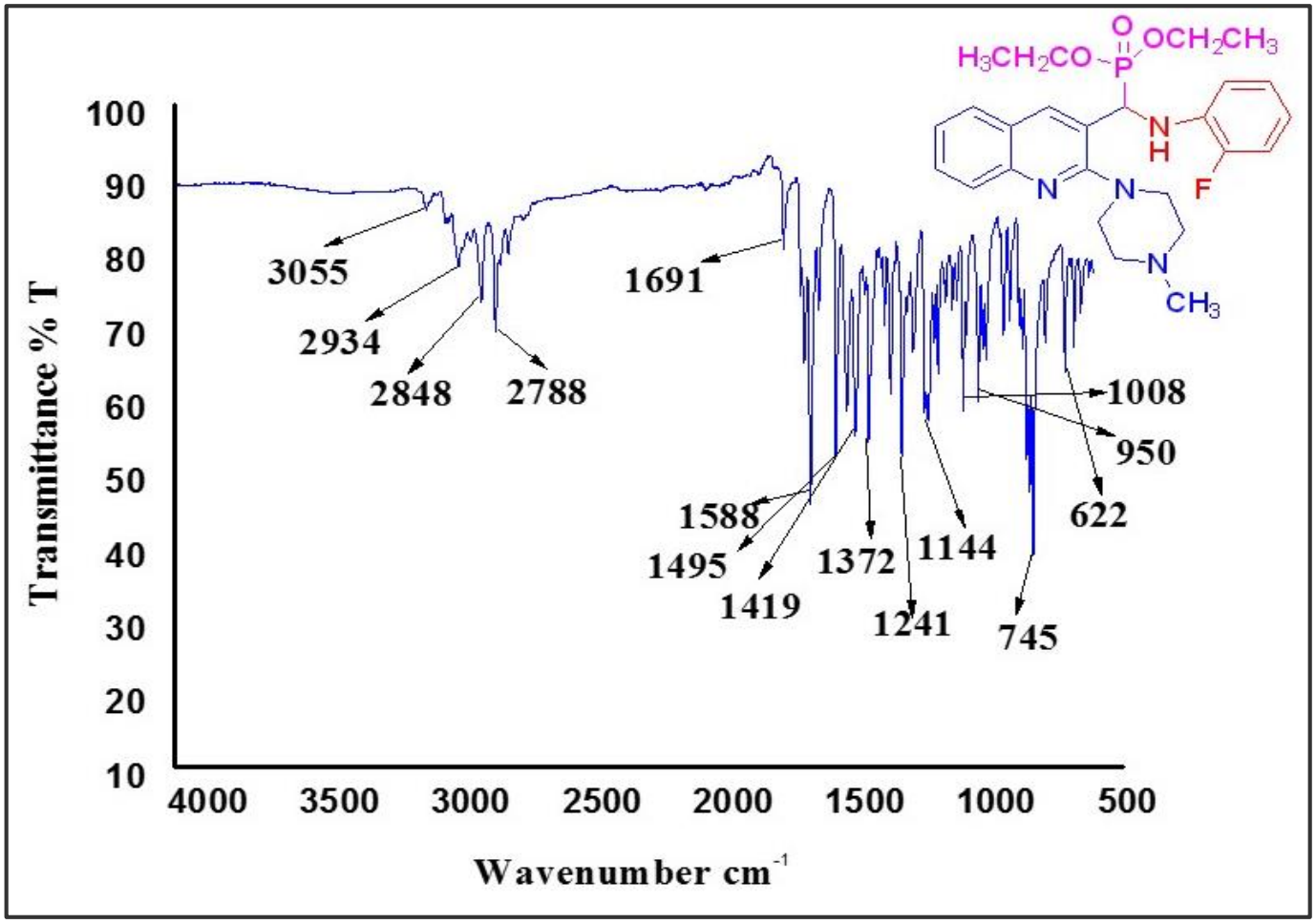

Figure S21: The IR Spectrum of 4d, diethyl (((2-fluorophenyl)amino)(2-(4-methylpiperazin-1-yl)quinolin-3-yl)methyl)phosphonate

Appendix 22

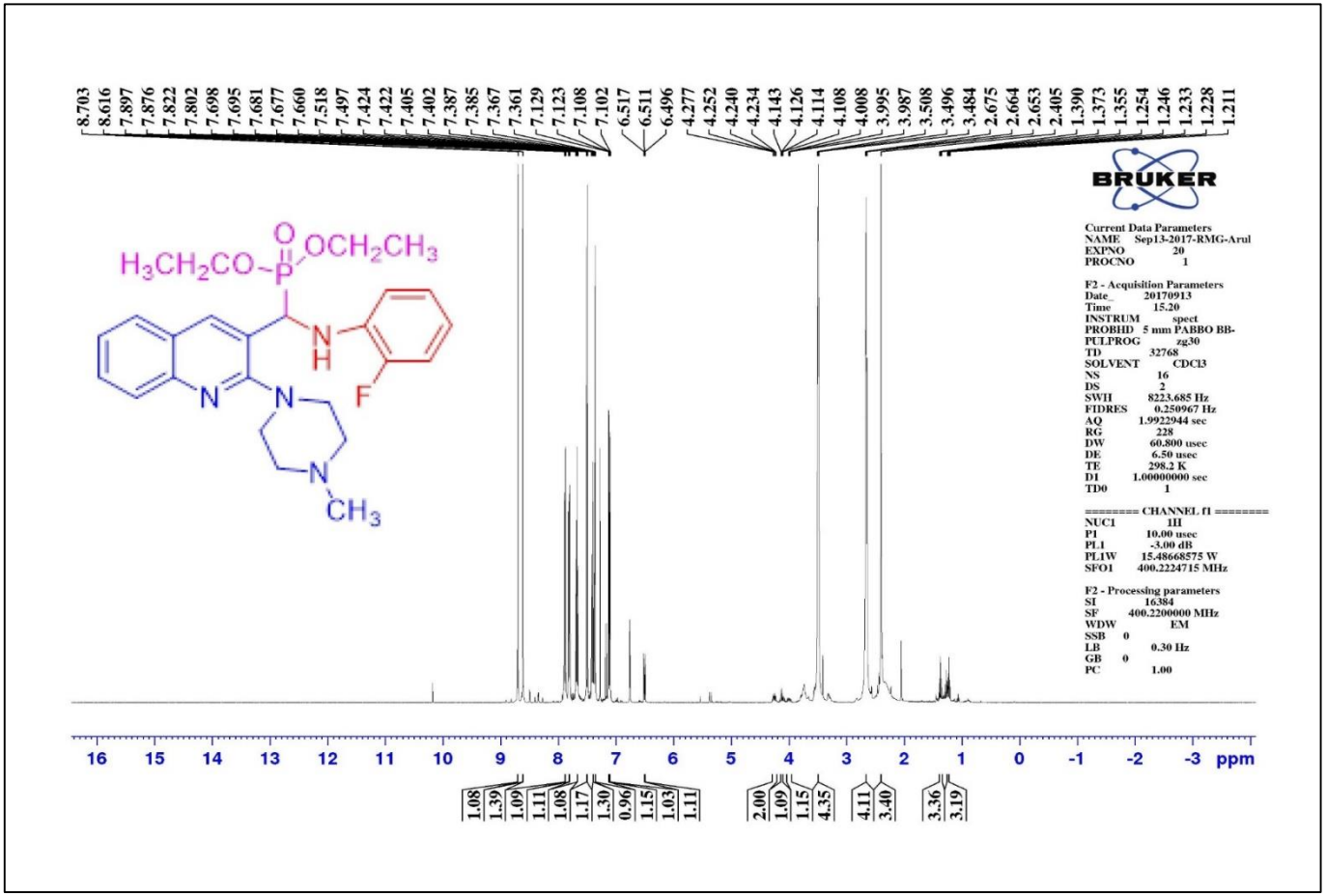

Figure S22: The ^{1}H NMR Spectrum of 4d, diethyl (((2-fluorophenyl)amino)(2-(4-methylpiperazin-1-yl)quinolin-3-yl)methyl)phosphonate

Appendix 23

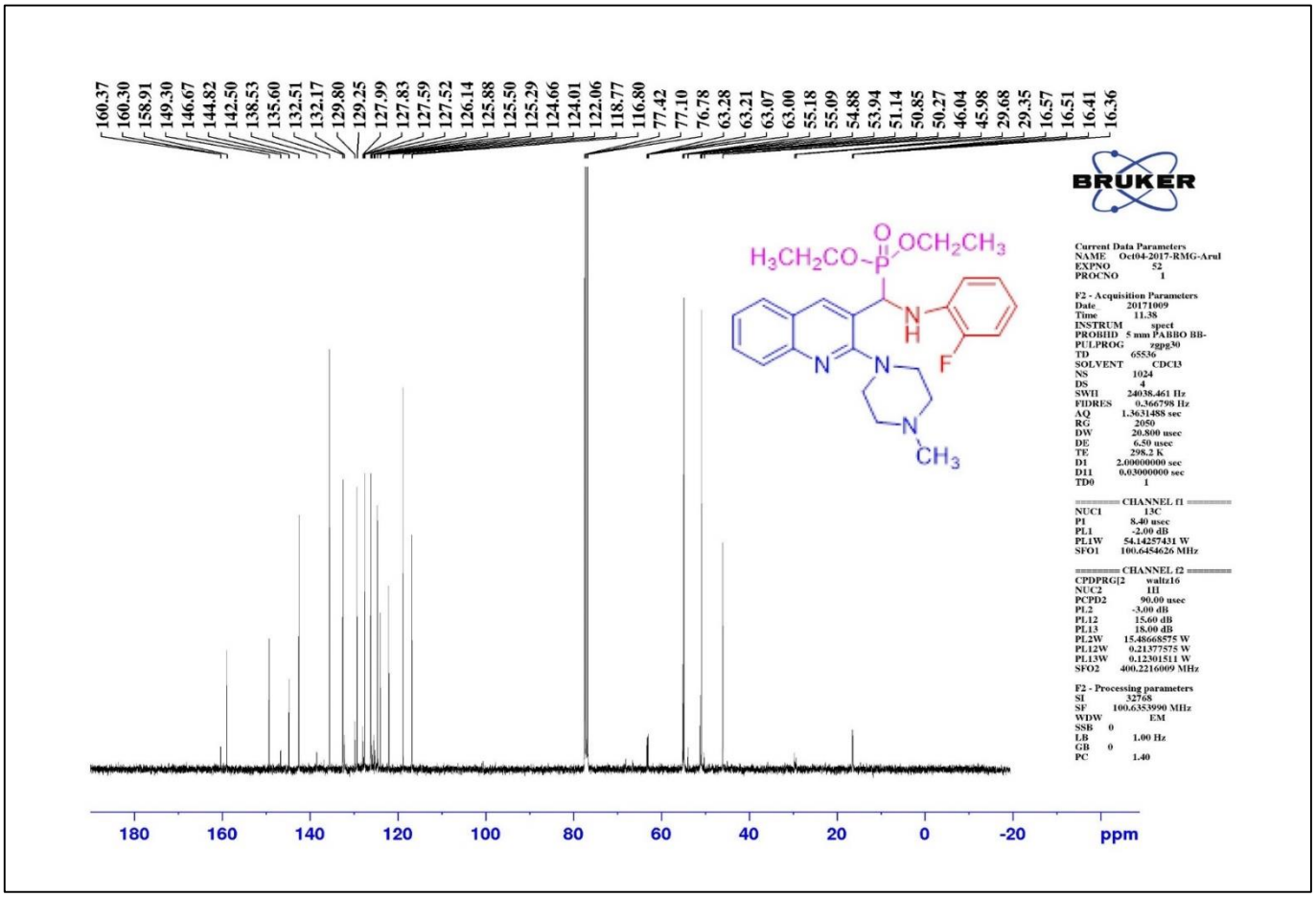

Figure S23: The ^{13}C NMR Spectrum of 4d, diethyl (((2-fluorophenyl)amino)(2-(4-methylpiperazin-1-yl)quinolin-3-yl)methyl)phosphonate

Appendix 24

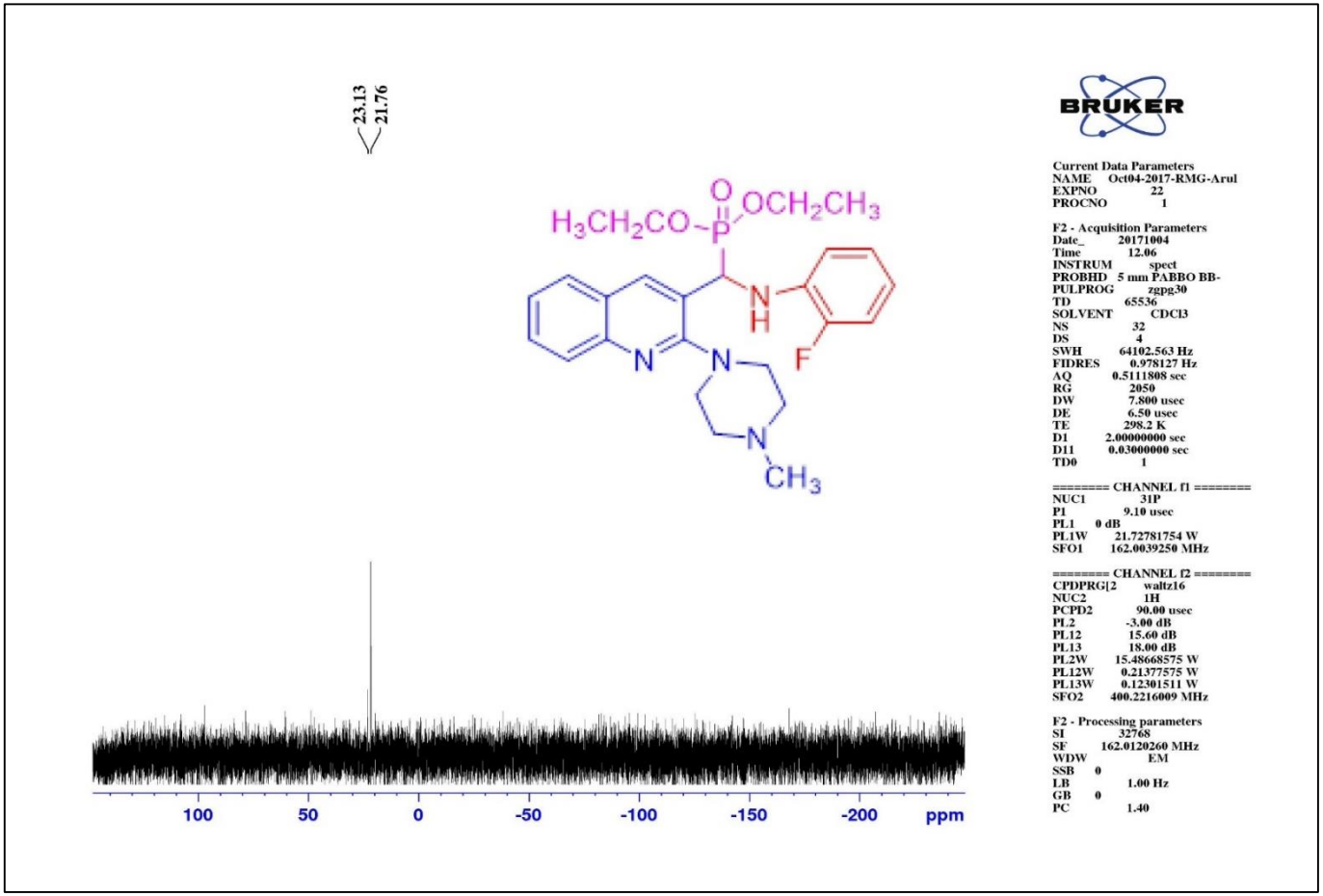

Figure S24: The ^{31}P NMR Spectrum of 4d, diethyl (((2-fluorophenyl)amino)(2-(4-methylpiperazin-1-yl)quinolin-3-yl)methyl)phosphonate

Appendix 25

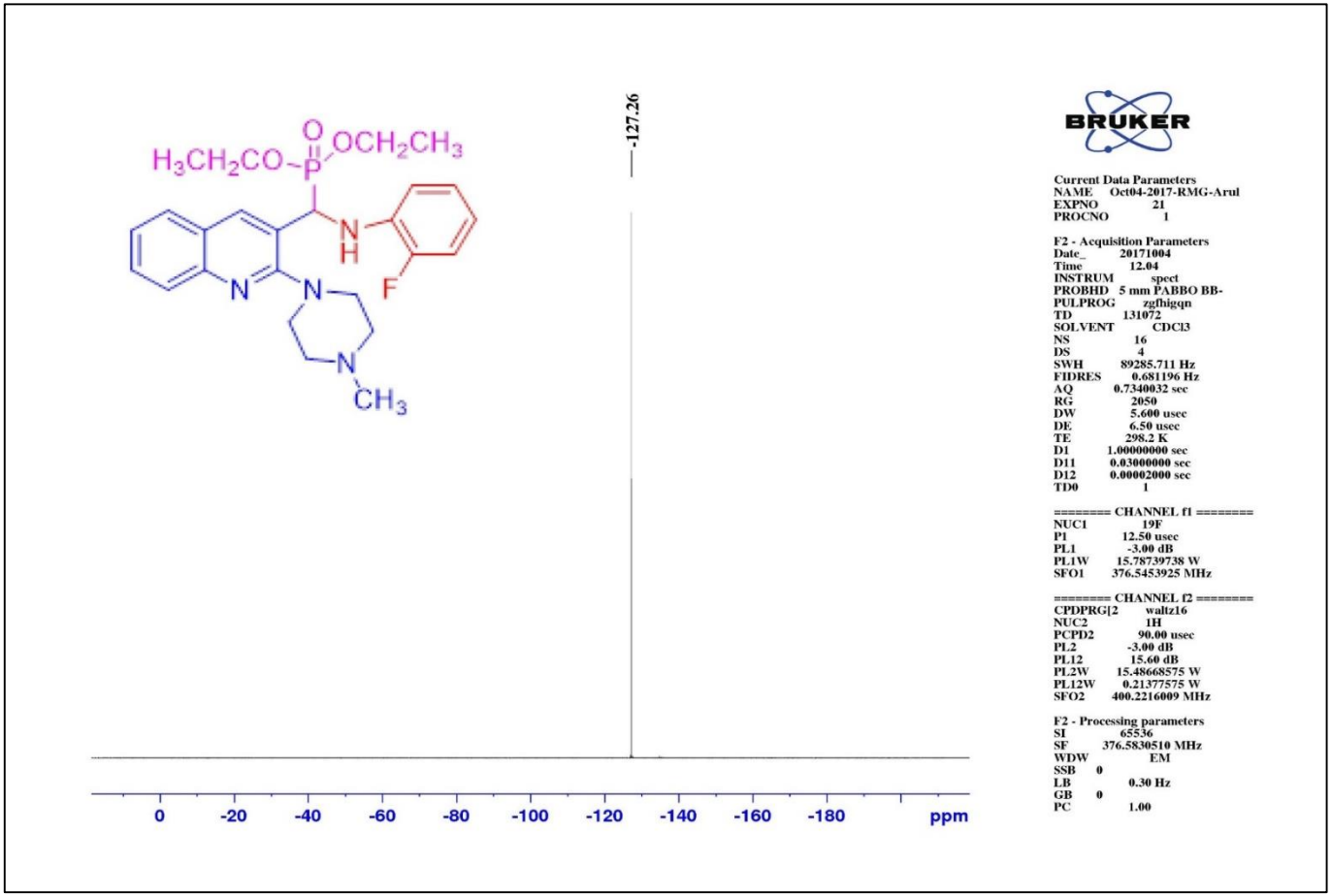

Figure S25: The ^{19}F NMR Spectrum of 4d, diethyl (((2-fluorophenyl)amino)(2-(4-methylpiperazin-1-yl)quinolin-3-yl)methyl)phosphonate

Appendix 26

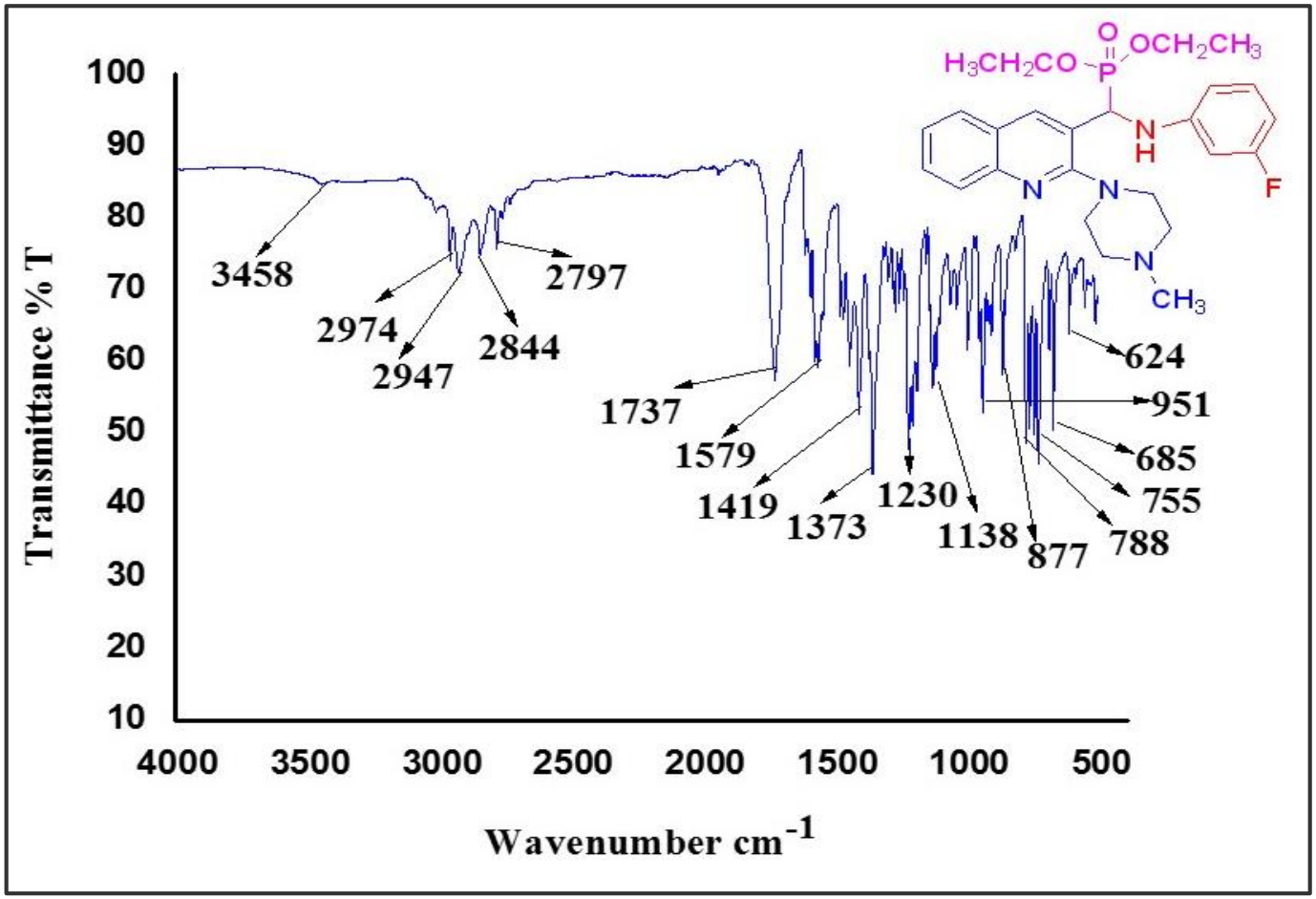

Figure S26: The IR Spectrum of 4e, diethyl(((3-fluorophenyl)amino)(2-(4-methylpiperazin-1-yl)quinolin-3-yl)methyl)phosphonate

Appendix 27

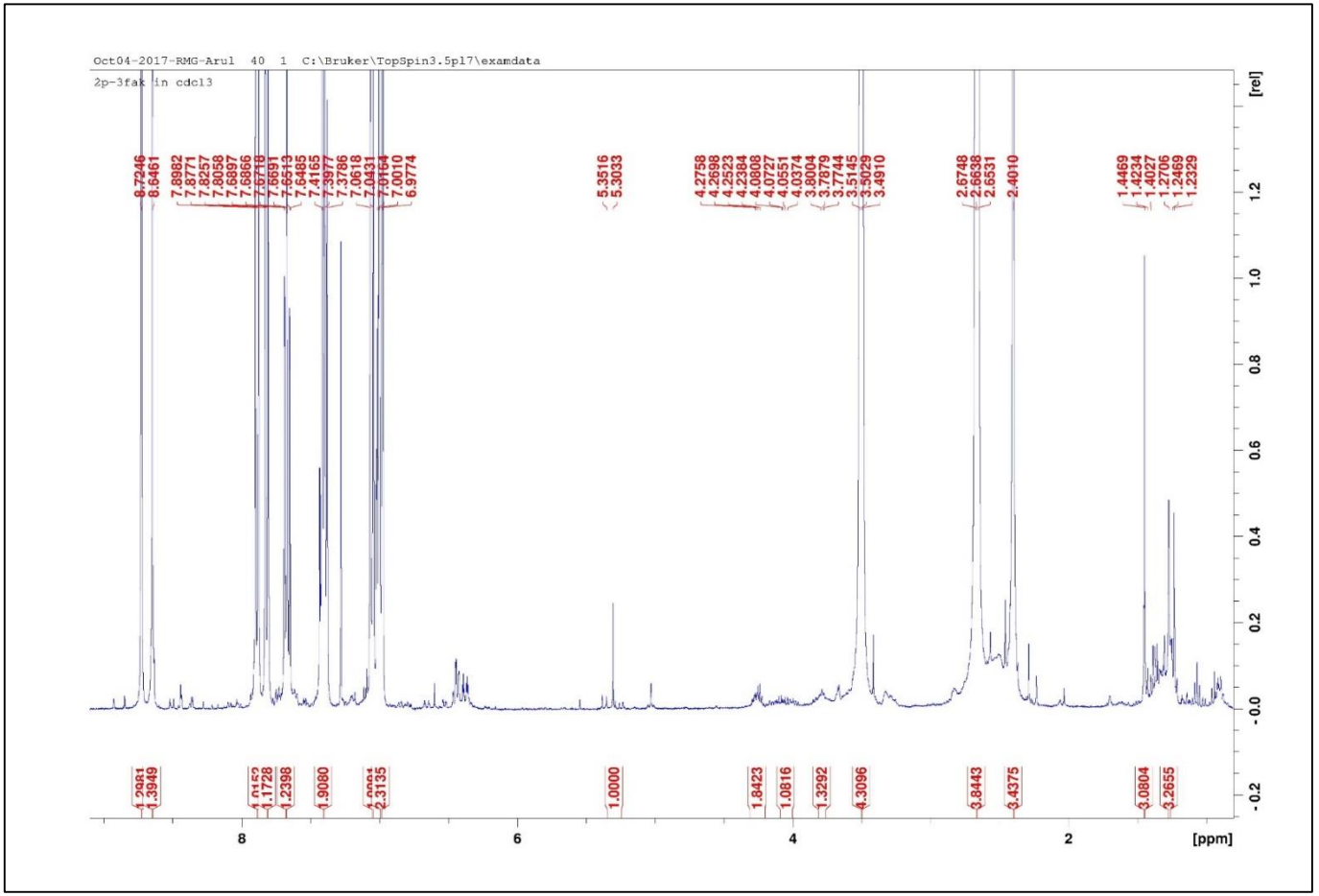

Figure S27: The ^{1}H NMR Spectrum of 4e, diethyl(((3-fluorophenyl)amino)(2-(4-methylpiperazin-1-yl)quinolin-3-yl)methyl)phosphonate

Appendix 28

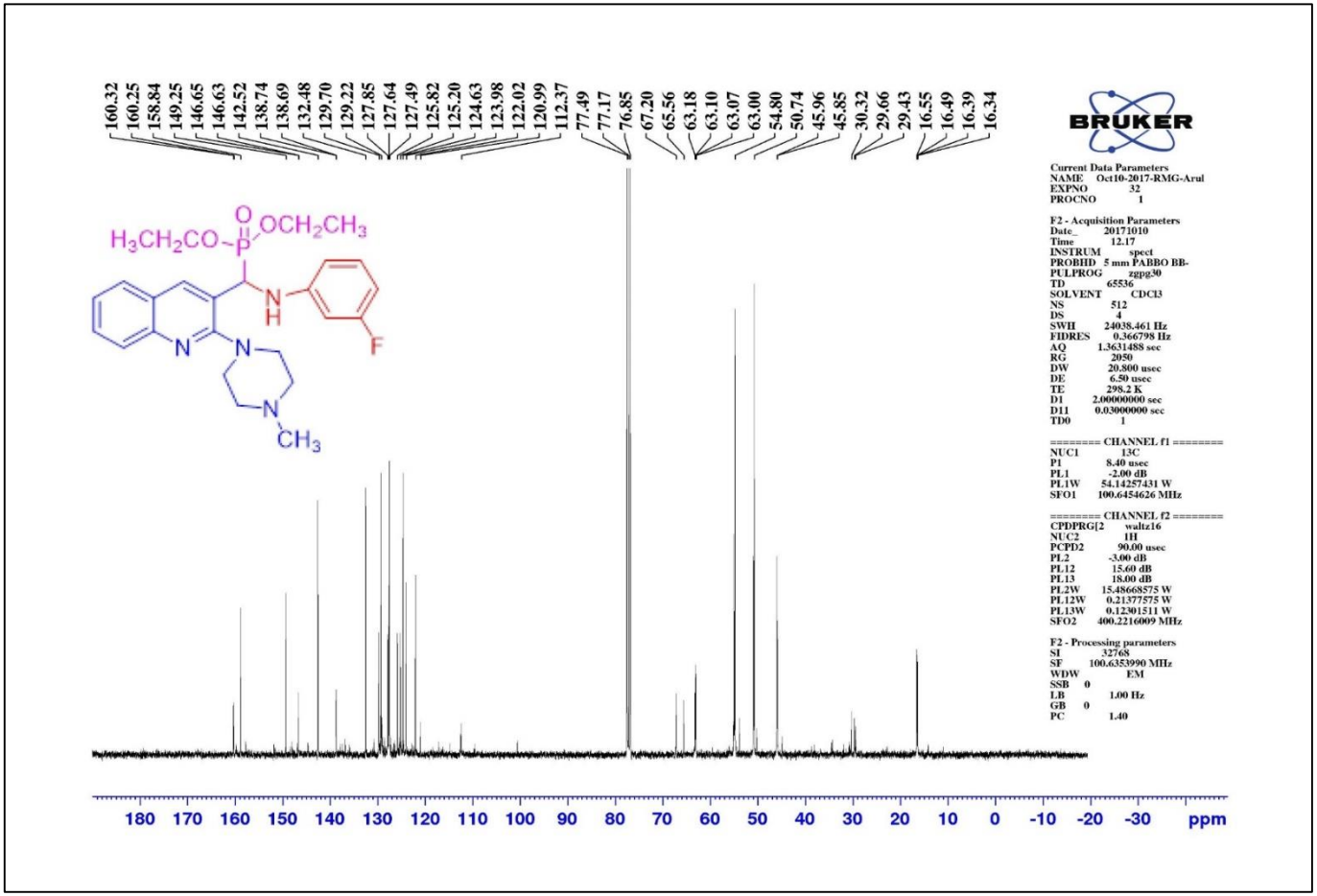

Figure S28: The ^{13}C NMR Spectrum of 4e, diethyl(((3-fluorophenyl)amino)(2-(4-methylpiperazin-1-yl)quinolin-3-yl)methyl)phosphonate

Appendix 29

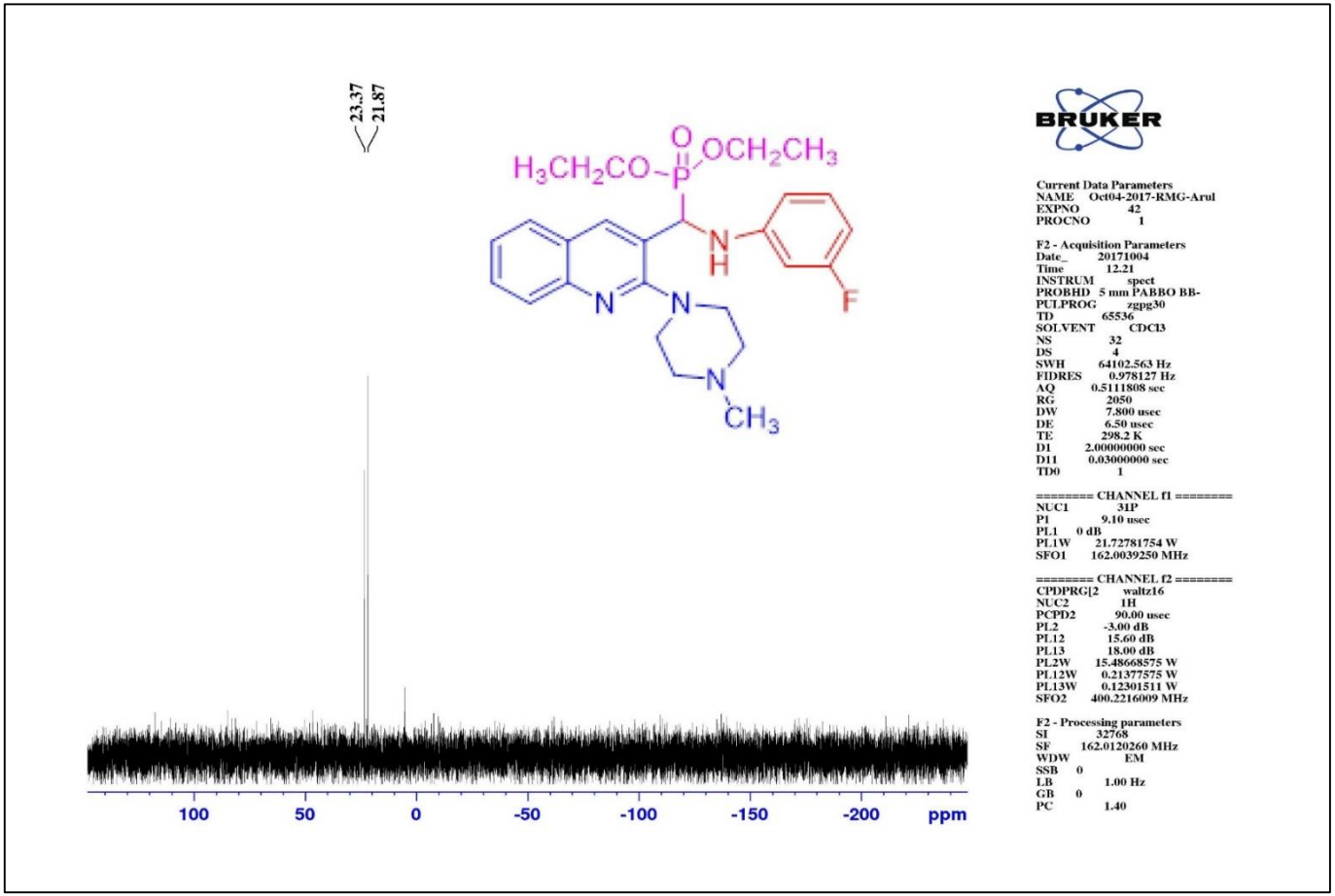

Figure S29: The ^{31}P NMR Spectrum of 4e, diethyl(((3-fluorophenyl)amino)(2-(4-methylpiperazin-1-yl)quinolin-3-yl)methyl)phosphonate

Appendix 30

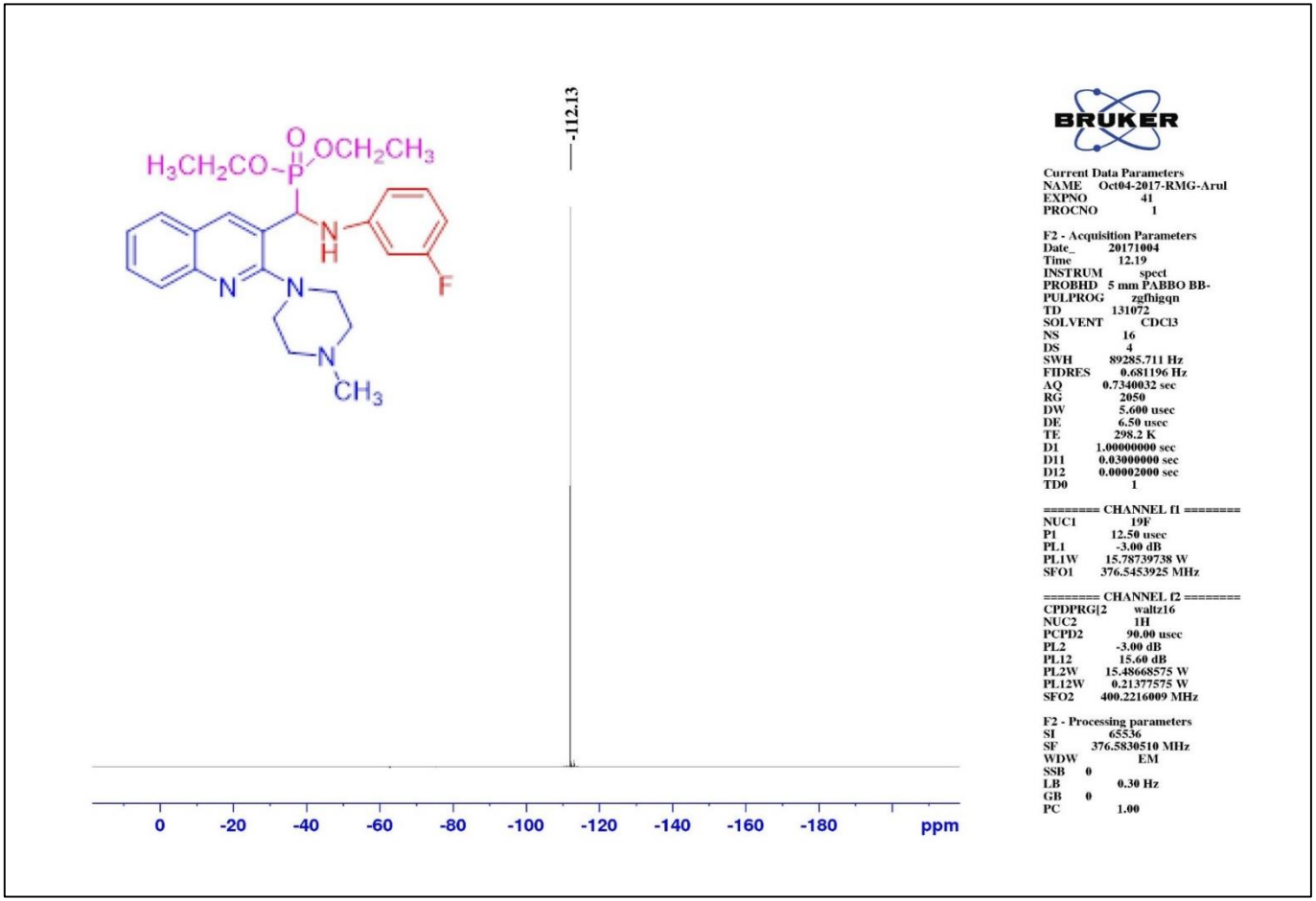

Figure S30: The ^{19}F NMR Spectrum of 4e, diethyl(((3-fluorophenyl)amino)(2-(4-methylpiperazin-1-yl)quinolin-3-yl)methyl)phosphonate

Appendix 31

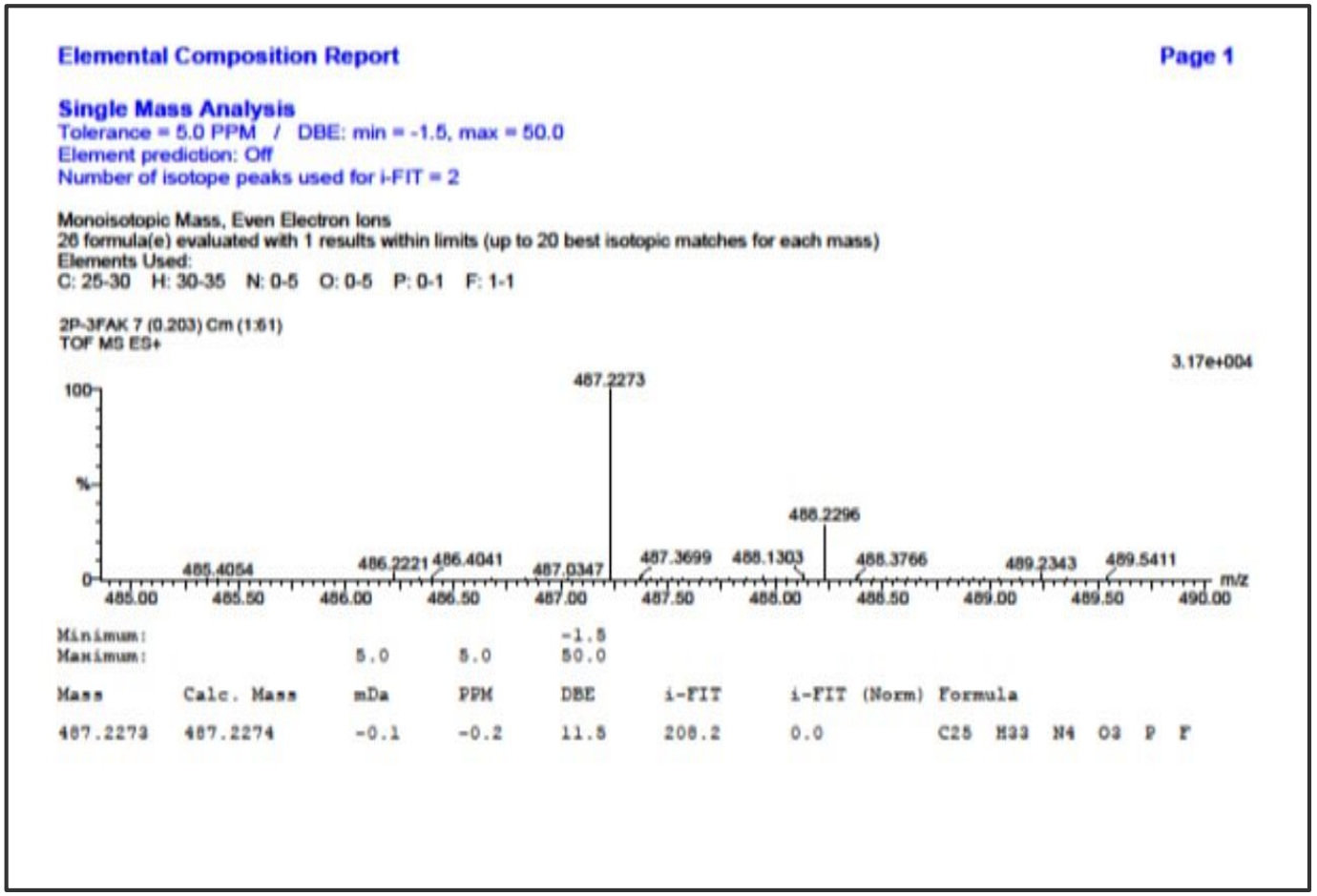

Figure S31: The HRMS Spectrum of 4e, diethyl(((3-fluorophenyl)amino)(2-(4-methylpiperazin-1-yl)quinolin-3-yl)methyl)phosphonate

Appendix 32

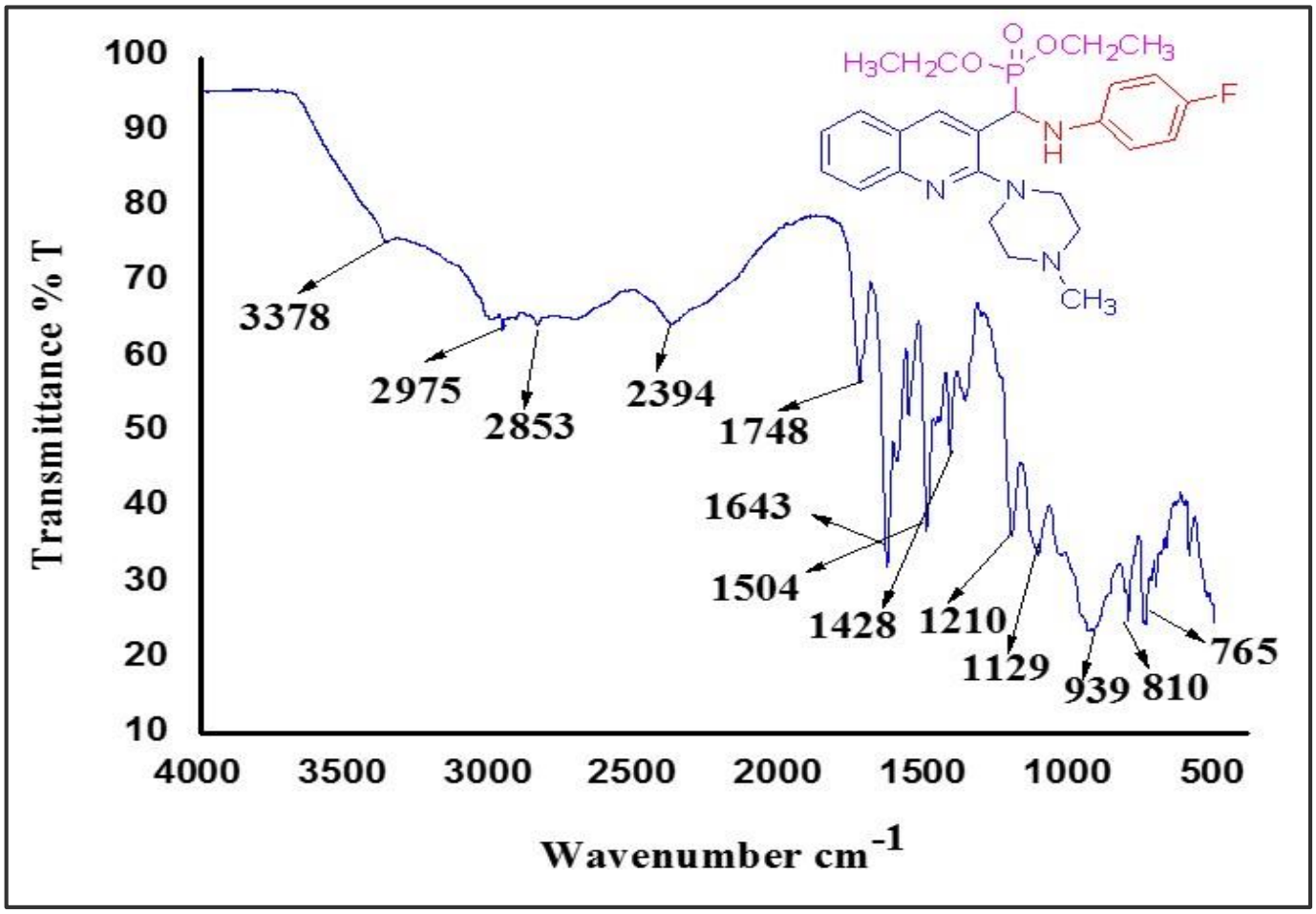

Figure S32: The IR Spectrum of 4f, diethyl(((4-fluorophenyl)amino)(2-(4-methylpiperazin-1-yl)quinolin-3-yl)methyl)phosphonate

Appendix 33

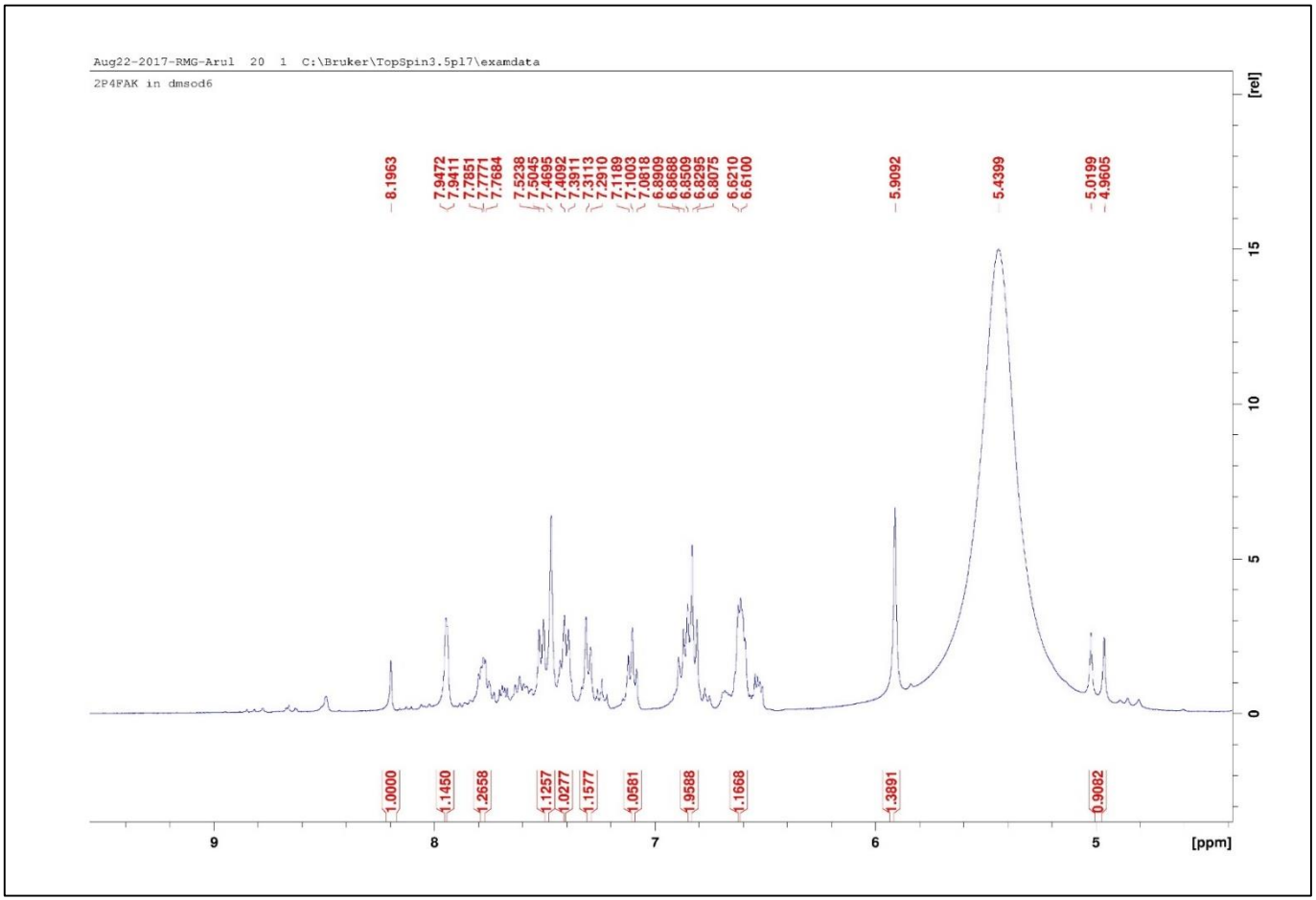

Figure S33: The ^{1}H NMR Spectrum of 4f, diethyl(((4-fluorophenyl)amino)(2-(4-methylpiperazin-1-yl)quinolin-3-yl)methyl)phosphonate

Appendix 34

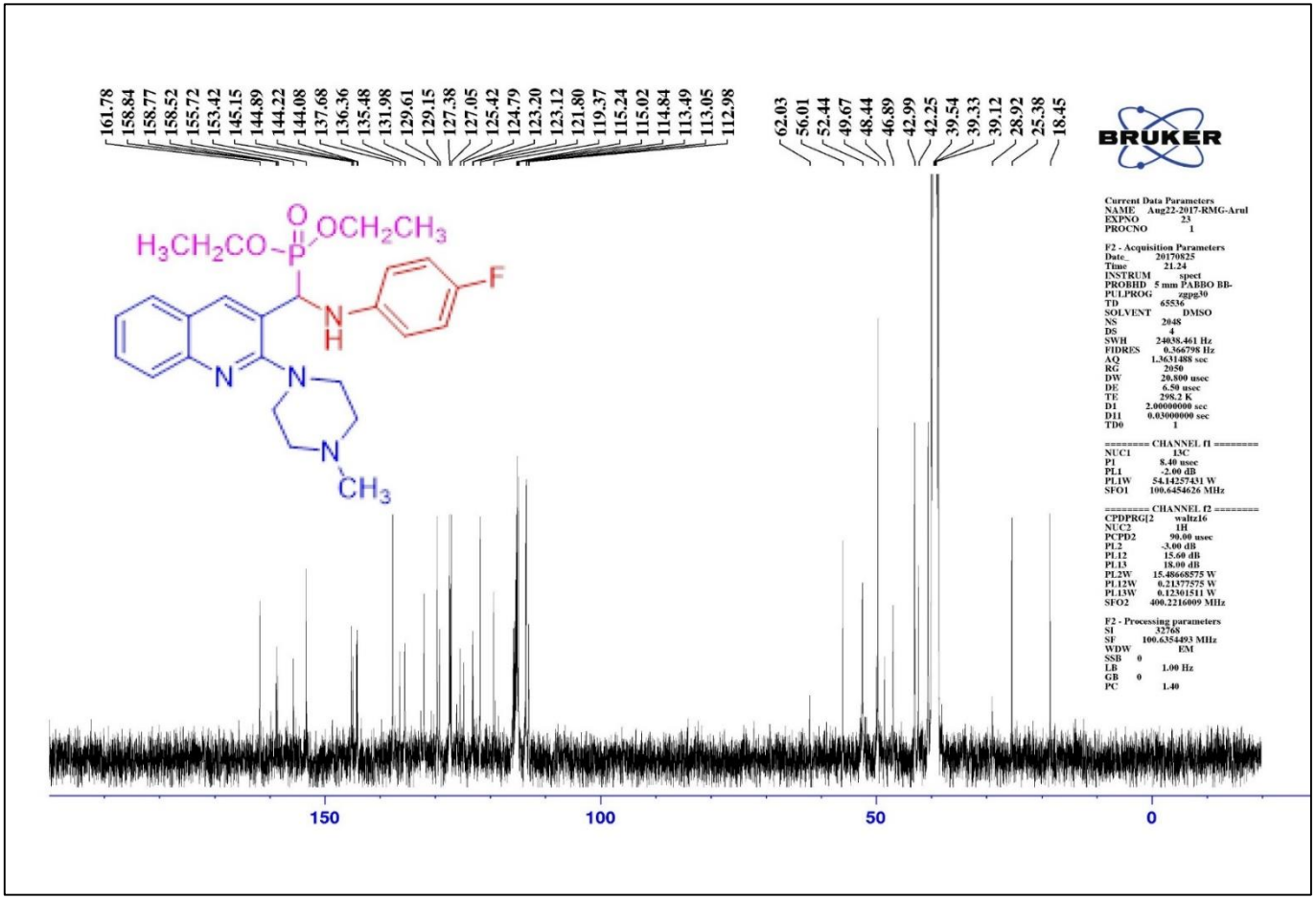

Figure S34: The ^{13}C NMR Spectrum of 4f, diethyl(((4-fluorophenyl)amino)(2-(4-methylpiperazin-1-yl)quinolin-3-yl)methyl)phosphonate

Appendix 35

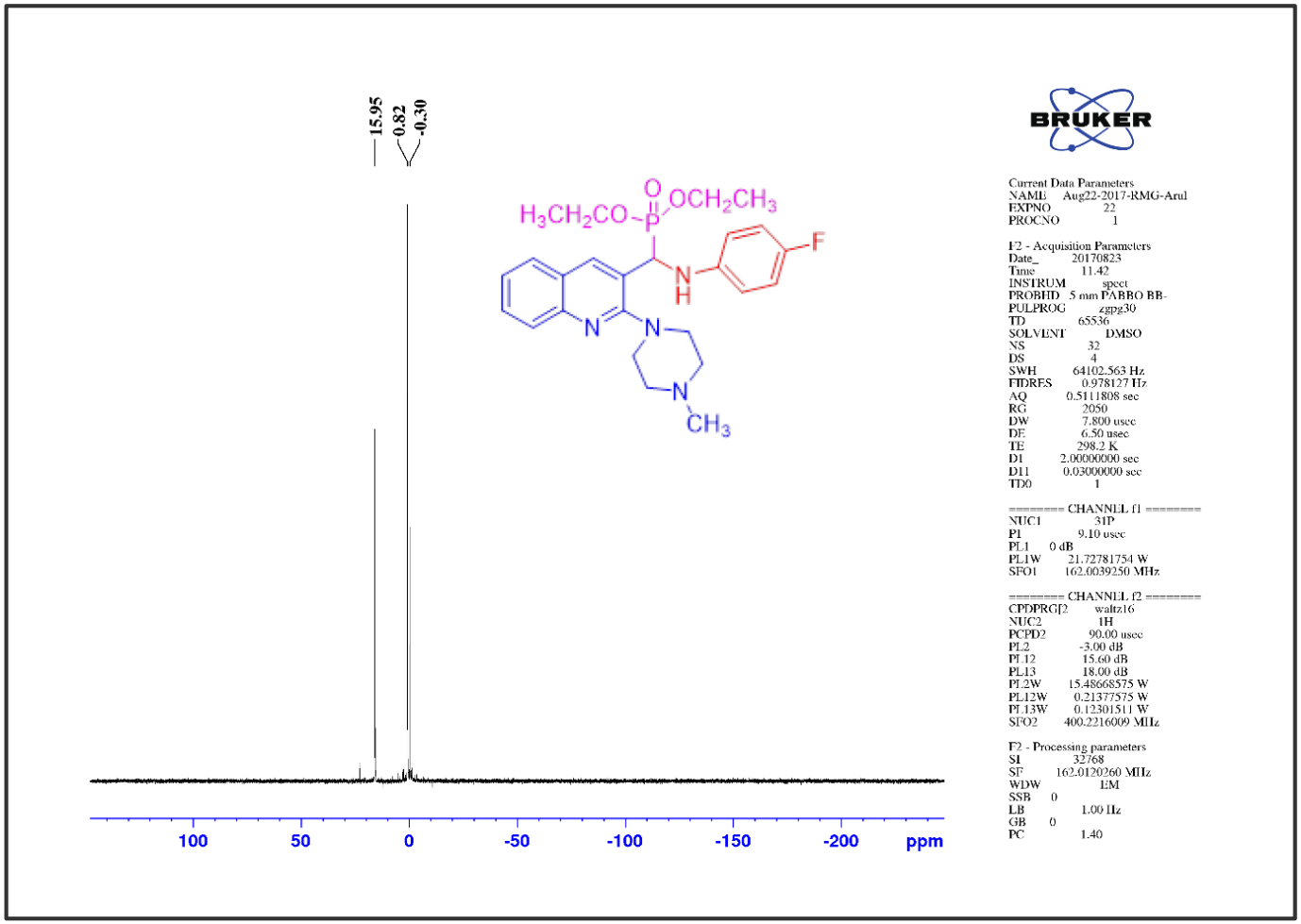

Figure S35: The ^{31}P NMR Spectrum of 4f, diethyl(((4-fluorophenyl)amino)(2-(4-methylpiperazin-1-yl)quinolin-3-yl)methyl)phosphonate

Appendix 36

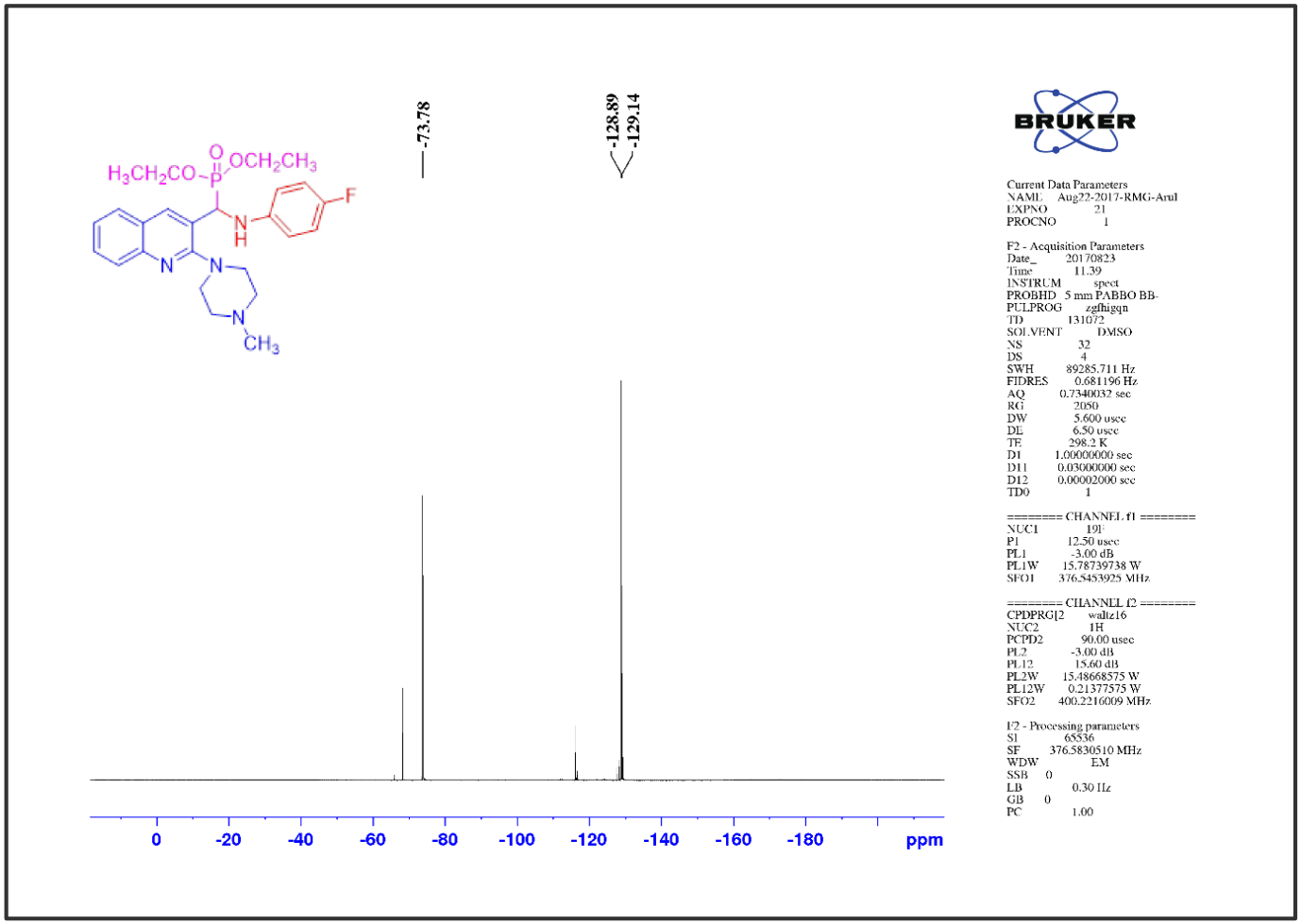

Figure S36: The ^{19}F NMR Spectrum of 4f, diethyl(((4-fluorophenyl)amino)(2-(4-methylpiperazin-1-yl)quinolin-3-yl)methyl)phosphonate

Appendix 37

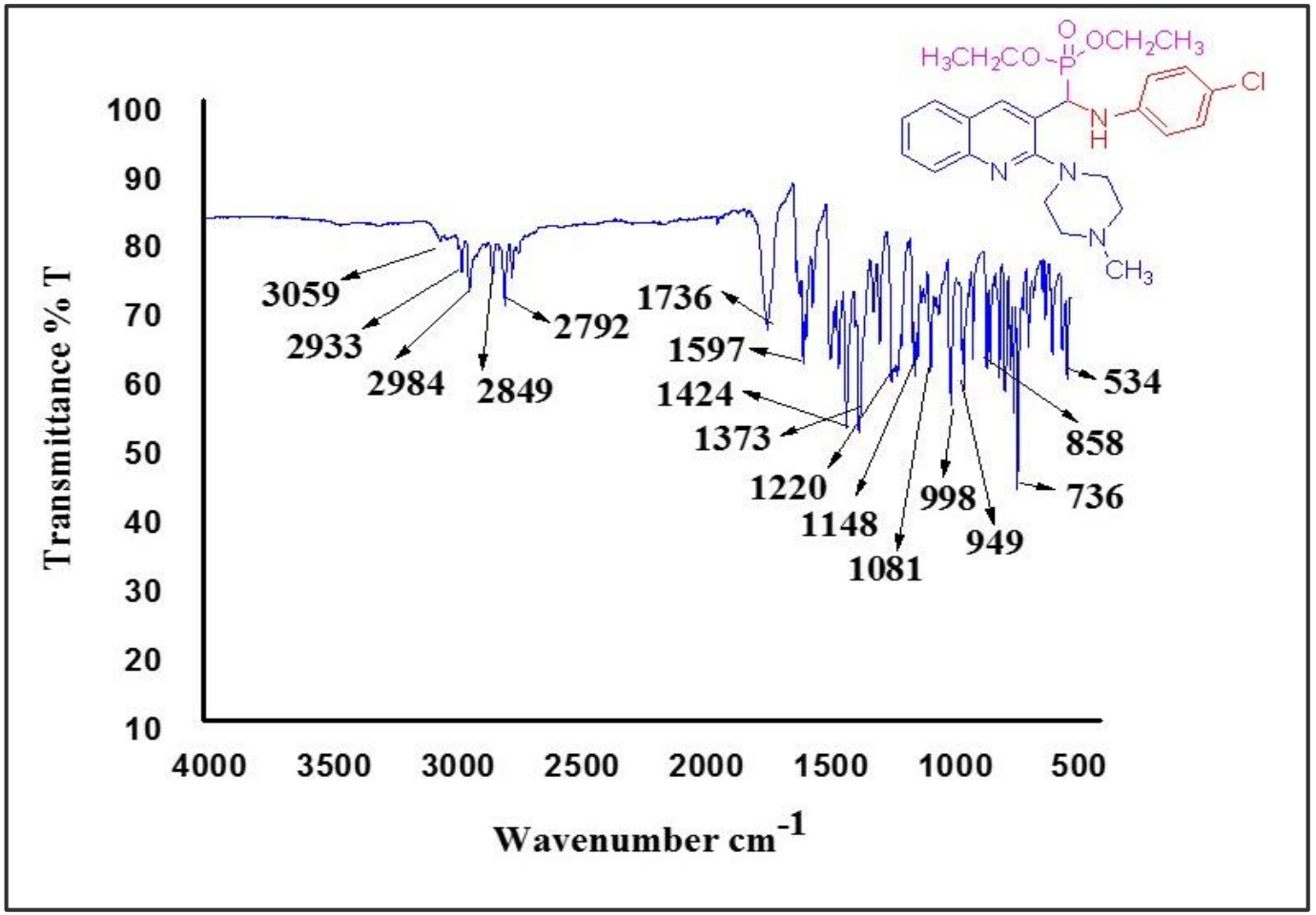

Figure S37: The IR Spectrum of 4g, diethyl(((4-chlorophenyl)amino)(2-(4-methylpiperazin-1-yl)quinolin-3-yl)methyl)phosphonate

Appendix 38

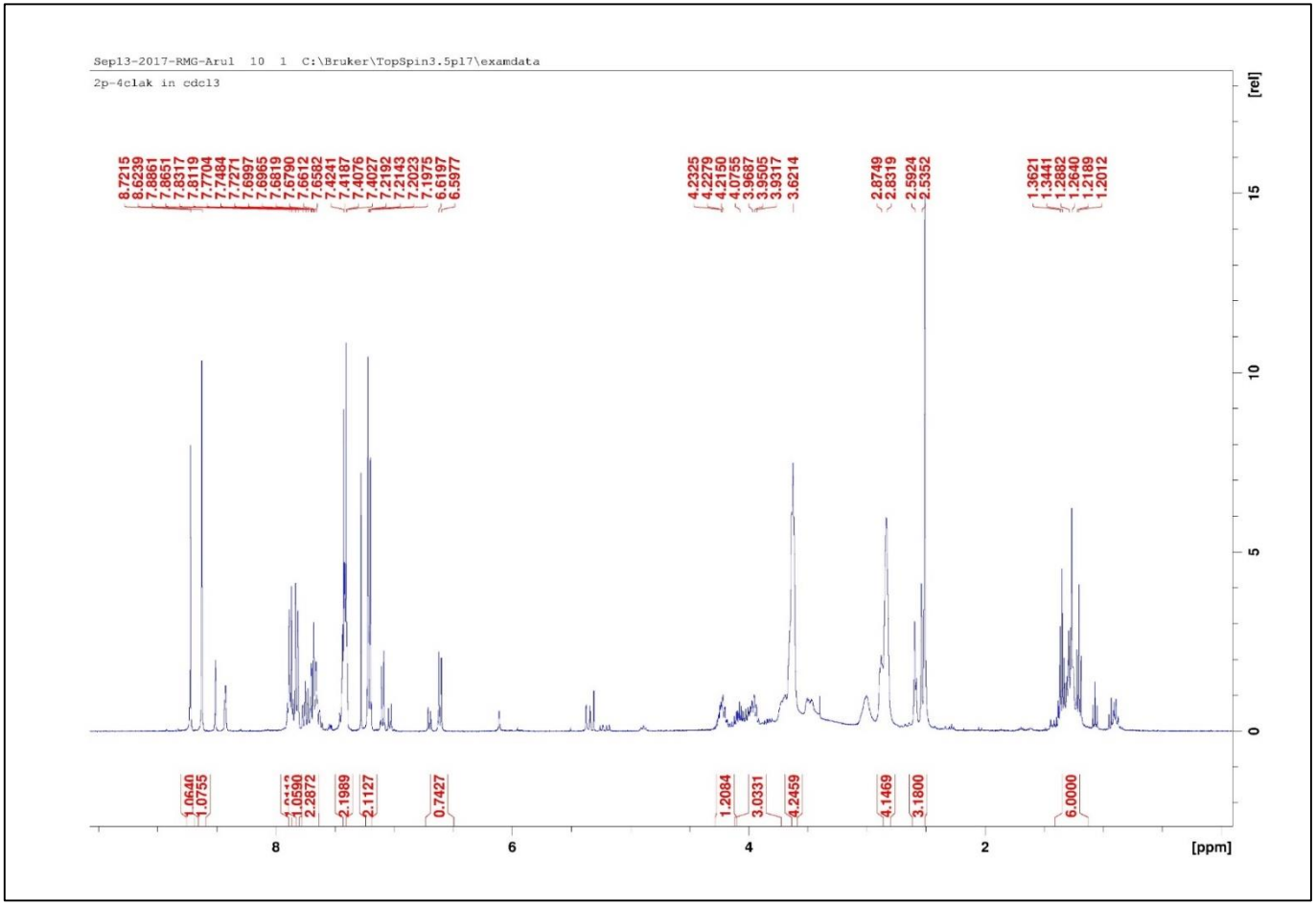

Figure S38: The ^{1}H NMR Spectrum of 4g, diethyl(((4-chlorophenyl)amino)(2-(4-methylpiperazin-1-yl)quinolin-3-yl)methyl)phosphonate

Appendix 39

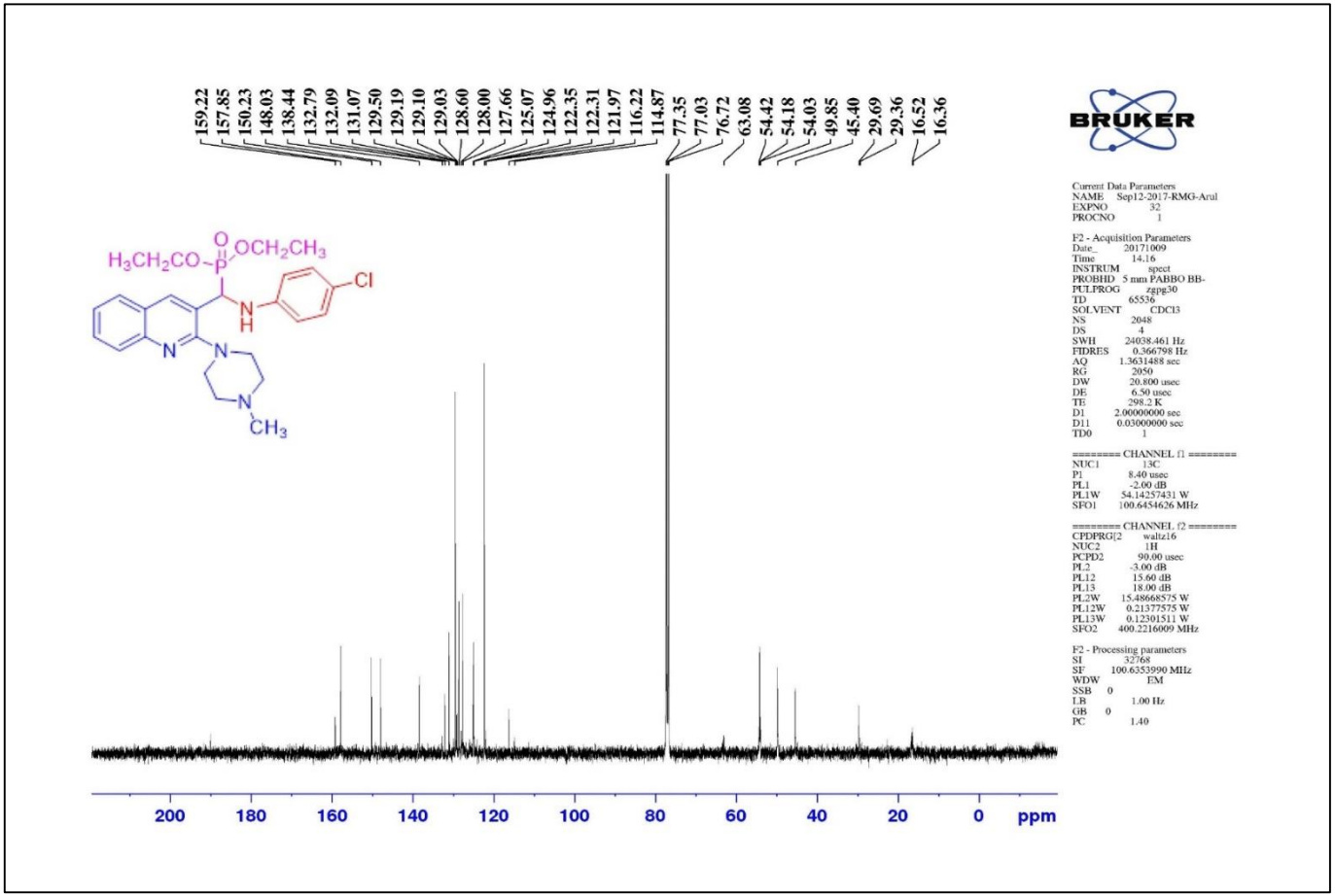

Figure S39: The ^{13}C NMR Spectrum of 4g, diethyl(((4-chlorophenyl)amino)(2-(4-methylpiperazin-1-yl)quinolin-3-yl)methyl)phosphonate

Appendix 40

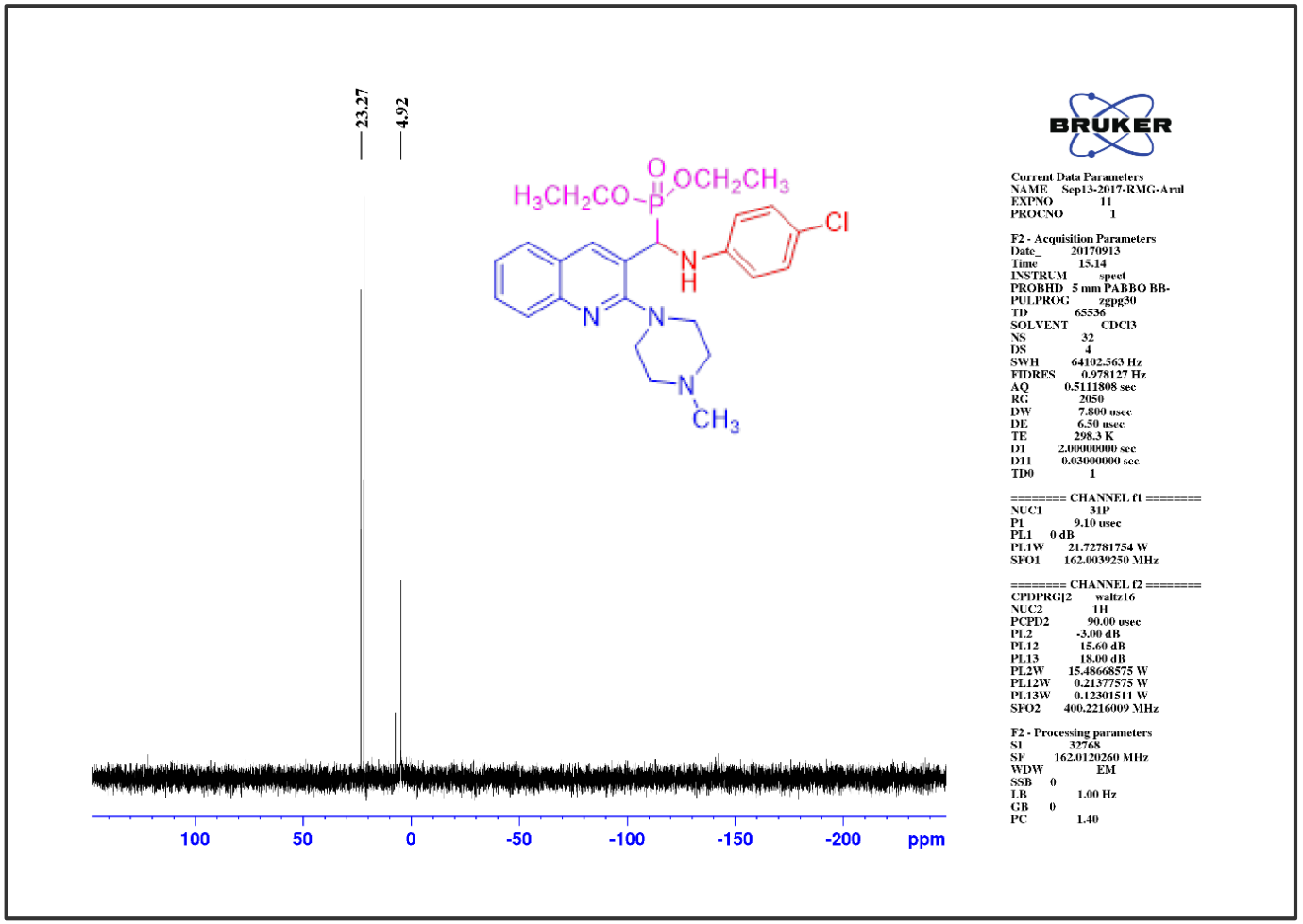

Figure S40: The ^{31}P NMR Spectrum of 4g, diethyl(((4-chlorophenyl)amino)(2-(4-methylpiperazin-1-yl)quinolin-3-yl)methyl)phosphonate

Appendix 41

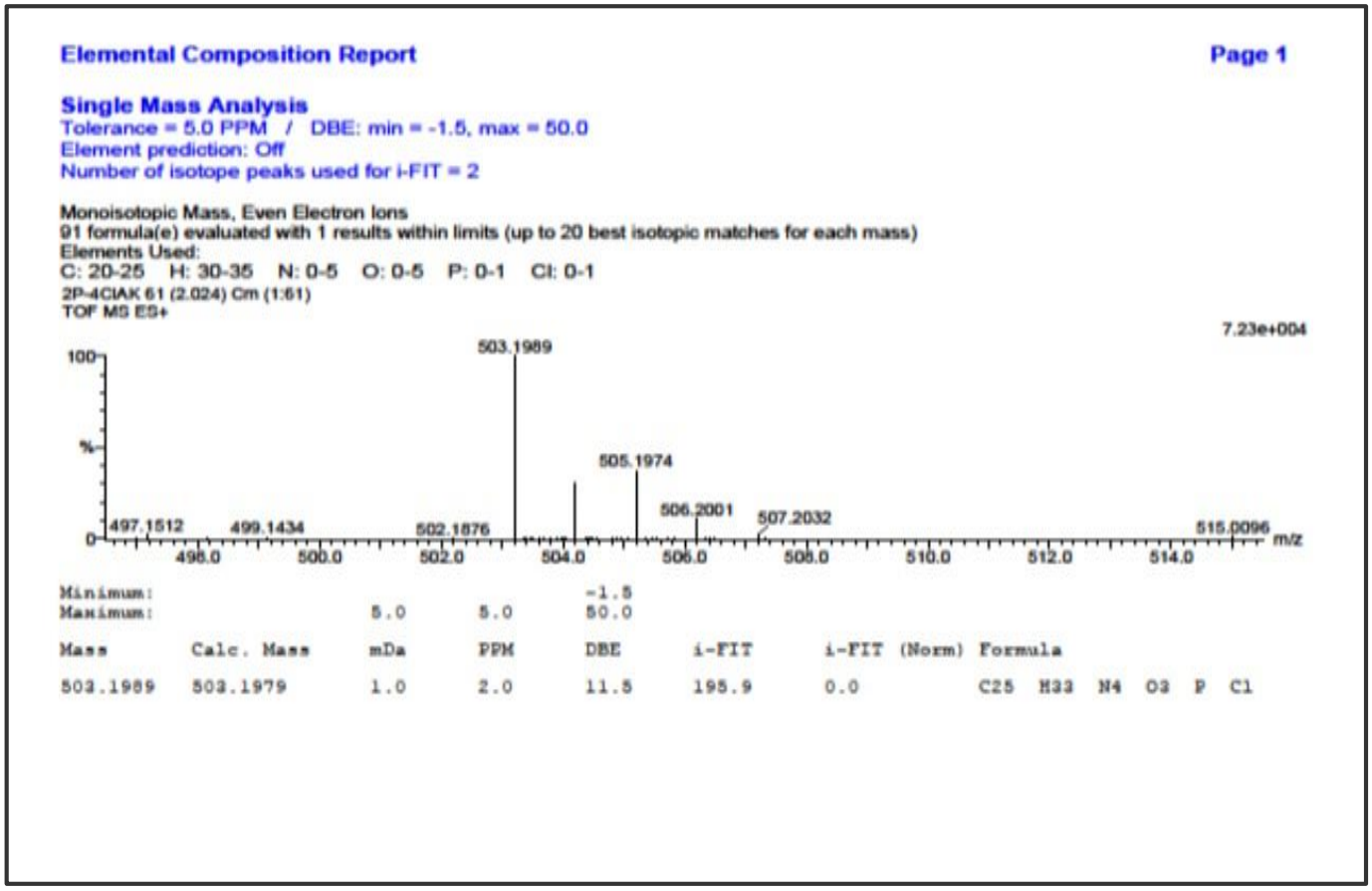

Figure S41: The HRMS Spectrum of 4g, diethyl(((4-chlorophenyl)amino)(2-(4-methylpiperazin-1-yl)quinolin-3-yl)methyl)phosphonate

Appendix 42

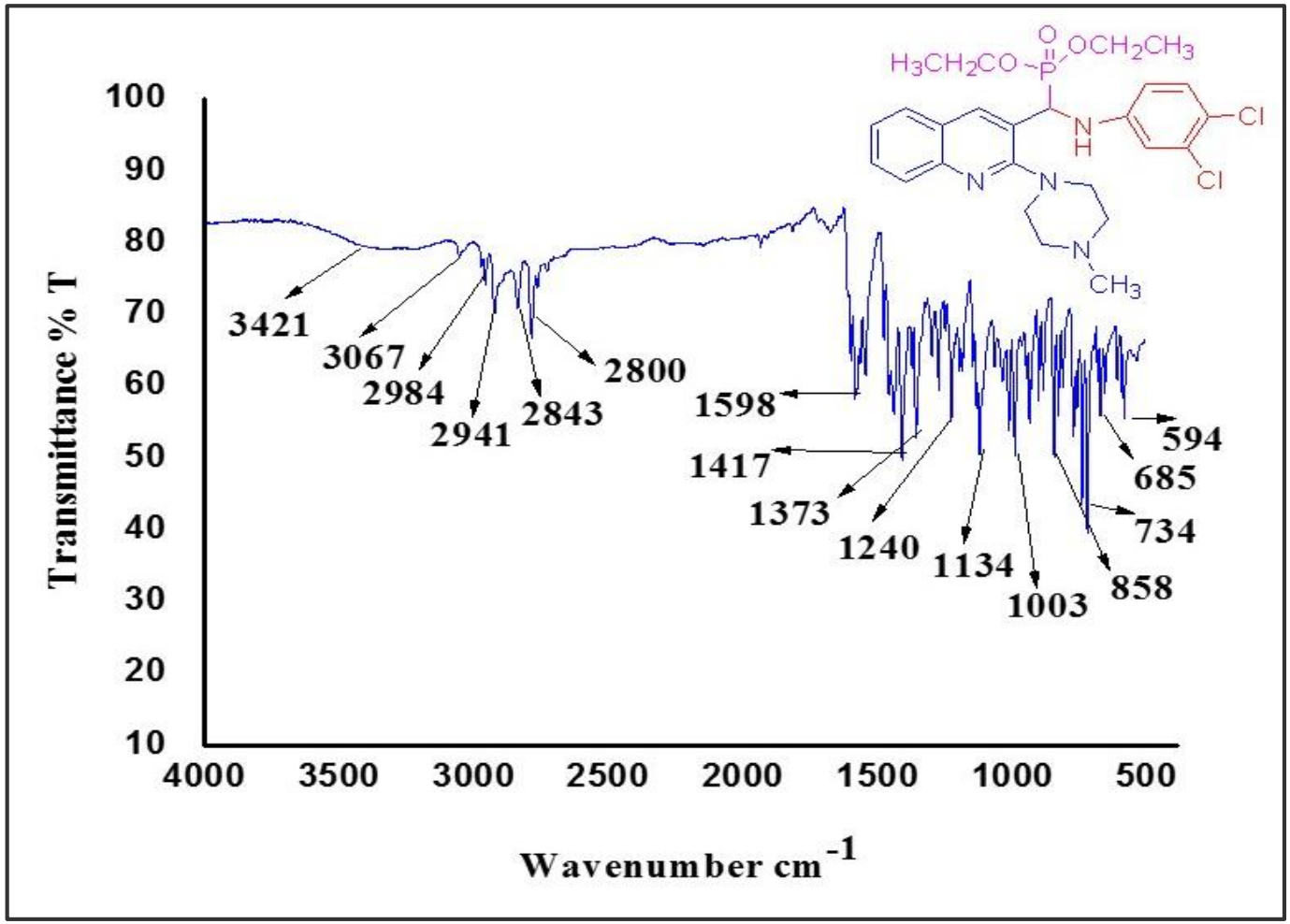

Figure S42: The IR Spectrum of 4h, diethyl(((3,4-dichlorophenyl)amino)(2-(4-methylpiperazin-1-yl)quinolin-3-yl)methyl)phosphonate

Appendix 43

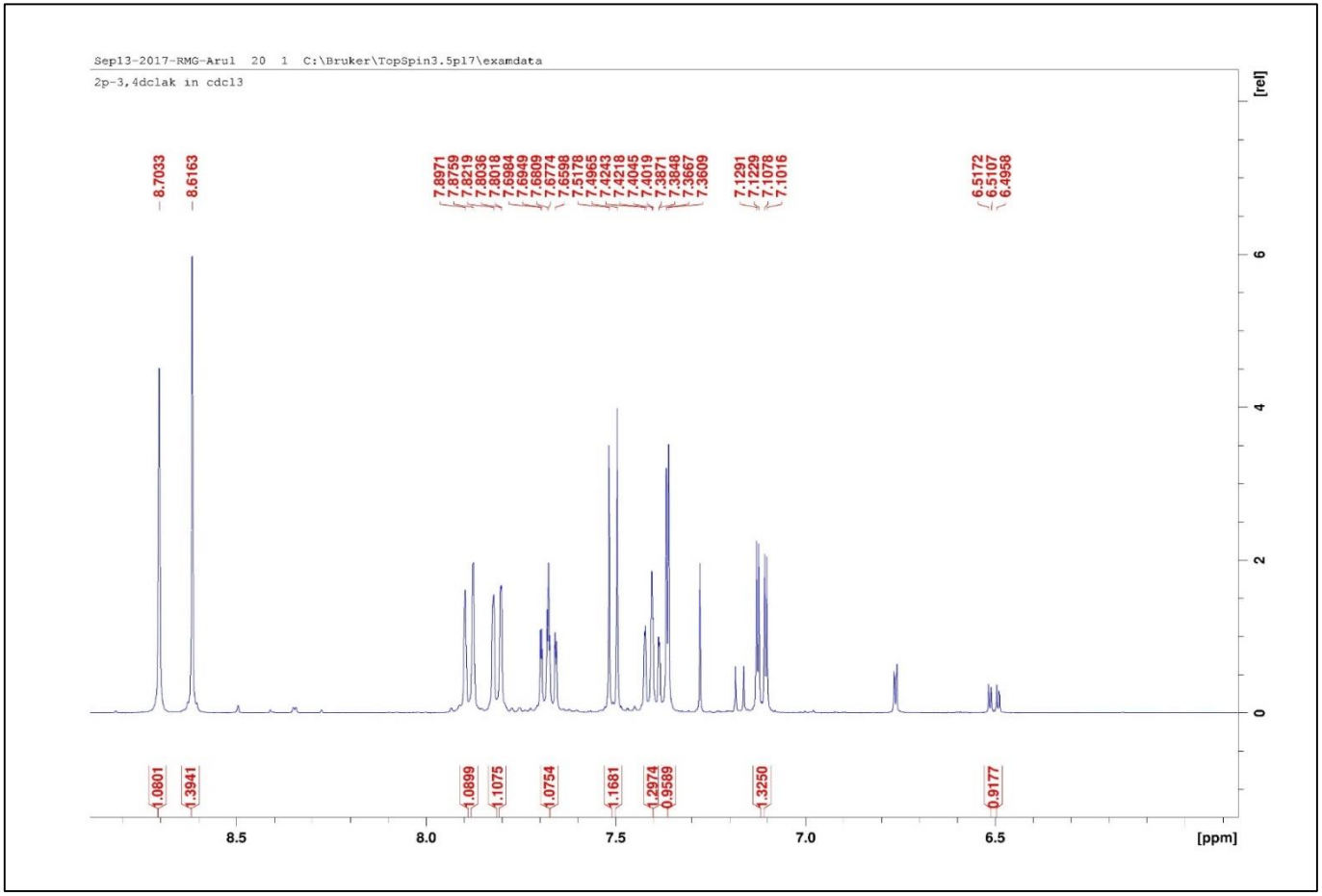

Figure S43: The ^{1}H NMR Spectrum of 4h, diethyl(((3,4-dichlorophenyl)amino)(2-(4-methylpiperazin-1-yl)quinolin-3-yl)methyl)phosphonate

Appendix 44

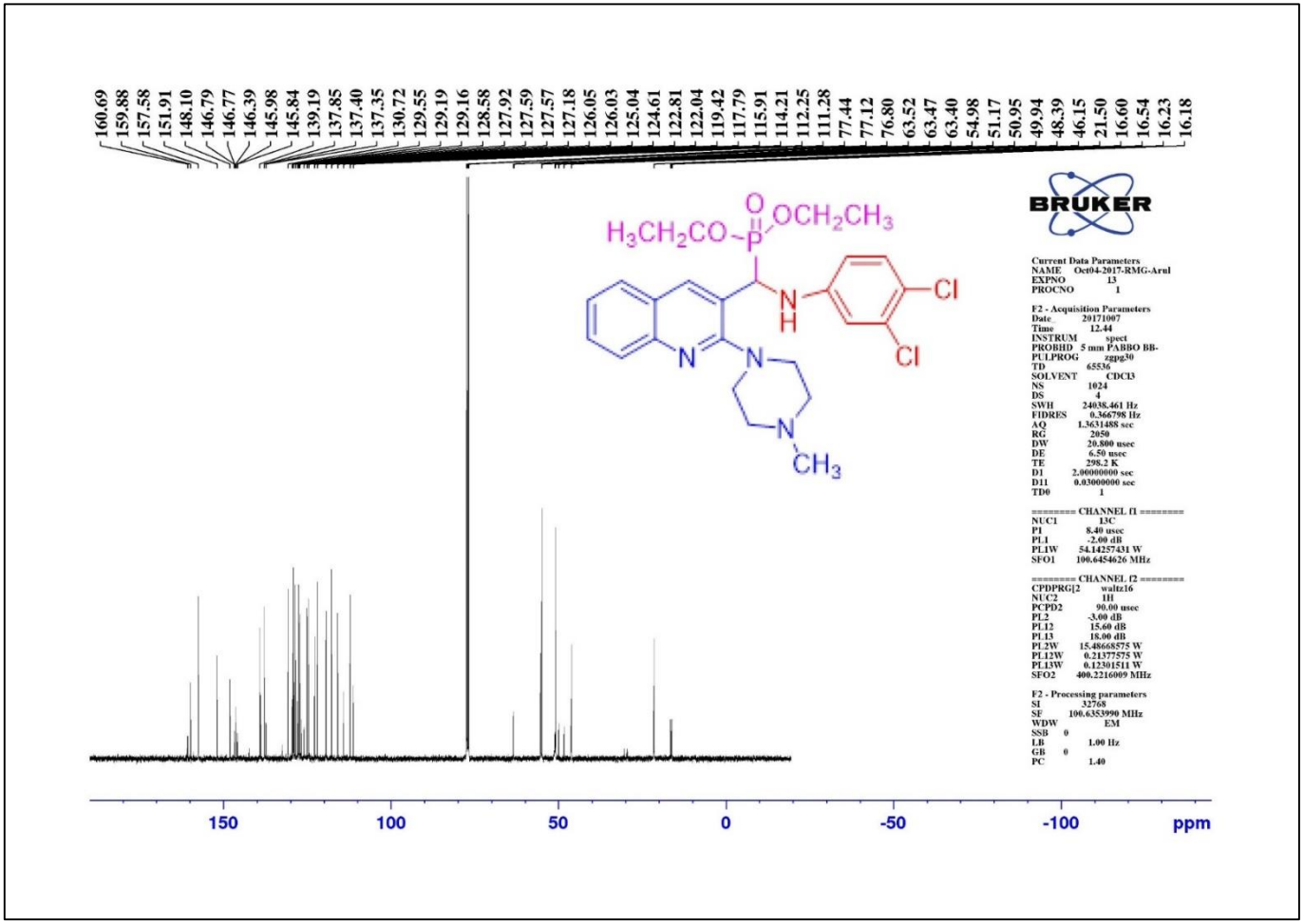

Figure S44: The ^{13}C NMR Spectrum of 4h, diethyl(((3,4-dichlorophenyl)amino)(2-(4-methylpiperazin-1-yl)quinolin-3-yl)methyl)phosphonate

Appendix 45

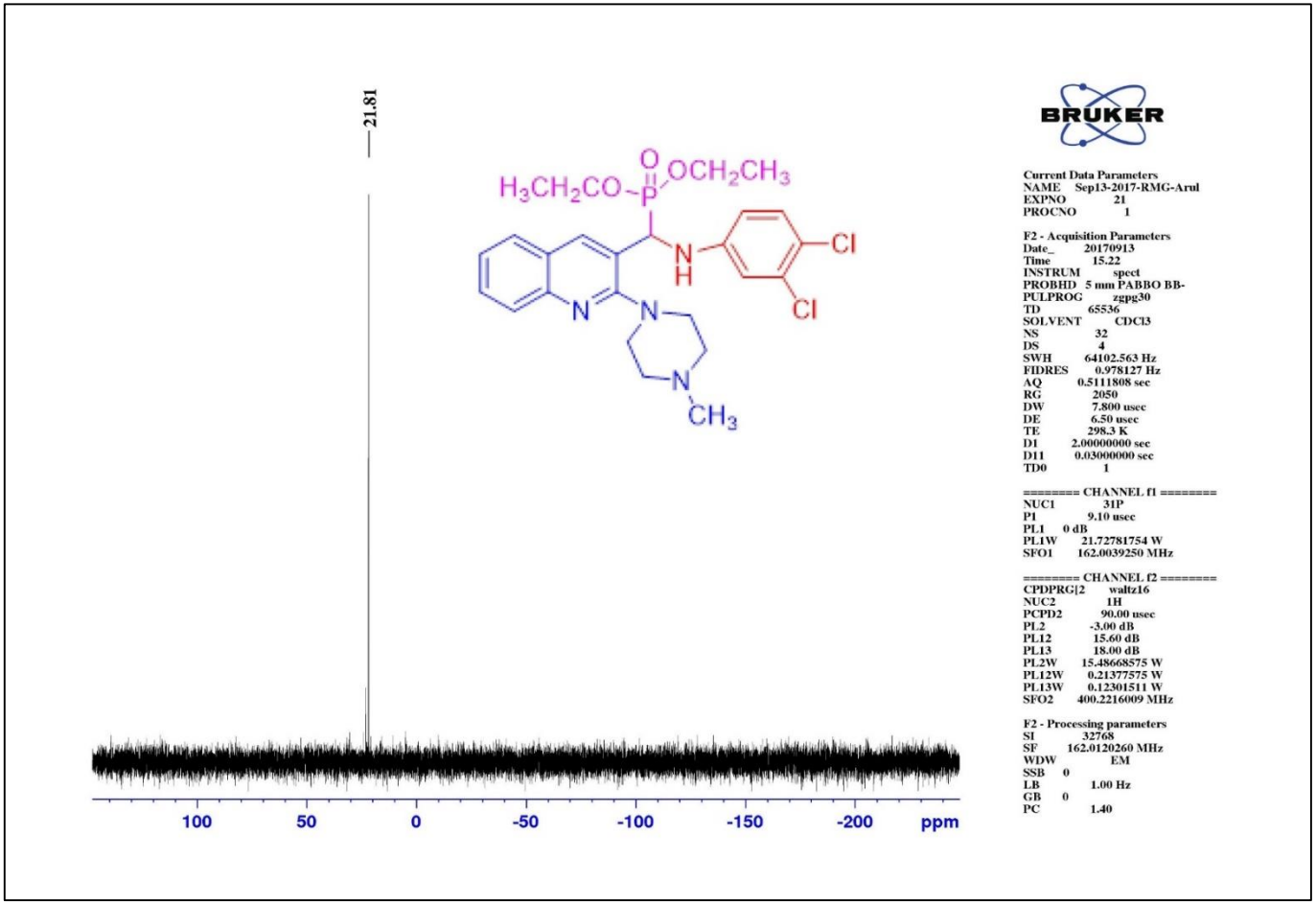

Figure S45: The ^{31}P NMR Spectrum of 4h, diethyl(((3,4-dichlorophenyl)amino)(2-(4-methylpiperazin-1-yl)quinolin-3-yl)methyl)phosphonate

Appendix 46

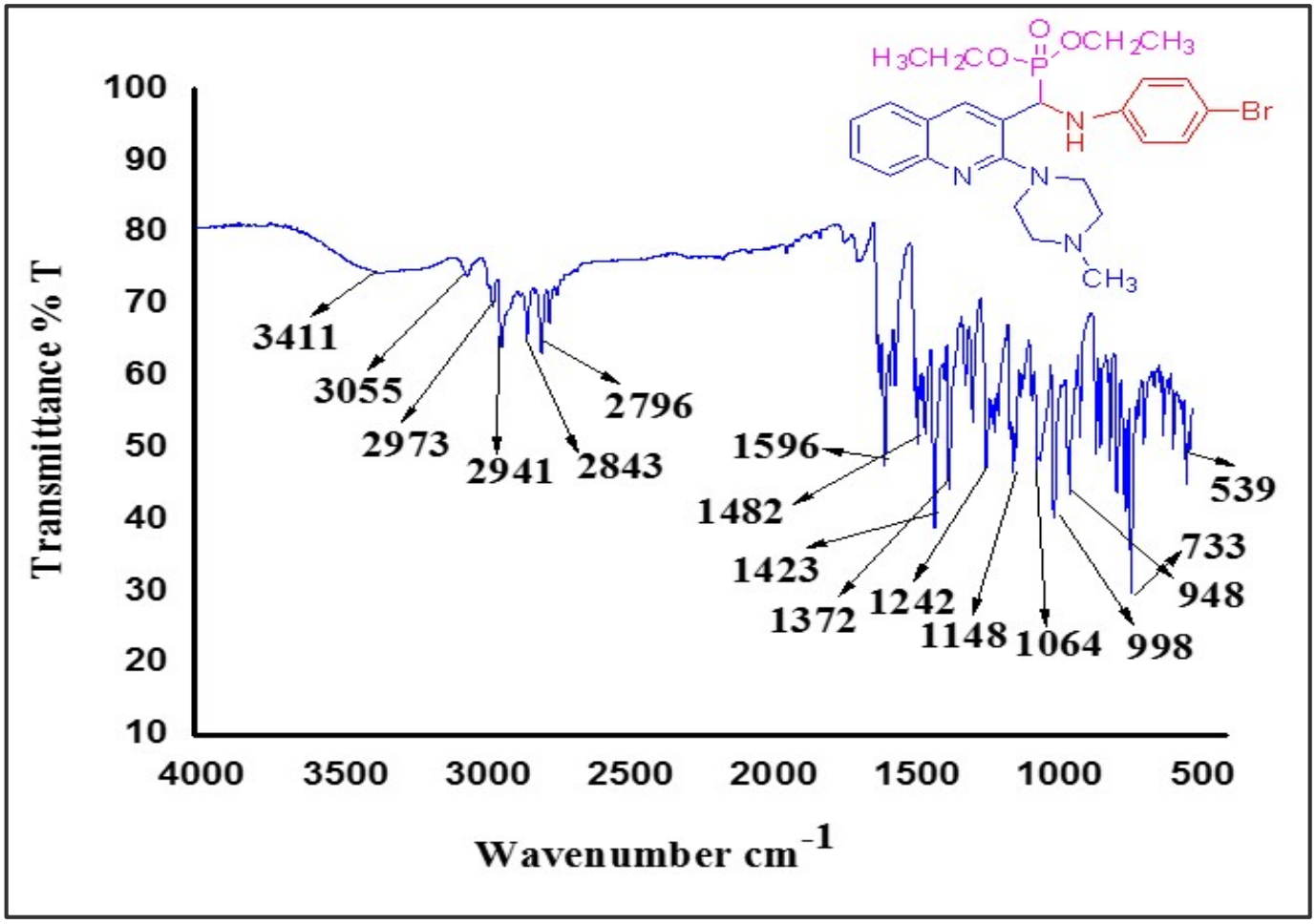

Figure S46: The IR Spectrum of 4i, diethyl(((4-bromophenyl)amino)(2-(4-methylpiperazin-1-yl)quinolin-3-yl)methyl)phosphonate

Appendix 47

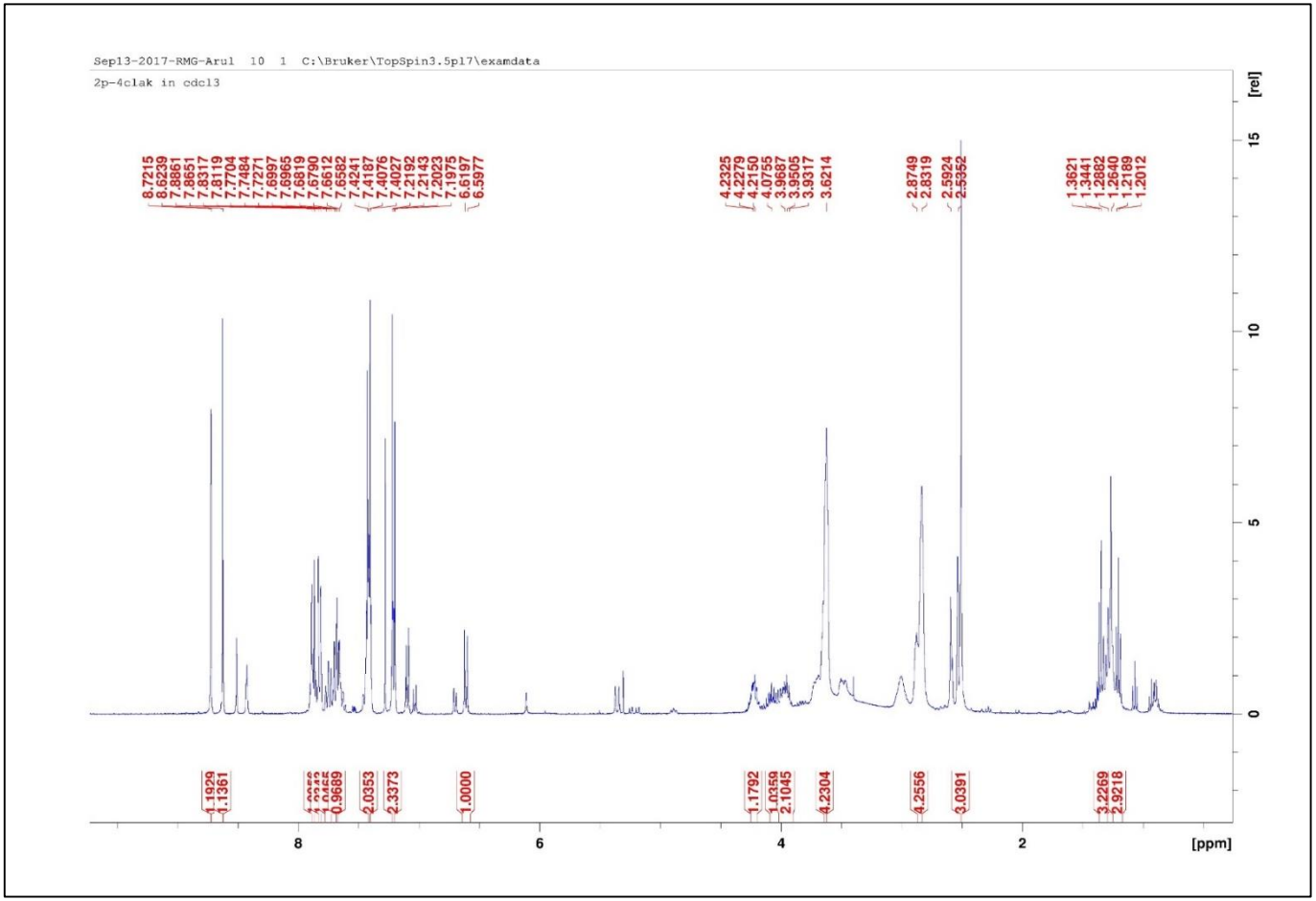

Figure S47: The ^{1}H NMR Spectrum of 4i, diethyl(((4-bromophenyl)amino)(2-(4-methylpiperazin-1-yl)quinolin-3-yl)methyl)phosphonate

Appendix 48

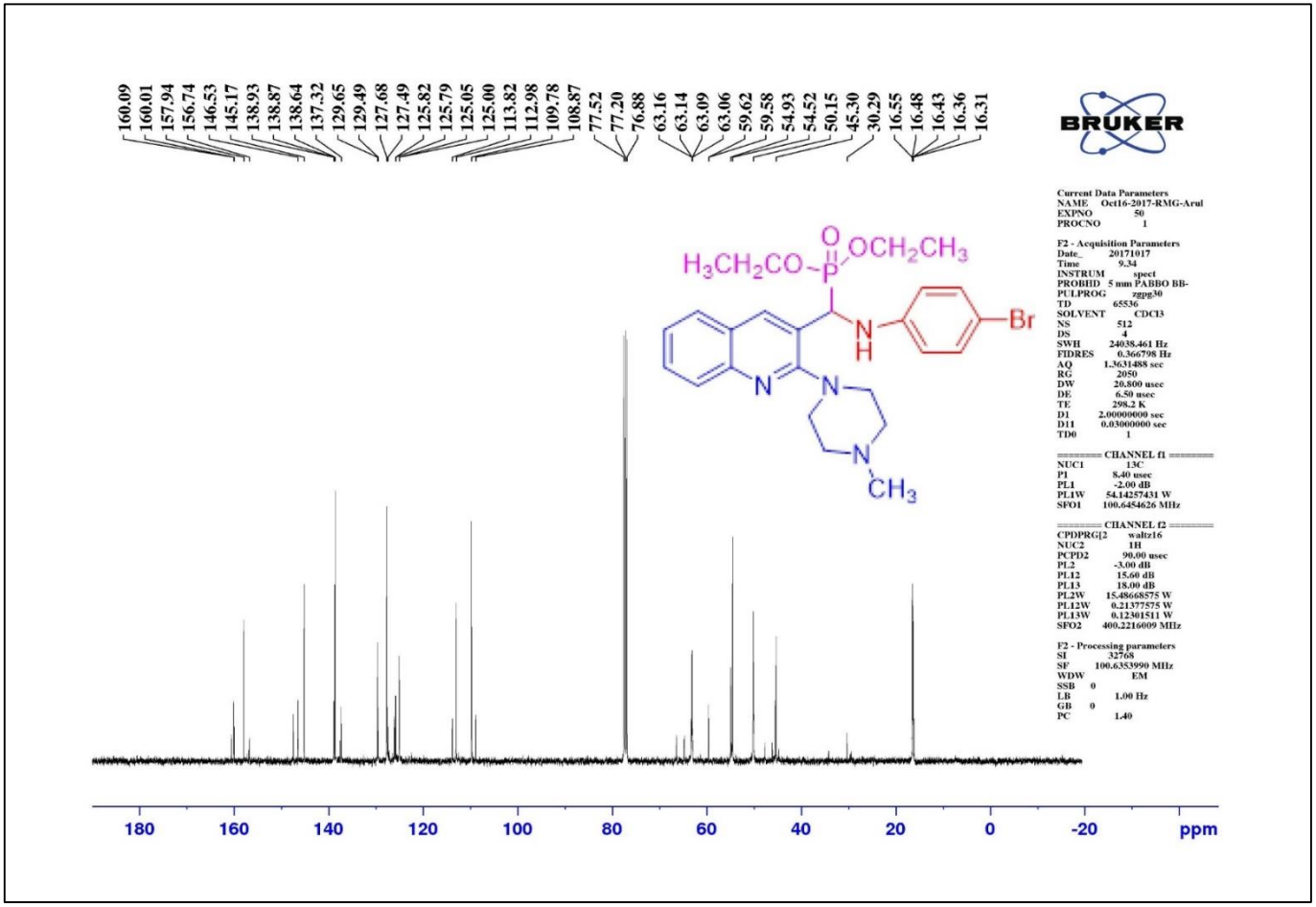

Figure S48: The ^{13}C NMR Spectrum of 4i, diethyl(((4-bromophenyl)amino)(2-(4-methylpiperazin-1-yl)quinolin-3-yl)methyl)phosphonate

Appendix 49

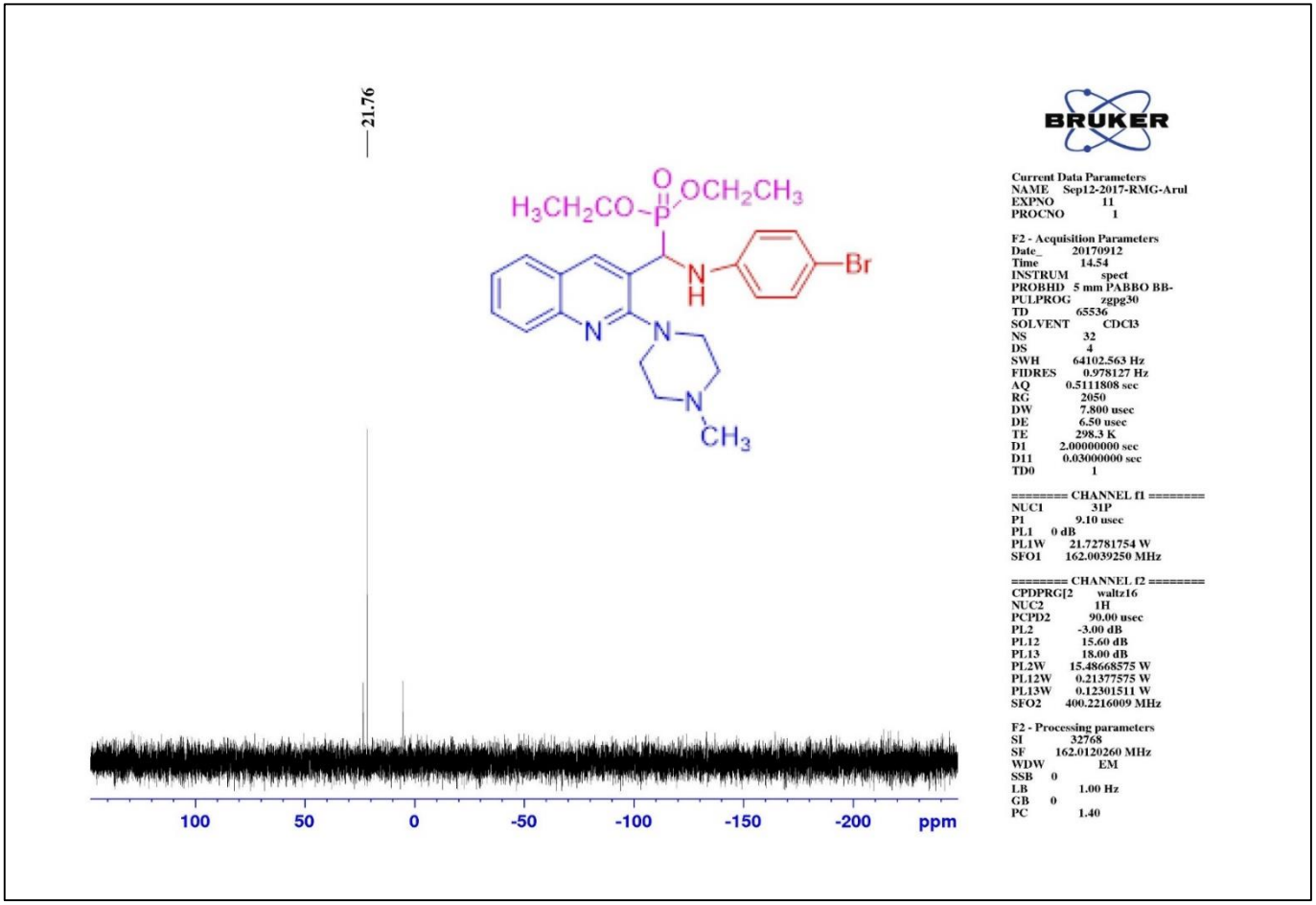

Figure S49: The ^{31}P NMR Spectrum of 4i, diethyl(((4-bromophenyl)amino)(2-(4-methylpiperazin-1-yl)quinolin-3-yl)methyl)phosphonate

Appendix 50

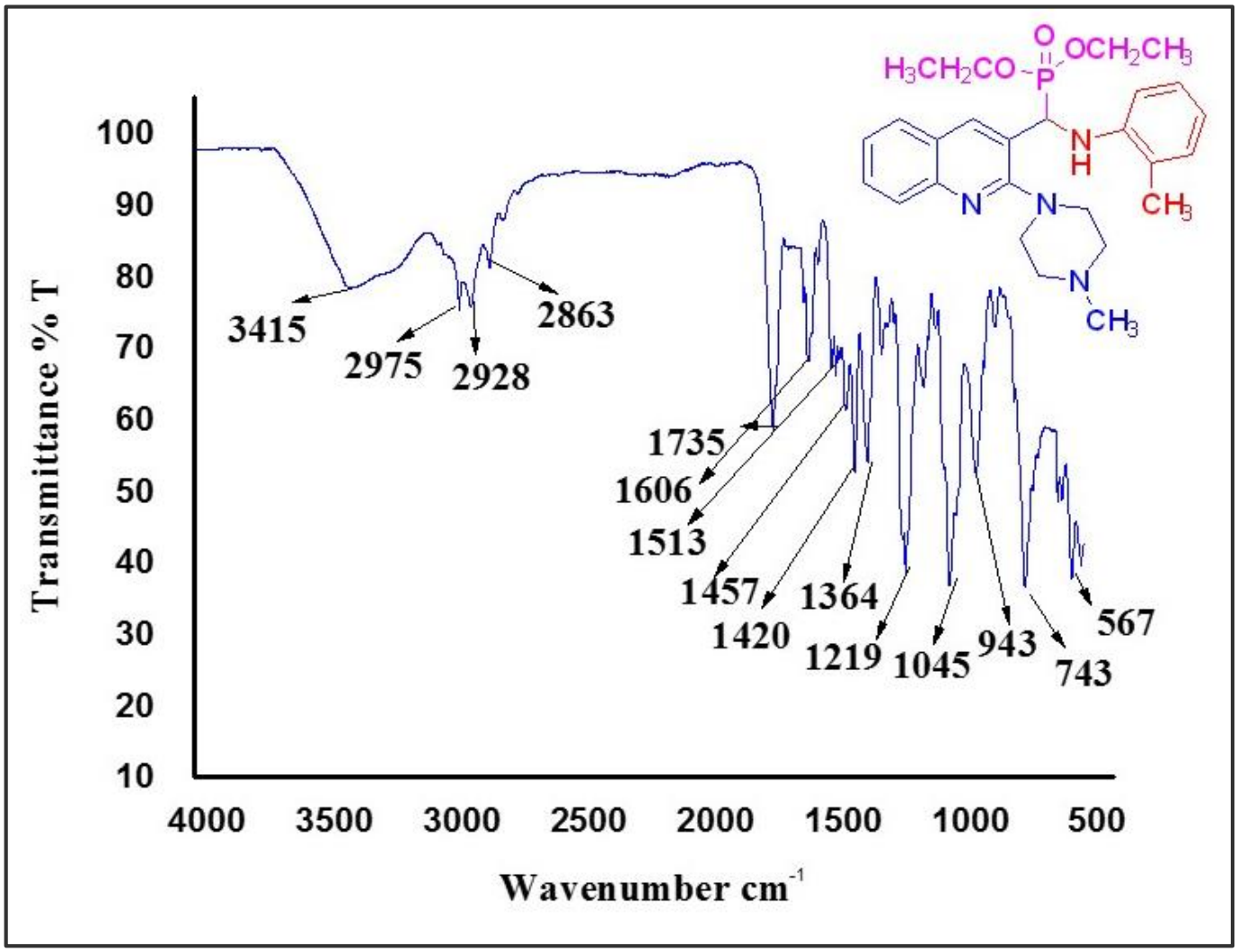

Figure S50: The IR Spectrum of 4j, diethyl ((2-(4-methylpiperazin-1-yl)quinolin-3-yl)(o-tolylamino)methyl)phosphonate

Appendix 51

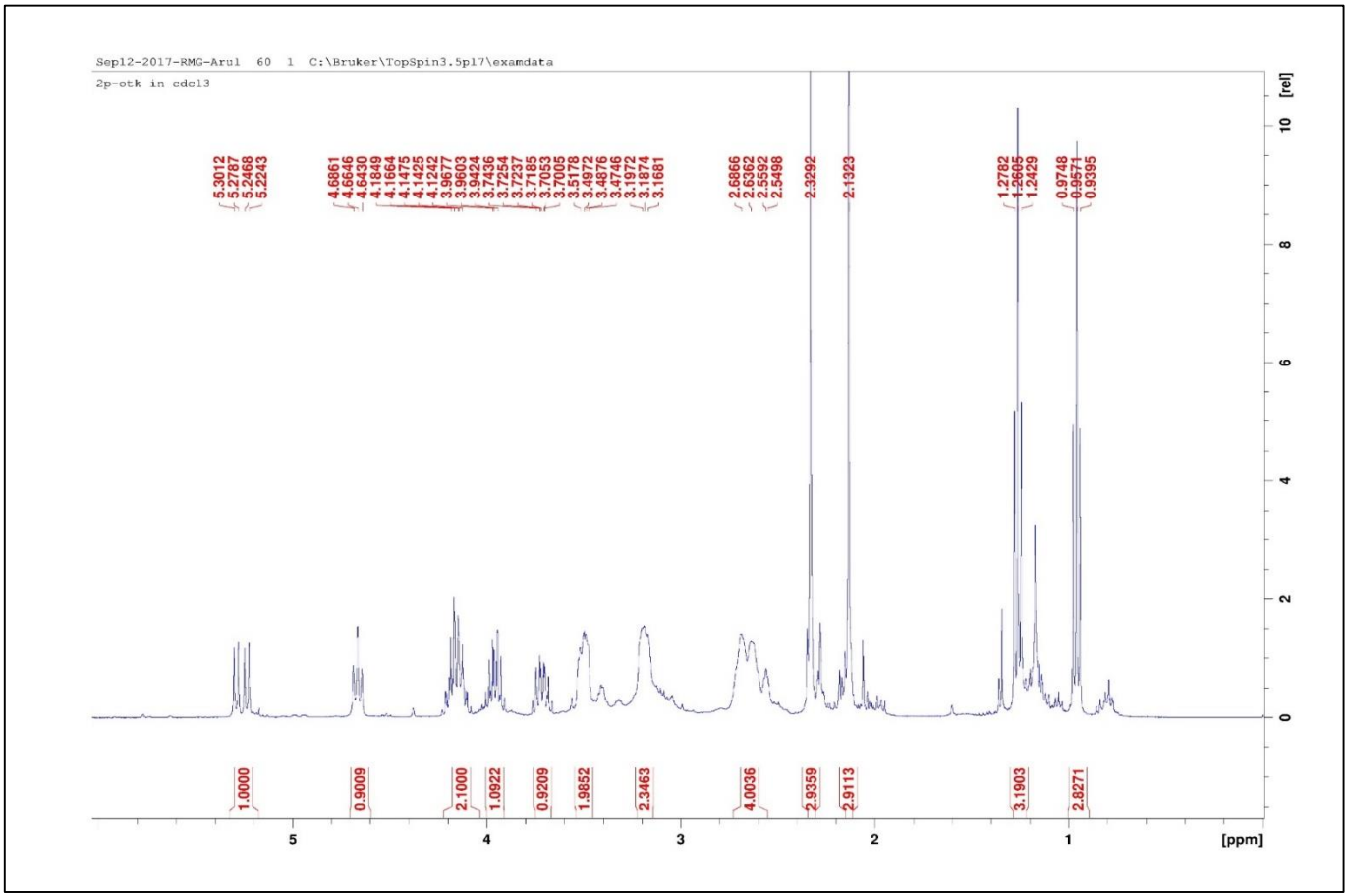

Figure S51: The ^{1}H NMR Spectrum of 4j, diethyl ((2-(4-methylpiperazin-1-yl)quinolin-3-yl)(o-tolylamino)methyl)phosphonate

Appendix 52

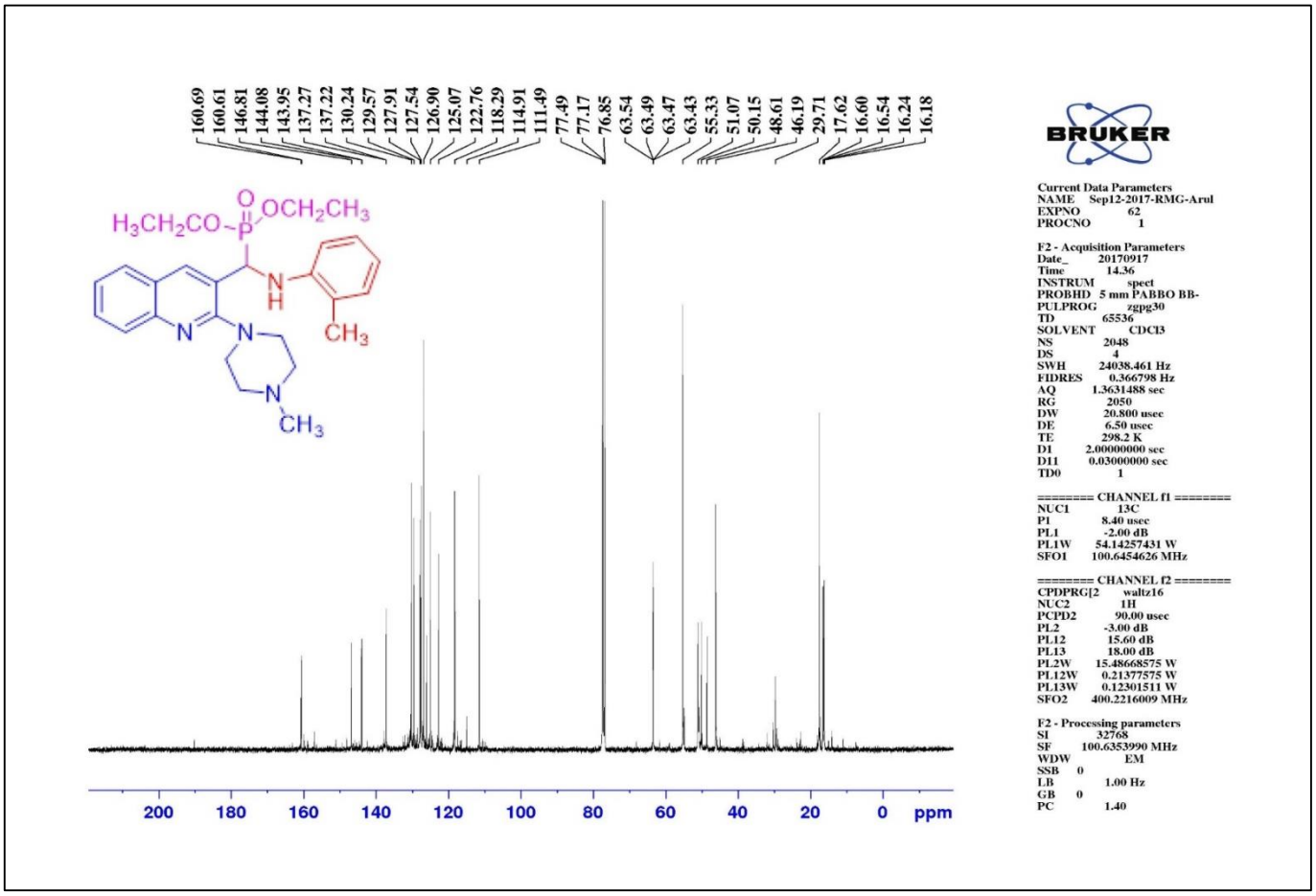

Figure S52: The ^{13}C NMR Spectrum of 4j, diethyl ((2-(4-methylpiperazin-1-yl)quinolin-3-yl)(o-tolylamino)methyl)phosphonate

Appendix 53

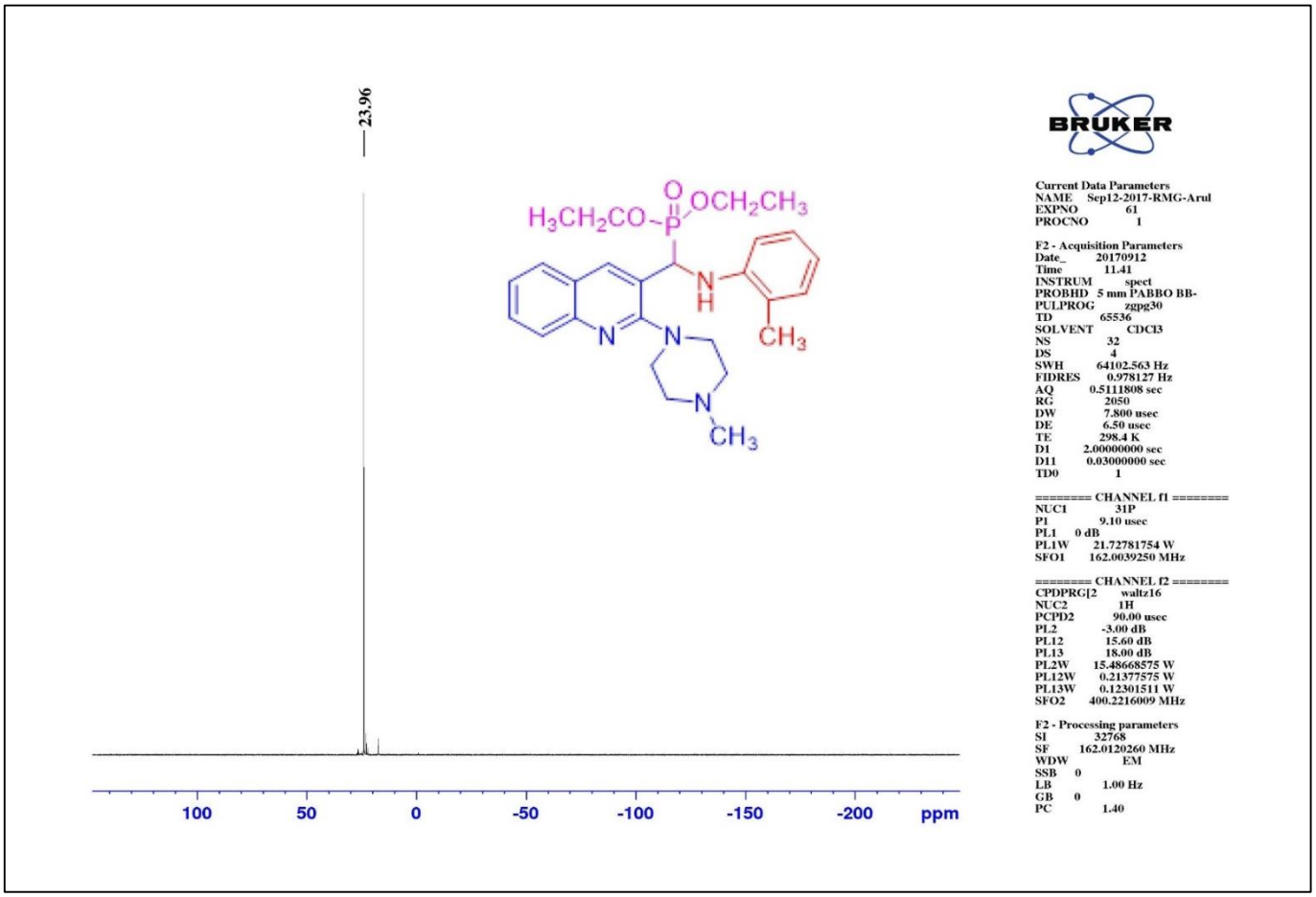

Figure S53: The ^{31}P NMR Spectrum of 4j, diethyl ((2-(4-methylpiperazin-1-yl)quinolin-3-yl)(o-tolylamino)methyl)phosphonate

Appendix 54

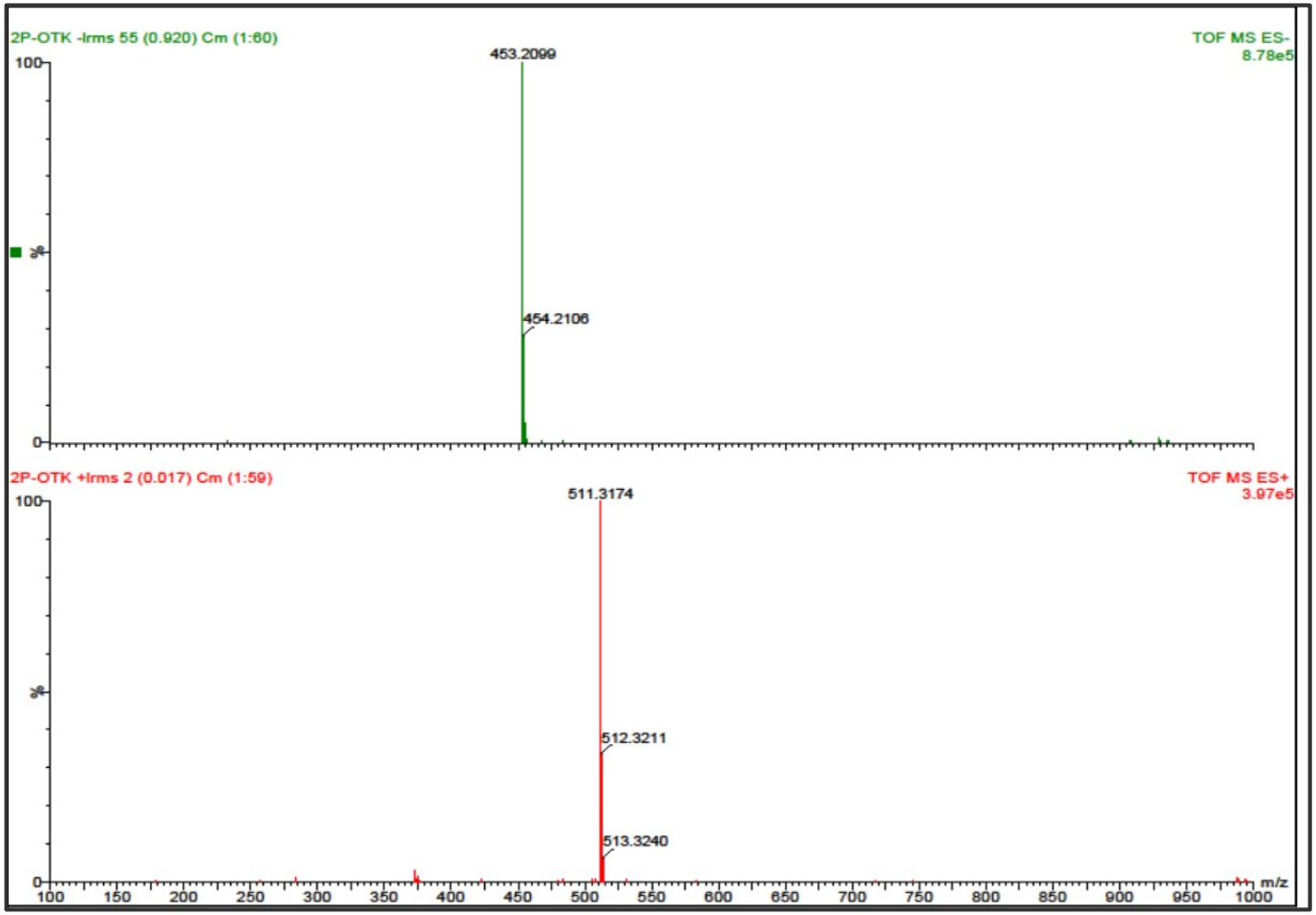

Figure S54: The HRMS Spectrum of 4j, diethyl ((2-(4-methylpiperazin-1-yl)quinolin-3-yl)(o-tolylamino)methyl)phosphonate

Appendix 55

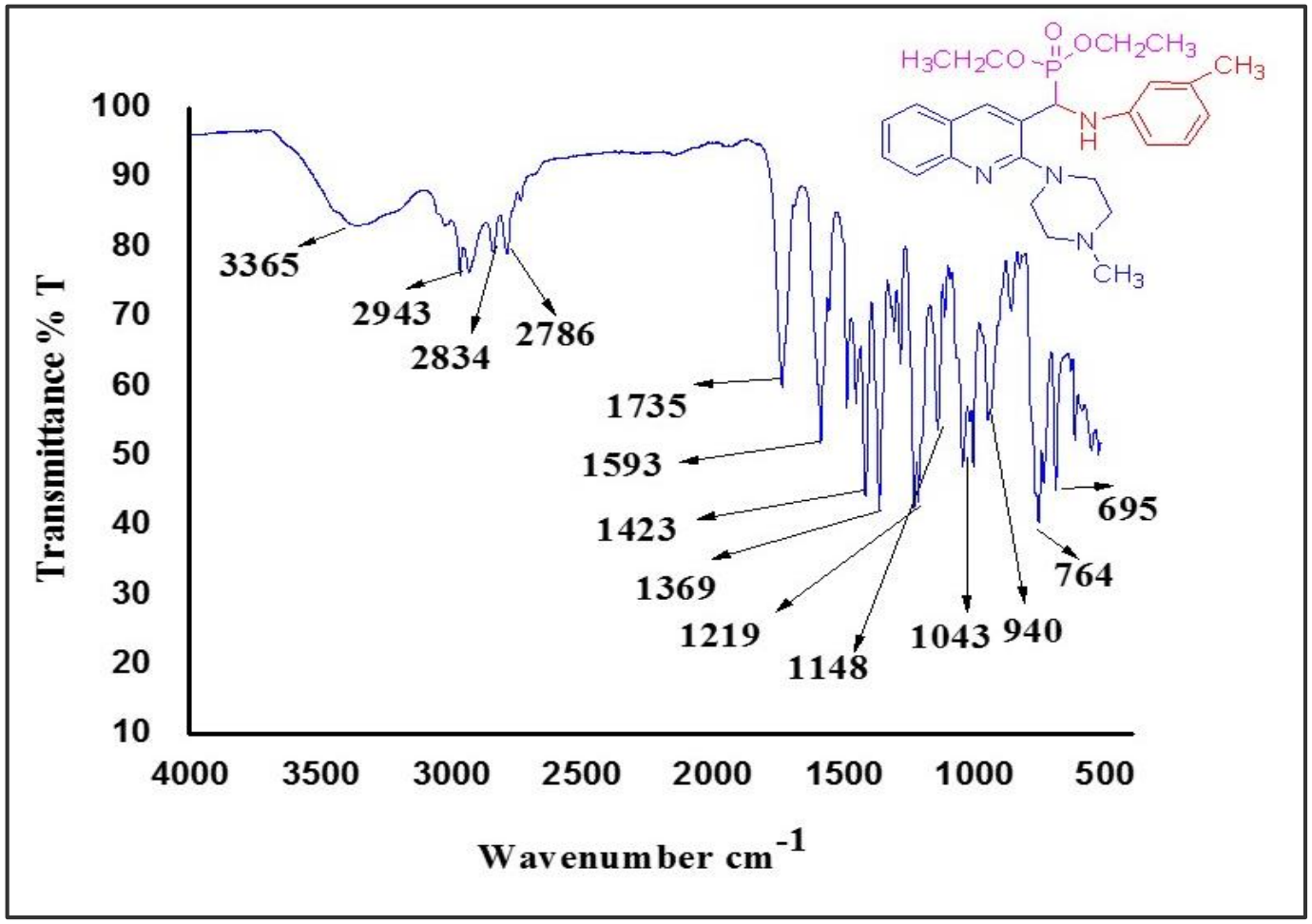

Figure S55: The IR Spectrum of 4k, diethyl ((2-(4-methylpiperazin-1-yl)quinolin-3-yl)(m-tolylamino)methyl)phosphonate

Appendix 56

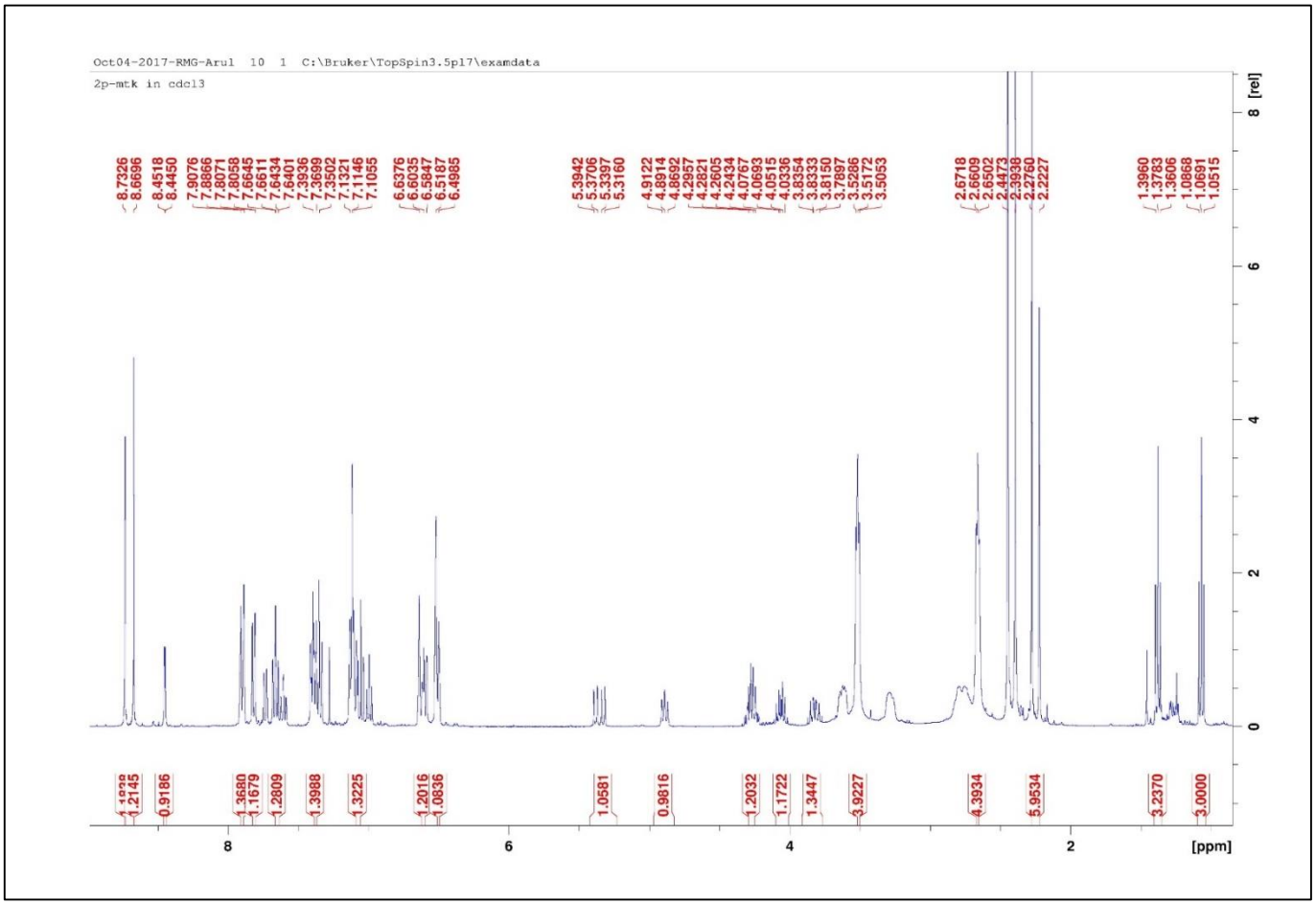

Figure S56: The ^{1}H NMR Spectrum of 4k, diethyl ((2-(4-methylpiperazin-1-yl)quinolin-3-yl)(m-tolylamino)methyl)phosphonate

Appendix 57

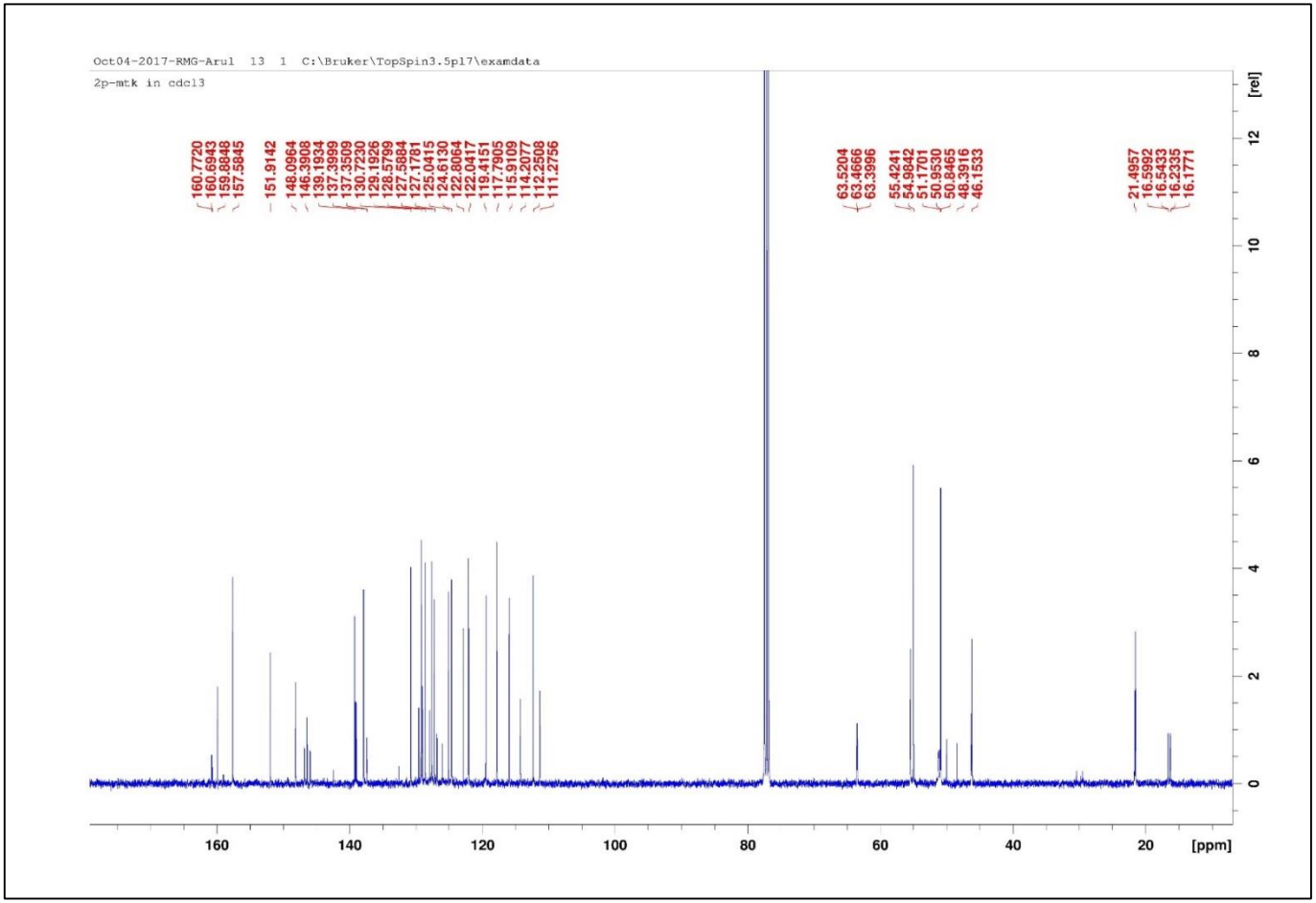

Figure S57: The ^{13}C NMR Spectrum of 4k, diethyl ((2-(4-methylpiperazin-1-yl)quinolin-3-yl)(m-tolylamino)methyl)phosphonate

Appendix 58

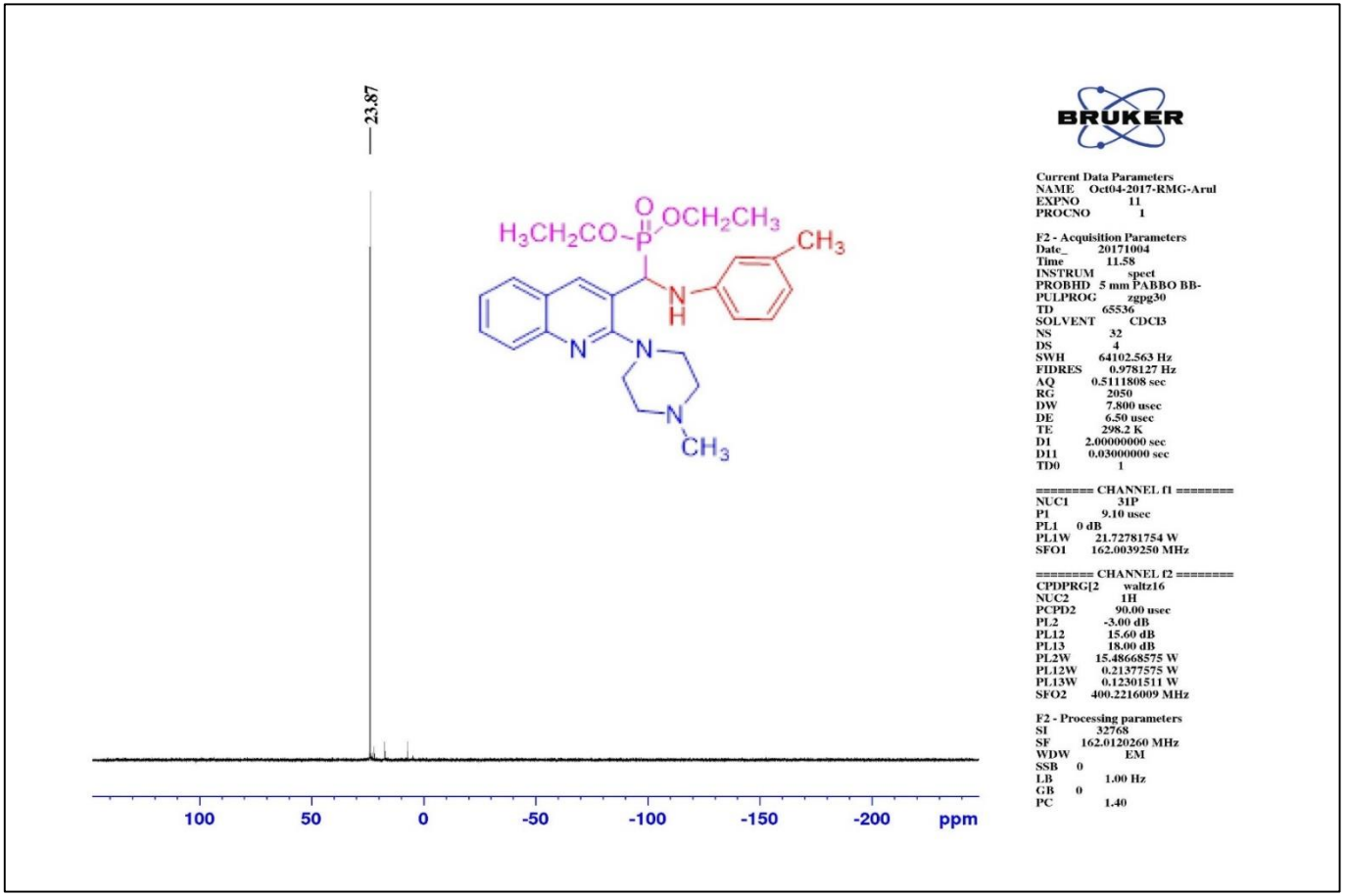

Figure S58: The ^{31}P NMR Spectrum of 4k, diethyl ((2-(4-methylpiperazin-1-yl)quinolin-3-yl)(m-tolylamino)methyl)phosphonate

Appendix 59

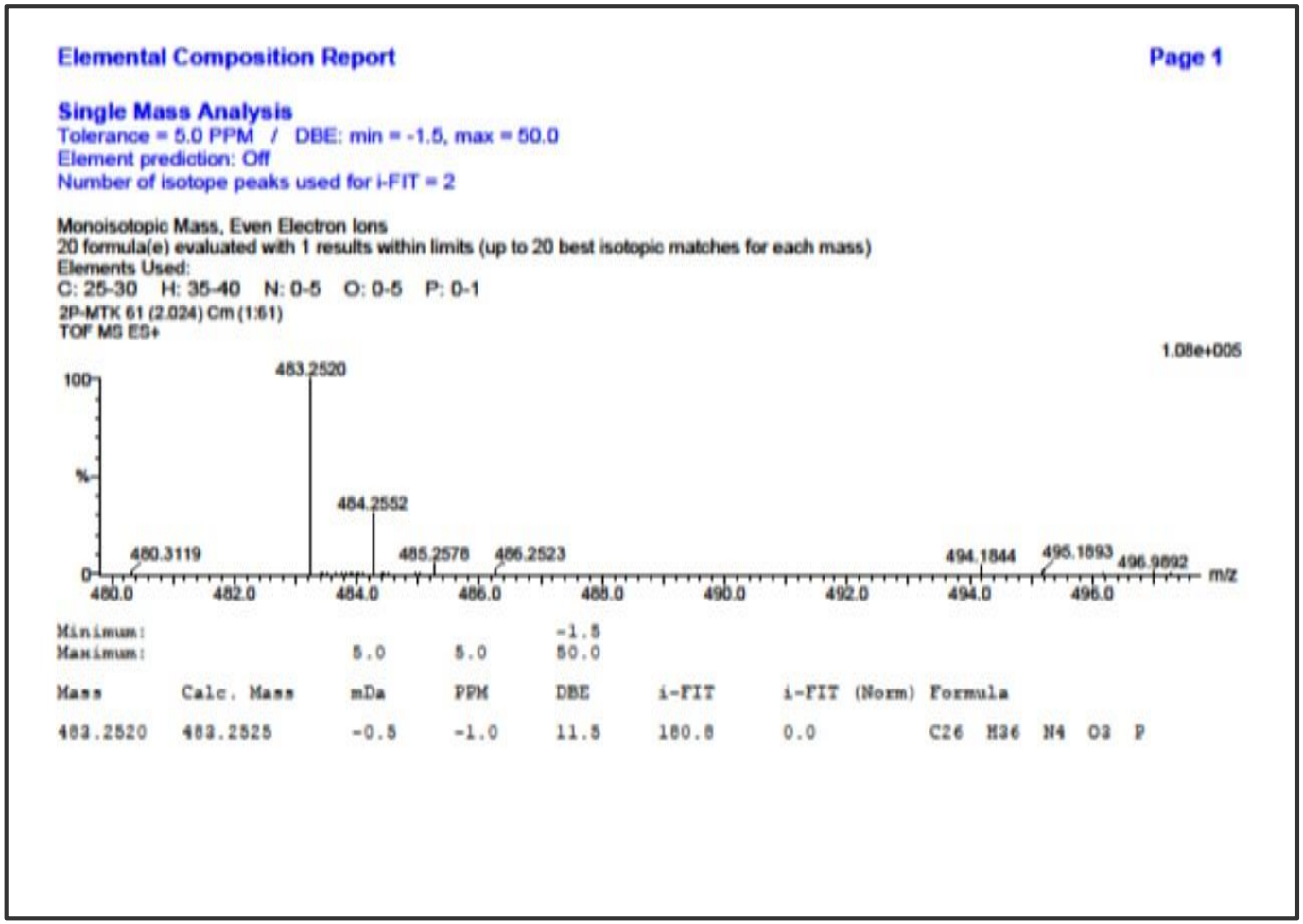

Figure S59: The HRMS Spectrum of 4k, diethyl ((2-(4-methylpiperazin-1-yl)quinolin-3-yl)(m-tolylamino)methyl)phosphonate

Appendix 60

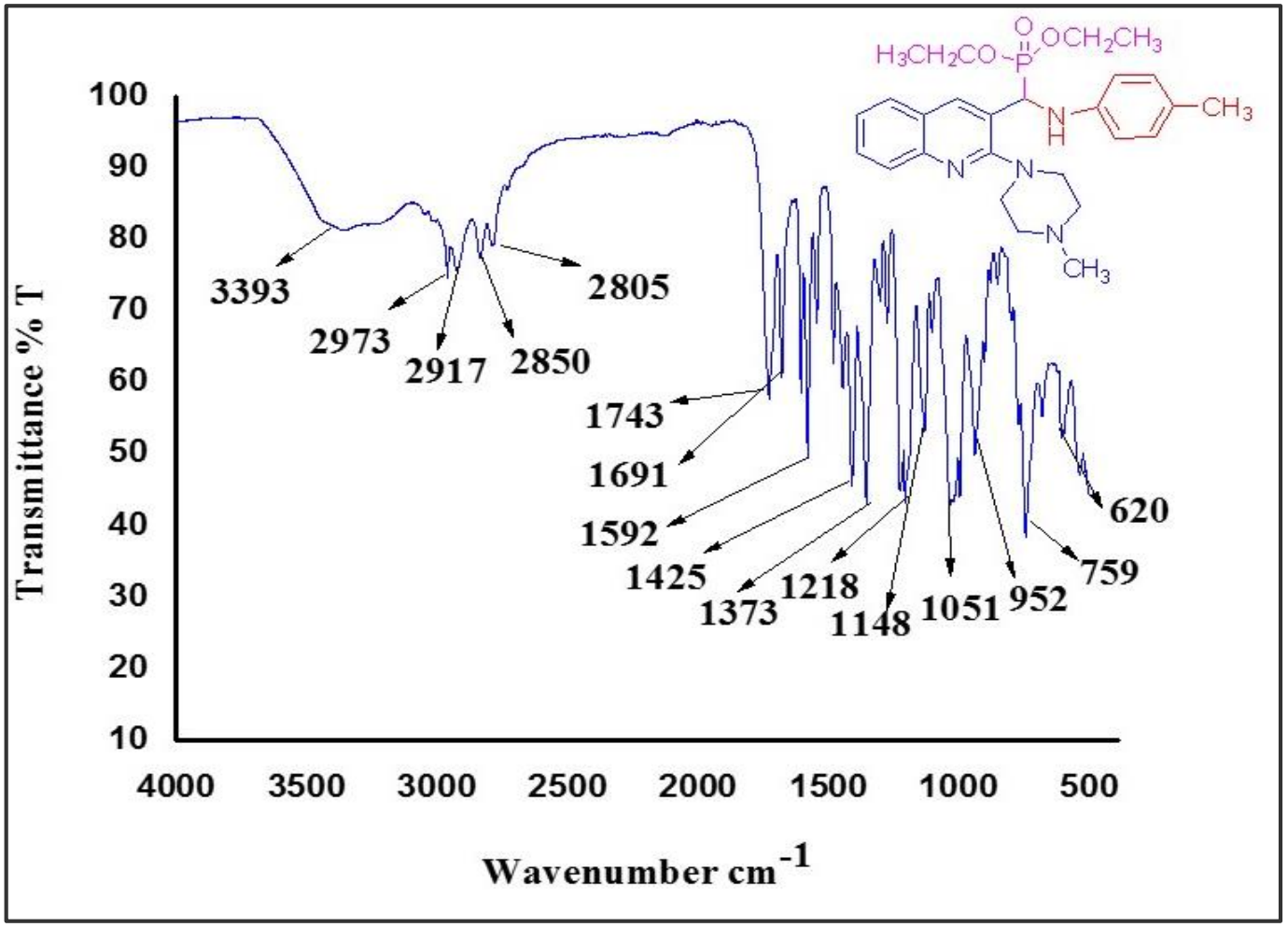

Figure S60: The IR Spectrum of 4l, diethyl ((2-(4-methylpiperazin-1-yl)quinolin-3-yl)(p-tolylamino)methyl)phosphonate

Appendix 61

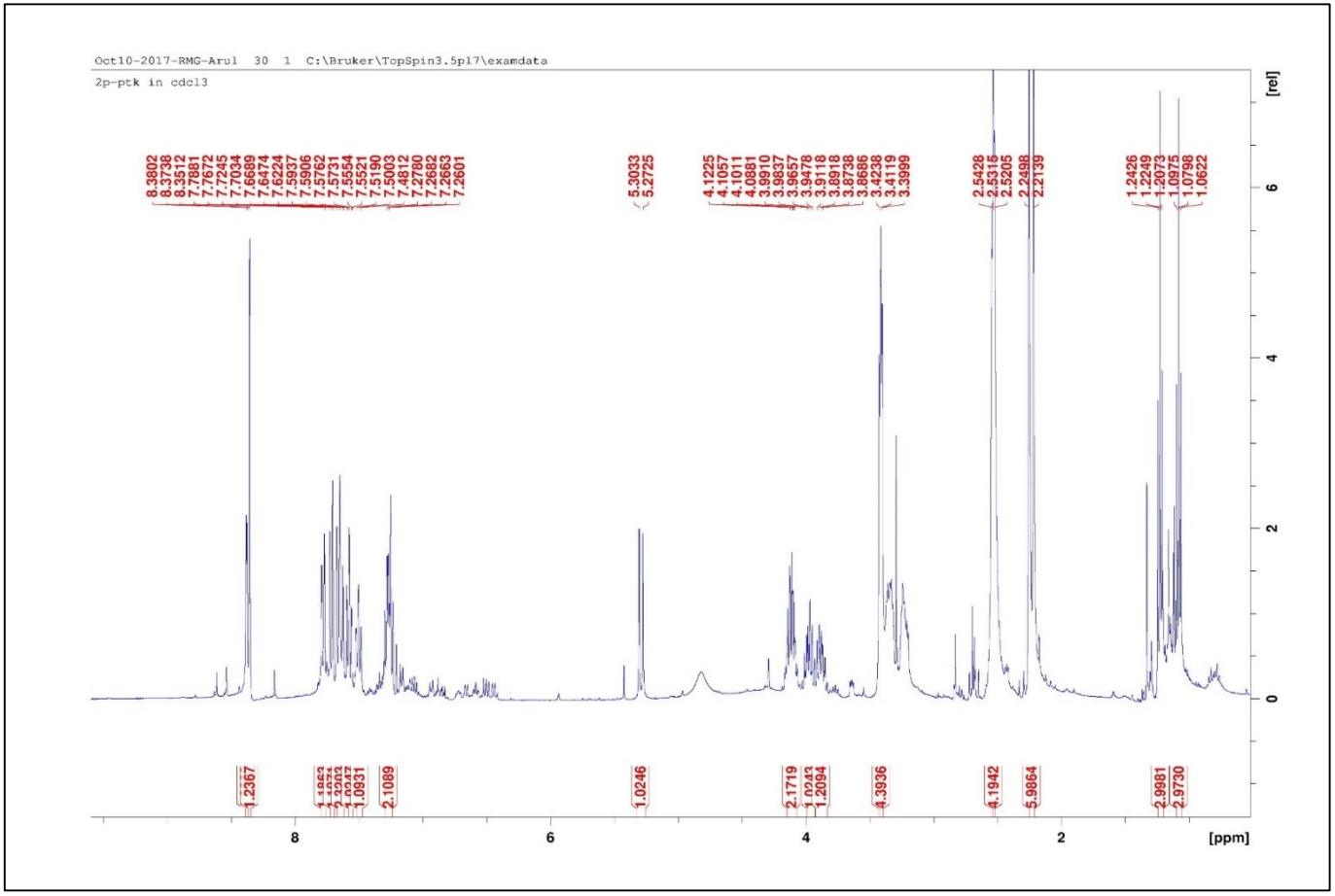

Figure S61: The ^{1}H NMR Spectrum of 4l, diethyl ((2-(4-methylpiperazin-1-yl)quinolin-3-yl)(p-tolylamino)methyl)phosphonate

Appendix 62

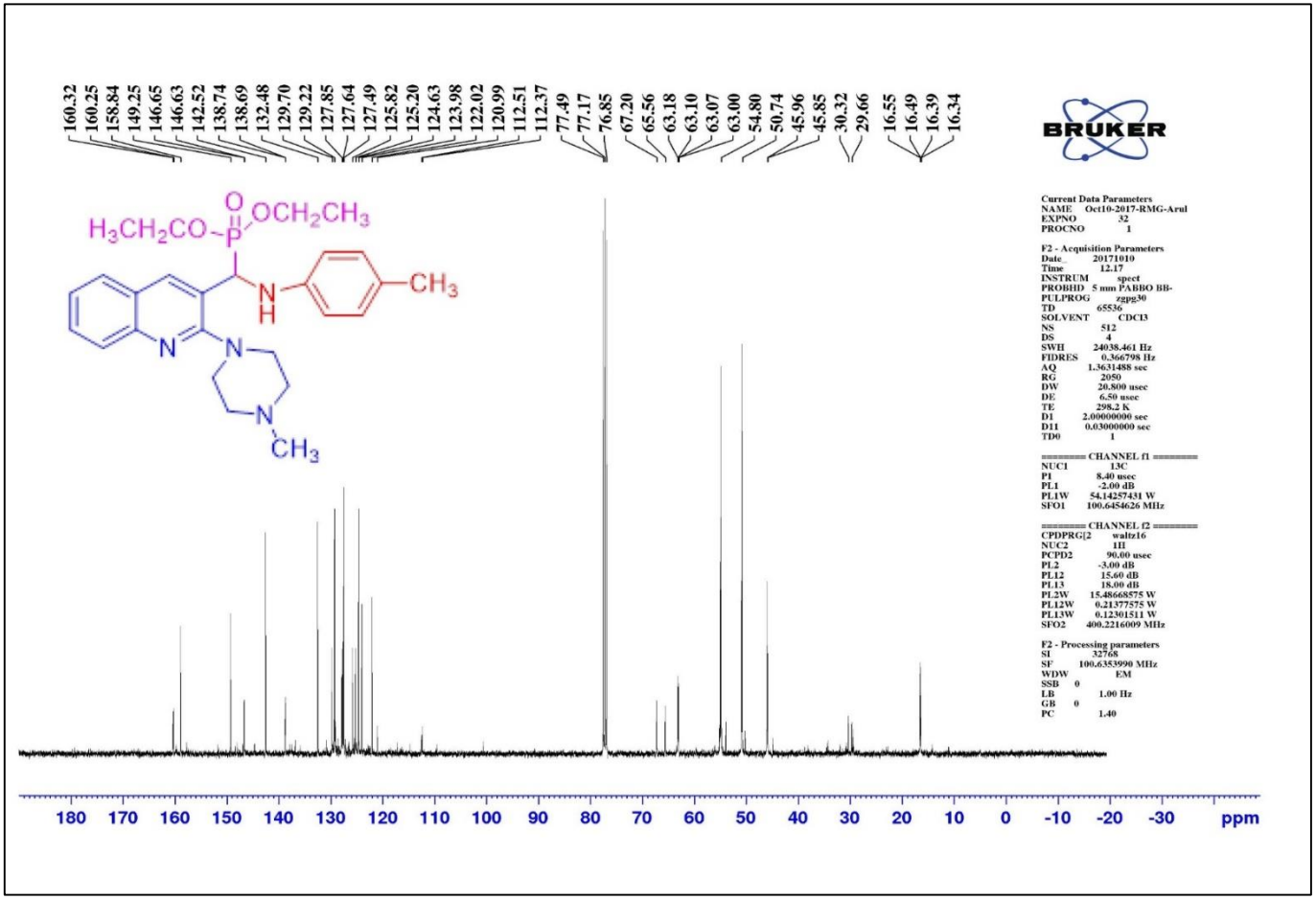

Figure S62: The ^{13}C NMR Spectrum of 4l, diethyl ((2-(4-methylpiperazin-1-yl)quinolin-3-yl)(p-tolylamino)methyl)phosphonate

Appendix 63

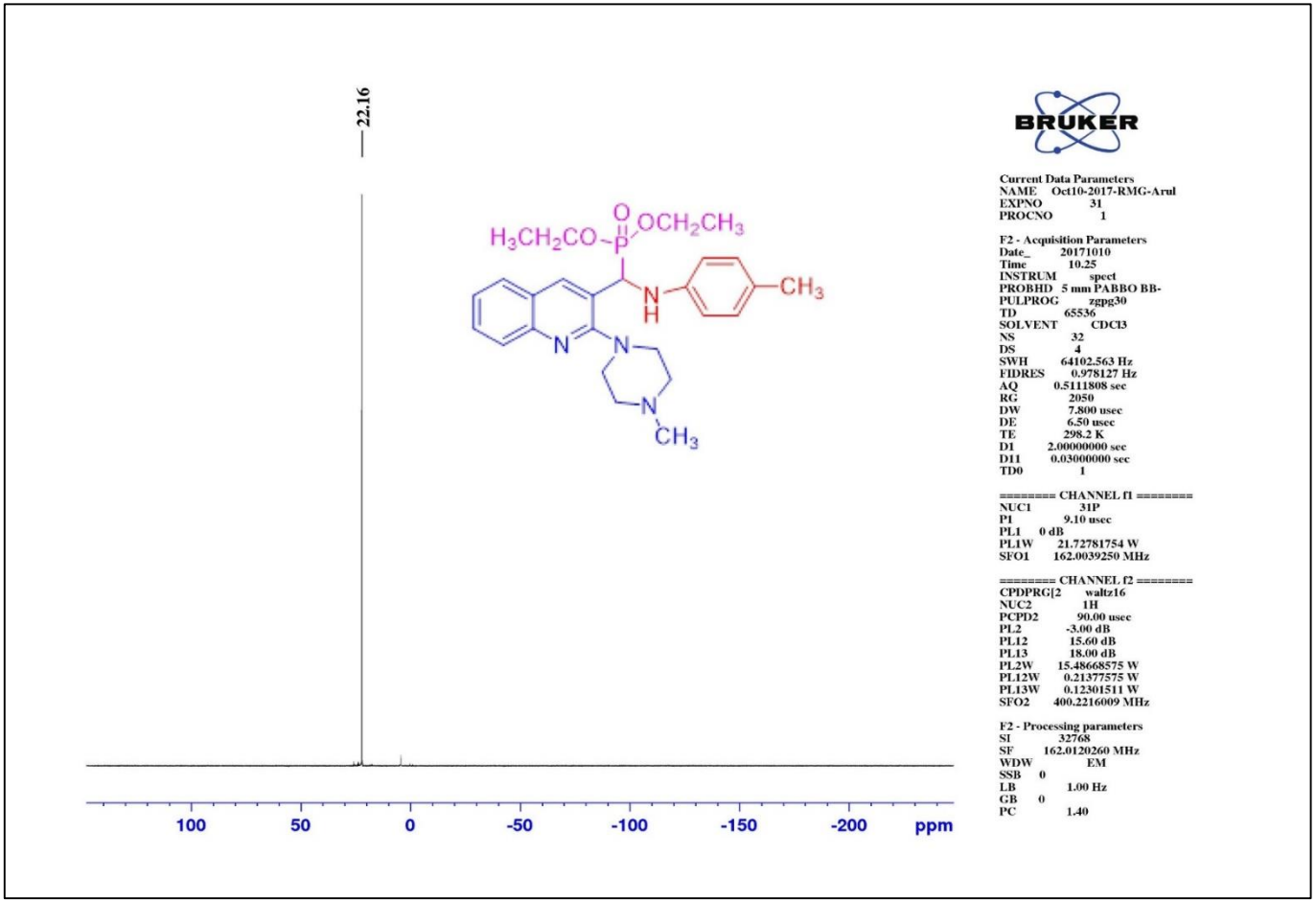

Figure S63: The ^{31}P NMR Spectrum of 4l, diethyl ((2-(4-methylpiperazin-1-yl)quinolin-3-yl)(p-tolylamino)methyl)phosphonate

Appendix 64

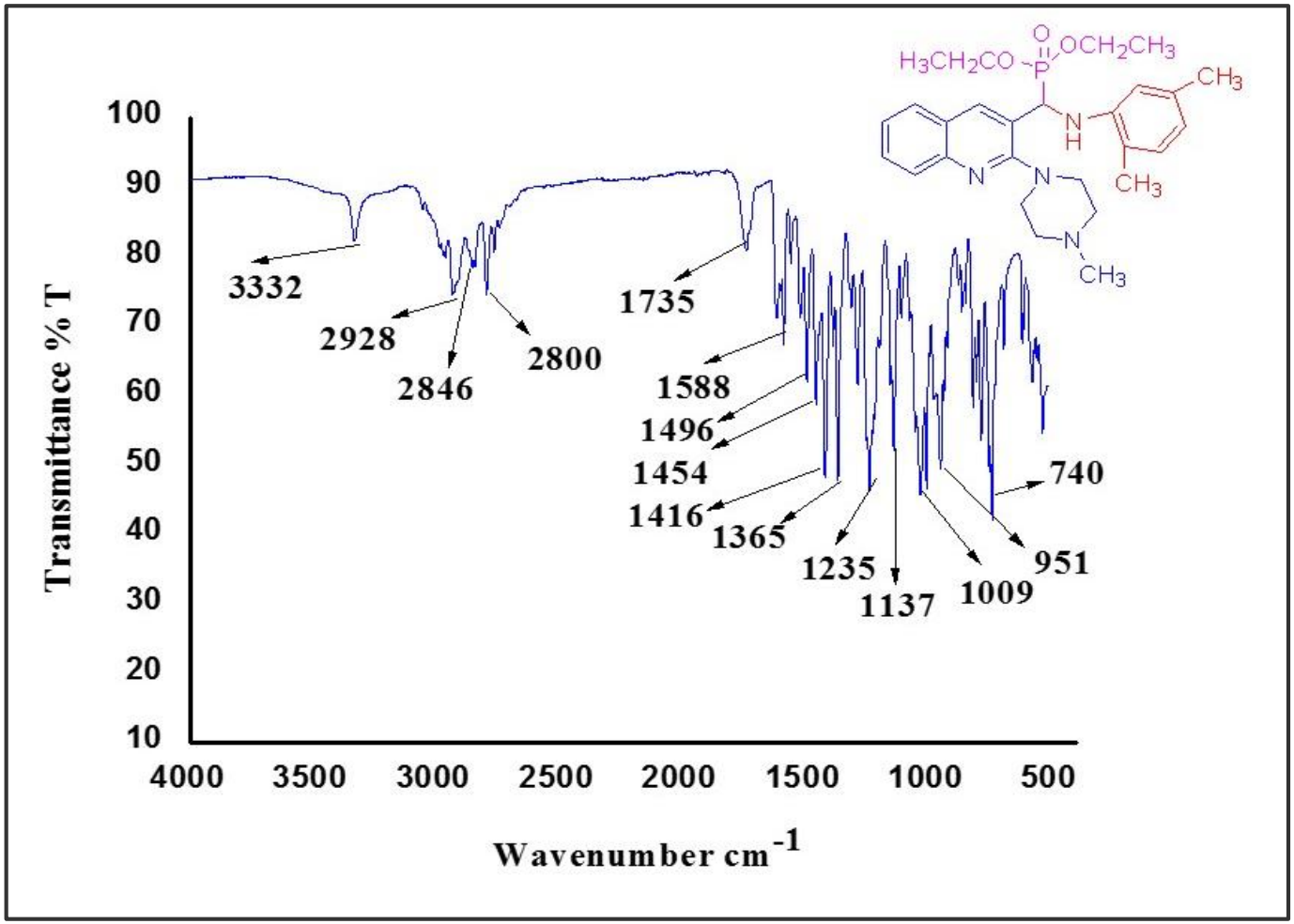

Figure S64: The IR Spectrum of 4m, diethyl(((2,5-dimethylphenyl)amino)(2-(4-methylpiperazin-1-yl)quinolin-3-yl)methyl)phosphonate

Appendix 65

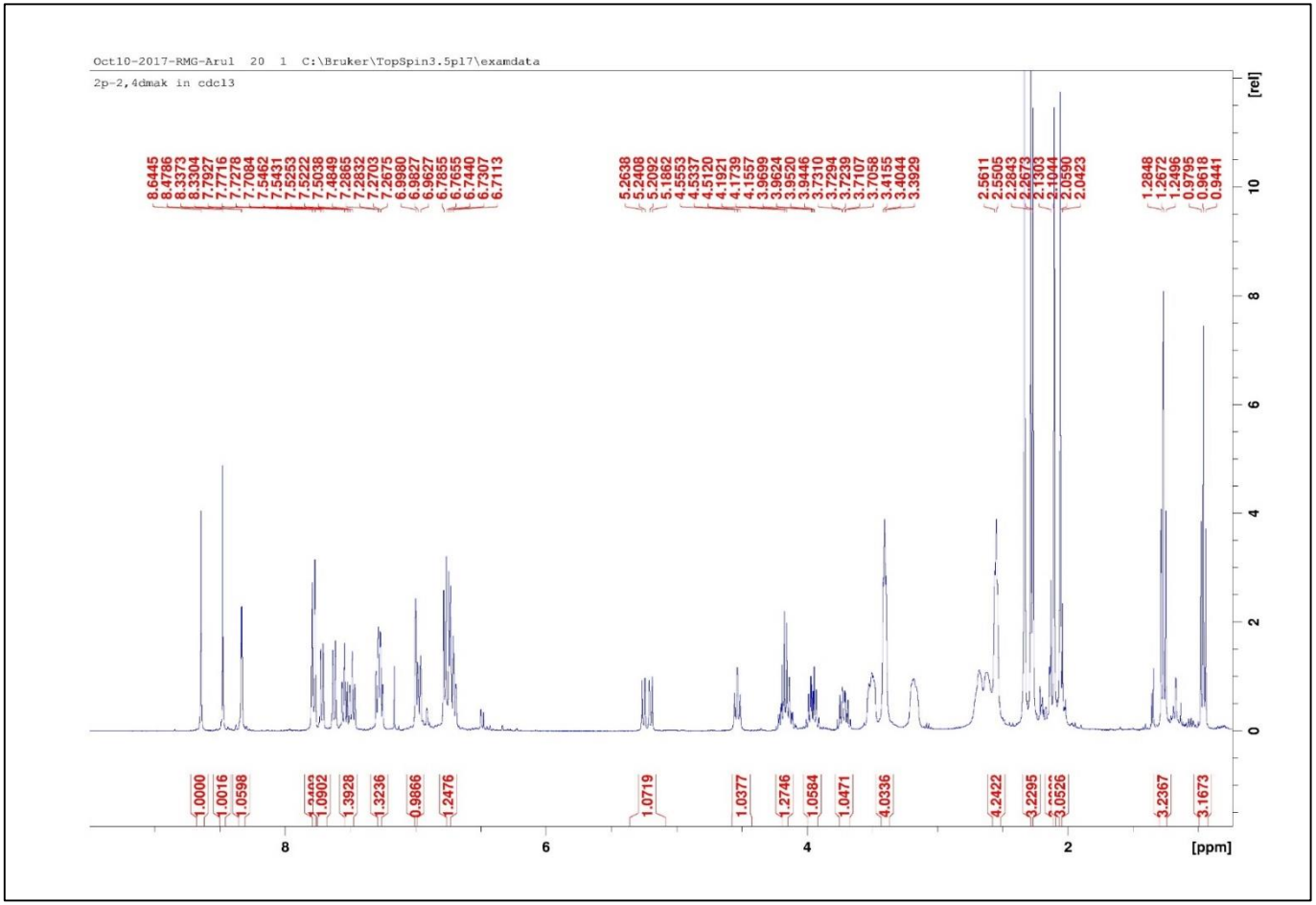

Figure S65: The ^{1}H NMR Spectrum of 4m, diethyl(((2,5-dimethylphenyl)amino)(2-(4-methylpiperazin-1-yl)quinolin-3-yl)methyl)phosphonate

Appendix 66

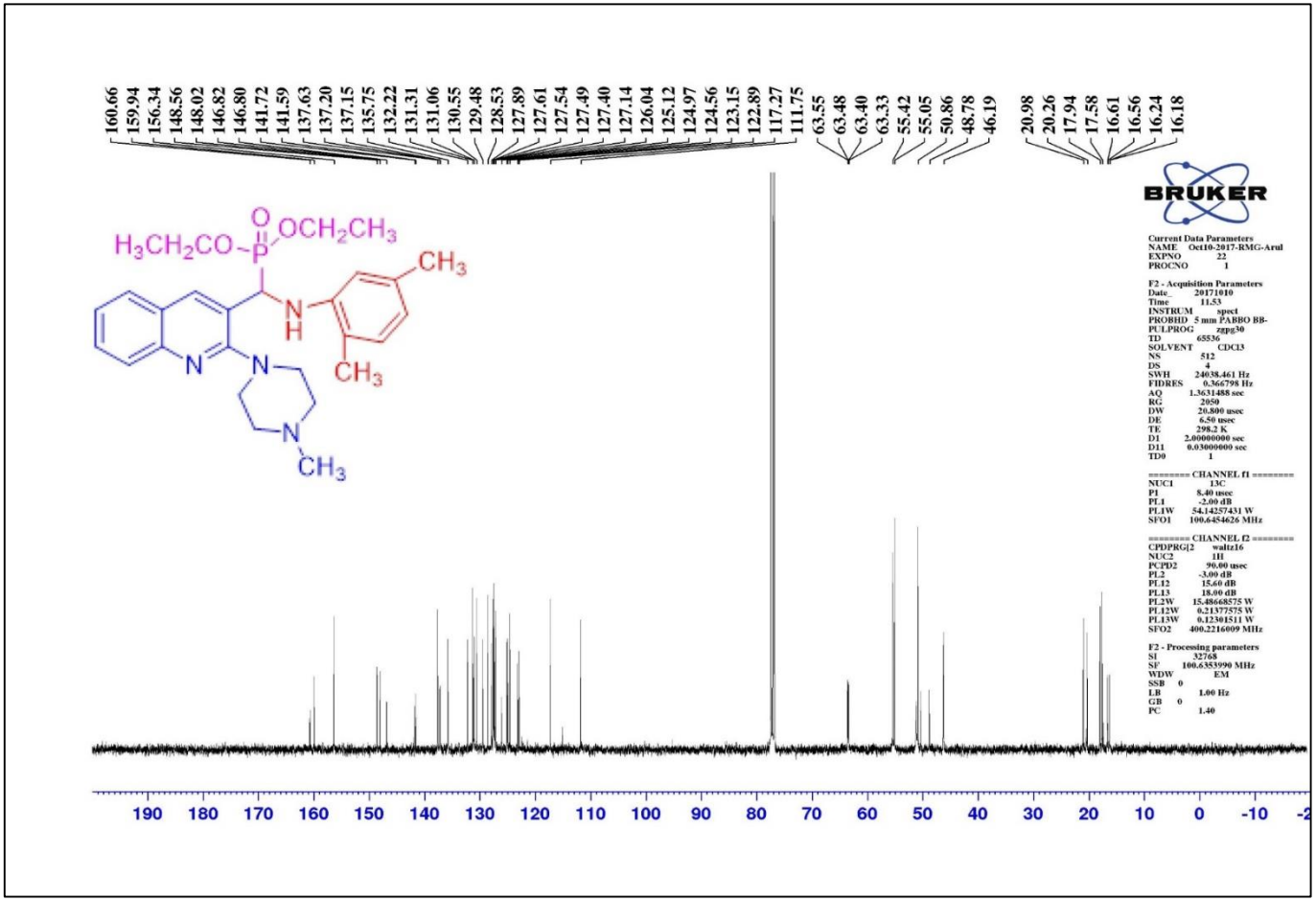

Figure S66: The ^{13}C NMR Spectrum of 4m, diethyl(((2,5-dimethylphenyl)amino)(2-(4-methylpiperazin-1-yl)quinolin-3-yl)methyl)phosphonate

Appendix 67

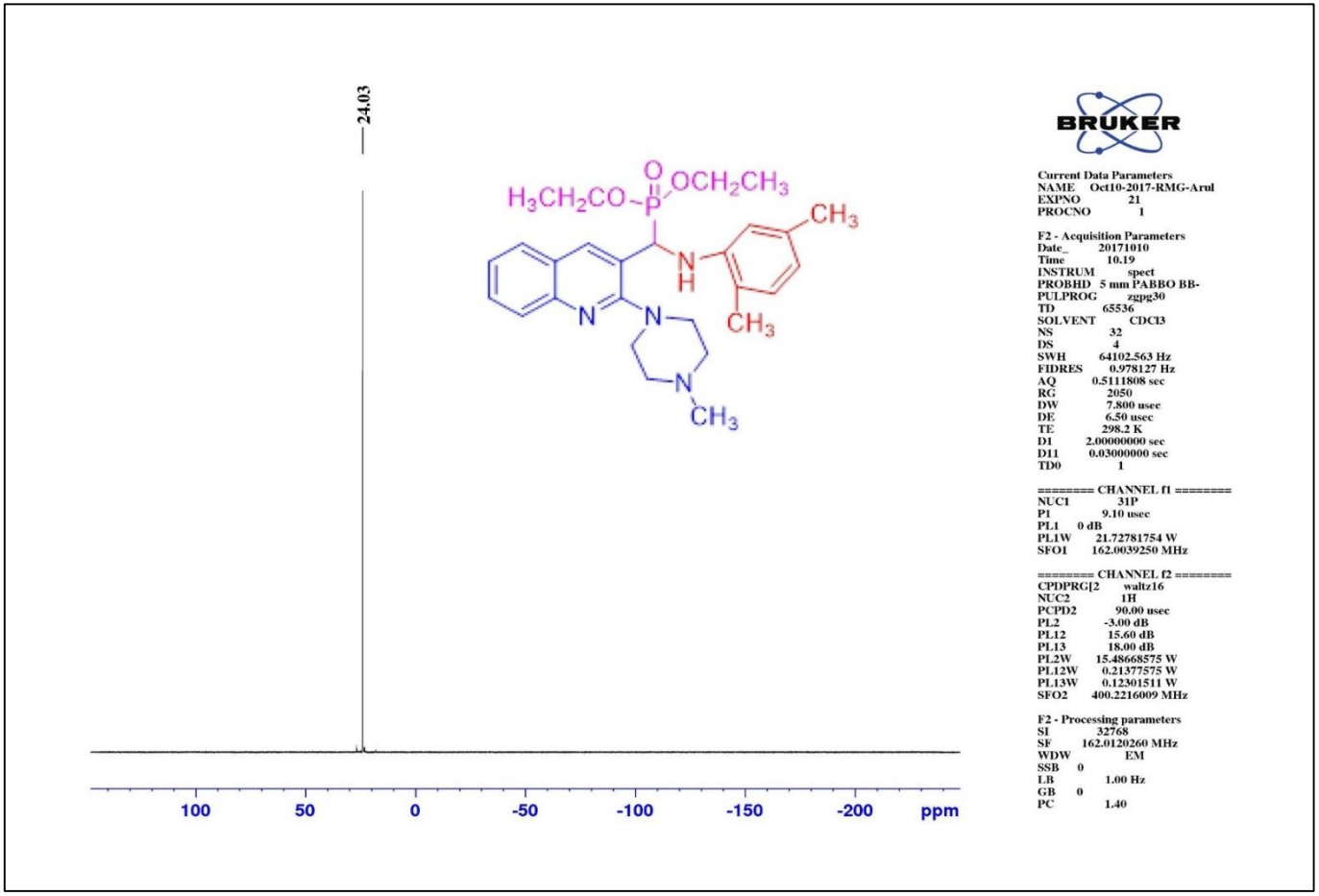

Figure S67: The ^{31}P NMR Spectrum of 4m, diethyl(((2,5-dimethylphenyl)amino)(2-(4-methylpiperazin-1-yl)quinolin-3-yl)methyl)phosphonate

Appendix 68

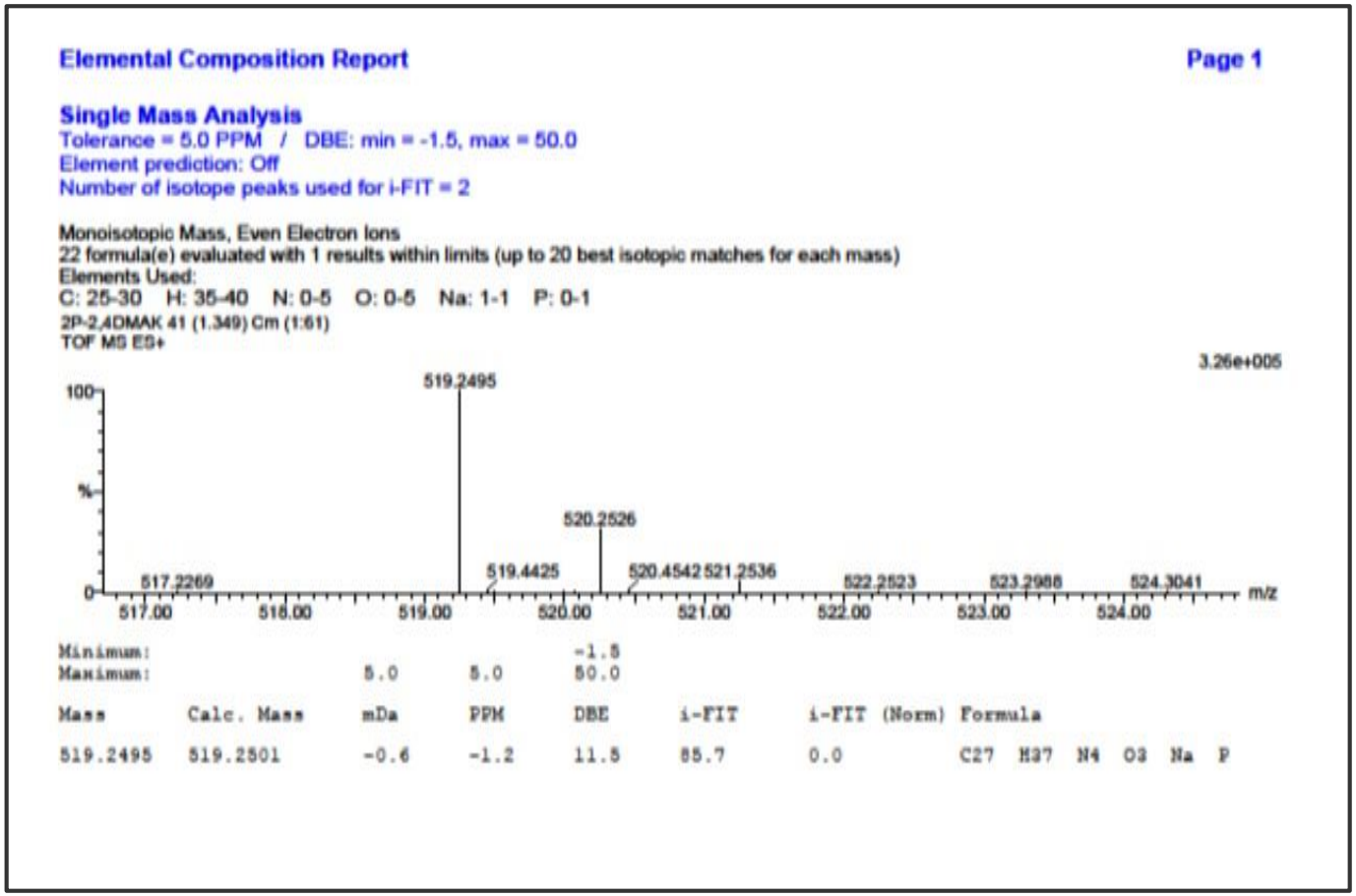

Figure S68: The HRMS Spectrum of 4m, diethyl(((2,5-dimethylphenyl)amino)(2-(4-methylpiperazin-1-yl)quinolin-3-yl)methyl)phosphonate

Appendix 69

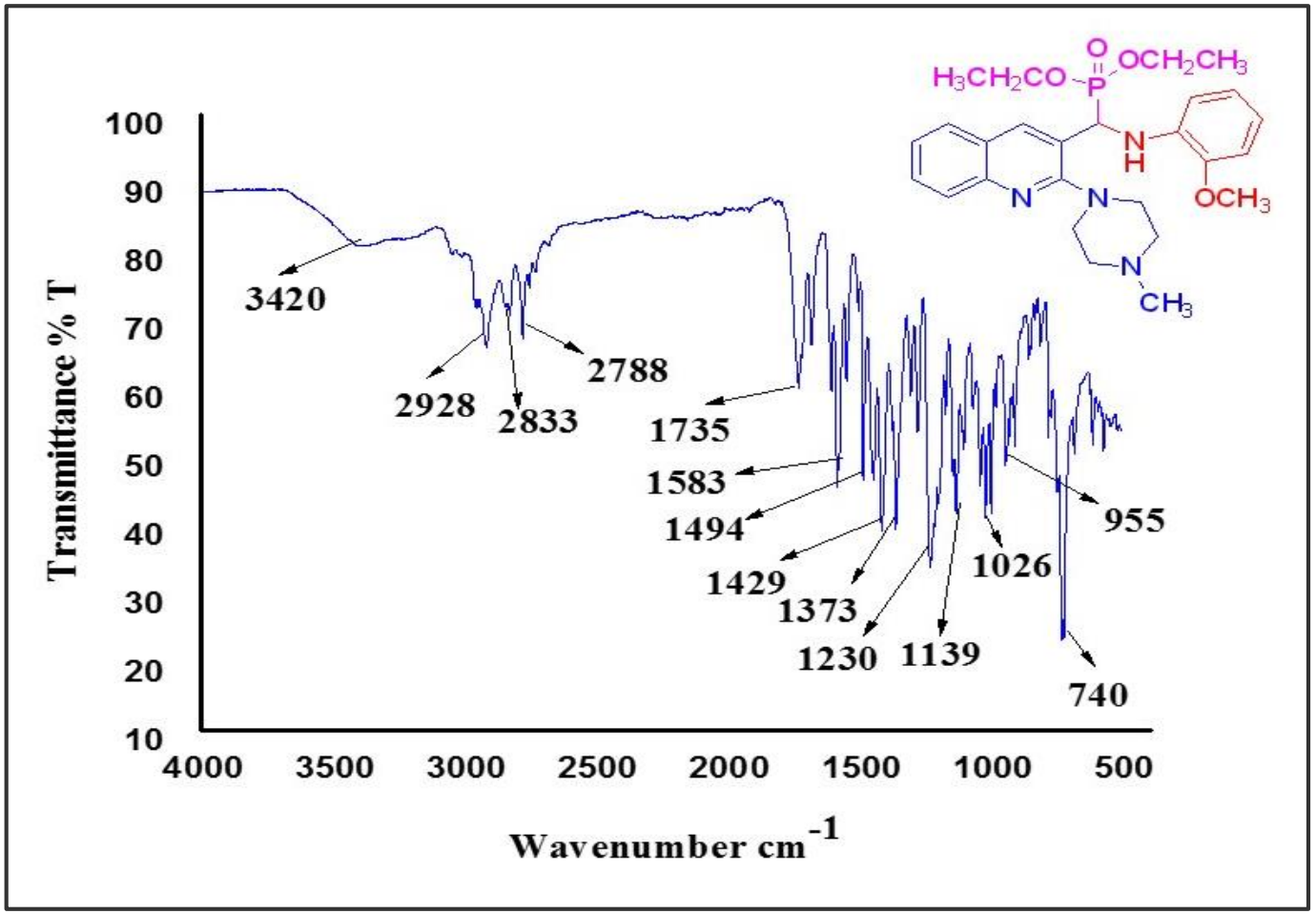

Figure S69: The IR Spectrum of 4p, diethyl (((2-methoxyphenyl)amino)(2-(4-methylpiperazin-1-yl)quinolin-3-yl)methyl)phosphonate

Appendix 70

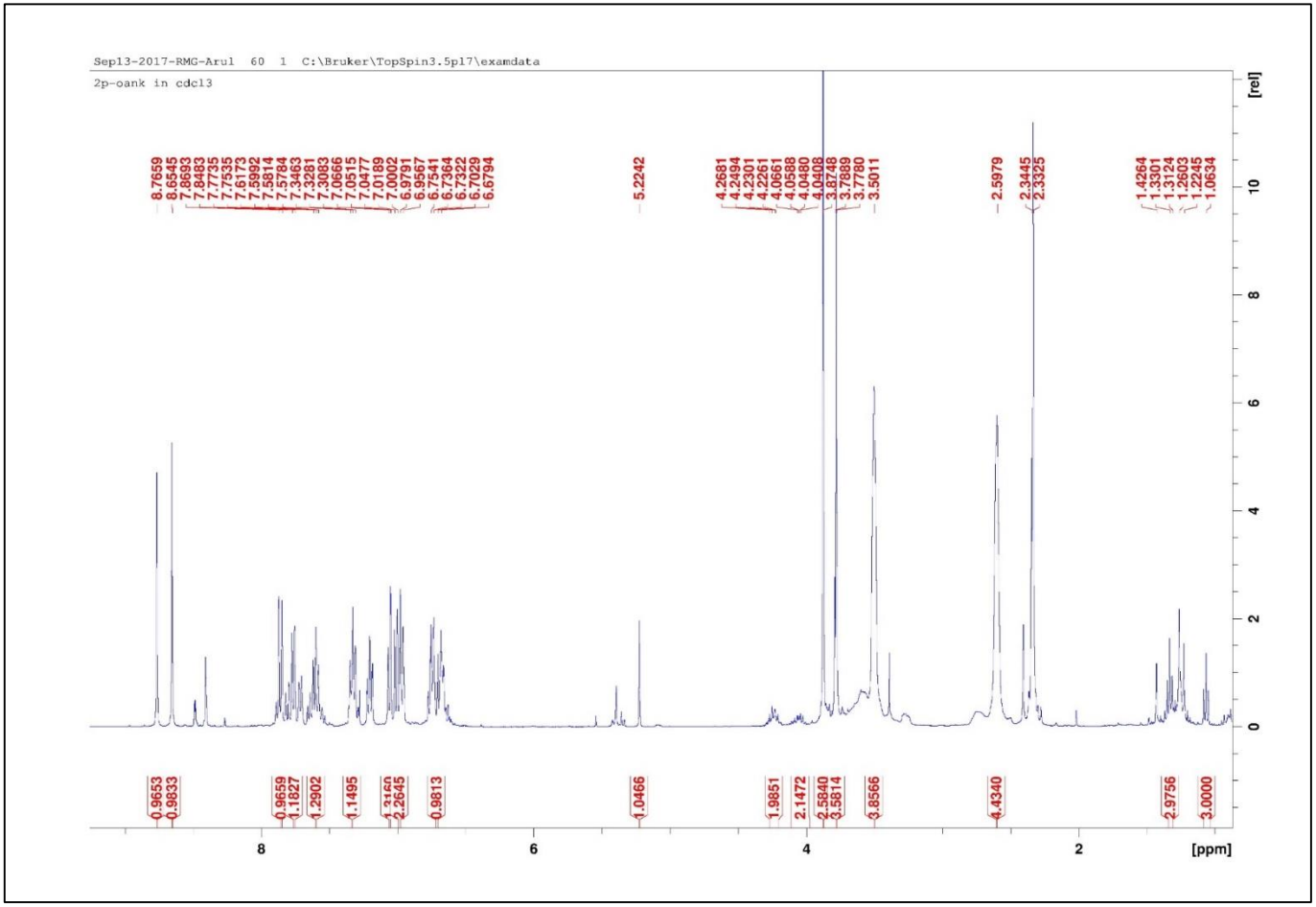

Figure S70: The ^{1}H NMR Spectrum of 4p, diethyl (((2-methoxyphenyl)amino)(2-(4-methylpiperazin-1-yl)quinolin-3-yl)methyl)phosphonate

Appendix 71

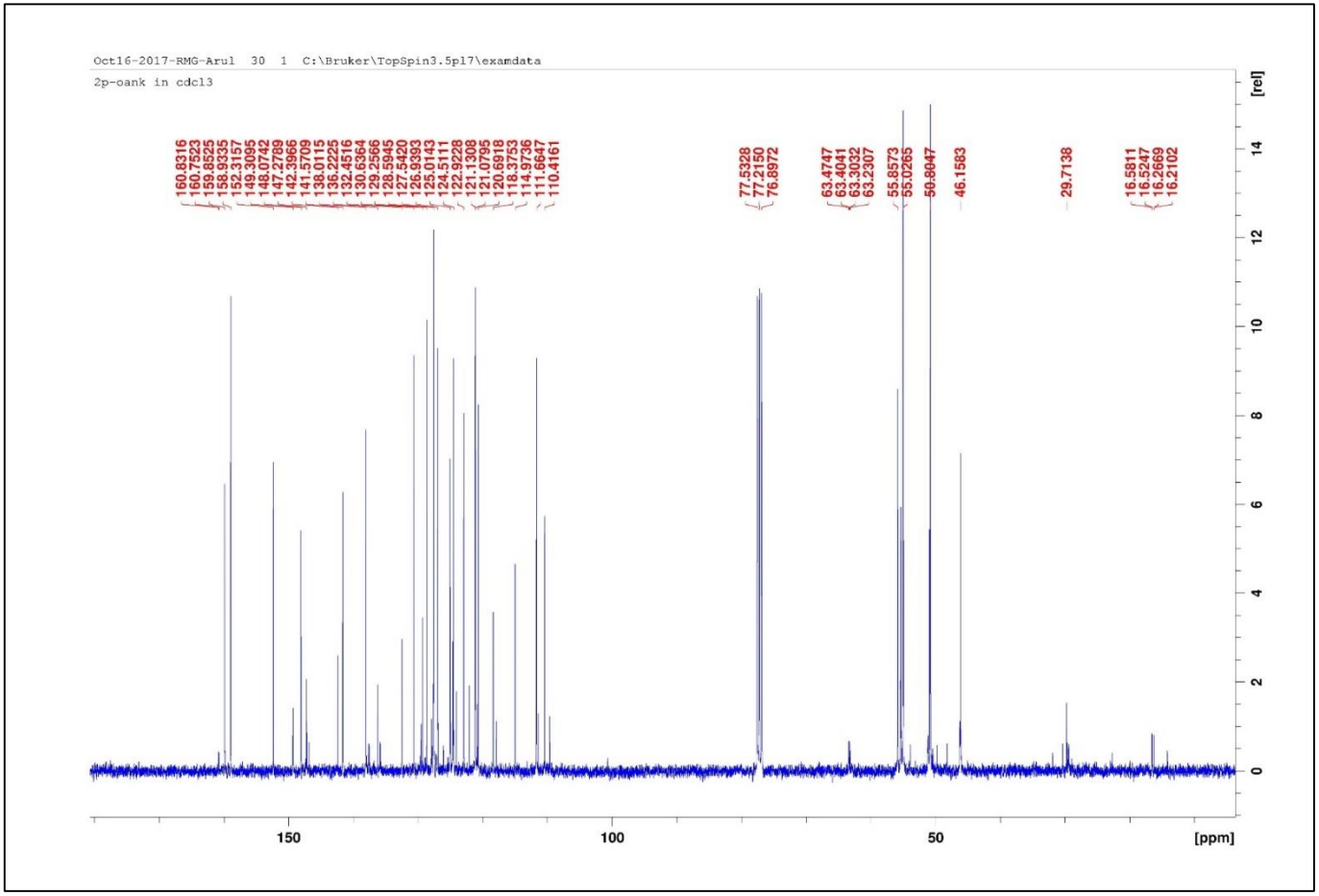

Figure S71: The ^{13}C NMR Spectrum of 4p, diethyl (((2-methoxyphenyl)amino)(2-(4-methylpiperazin-1-yl)quinolin-3-yl)methyl)phosphonate

Appendix 72

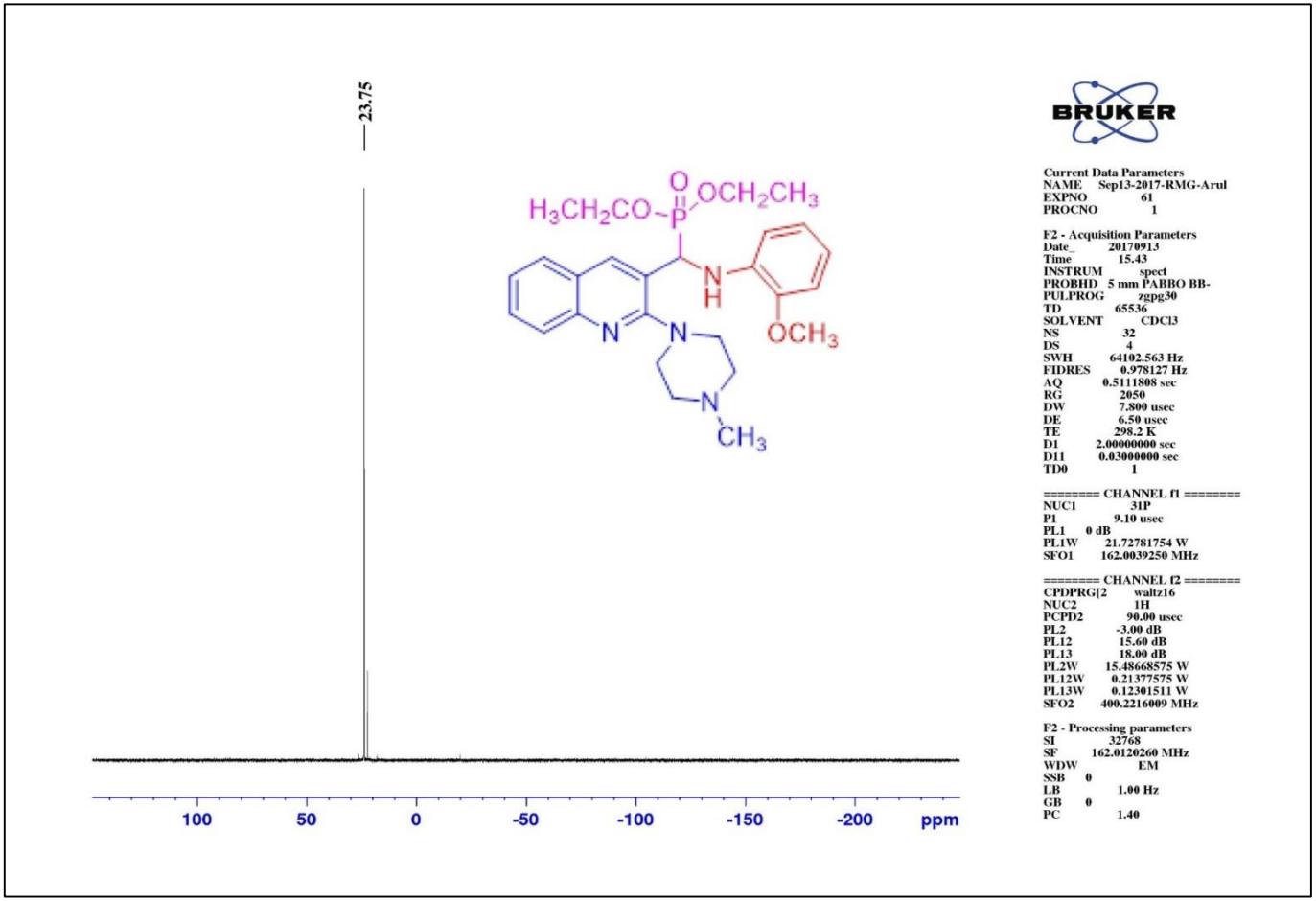

Figure S72: The ^{31}P NMR Spectrum of 4p, diethyl (((2-methoxyphenyl)amino)(2-(4-methylpiperazin-1-yl)quinolin-3-yl)methyl)phosphonate

Appendix 73

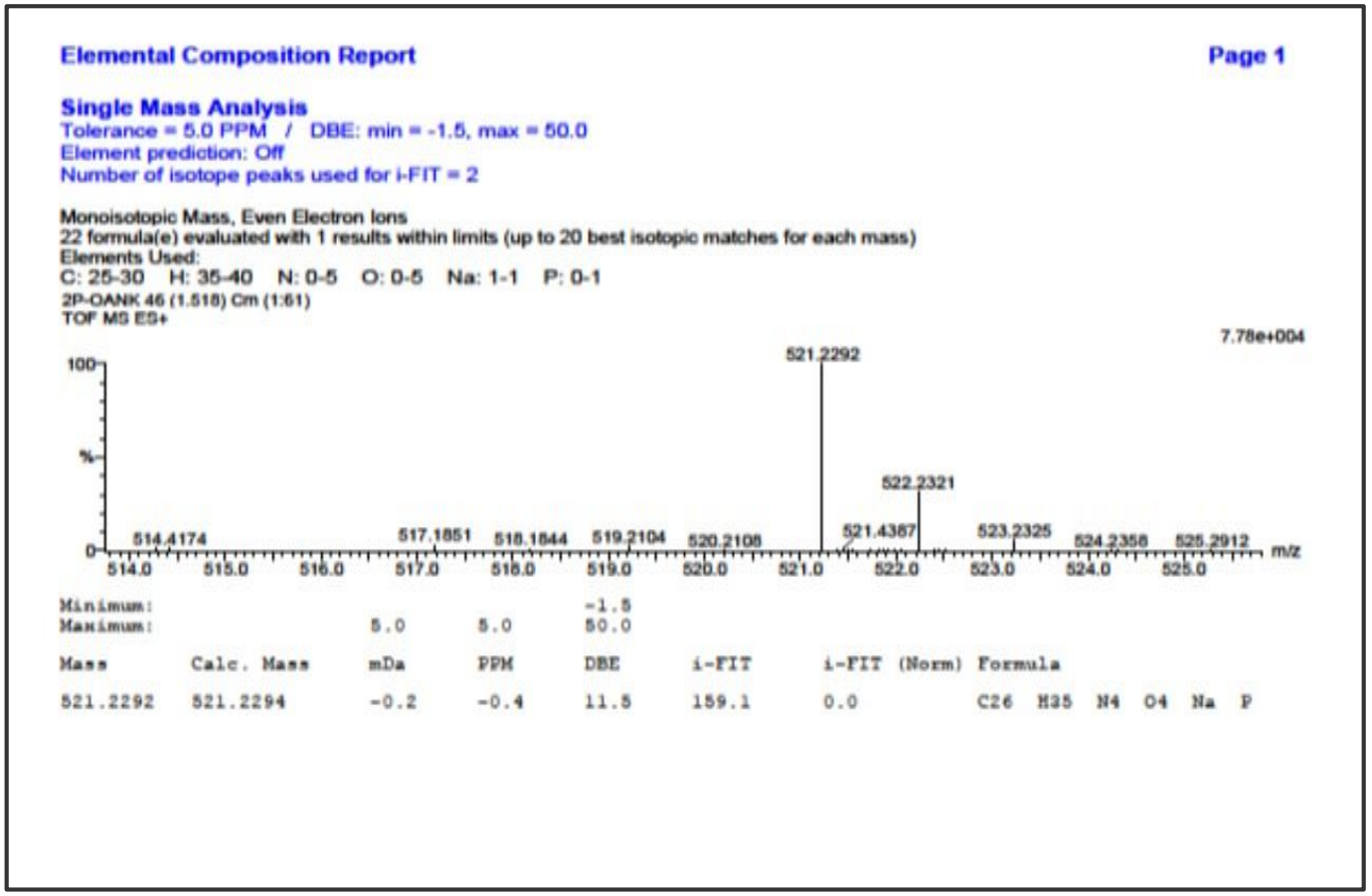

Figure S73: The HRMS Spectrum of 4p, diethyl (((2-methoxyphenyl)amino)(2-(4-methylpiperazin-1-yl)quinolin-3-yl)methyl)phosphonate

Appendix 74

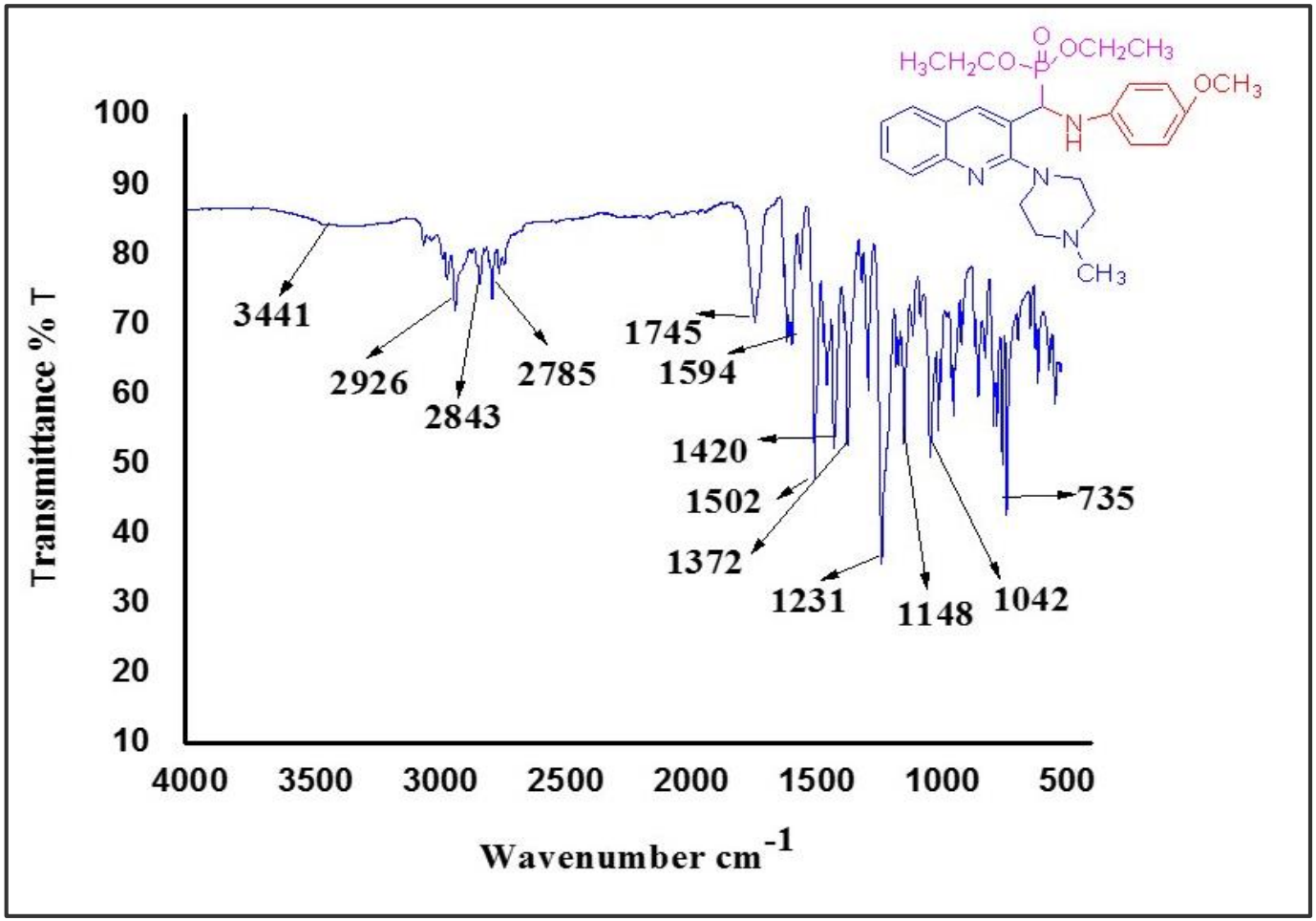

Figure S74: The IR Spectrum of 4q, diethyl(((4-methoxyphenyl)amino)(2-(4-methylpiperazin-1-yl)quinolin-3-yl)methyl)phosphonate

Appendix 75

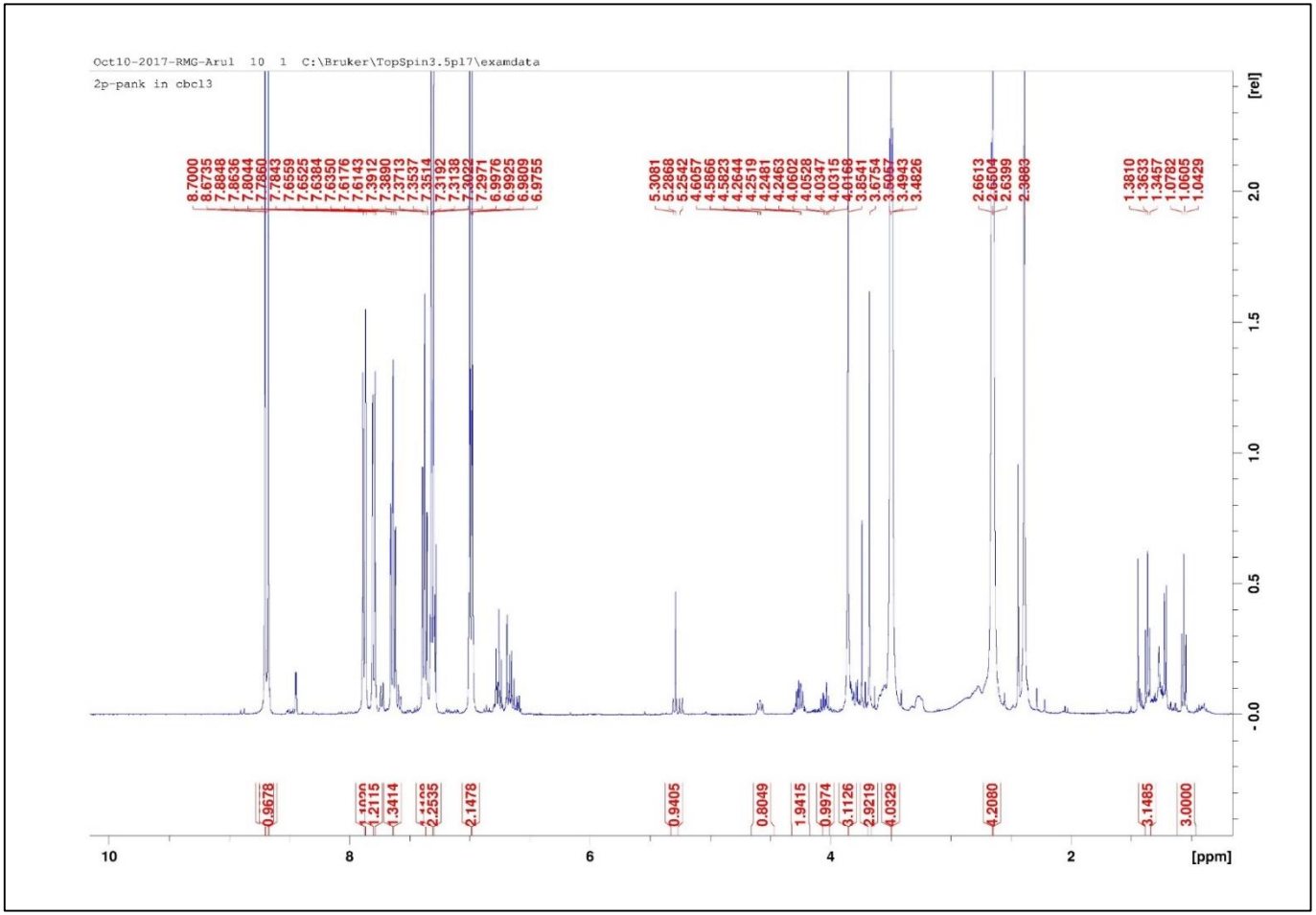

Figure S75: The ^{1}H NMR Spectrum of 4q, diethyl(((4-methoxyphenyl)amino)(2-(4-methylpiperazin-1-yl)quinolin-3-yl)methyl)phosphonate

Appendix 76

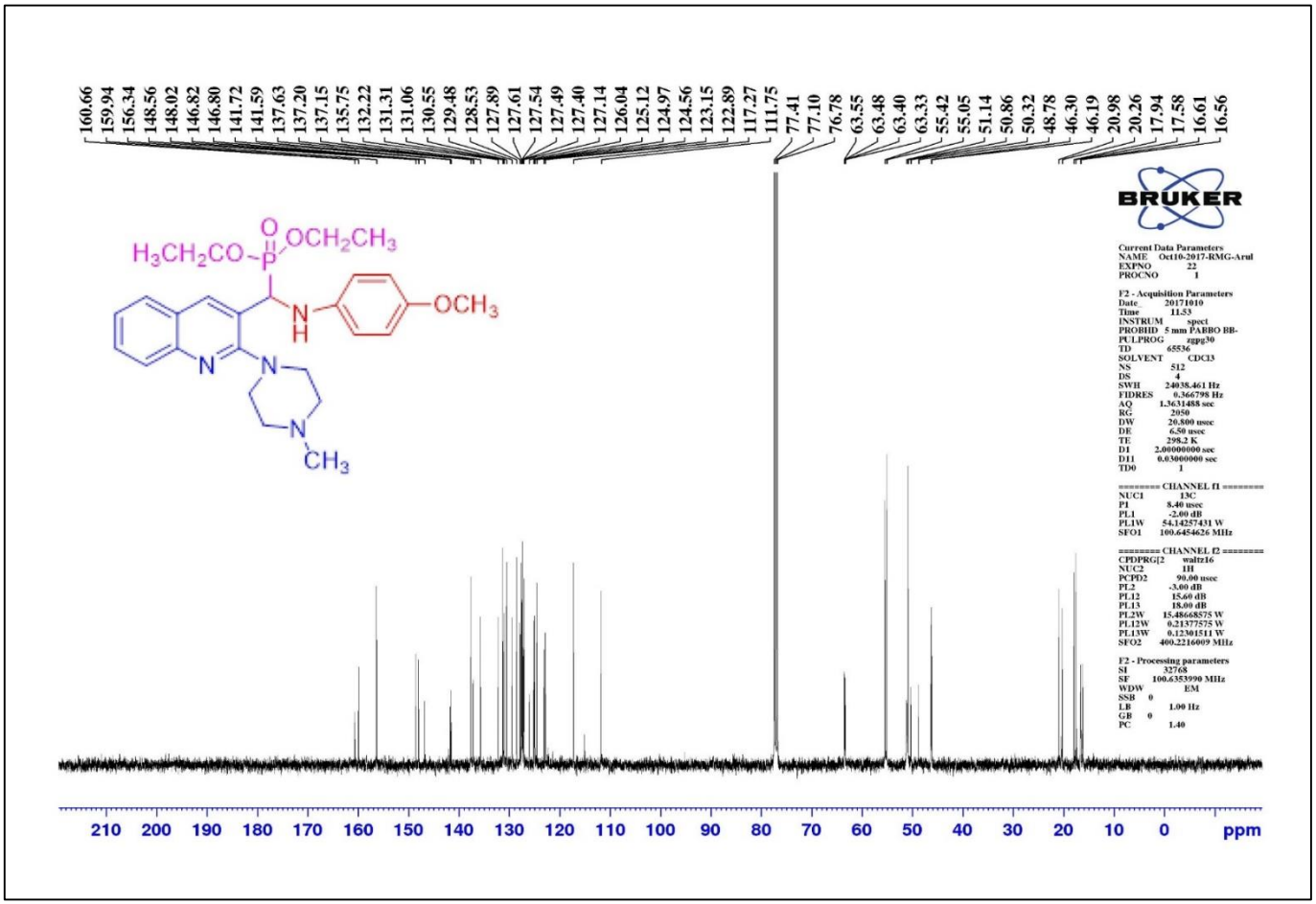

Figure S76: The ^{13}C NMR Spectrum of 4q, diethyl(((4-methoxyphenyl)amino)(2-(4-methylpiperazin-1-yl)quinolin-3-yl)methyl)phosphonate

Appendix 77

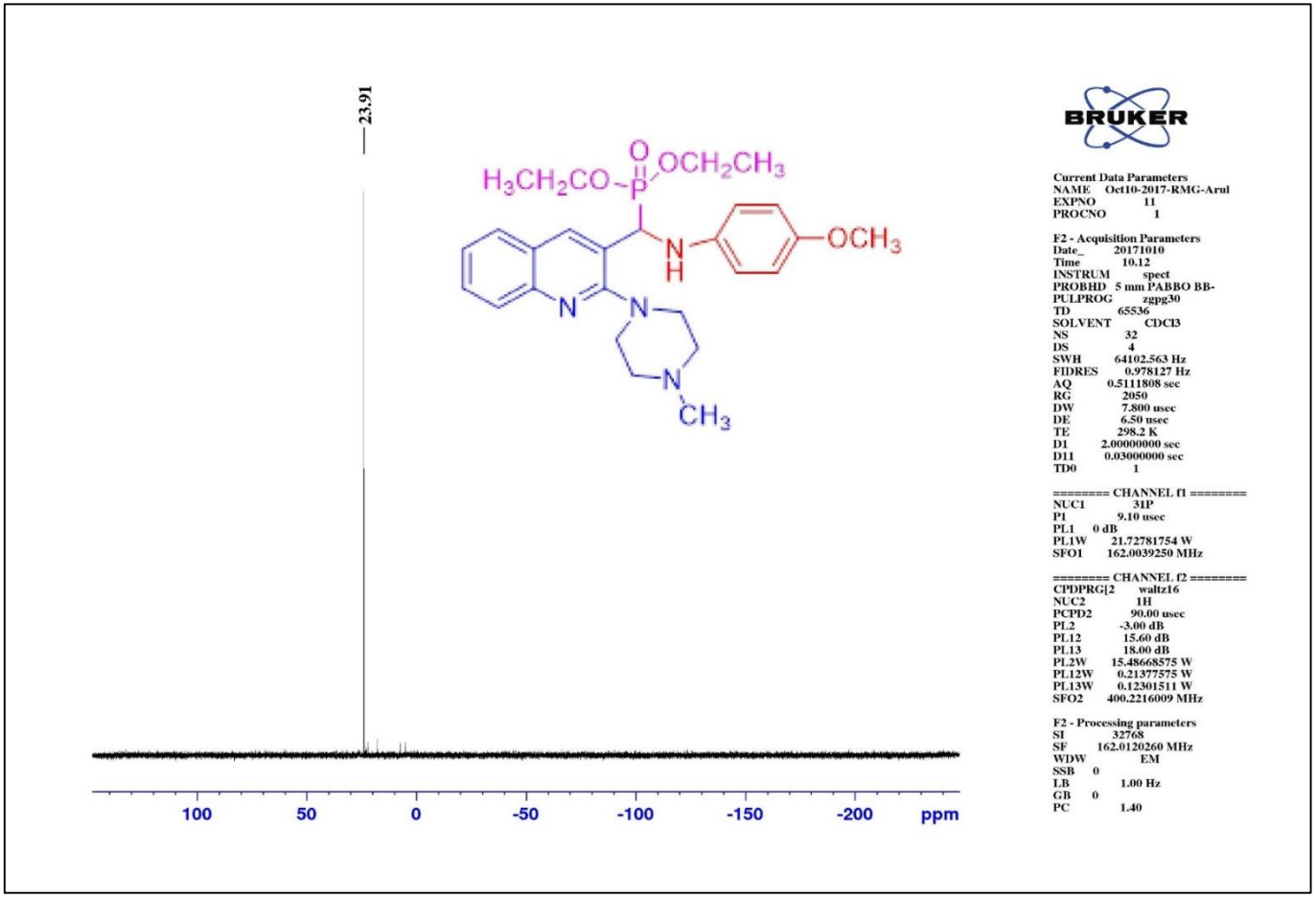

Figure S77: The ^{31}P NMR Spectrum of 4q, diethyl(((4-methoxyphenyl)amino)(2-(4-methylpiperazin-1-yl)quinolin-3-yl)methyl)phosphonate

Appendix 78

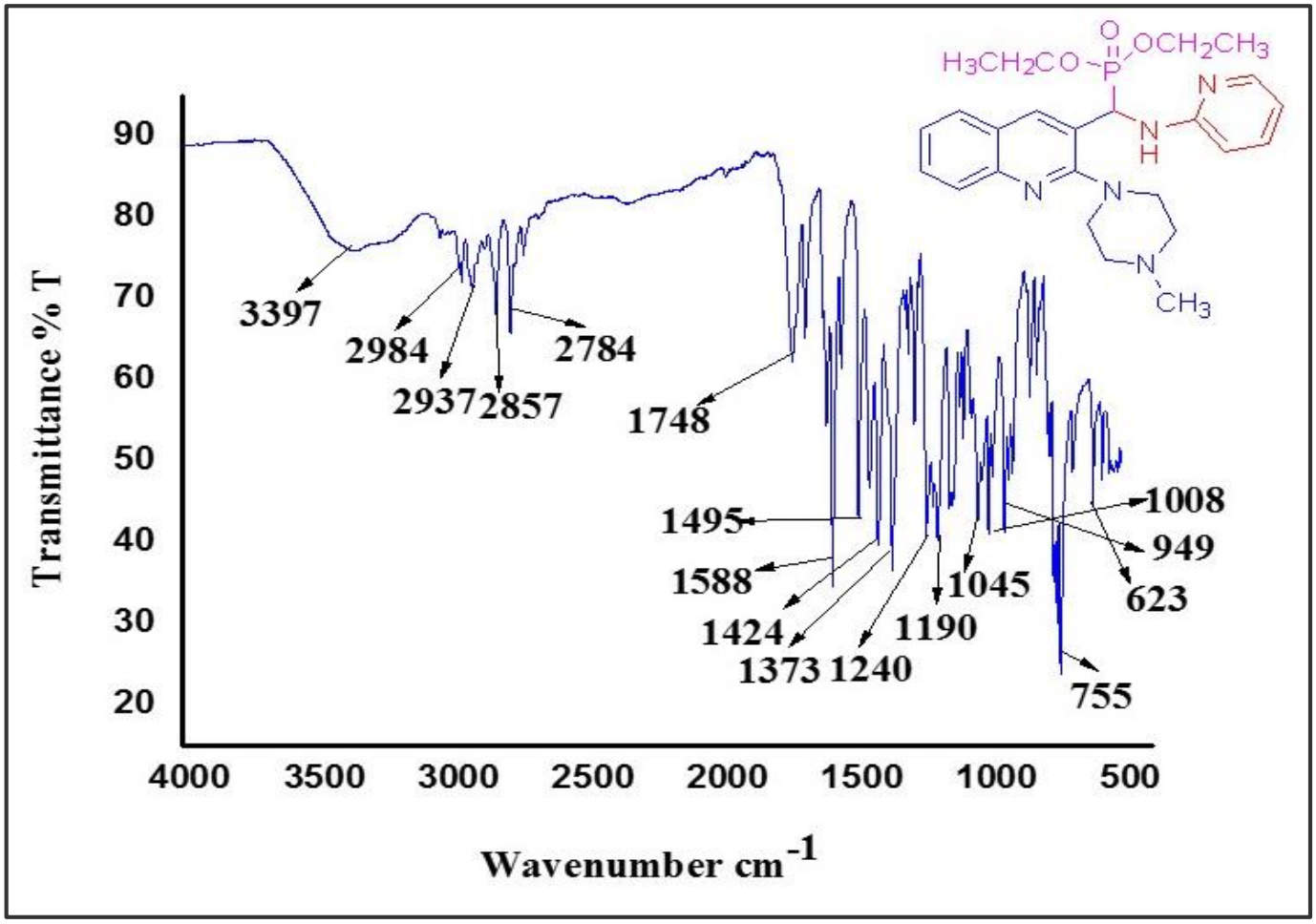

Figure S78: The HRMS Spectrum of 4q, diethyl(((4-methoxyphenyl)amino)(2-(4-methylpiperazin-1-yl)quinolin-3-yl)methyl)phosphonate

Appendix 79

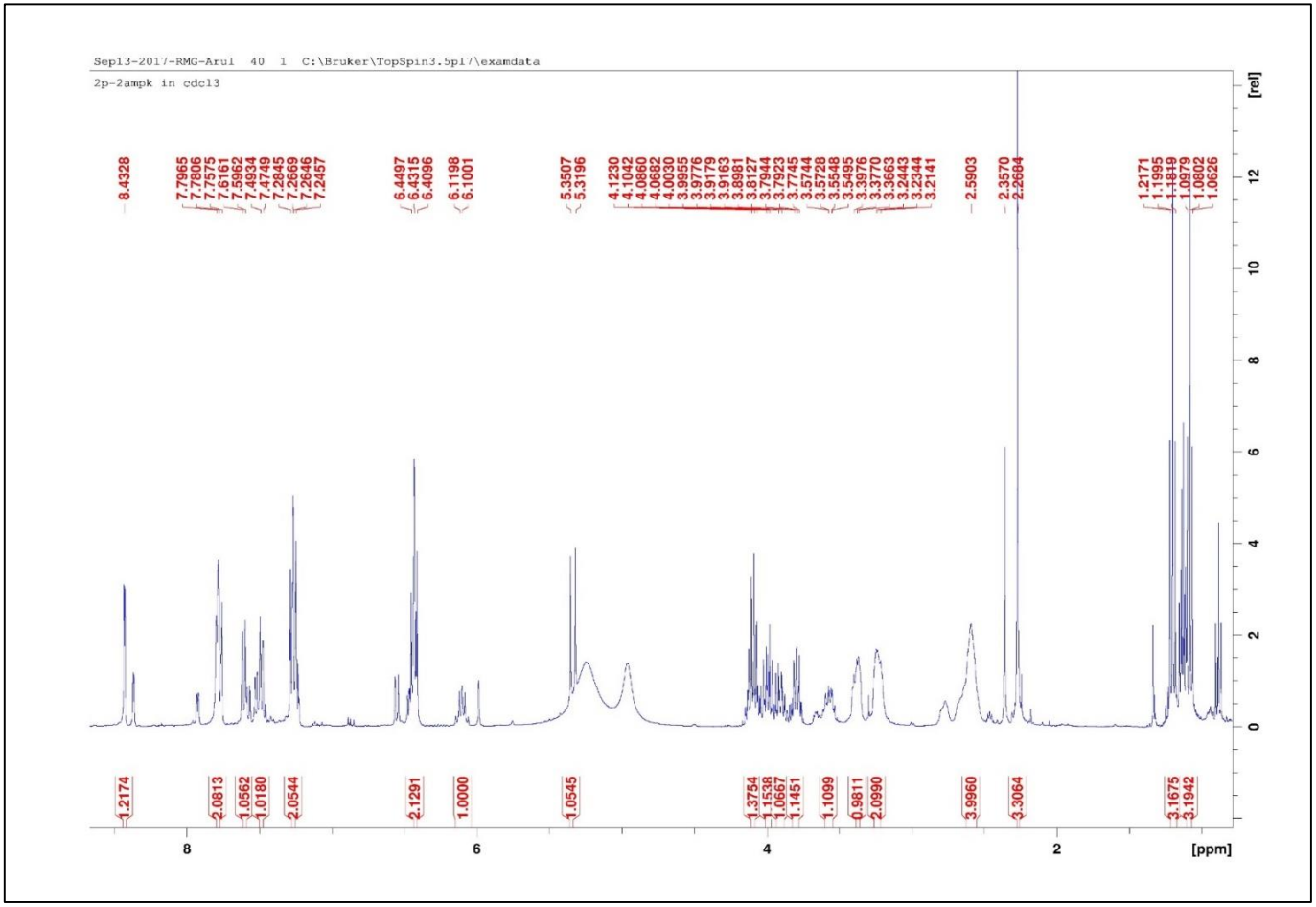

Figure S79: The IR Spectrum of 4n, diethyl((2-(4-methylpiperazin-1-yl)quinolin-3-yl)(pyridin-2-ylamino)methyl)phosphonate

Appendix 80

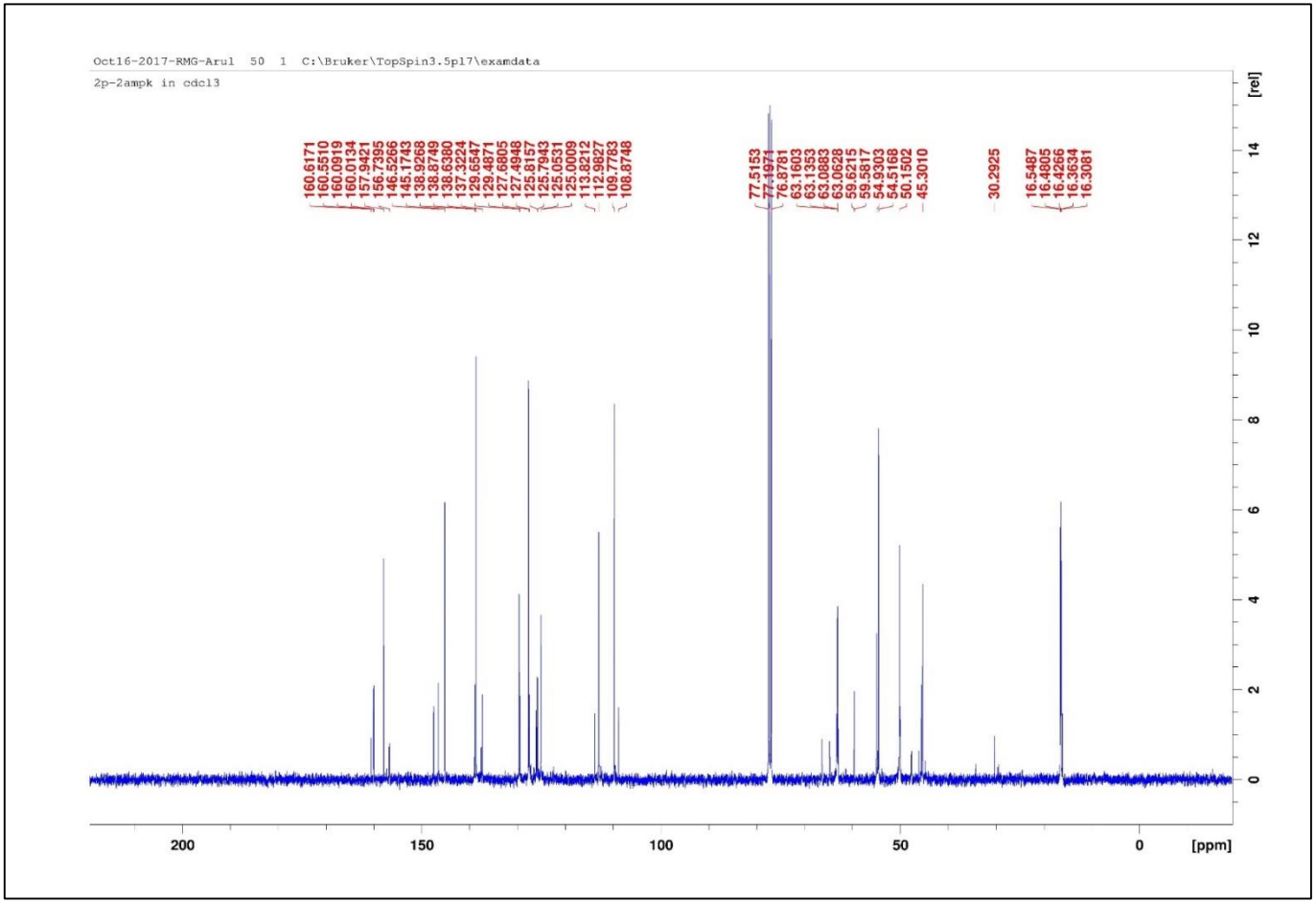

Figure S80: The ^{1}H NMR Spectrum of 4n, diethyl((2-(4-methylpiperazin-1-yl)quinolin-3-yl)(pyridin-2-ylamino)methyl)phosphonate

Appendix 81

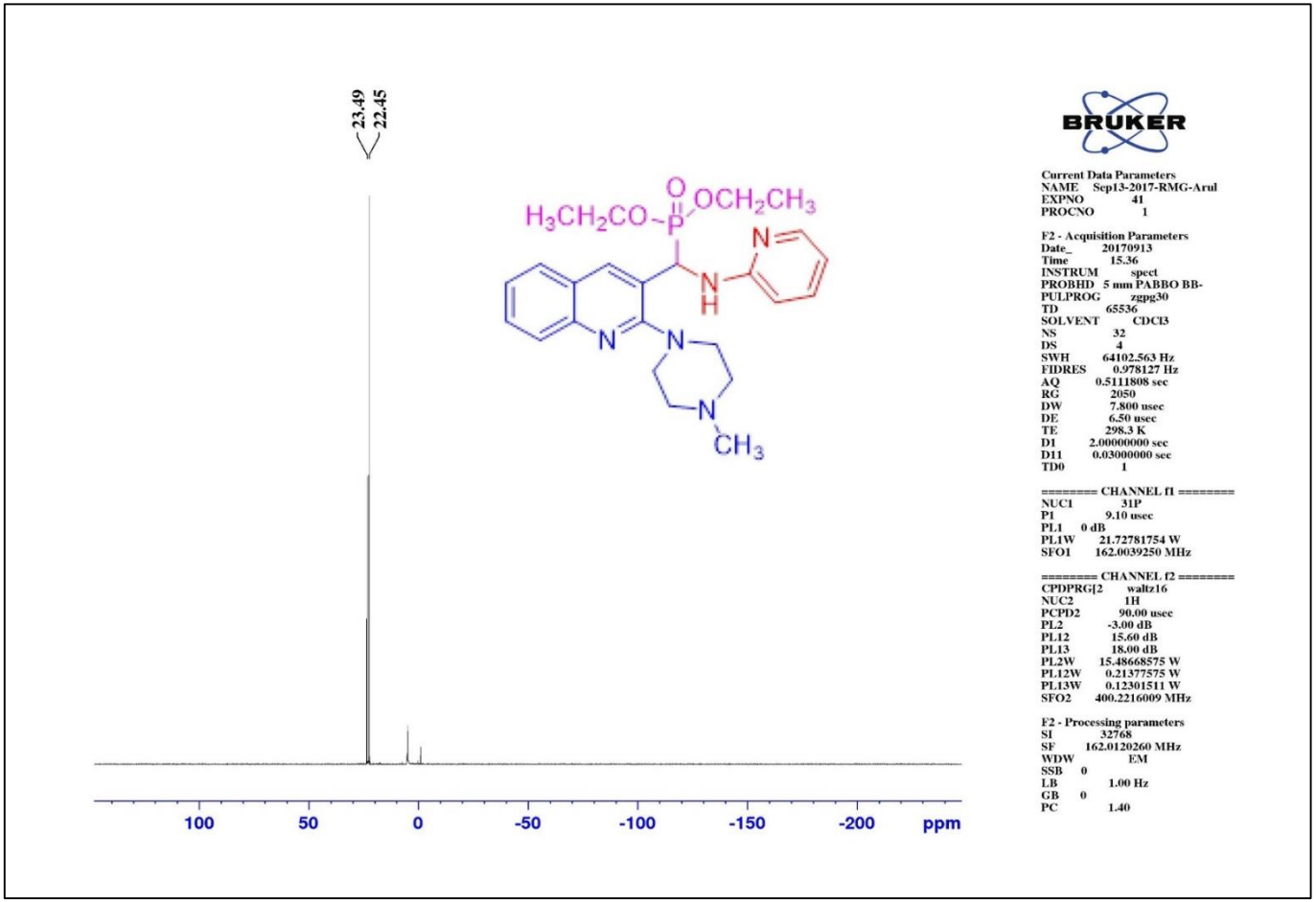

Figure S81: The ^{13}C NMR Spectrum of 4n, diethyl((2-(4-methylpiperazin-1-yl)quinolin-3-yl)(pyridin-2-ylamino)methyl)phosphonate

Appendix 82

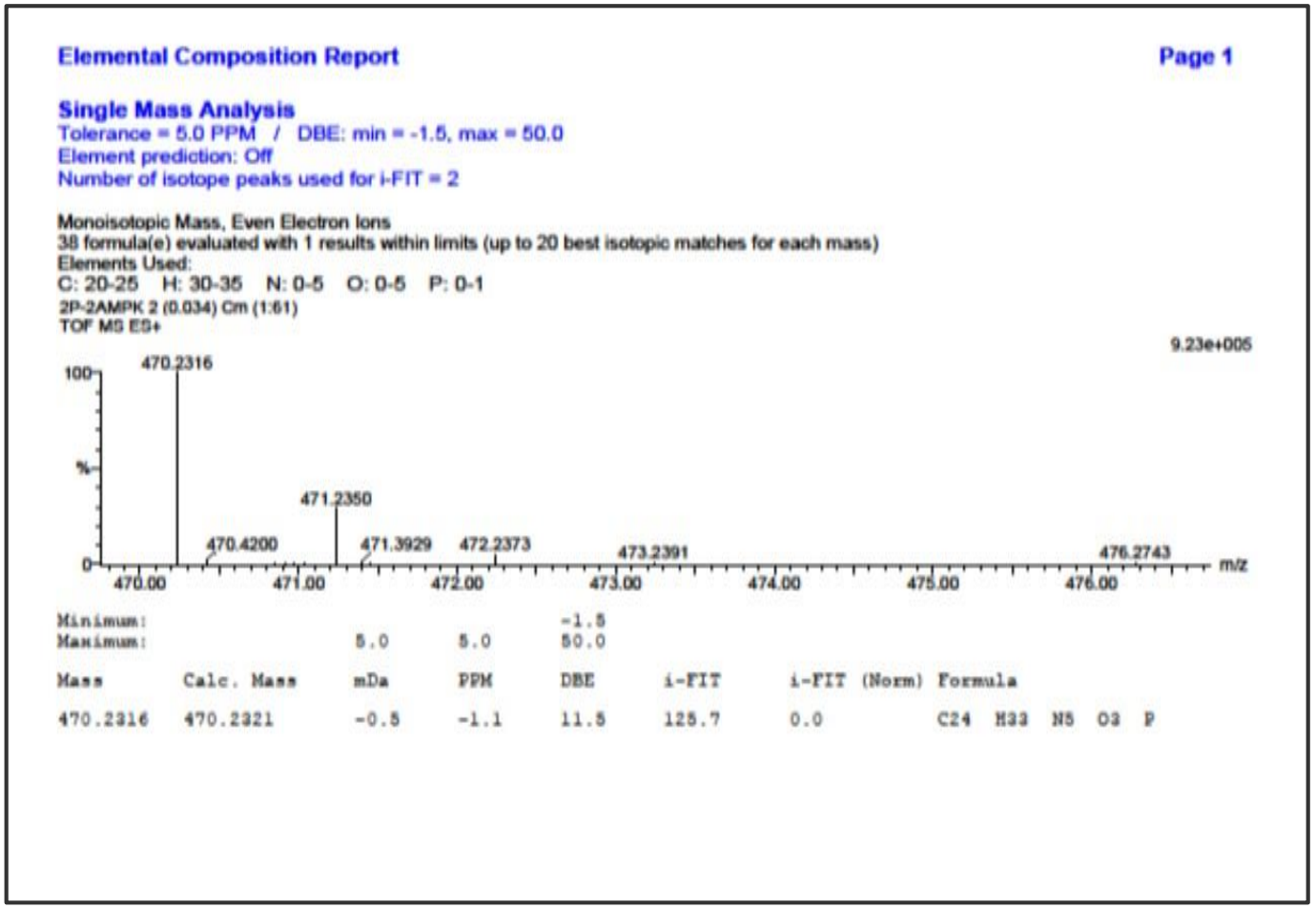

Elemental Composition Report Page 1

Single Mass Analysis
Tolerance = 5.0 PPM / DBE: min = -1.5, max = 50.0
Element prediction: Off
Number of isotope peaks used for i-FIT = 2

Monoisotopic Mass, Even Electron Ions
38 formula(e) evaluated with 1 results within limits (up to 20 best isotopic matches for each mass)
Elements Used:
C: 20-25 H: 30-35 N: 0-5 O: 0-5 P: 0-1
2P-2AMPK 2 (0.034) Cm (1:61)
TOF MS ES+

9.23e+005

Minimum:				-1.5			
Maximum:		5.0	5.0	50.0			
Mass	Calc. Mass	mDa	PPM	DBE	i-FIT	i-FIT (Norm)	Formula
470.2316	470.2321	-0.5	-1.1	11.5	125.7	0.0	C24 H33 N5 O3 P

Figure S82: The ^{31}P NMR Spectrum of 4n, diethyl((2-(4-methylpiperazin-1-yl)quinolin-3-yl)(pyridin-2-ylamino)methyl)phosphonate

Appendix 83

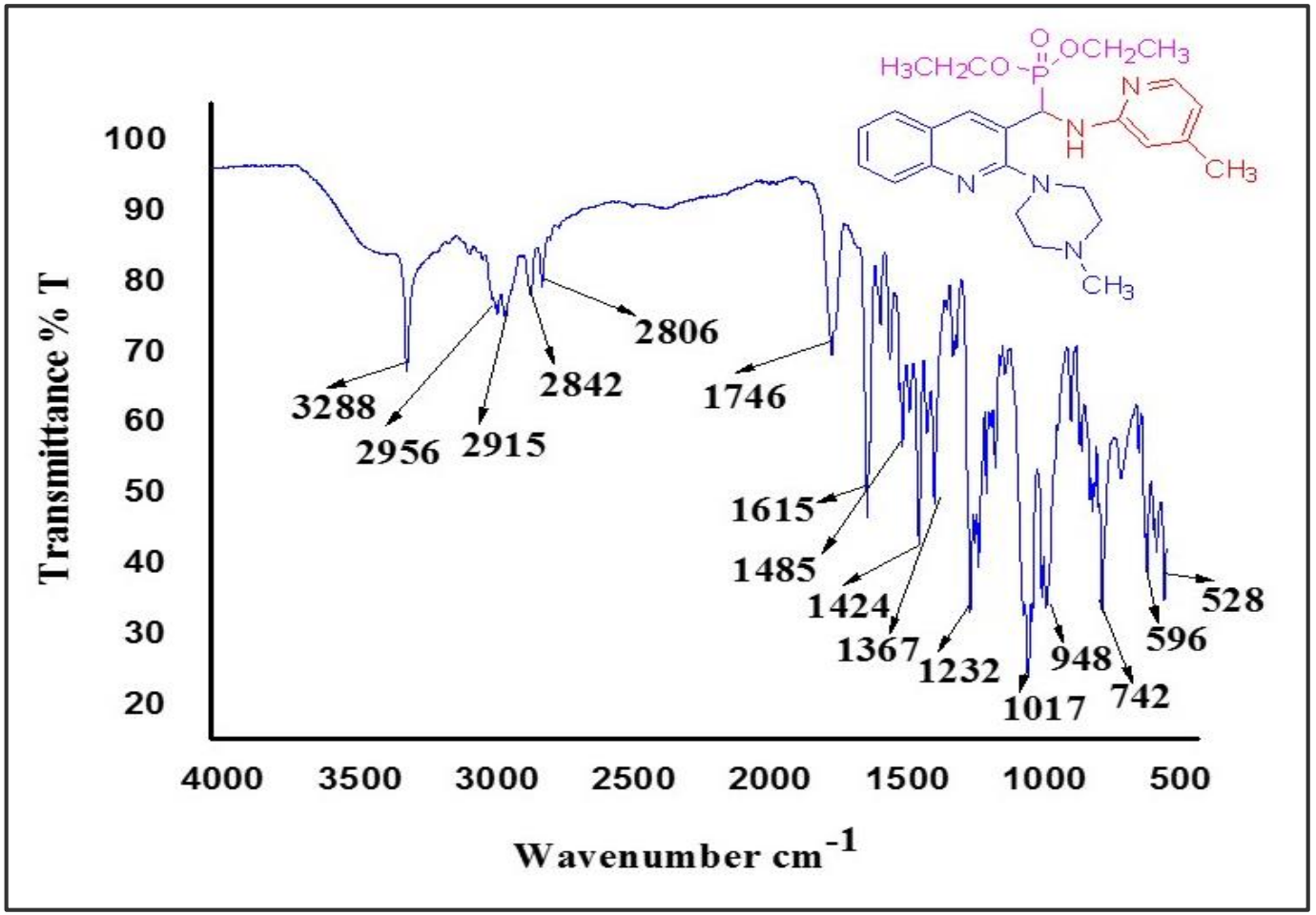

Figure S83: The HRMS Spectrum of 4n, diethyl((2-(4-methylpiperazin-1-yl)quinolin-3-yl)(pyridin-2-ylamino)methyl)phosphonate

Appendix 84

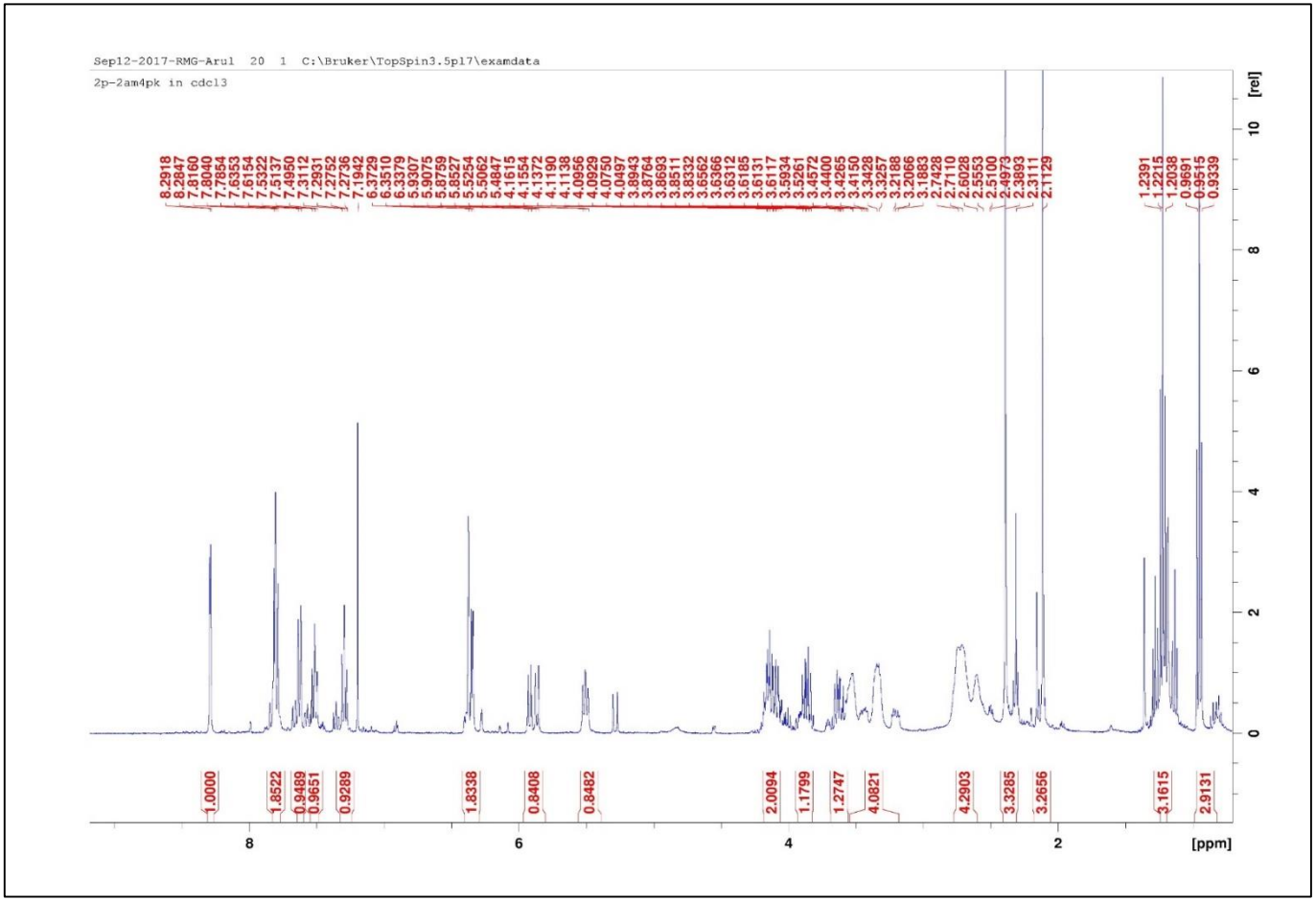

Figure S84: The IR Spectrum of 4o, diethyl((2-(4-methylpiperazin-1-yl)quinolin-3-yl)((4-methylpyridin-2-yl)amino)methyl)phosphonate

Appendix 85

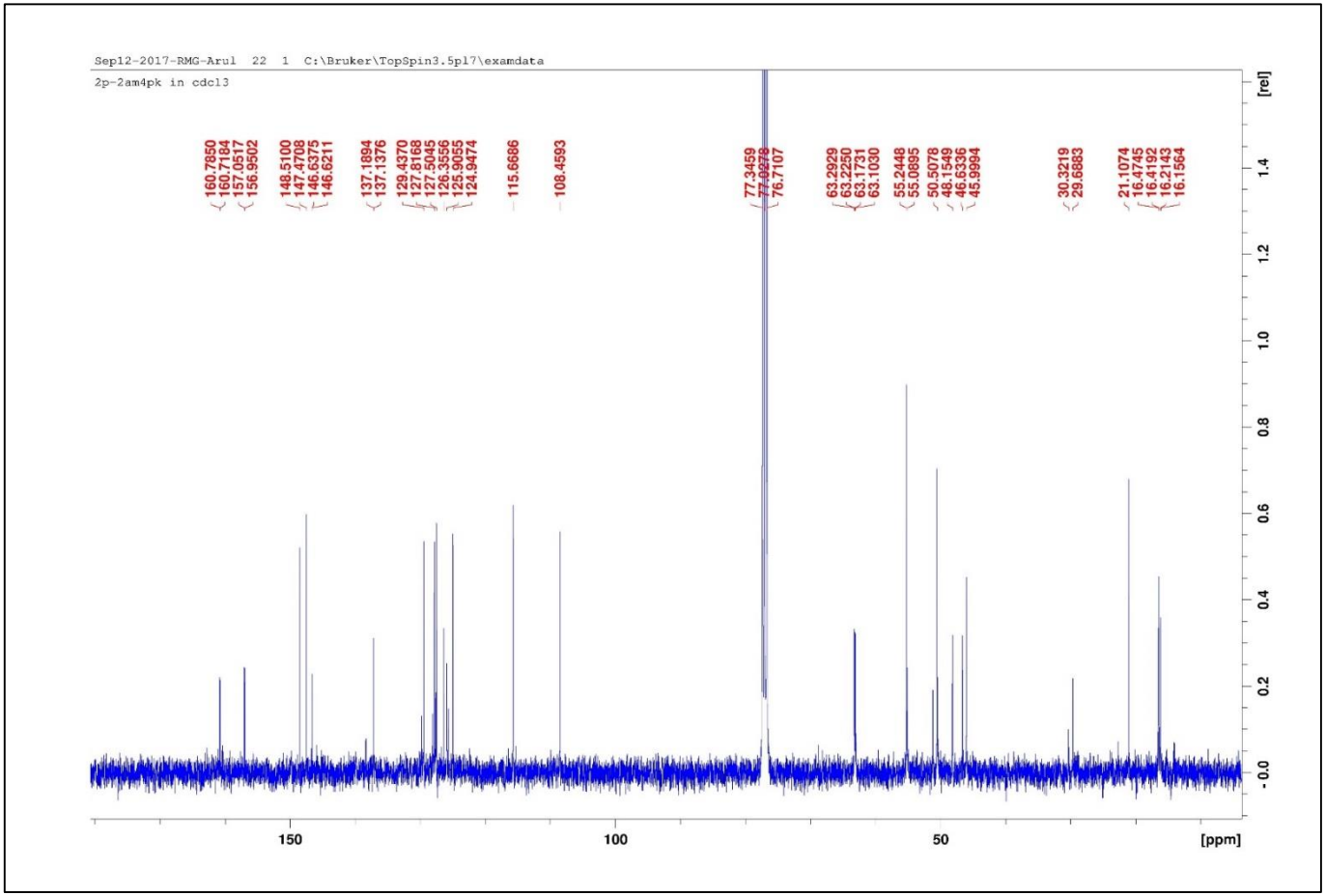

Figure S85: The ^{1}H NMR Spectrum of 4o, diethyl((2-(4-methylpiperazin-1-yl)quinolin-3-yl)((4-methylpyridin-2-yl)amino)methyl)phosphonate

Appendix 86

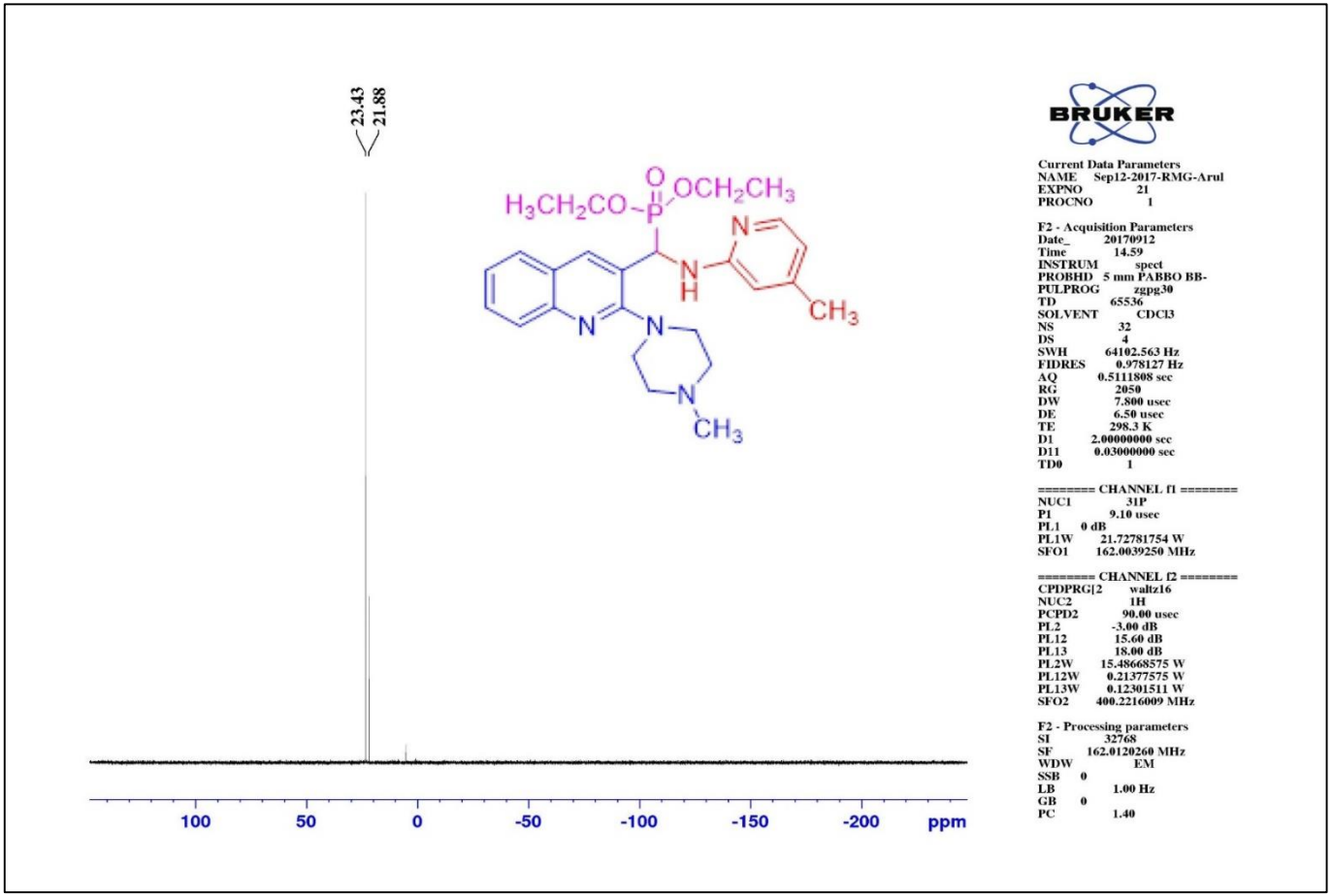

Figure S86: The ^{13}C NMR Spectrum of 4o, diethyl((2-(4-methylpiperazin-1-yl)quinolin-3-yl)((4-methylpyridin-2-yl)amino)methyl)phosphonate

Appendix 87

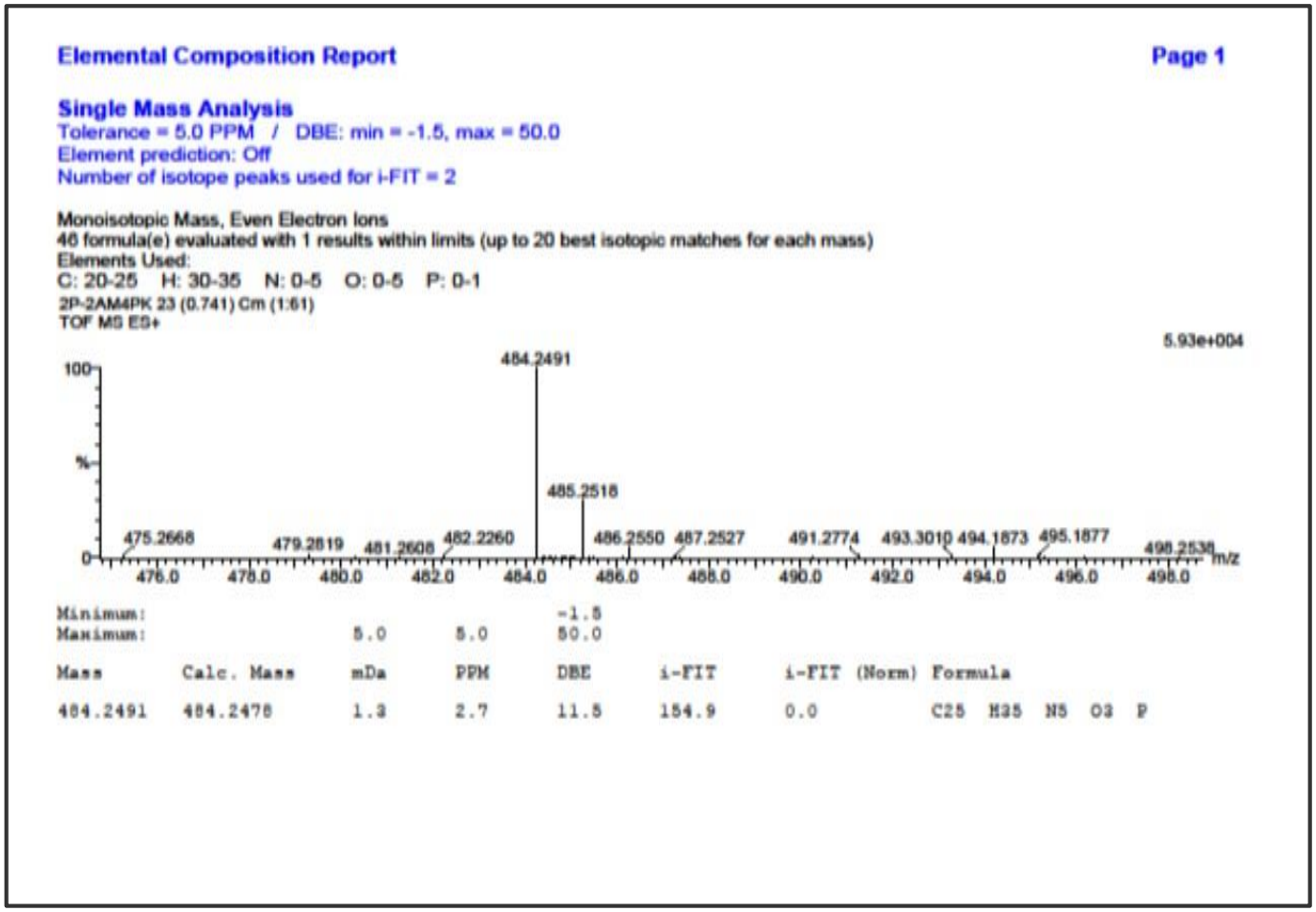

Figure S87: The ^{31}P NMR Spectrum of 4o, diethyl((2-(4-methylpiperazin-1-yl)quinolin-3-yl)((4-methylpyridin-2-yl)amino)methyl)phosphonate

Appendix 88

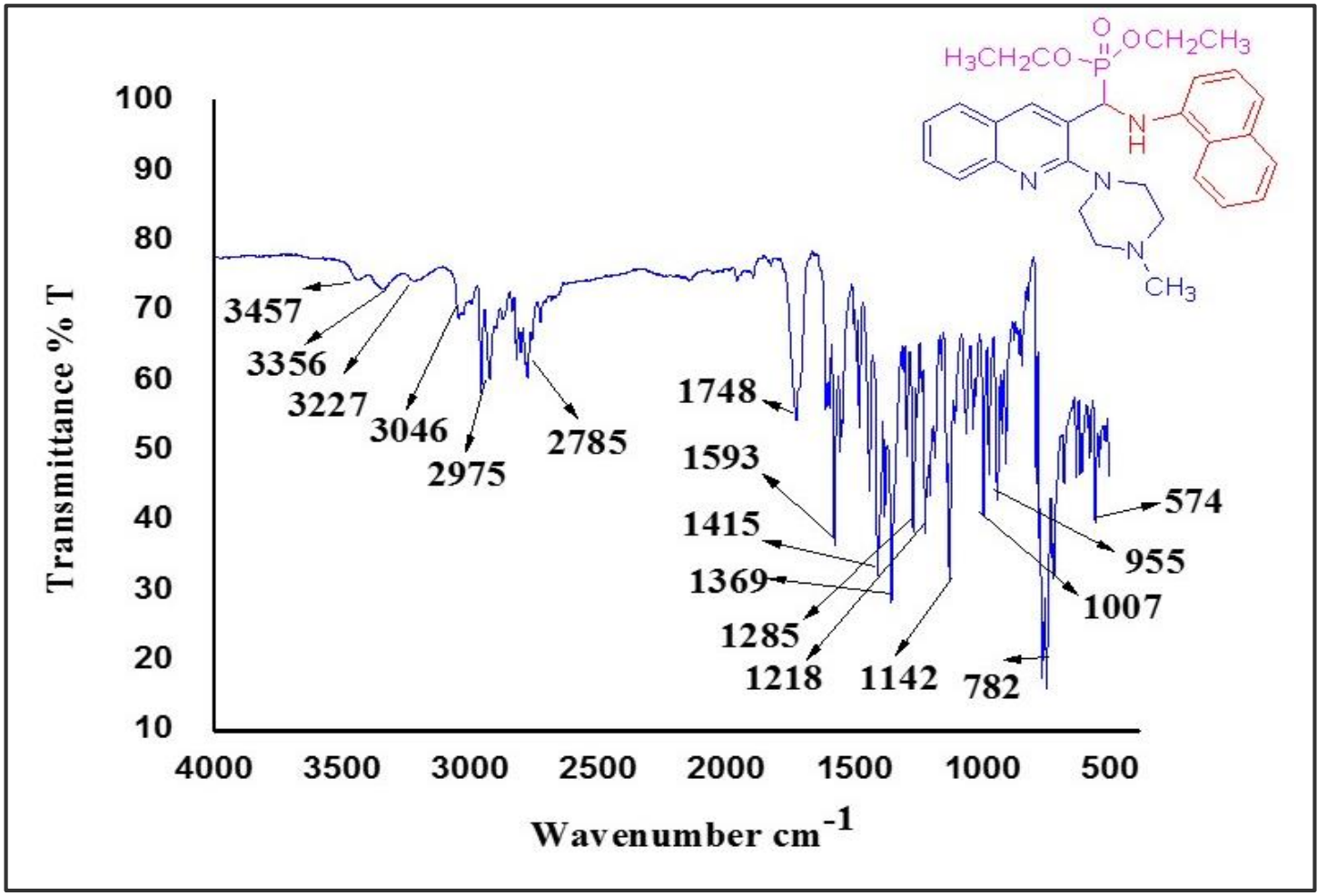

Figure S88: The IR Spectrum of 4r, diethyl ((2-(4-methylpiperazin-1-yl)quinolin-3-yl)(naphthalen-1-ylamino)methyl)phosphonate

Appendix 89

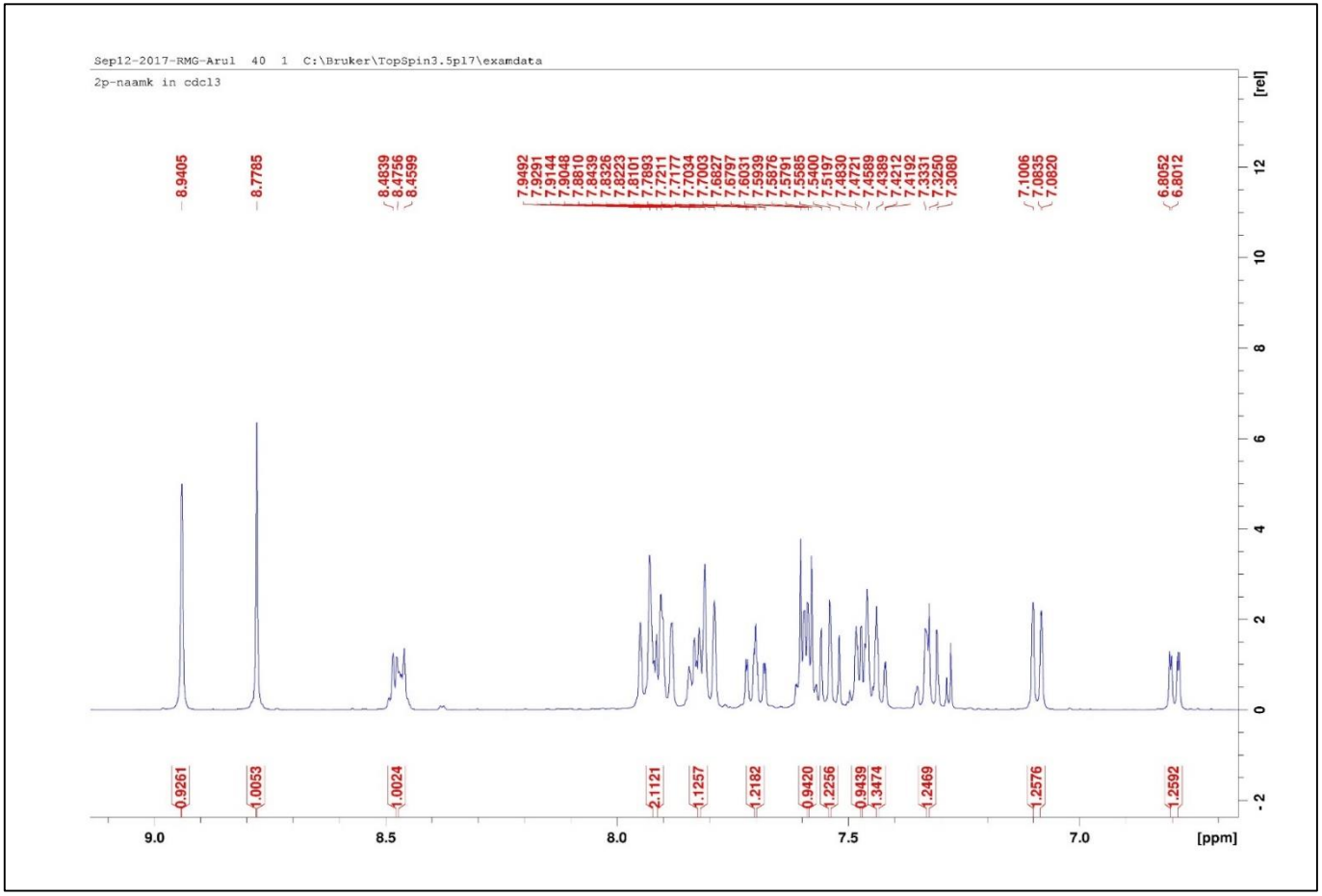

Figure S89: The ^{1}H NMR Spectrum of 4r, diethyl ((2-(4-methylpiperazin-1-yl)quinolin-3-yl)(naphthalen-1-ylamino)methyl)phosphonate

Appendix 90

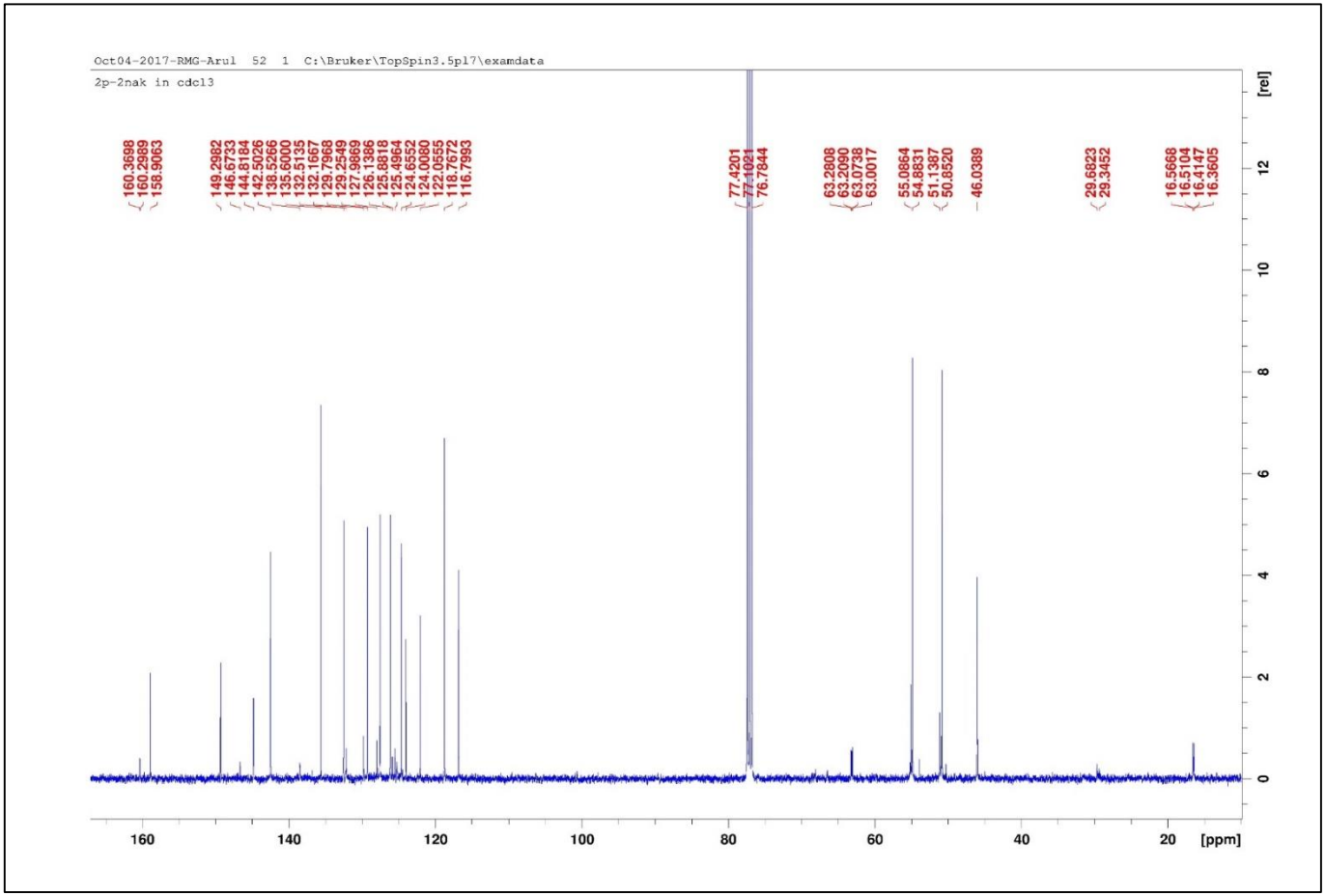

Figure S90: The ^{13}C NMR Spectrum of 4r, diethyl ((2-(4-methylpiperazin-1-yl)quinolin-3-yl)(naphthalen-1-ylamino)methyl)phosphonate

Appendix 91

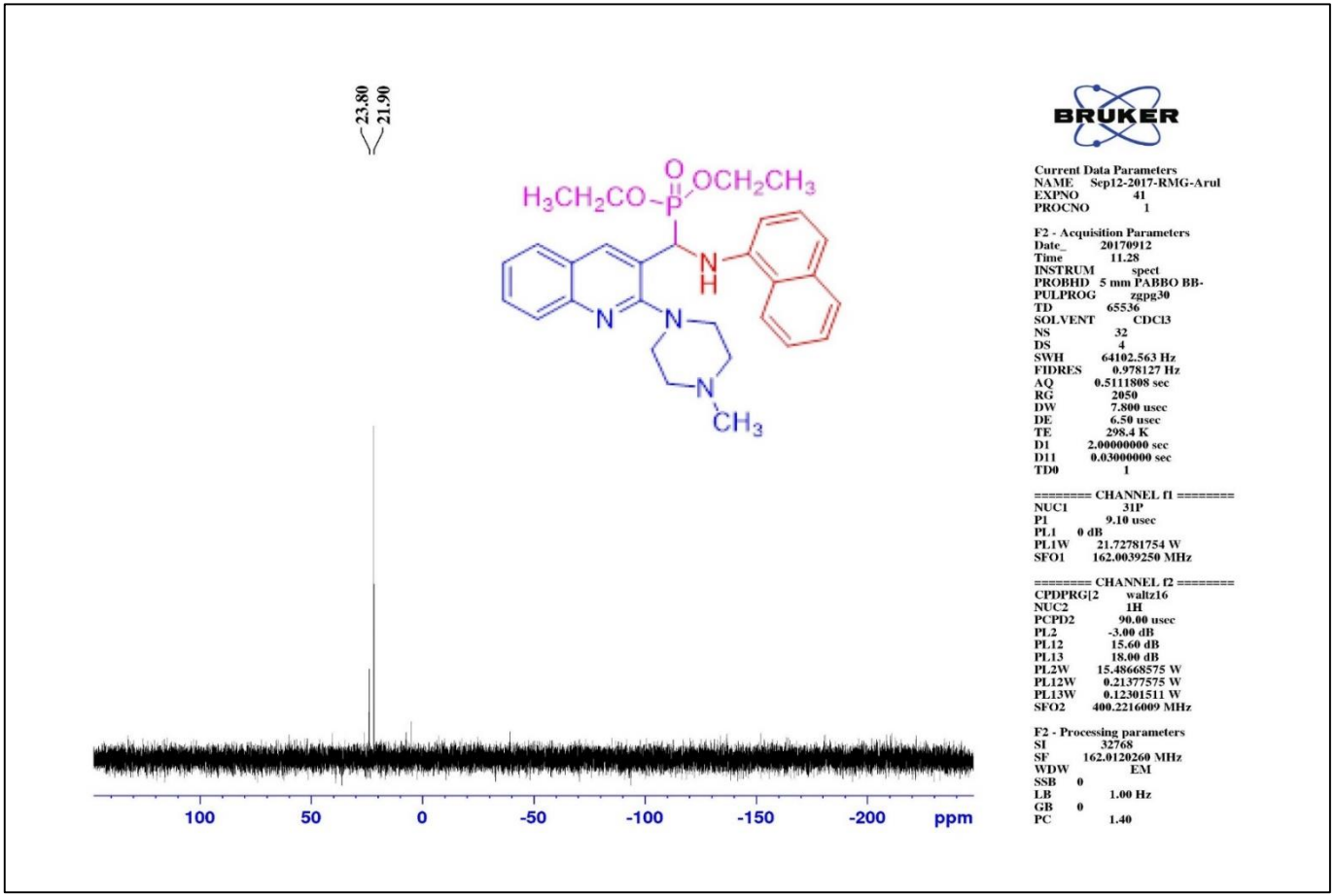

Figure S91: The ^{31}P NMR Spectrum of 4r, diethyl ((2-(4-methylpiperazin-1-yl)quinolin-3-yl)(naphthalen-1-ylamino)methyl)phosphonate

Appendix 92

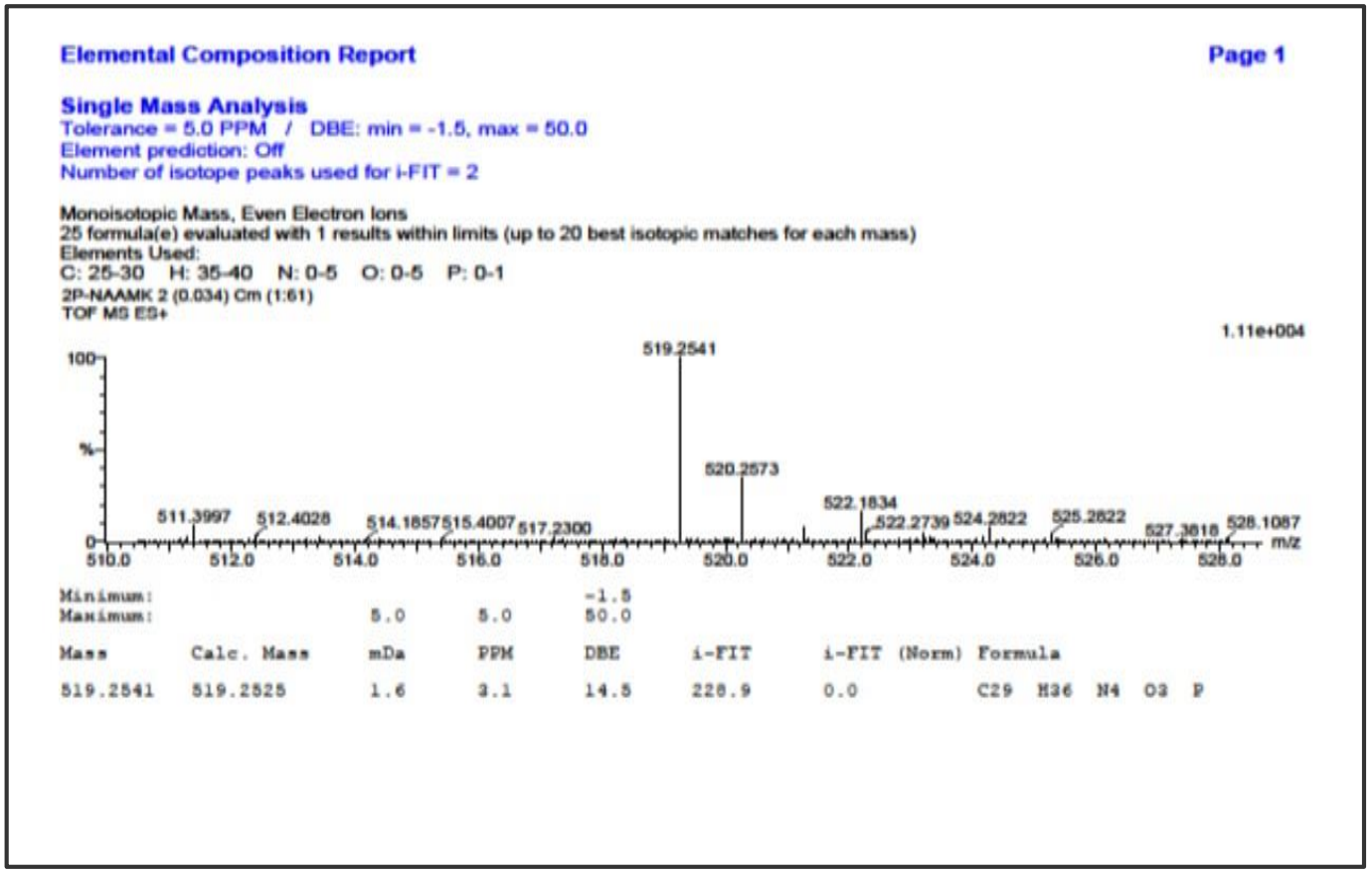

Figure S92: The HRMS Spectrum of 4r, ((2-(4-methylpiperazin-1-yl)quinolin-3-yl)(naphthalen-1-ylamino)methyl)phosphonate

Appendix 93

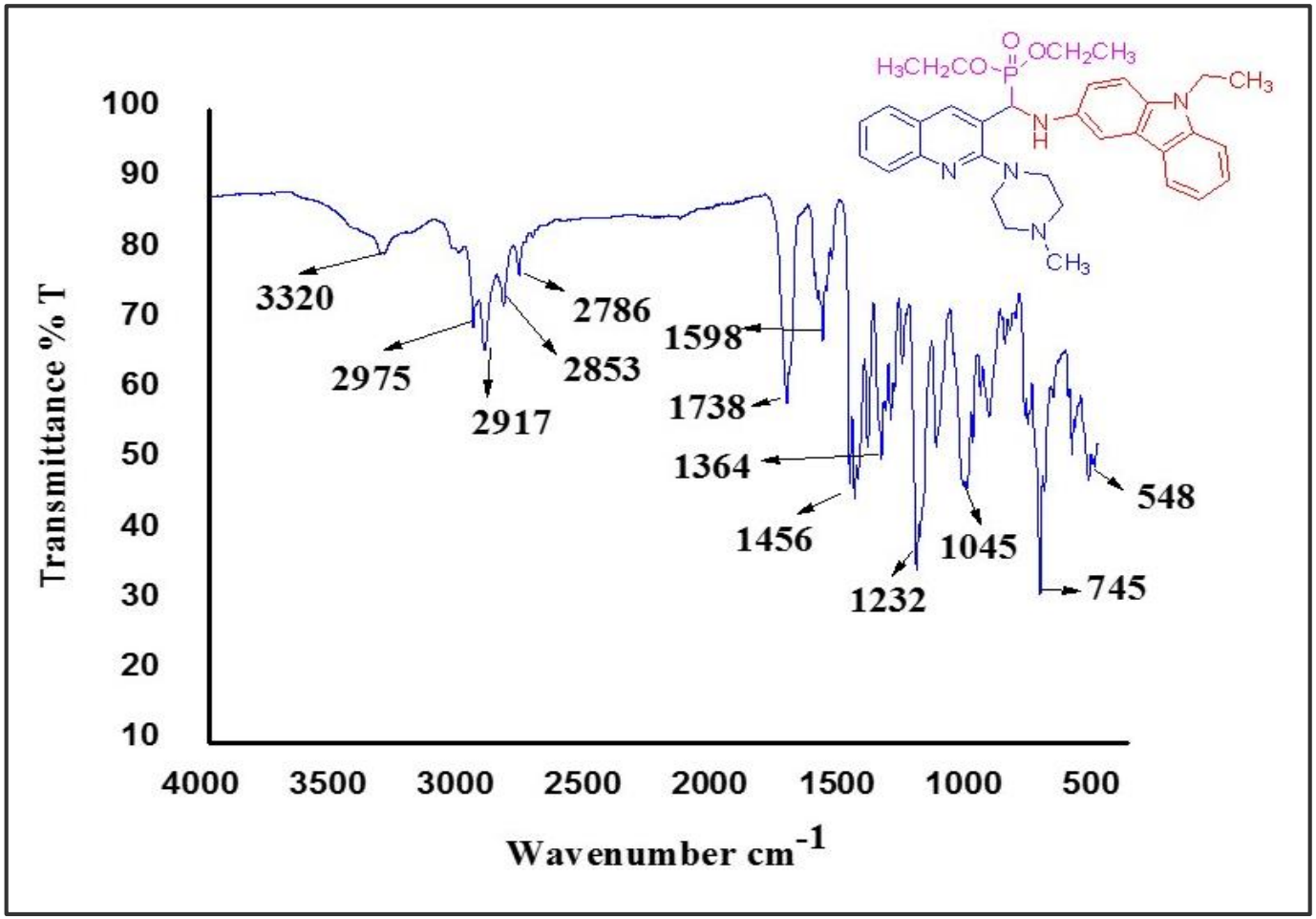

Figure S94: The ^{1}H NMR Spectrum of 4s, diethyl(((9-ethyl-9H-carbazol-3-yl)amino)(2-(4-methylpiperazin-1-yl)quinolin-3-yl)methyl)phosphonate

Appendix 94

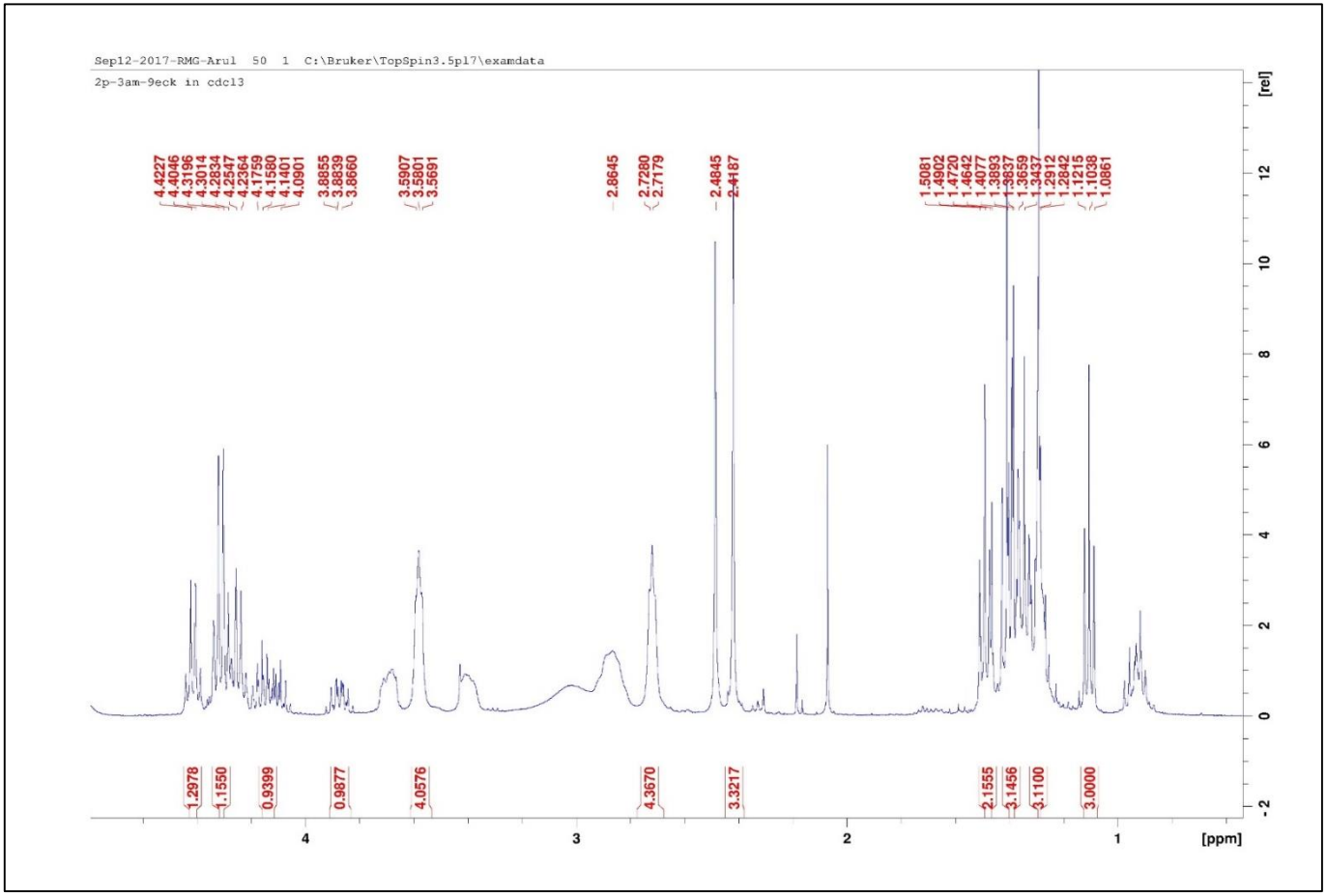

Figure S95: The ^{13}C NMR Spectrum of 4s, diethyl(((9-ethyl-9H-carbazol-3-yl)amino)(2-(4-methylpiperazin-1-yl)quinolin-3-yl)methyl)phosphonate

Appendix 95

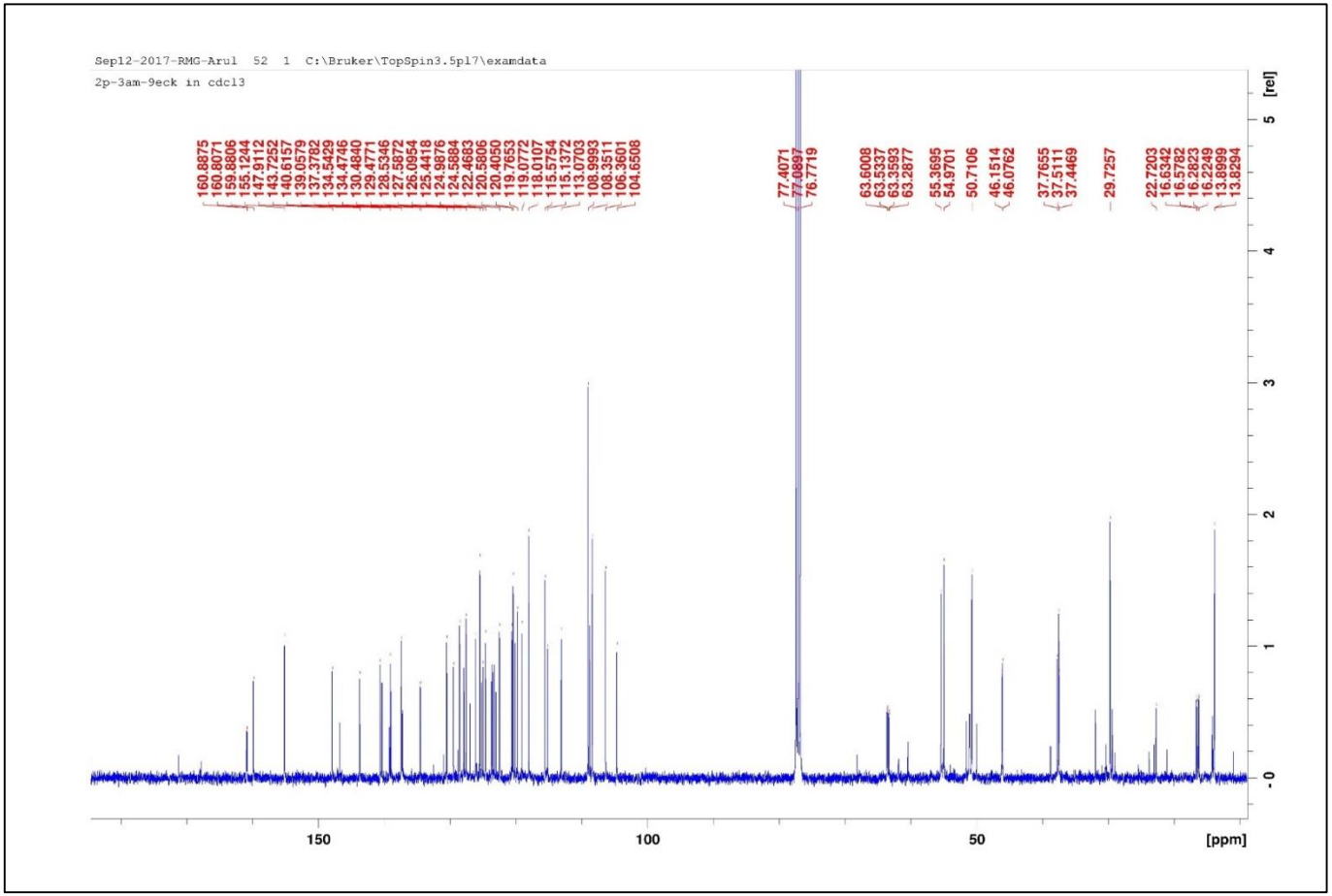

Figure S95: The ^{13}C NMR Spectrum of 4s, diethyl(((9-ethyl-9H-carbazol-3-yl)amino)(2-(4-methylpiperazin-1-yl)quinolin-3-yl)methyl)phosphonate

Appendix 96

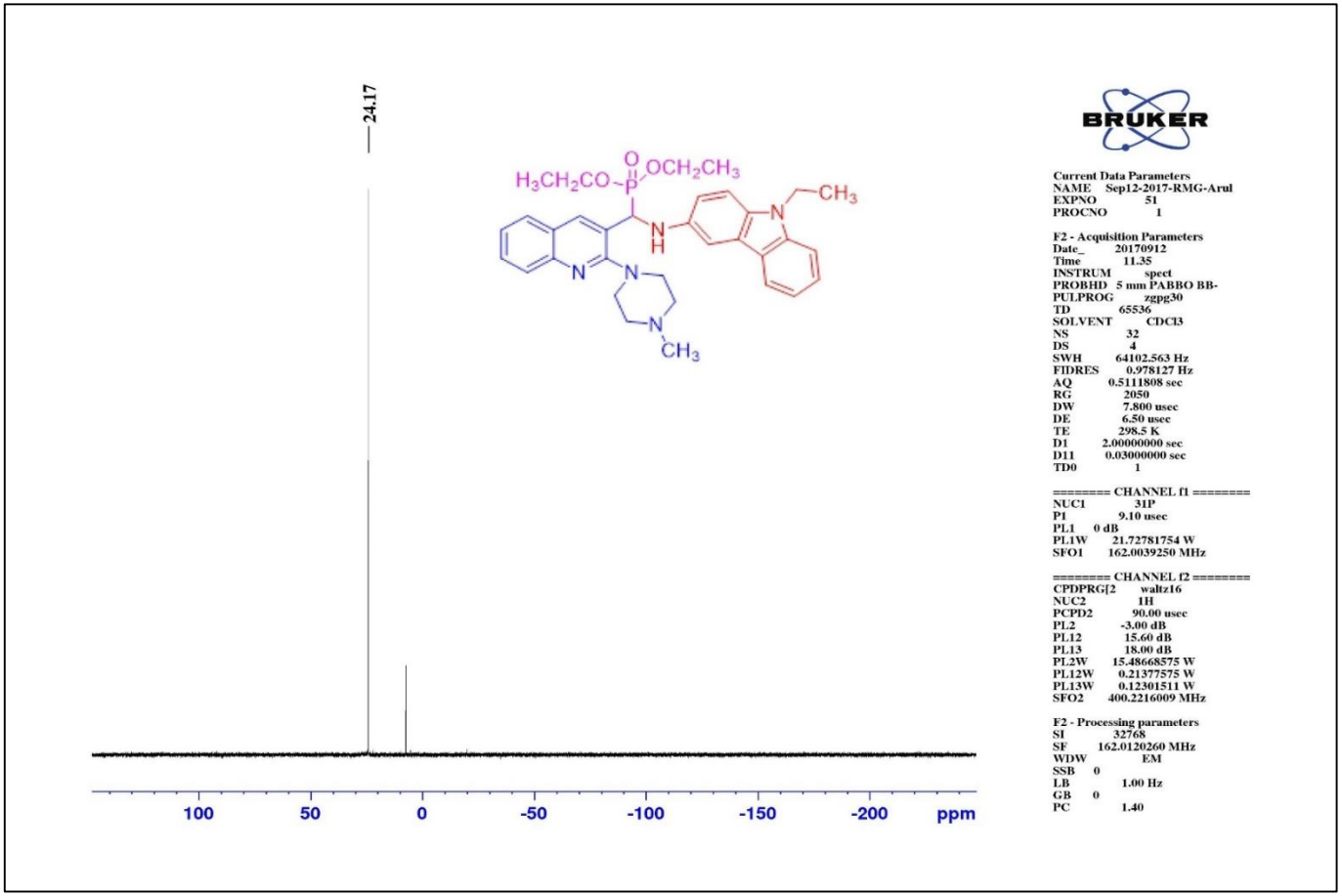

Figure S96: The ^{31}P NMR Spectrum of 4s, diethyl(((9-ethyl-9H-carbazol-3-yl)amino)(2-(4-methylpiperazin-1-yl)quinolin-3-yl)methyl)phosphonate

Appendix 97

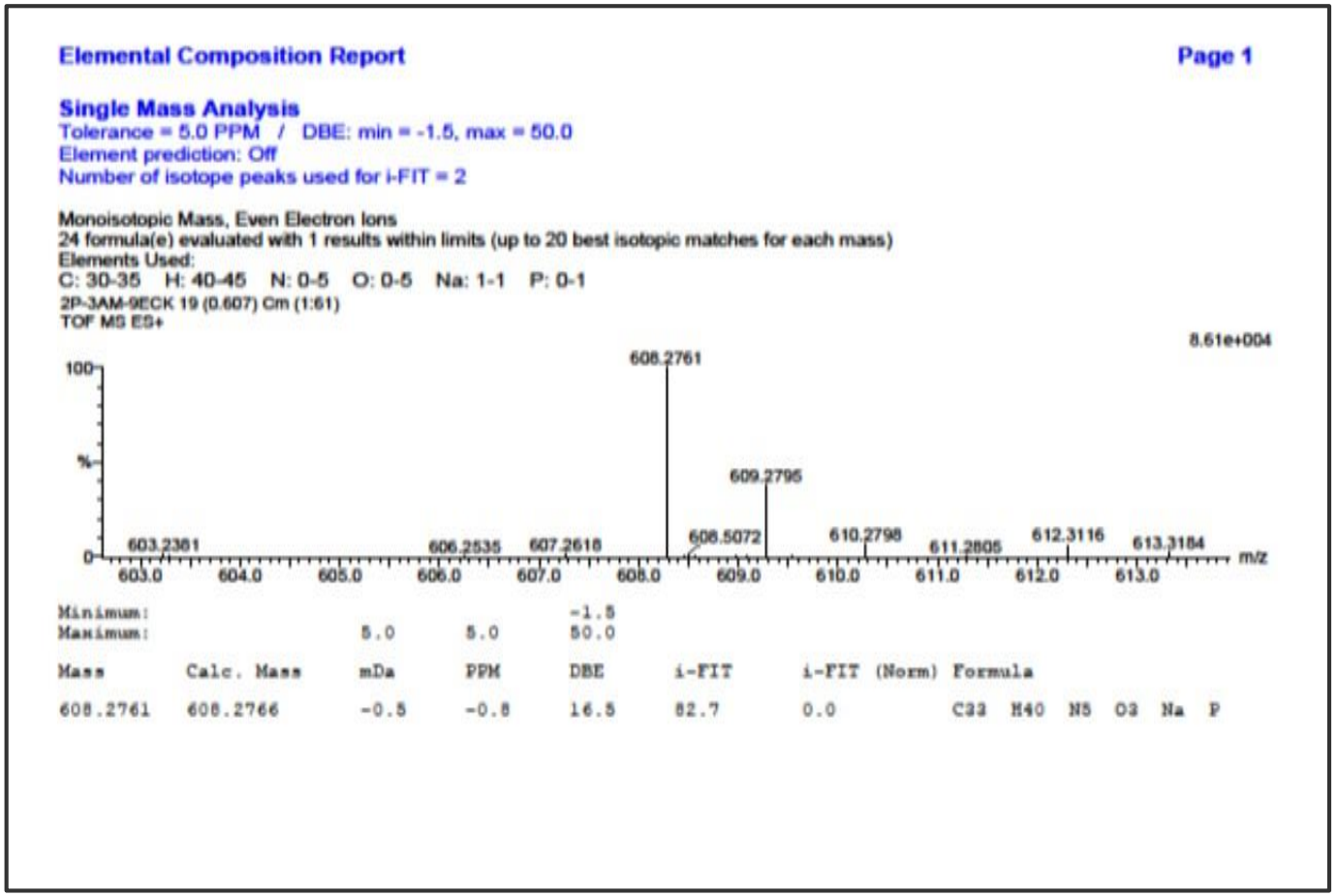

Figure S97: The HRMS Spectrum of 4s, diethyl(((9-ethyl-9H-carbazol-3-yl)amino)(2-(4-methylpiperazin-1-yl)quinolin-3-yl)methyl)phosphonate

Appendix 98

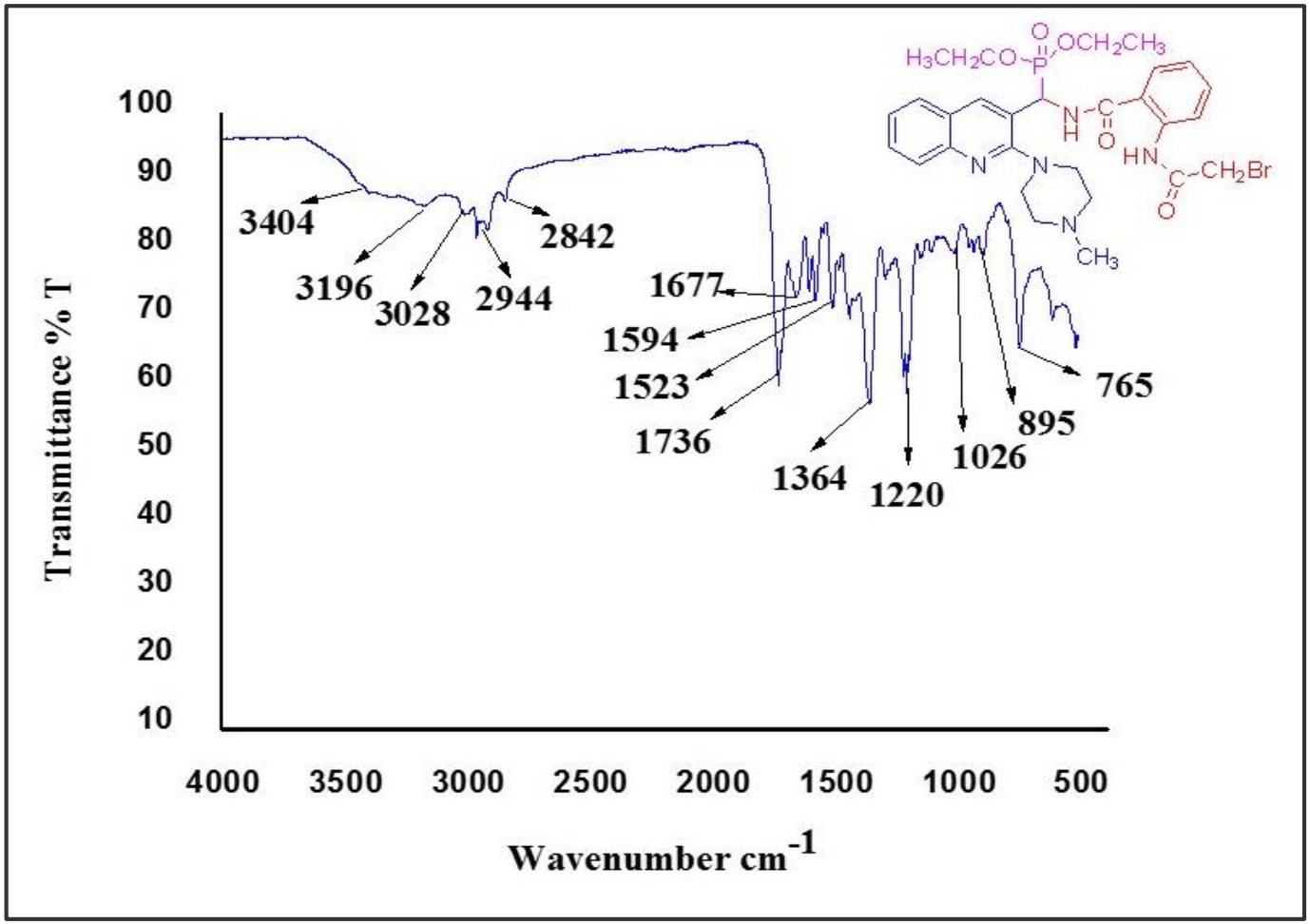

Figure S98: The IR Spectrum of 4t, diethyl((2-(2-bromoacetamido)benzamido)(2-(4-methylpiperazin-1-yl)quinolin-3-yl)methyl)phosphonate

Appendix 99

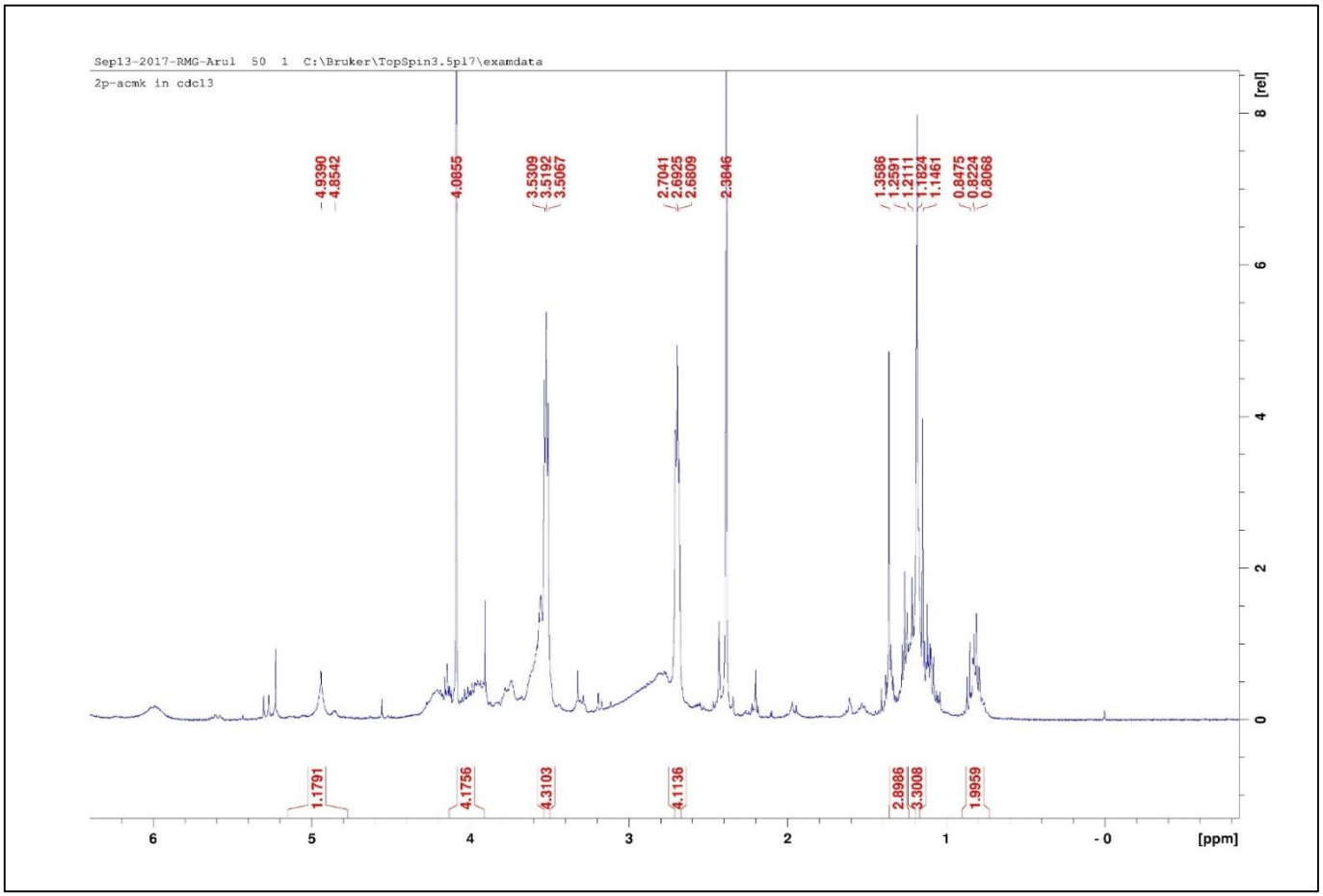

Figure S99: The ^{1}H NMR Spectrum of 4t, diethyl((2-(2-bromoacetamido)benzamido)(2-(4-methylpiperazin-1-yl)quinolin-3-yl)methyl)phosphonate

Appendix 100

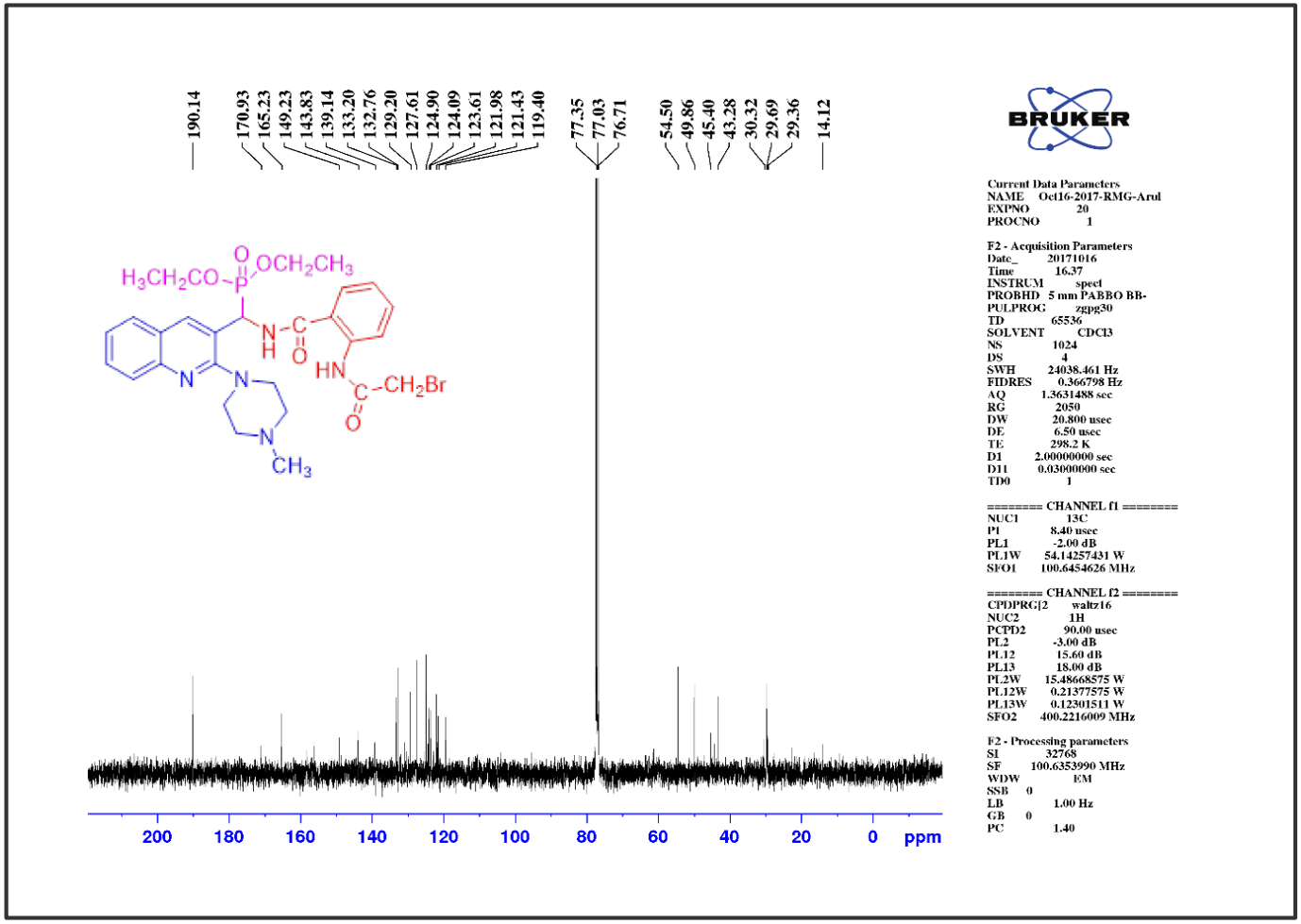

Figure S100: The ^{13}C NMR Spectrum of 4t, diethyl((2-(2-bromoacetamido)benzamido)(2-(4-methylpiperazin-1-yl)quinolin-3-yl)methyl)phosphonate

Appendix 101

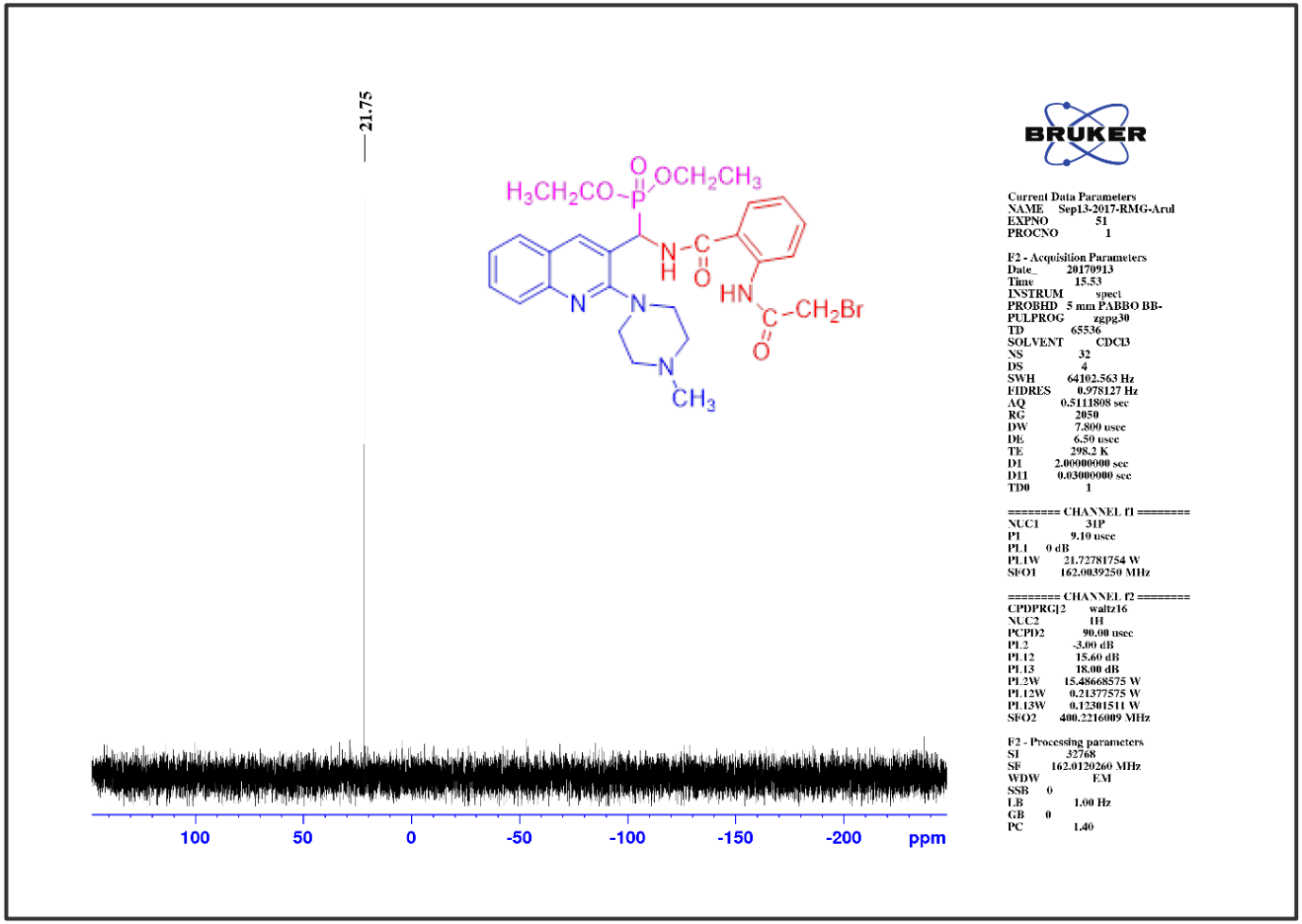

Figure S101: The ^{31}P NMR Spectrum of 4t, diethyl((2-(2-bromoacetamido)benzamido)(2-(4-methylpiperazin-1-yl)quinolin-3-yl)methyl)phosphonate

Appendix 102

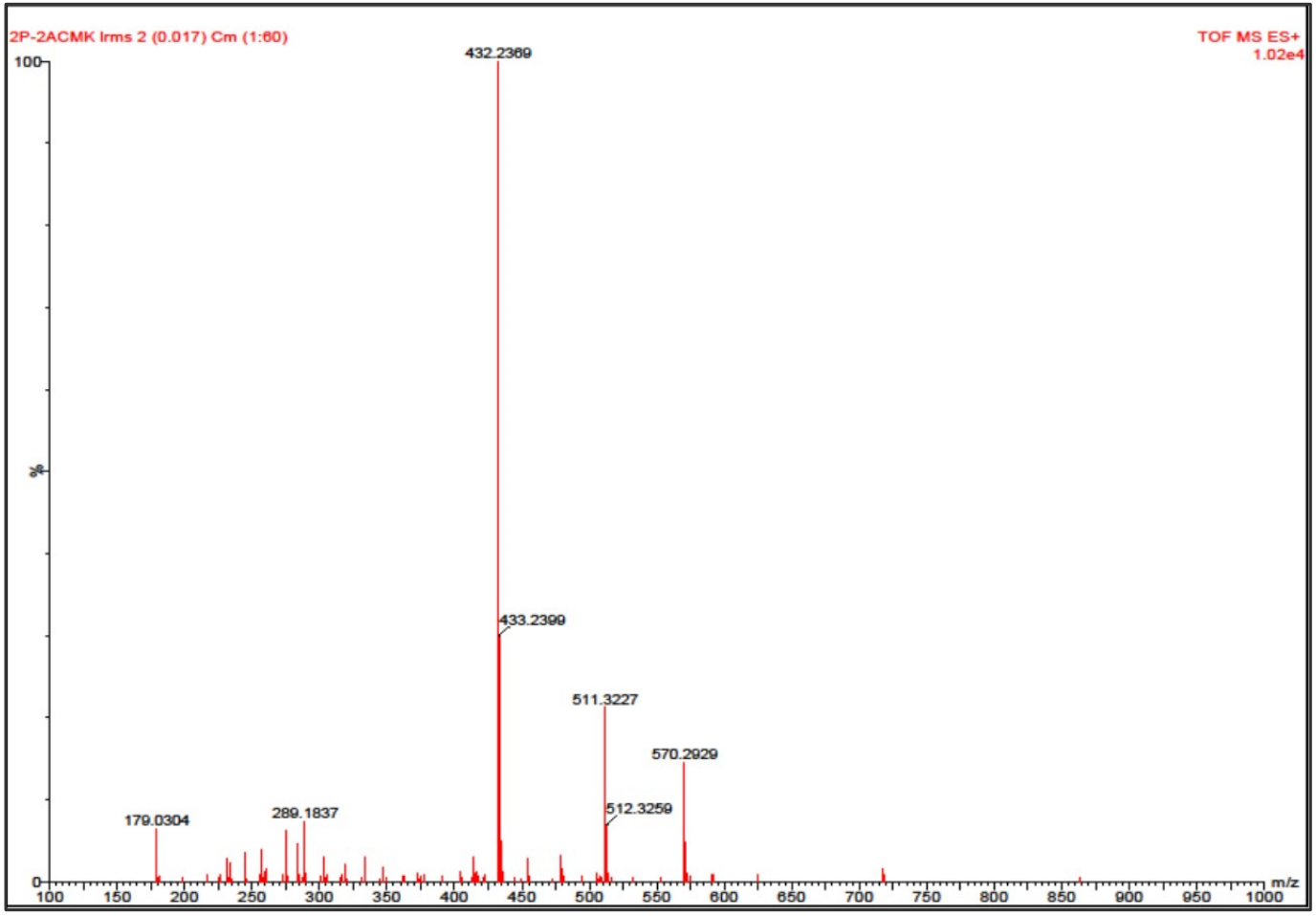

Figure S102: The HRMS Spectrum of 4t, diethyl((2-(2-bromoacetamido)benzamido)(2-(4-methylpiperazin-1-yl)quinolin-3-yl)methyl)phosphonate

Research Paper Submitted

Enhancing the effect of microwave irradiation with Pd-$SrTiO_3$ catalyst for the synthesis of methyl piperazinyl-quinolinyl α-aminophosphonates and their antibacterial and antioxidant activities

Nikisha Rajkoomar[1], Arul Murugesan[1]*, Samikannu Prabu[2], Robert M Gengan[1]*

[1]Department of Chemistry, Faculty of Applied Sciences, Durban University of Technology, Durban 4001, South Africa.

[2]Department of Chemistry, Chung-Yuan Christian University, Zhongli, 320, Taiwan, R.O.C.

*Corresponding author. Tel: (+27) 31 3732309; Fax: (+27) 866740441; E-mail: chemarul91@gmail.com; genganrm@dut.ac.za

Abstract

Novel methyl piperazinyl-quinolinyl α-aminophosphonates (MPQ-APs) (**4a-4t**) were synthesised by a one-pot reaction under microwave conditions, in the presence of a new Pd-$SrTiO_3$ catalyst. **4a-4t** were prepared from the substrates methyl piperazinyl-quinolinyl carbaldehyde, selected aniline derivatives and diethyl phosphite. MPQ-APs were characterized by FT-IR, ^{1}H-NMR, ^{13}C-NMR, 2D-NMR, ^{31}P-NMR and high resolution mass spectroscopy. The catalyst was prepared by a sequential reaction of Sr (II) nitrate, citric acid and Ti (IV) butoxide followed by reflux in the presence of Pd (II) nitrate. Pd-$SrTiO_3$ was characterized by FT-IR, P-XRD, SEM, BET, SEM-EDX and Raman spectroscopy techniques. The MPQ-APs were screened *in vitro* for antibacterial activity against 4 strains of bacteria and 3 yeast cultures. Compounds **4m** and **4**r showed good positive results for antimicrobial activity for some bacterial strains whilst **4m**, **4r** and **4f** gave positive results for antioxidant activity.

Keywords: Kabachnik Fields reaction; Palladium; 2D-NMR; Antibacterial; Antioxidant

1. Introduction

Since time immemorial, diseases that originated from pathogenic microorganisms was a leading cause of human death. However, in modern times, there has been a dramatic shift to non-microbial deaths such as cancer, diabetes, cardiac and kidney failure. Although there is an abundance of natural and synthetic medicinal drugs, these cannot completely eradicate some microorganisms. Furthermore, the development of resistance of the human body to drugs has resulted in its low efficacy. Hence the design and synthesis of new compounds that might act as better drugs, is an important research area of study for the well-being of humankind.

The heterocyclic ring is a biologically active scaffold [1-3] found in many organic compounds. The nitrogen and oxygen containing heterocycles are the most important because of their wide application as medicines. The α-aminophosphonates (α-APs), an important class of organophosphorus compounds, possess a reduced level of toxicity and has the ability to substitute natural amino acids [4]. They exhibit a wide range of biological properties such as enzyme [5] and HIV protease inhibitors [6], as peptide mimics [7] as well as anti-bacterial [8], anti-fungal [9], anti-oxidant [10] and anti-viral agents [11]. Among the number of synthetic approaches to α-APs, one of the most suitable method is the Kabachnik Fields reaction.

This involves a one-pot three-component condensation of a primary or secondary amine, aldehyde or ketone and a diethyl phosphate in the presence of an acid or base catalyst [12]. Catalysts such as $CdCl_2$ [13], Cd $(ClO_4)_2.xH_2O$ [14], $Zr4^+$ [15], In $(OTF)_3$ [16], $TaCl_5$-SiO_2 [17], L-lactic acid [18], and montmorillonite clay [19] were reported. Some of these catalysts are inefficient because of their low activation in reaction mixtures. In addition, the use of hazardous solvents, long reaction times and the low yield of products has encouraged the search for better catalysts for the synthesis of novel α-APs that possess functional groups that might improve their biological activity.

In this current work, a new material, viz., Pd-$SrTiO_3$ catalyst was prepared, characterised and subsequently used in the Kabachnik Fields reaction to produce a new series of methyl piperazinyl-quinolinyl α-aminophosphonates. The synthesized compounds were also evaluated for their antimicrobial and antioxidant activities.

2. Experimental

2.1. Material and Methods

All chemicals were purchased from Merck and Sigma Aldrich. Both monitoring of the reaction and product purity was accomplished using TLC. The FTIR spectra was documented within the range of 4000-400 cm^{-1} using KBr pellets on a JASCO FT/IR-460 spectrophotometer. A Bruker D2 PHASER powder diffraction instrument; Cu Kα ray (wavelength λ = 0.154056 nm), was used to measure in a continuous step-scan mode: the minimum width of the stage 0.031°, equilibrium time of 256 seconds, the operating voltage to 30 kV with 10 mA. Characterization of the morphology was employed by scanning electron microscopy (SEM, Joel JSM 7600F). The Micromeritics Auto pore 9500 system was used for the BET gas sorption isotherms, measured at 77 K for N_2 and H_2, and 273 and 298 K for CO_2. The sample was dehydrated to begin with at 423 K for 24 h under vacuum before gas sorption measurements were recorded.
The detector CCD (Triaxle) and the laser (He-Ne laser 632.8 nm) was used in the measurement of Raman Spectroscopy. All NMR spectra were recorded in a Bruker Avance 400 MHz instrument. Accurate (HRMS) was attained using a TOF-MS analyser. A Buchi B-545 apparatus was used to record melting points (m.p) along with open capillary tubes.

2.2. Preparation of $SrTiO_3$

An aliquot of Sr $(NO_3)_2$ (2.12 g) and citric acid (2.10 g) was dissolved in 40 ml of H_2O. Thereafter, Titanium (IV) butoxide (TBT) (3.4g), dissolved in 20 ml of ethanol, was added and the mixture stirred for 24 h at 70˚C. The solid was washed with water, and air- dried to produce solid $SrTiO_3$.

2.3. Preparation of Catalyst Pd-$SrTiO_3$

2g of $SrTiO_3$ and 0.12 g of metal source powders ($PdCl_2$) was transferred to a beaker and heated with water for 12h at 80˚C. Thereafter the solid was transferred into a furnace set at 1000 ˚C for 2h. An aliquot of 10 ml ethanol was added to the material, it was then filtered, washed again with acetone and water. The solid was air-dried to produce Pd-$SrTiO_3$.

2.4. General experimental procedures

2-(4-methylpiperazin-1-yl) quinoline-3-carbaldehyde (**3**), used as a starting material, was synthesized using 2-chloro-3-formyl quinoline (0.001 mol) and potassium carbonate (0.002

mol). Thereafter an excess amount of 1-methylpiperazine was added and the mixture refluxed at 200 °C for 24 h [20-22].

The metal doping Pd-$SrTiO_3$ catalyst (0.05g) (see preparation method in supplementary file) was activated at 100 °C under vacuum followed by cooling to room temperature before adding it to 2-(4-methylpiperazin-1-yl) quinoline-3-carbaldehyde (1.0 mmol), diethyl phosphite (1.0 mmol), and aniline derivatives (1.0 mmol). This mixture was refluxed in THF under microwave conditions at 140 °C: these conditions are associated with a suitable reaction time as shown in **Table 3**.

The course of the reaction was monitored using TLC. Once the reaction reached completion, ethanol was used to dissolve the mixture as a way to separate the catalyst. The crude product was cooled, filtered and purified by column chromatography using silica gel and a mobile phase of acetone: hexane (80:20). The catalyst was then washed with a dilute acid solution, distilled water and finally with acetone. The catalyst was dried under vacuum and re-used.

The spectral data (^{1}H-NMR, ^{13}C-NMR, MS, elemental analysis and FT-IR) of **4b-4t** are presented in supplementary file. The synthesis of diethyl((2-(4-methylpiperazin-1-yl)quinolin-3-yl)(phenylamino)methyl)phosphonate derivatives (4b-4t):

2.4.1. diethyl((2-(4-methylpiperazin-1-yl)quinolin-3-yl)(phenylamino)methyl)phosphonate (4a)

Yellow colour solid: FT-IR (KBr): 3320, 3058, 2940, 2842, 2789, 1588, 1426, 1368, 1285, 1243, 1137, 1010, 947, 742, 694, 576, 529 cm^{-1}. ^{1}H-NMR ($CDCl_3$, 400 MHz): δ 8.74 (1H, s, N-H), 8.68 (1H, s, Ar-H), 8.44 (1H, d, J = 2.72 Hz, Ar-H), 7.88 (1H, d, J = 8.44 Hz, Ar-H), 7.82 (1H, d, J = 8 Hz, Ar-H), 7.64-7.68 (1H, m, Ar-H), 7.44-7.48 (1H, t, J = 7.48 Hz, Ar-H), 7.38-7.40 (1H, m, J = 2.52 Hz, Ar-H), 7.08-7.12 (1H, dd, J = 0.84 Hz, Ar-H), 6.81 (1H, d, J = 7.96 Hz, Ar-H), 6.66-6.70 (1H, dd, J = 2.5 Hz, Ar-H), 5.29-5.37 (1H, d, CH), 4.83-4.07 (1H, t, CH_2), 4.24-4.28 (1H, t, CH_2), 4.02-4.06 (1H, m, CH_2), 3.77-3.84 (1H, m, CH_2), 3.51-3.54 (4H, t, CH_2), 2.66-2.69 (4H, t, CH_2), 2.46 (3H, s, CH_3), 1.34-1.38 (3H, t, CH_3), 1.04-1.08 (3H, t, CH_3). ^{13}C-NMR ($CDCl_3$, 100 MHz): δ 160.64, 160.56, 159.85, 157.79, 151.87, 146.12, 146.75, 145.97, 145.85, 137.92, 129.36, 128.58, 127.60, 126.40, 124.64, 122.73, 121.03, 118.54, 113.81, 63.49, 63.44, 63.37, 54.95, 50.79, 50.05, 48.51, 46.11, 16.57, 16.52, 16.22, 16.16. ^{31}P-NMR ($CDCl_3$, 400 MHz): δ 23.76 TOFMS ES *m/z* (rel. int.): 469.23 $[M]^+$. Anal. Calc. for $C_{25}H_{33}N_4O_3P$: C, 64.09; H, 7.10; N, 11.96 %. Found: C, 64.11; H, 7.12; N, 11.98 %.

2.4.2. diethyl((2-(4-methylpiperazin-1-yl)quinolin-3-yl)((2

nitrophenyl)amino)methyl)phosphonate(4b)

Yellow colour solid: FT-IR (KBr): 3471, 3378, 3190, 2982, 2839, 1736, 1625, 1503, 1427, 1343, 1239, 1014, 745 cm^{-1}. ^{1}H-NMR ($CDCl_3$, 400 MHz): δ 8.38 (1H, s, Ar-H), 7.98-8.01 (1H, dd, *J* = 1.2 Hz, Ar-H), 7.73 (1H, d, *J* = 8.48 Hz, Ar-H), 7.70 (1H, d, *J* = 8.04 Hz, Ar-H), 7.60 (1H, t, *J* = 8.24 Hz, Ar-H), 7.27 (1H, t, *J* = 7.36 Hz, Ar-H), 6.70 (2H, t, *J* = 0.76 Hz, Ar-H), 6.56-6.59 (1H, dd, *J* = 0.88 Hz, Ar-H), 6.10 (1H, s, C-H), 5.3 (1H, d, *J* = 12.48 Hz, N-H), 4.12-4.15 (2H, m, CH_2), 3.89-4.01 (2H, m, CH_2), 3.44 (4H, t, CH_2), 2.56 (4H, t, CH_2), 2.28 (3H, s, CH_3), 1.25 (3H, t, CH_3), 1.11 (3H, t, CH_3). ^{13}C-NMR ($CDCl_3$, 100 MHz): δ 160.37, 160.30, 158.91, 149.30, 144.02, 142.50, 135.60, 132.51, 129.25, 127.52, 126.14, 124.66, 124.01, 122.06, 118.77, 116.80, 63.28, 63.21, 63.97, 63, 58.09, 54.88, 51.14, 50.85, 46.03, 29.68, 29.35, 16.59, 16.81, 16.41, 16.36. ^{31}P-NMR ($CDCl_3$, 400 MHz): δ 21.95 TOFMS ES *m/z* (rel. int.): 513.21 $[M]^+$. Anal. Calc. for $C_{25}H_{22}N_5O_5P$: C, 58.47; H, 6.28; N, 13.64 %. Found: C, 58.49; H, 6.30; N, 13.66 %.

2.4.3. diethyl((2-(4-methylpiperazin-1-yl)quinolin-3-yl)((3

nitrophenyl)amino)methyl)phosphonate (4c)

Yellow colour solid: FT-IR (KBr): 3406, 2937, 2844, 2794, 1549, 1521, 1420, 1349, 1139, 1008, 961, 733, 676 cm^{-1}. ^{1}H-NMR ($CDCl_3$, 400 MHz): δ 8.75 (1H, s, N-H), 8.70 (1H, s, Ar-H), 8.13-8.15 (1H, dd, *J* = 1.64 Hz, Ar-H), 8.09 (1H, s, Ar-H), 7.90 (1H, d, *J* = 8.52 Hz, Ar-H), 7.84 (1H, d, *J* = 0.76 Hz, Ar-H), 7.67-7.71 (1H, m, Ar-H), 7.58-7.62 (1H, q, *J* = 1.56 Hz, Ar-H), 7.49 (1H, t, *J* = 2.28 Hz, Ar-H), 7.40-7.44 (1H, q, *J* = 0.8 Hz, Ar-H), 6.95 (1H, d, C-H), 4.02 (4H, s, CH_2), 3.51 (4H, t, CH_2), 2.68 (4H, t, CH_2), 2.40 (3H, s, CH_3), 1.37 (3H, t, CH_3), 1.23 (3H, t, CH_3). ^{13}C-NMR ($CDCl_3$, 100 MHz): δ 160.32, 160.05, 158.84, 149.25, 146.65, 146.63, 142.52, 138.74, 138.69, 132.48, 129.22, 127.85, 125.82, 124.63, 123.48, 122.02, 122.51, 110.87, 65.56, 63.18, 63.10, 63.07, 63, 54.80, 50.74, 45.96, 45.85, 34.46, 44.21, 30.32, 29.66, 16.55, 16.49, 16.39, 16.34. ^{31}P-NMR ($CDCl_3$, 400 MHz): δ 23.04 Anal. Calc. for $C_{25}H_{32}N_5O_5P$: C, 58.47; H, 6.28; N, 13.64 %. Found: C, 58.48; H, 6.30; N, 13.67 %.

2.4.4. diethyl(((2-fluorophenyl)amino)(2-(4-methylpiperazin-1-yl)quinolin-3 yl)methyl)phosphonate (4d)

Yellow colour solid: FT-IR (KBr): 3055, 2934, 2849, 2788, 1691, 1588, 1495, 1419, 1372, 1241, 1144, 1008, 950, 745, 622 cm^{-1}. ^{1}H-NMR ($CDCl_3$, 400 MHz): δ 8.70 (1H, s, N-H), 8.61 (1H, s, Ar-H), 7.88 (1H, d, *J* = 8.44 Hz, Ar-H), 7.82 (1H, d, *J* = 7.96 Hz, Ar-H), 7.68-7.69 (1H, m, Ar-H), 7.42 (1H, t, *J* = 6.8 Hz, Ar-H), 7.36-7.38 (2H, dd, *J* = 8 Hz, Ar-H), 7.10-7.12 (2H, dd, *J* = 6 Hz, Ar-H), 6.51 (1H, s, C-H), 4.23-4.27 (2H, q, CH_2), 4.12 (1H, t, CH_2), 4.10 (1H, d, CH_2), 3.50 (4H, t, CH_2), 2.66 (4H, t, CH_2), 2.46 (3H, s, CH_3), 1.37 (3H, t, CH_3), 1.23 (3H, t, CH_3). ^{13}C-NMR ($CDCl_3$, 100 MHz): δ 160.37, 160.30, 158.91, 149.30, 146.67, 144.82, 142.50 138.53, 135.60, 132.51, 132.17, 129.80, 129.25, 127.99, 127.83, 127.59, 127.52, 126.14, 125.88, 125.30, 125.29, 124.66, 124.01, 122.06, 118.77, 116.80, 63.28, 63.21, 63.07, 63, 55.18, 55.09, 54.88, 53.94, 51.14, 50.85, 55.27, 46.04, 45.98, 29.68, 29.35, 16.57, 16.51, 16.41, 16.36. ^{19}F-NMR ($CDCl_3$, 400 MHz): δ -127.26. ^{31}P-NMR ($CDCl_3$, 400 MHz): δ 23.13, 21.76 Anal. Calc. for $C_{25}H_{32}FN_4O_3P$: C, 61.72; H, 6.63; N, 11.52 %. Found: C, 61.75; H, 6.62; N, 11.50 %.

2.4.5. diethyl(((3-fluorophenyl)amino)(2-(4-methylpiperazin-1-yl)quinolin-3 yl)methyl)phosphonate (4e)

Yellow colour solid: FT-IR (KBr): 3458, 2974, 2947, 2844, 2797, 1737, 1579, 1419, 1373, 1230, 1138, 951, 877, 788, 755, 685, 624 cm^{-1}. ^{1}H-NMR ($CDCl_3$, 400 MHz): δ 8.72 (1H, s, N-H), 8.64 (1H, s, Ar-H), 7.88 (1H, d, *J* = 8.44 Hz, Ar-H), 7.81 (1H, d, *J* = 7.96 Hz, Ar-H), 7.62-7.64 (1H, m, Ar-H), 7.39 (2H, t, *J* = 7.64 Hz, Ar-H), 7.05 (1H, d, *J* = 7.48 Hz, Ar-H), 7 (2H, t, *J* = 9.44 Hz, Ar-H), 5.35 (1H, d, C-H), 4.23-4.27 (2H, q, CH_2), 4.03-4.08 (1H, q, CH_2), 3.78 (1H, t, CH_2), 3.50 (4H, t, CH_2), 2.68 (4H, t, CH_2), 2.40 (3H, s, CH_3), 1.42 (3H, t, CH_3), 1.24 (3H, t, CH_3). ^{13}C-NMR ($CDCl_3$, 100 MHz): δ 160.32, 160.25, 158.84, 149.25, 146.65, 146.63, 142.52, 138.74, 138.69, 132.48, 129.79, 129.22, 127.85, 127.64, 127.49, 125.82, 125.29, 124.63, 123.98, 122.02, 120.99, 112.37, 67.20, 65.56, 63.18, 63.10, 63.07, 63, 54.80, 50.74, 45.96, 45.85, 30.32, 29.66, 29.43, 16.55, 16.49, 16.39, 16.34. ^{19}F-NMR ($CDCl_3$, 400 MHz): δ -112.13. ^{31}P-NMR ($CDCl_3$, 400 MHz): δ 23.37, 21.87. TOFMS ES *m/z* (rel. int.): 487.22 $[M]^+$. Anal. Calc. for $C_{25}H_{32}FN_4O_3P$: C, 61.72; H, 6.63; N, 11.52 %. Found: C, 61.74; H, 6.65; N, 11.55 %.

2.4.6. diethyl(((4-fluorophenyl)amino)(2-(4-methylpiperazin-1-yl)quinolin-3 yl)methyl)phosphonate (4f)

Yellow colour solid: FT-IR (KBr): 3378, 2975, 2853, 2394, 1748, 1643, 1504, 1428, 1210, 1129, 939, 810, 765 cm^{-1}. ^{1}H-NMR ($DMSOd_6$, 400 MHz): δ 8.19 (1H, s, Ar-H), 7.94 (1H, d, N-H), 7.76-7.78 (1H, t, *J* = 3.2 Hz, Ar-H), 7.46-7.52 (1H, t, *J* = 7.72 Hz, Ar-H), 7.40 (1H, d, *J* = 7.24 Hz, Ar-H), 7.25 (1H, d, *J* = 8.12 Hz, Ar-H), 7.08-7.11 (1H, t, *J* = 7.4 Hz, Ar-H), 6.80-6.89 (2H, dd, *J* = 8.56 Hz, Ar-H), 6.61 (1H, d, *J* = 4.4 Hz, Ar-H), 5.90 (1H, s, C-H), 5.01 (1H, d, CH_2), 3.76-3.80 (1H, m, CH_2), 3.40-3.44 (2H, t, CH_2), 3.29 (4H, d, CH_2), 2.84 (4H, d, CH_2), 2.61 (3H, s, CH_3), 1.13-1.17 (3H, t, CH_3), 1.02-1.06 (3H, m, CH_3). ^{13}C-NMR ($DMSOd_6$, 100 MHz): δ 161.77, 158.83, 158.76, 158.52, 155.71, 153.41, 145.15, 144.88, 144.22, 144.08, 137.87, 136.36, 135.47, 131.97, 129.61, 129.15, 127.38, 127.05, 125.42, 124.79, 123.20, 123.11, 121.79, 119.36, 114.84-115.23, 112.92-113.48, 62.03, 56, 52.43, 49.66, 48.44, 46.89, 42.99, 42.25, 28.92, 25.37, 18.45. ^{19}F-NMR ($DMSOd_6$, 400 MHz): δ -129.13, -128.89. ^{31}P-NMR ($DMSOd_6$, 400 MHz): δ 15.95. Anal. Calc. for $C_{25}H_{32}FN_4O_3P$: C, 61.72; H, 6.63; N, 11.52 %. Found: C, 61.75; H, 6.65; N, 11.55 %.

2.4.7. diethyl(((4-chlorophenyl)amino)(2-(4-methylpiperazin-1-yl)quinolin-3 yl)methyl)phosphonate (4g)

Yellow colour solid: FT-IR (KBr): 3059, 2933, 2984, 2849, 2792, 1736, 1597, 1424, 1373, 1220, 1148, 1018, 998, 949, 858, 736, 534 cm^{-1}. ^{1}H-NMR ($CDCl_3$, 400 MHz): δ 8.72 (1H, s, N-H), 8.62 (1H, s, Ar-H), 7.87 (1H, d, *J* = 8.4 Hz, Ar-H), 7.82 (1H, d, *J* = 7.92 Hz, Ar-H), 7.74 (1H, t, *J* = 8.5 Hz, Ar-H), 7.65-7.69 (1H, m, Ar-H), 7.40-7.42 (2H, dd, *J* = 1.96 Hz, Ar-H), 7.19-7.21 (2H, dd, *J* = 1.92 Hz, Ar-H), 6.61 (1H, d, C-H), 4.22 (1H, t, CH_2), 3.95 (3H, t, CH_2), 3.62 (4H, s, CH_2), 2.87 (4H, d, CH_2), 2.59 (3H, d, CH_3), 1.20-1.36 (6H, m, CH_3). ^{13}C-NMR ($CDCl_3$, 100 MHz): δ 159.22, 157.85, 150.22, 148.03, 138.43, 132.78, 132.09, 131.06, 129.49, 129.18, 129.09, 129, 128,.60, 127.99, 127.65, 125.06, 124.96, 122.34, 122.31, 121.97, 116.21, 114.87, 63.07, 54.41, 54.17, 54.02, 49.85, 45.39, 29.69, 29.35, 16.52, 16.36. ^{31}P-NMR ($CDCl_3$, 400 MHz): δ 23.27 TOFMS ES *m/z* (rel. int.): 503.19 $[M]^+$. Anal. Calc. for $C_{25}H_{32}ClN_4O_3P$: C, 59.70; H, 6.41; N, 11.14 %. Found: C, 59.72; H, 6.43; N, 11.16 %.

2.4.8. diethyl(((3,4-dichlorophenyl)amino)(2-(4-methylpiperazin-1-yl)quinolin-3 yl)methyl)phosphonate (4h)

Yellow colour solid: FT-IR (KBr): 3421, 3067, 2984, 2941, 2843, 2800, 1598, 1417, 1373, 1240, 1134, 1003, 858, 734, 685, 594 cm^{-1}. ^{1}H-NMR ($CDCl_3$, 400 MHz): δ 8.70 (1H, s, N-H), 8.61 (1H, s, Ar-H), 7.88 (1H, d, *J* = 8.48 Hz, Ar-H), 7.82 (1H, d, *J* = 8.04 Hz, Ar-H), 7.65-7.69 (1H, m, Ar-H), 7.51 (1H, d, *J* = 8.52 Hz, Ar-H), 7.38-7.42 (1H, m, Ar-H), 7.16 (1H, d, *J* = 2.32 Hz, Ar-H), 7.12 (1H, d, *J* = 2.48 Hz, Ar-H), 7.10 (1H, d, *J* = 2.48 Hz, C-H), 4.23-4.27 (2H, q, CH_2), 4.10-4.14 (1H, q, CH_2), 3.98-4 (1H, q, CH_2), 3.49 (4H, t, CH_2), 2.66 (4H, t, CH_2), 2.40 (3H, s, CH_3), 1.37 (3H, t, CH_3), 1.23 (3H, t, CH_3). ^{13}C-NMR ($CDCl_3$, 100 MHz): δ 160.77, 160.69, 159.88, 151.90, 148.09, 146.39, 139.19, 137.39, 137.35, 130.72, 129.19, 128.57, 127.58, 127.17, 125.04, 124.61, 122.80, 122.04, 119.41, 117.79, 115.91, 114.20, 112.25, 111.27, 63.52, 63.46, 63.39, 55.42, 54.98, 51.17, 50.95, 50.54, 48.39, 46.15, 21.49, 16.59, 16.54, 16.23, 16.17. ^{31}P-NMR ($CDCl_3$, 400 MHz): δ 21.81 Anal. Calc. for $C_{25}H_{32}Cl_2N_4O_3P$: C, 55.87; H, 5.81; N, 10.43 %. Found: C, 55.89; H, 5.83; N, 10.45 %.

2.4.9. diethyl(((4-bromophenyl)amino)(2-(4-methylpiperazin-1-yl)quinolin-3 yl)methyl)phosphonate (4i)

Yellow colour solid: FT-IR (KBr): 3411, 3055, 2973, 2941, 2843, 2796, 1596, 1482, 1423, 1372, 1242, 1148, 1064, 998, 948, 733, 539 cm^{-1}. ^{1}H-NMR ($CDCl_3$, 400 MHz): δ 8.72 (1H, s, N-H), 8.62 (1H, s, Ar-H), 7.87 (1H, d, *J* = 8.4 Hz, Ar-H), 7.82 (1H, d, *J* = 7.92 Hz, Ar-H), 7.74 (1H, t, *J* = 8.8 Hz, Ar-H), 7.65-7.69 (1H, m, Ar-H), 7.40-7.42 (2H, dd, *J* = 2.16 Hz, Ar-H), 7.19-7.21 (2H, dd, *J* = 1.96 Hz, Ar-H), 6.61 (1H, d, *J* = 8.8 Hz, C-H), 4.22 (1H, t, CH_2), 4.07 (1H, t, CH_2), 3.95 (2H, t, CH_2), 3.62 (4H, s, CH_2), 2.87 (4H, d, CH_2), 2.53 (3H, s, CH_3), 1.34 (3H, t, CH_3), 1.21 (3H, t, CH_3). ^{13}C-NMR ($CDCl_3$, 100 MHz): δ 160.09, 160.01, 157.94, 156.74, 146.53, 145.17, 138.93, 138.87, 138.63, 137.32, 129.63, 129.49, 127.68, 127.49, 125.82, 125.79, 125.05, 125, 113.82, 112.08, 109.78, 108.87, 63.16, 63.07, 63.06, 59.62, 54.93, 54.52, 50.15, 45.30, 30.29, 16.35, 16.48, 16.43,16.36, 16.31. ^{31}P-NMR ($CDCl_3$, 400 MHz): δ 21.76 Anal. Calc. for $C_{25}H_{32}BrN_4O_3P$: C, 54.85; H, 5.89; N, 10.23 %. Found: C, 54.87; H, 5.91; N, 10.25 %.

2.4.10. diethyl ((2-(4-methylpiperazin-1-yl)quinolin-3-yl)(o-tolylamino)methyl)phosphonate (4j)

Yellow colour solid: FT-IR (KBr): 3415, 2975, 2928, 2863, 1735, 1606, 1513, 1457, 1420, 1364, 1045, 943, 743, 567 cm^{-1}. ^{1}H-NMR ($CDCl_3$, 400 MHz): δ 8.34 (1H, s, Ar-H), 7.80 (1H, d, J = 8.44 Hz, Ar-H), 7.63 (1H, d, J = 8.04 Hz, Ar-H), 7.48 (1H, t, J = 7.72 Hz, Ar-H), 7.27 (1H, t, J = 7.32 Hz, Ar-H), 6.89 (2H, t, J = 7.32 Hz, Ar-H), 6.82 (1H, d, J = 7.11 Hz, Ar-H), 6.53 (1H, t, J = 7.44 Hz, Ar-H), 5.27 (1H, d, N-H), 4.65 (1H, t, C-H), 4.12-4.18 (2H, m, CH_2), 3.96 (1H, t, CH_2), 3.70-3.74 (1H, m, CH_2), 3.49 (2H, q, CH_2), 3.18 (2H, t, CH_2), 2.63 (4H, q, CH_2), 2.32 (3H, s, CH_3), 2.13 (3H, s, CH_3), 1.26 (3H, t, CH_3), 0.95 (3H, t, CH_3). ^{13}C-NMR ($CDCl_3$, 100 MHz): δ 160.69, 160.61, 146.81, 144.08, 143.95, 137.27, 137.22, 130.24, 129.57, 127.91, 127.54, 126.90, 125.07, 122.76, 118.29, 114.91, 111.49, 63.54, 63.49, 63.47, 63.43, 55.33, 51.07, 50.15, 48.61, 46.19, 29.71, 17.62, 16.60, 16.54, 16.24, 16.18. ^{31}P-NMR ($CDCl_3$, 400 MHz): δ 23.96 TOFMS ES *m/z* (rel. int.): 511.31 $[M]^+$. Anal. Calc. for $C_{26}H_{35}N_4O_3P$: C, 64.71; H, 7.31; N, 11.61 %. Found: C, 64.73; H, 7.32; N, 11.63 %.

2.4.11. diethyl ((2-(4-methylpiperazin-1-yl)quinolin-3-yl)(m-tolylamino)methyl)phosphonate (4k).

Yellow colour solid: FT-IR (KBr): 3365, 2943, 2834, 2786, 1735, 1593, 1423, 1369, 1219, 1148, 1043, 940, 764, 695 cm^{-1}. ^{1}H-NMR ($CDCl_3$, 400 MHz): δ 8.73 (1H, s, N-H), 8.66 (1H, s, Ar-H), 8.45 (1H, d, J = 2.72 Hz, Ar-H), 7.90 (1H, d, J = 8.4 Hz, Ar-H), 7.80 (1H, d, J = 0.52 Hz, Ar-H), 7.64-7.66 (1H, dd, J = 1.32 Hz, Ar-H), 7.36 (1H, t, J = 7.88 Hz, Ar-H), 7.11 (1H, t, J = 3.64 Hz, Ar-H), 6.60 (1H, t, J = 7.52 Hz, Ar-H), 6.55 (1H, d, J = 8.08 Hz, Ar-H), 5.31-5.39 (1H, dd, J = 9.48 Hz, C-H), 4.86 (1H, t, CH_2), 4.24-4.29 (1H, q, CH_2), 4.03-4.07 (1H, q, CH_2), 3.78-3.83 (1H, q, CH_2), 3.51 (4H, t, CH_2), 2.66 (4H, t, CH_2), 2.27 (3H, s, CH_3), 2.22 (3H, s, CH_3), 1.37 (3H, t, CH_3), 1.06 (3H, t, CH_3). ^{13}C-NMR ($CDCl_3$, 100 MHz): δ 160.77, 160.69, 159.88, 151.58, 151.91, 148.09, 146.39, 139.19, 137.39, 137.35, 130.72, 129.19, 128.57, 127.58, 127.17, 125.04, 124.61, 122.80, 122.04, 119.41, 117.79, 115.91, 114.20, 112.25, 111.27, 63.52, 63.46, 63.39, 55.42, 54.98, 51.17, 50.95, 50.84, 48.39, 46.15, 21.49, 16.59, 16.54, 16.23, 16.17. ^{31}P-NMR ($CDCl_3$, 400 MHz): δ 23.86 TOFMS ES *m/z* (rel. int.): 483.25 $[M]^+$. Anal. Calc. for $C_{26}H_{35}N_4O_3P$: C, 64.71; H, 7.31; N, 11.61 %. Found: C, 64.73; H, 7.34; N, 11.63 %.

2.4.12. diethyl ((2-(4-methylpiperazin-1-yl)quinolin-3-yl)(p-tolylamino)methyl)phosphonate (4l)

Yellow colour solid: FT-IR (KBr): 3393, 2973, 2917, 2850, 2805, 1743, 1691, 1592, 1425, 1373, 1218, 1148, 1015, 952, 789, 620 cm^{-1}. ^{1}H-NMR ($CDCl_3$, 400 MHz): δ 8.38 (1H, d, J = 2.56 Hz, N-H), 8.35 (1H, s, Ar-H), 7.77 (1H, d, J = 8.36 Hz, Ar-H), 7.72 (1H, d, J = 8.44 Hz, Ar-H), 7.64 (2H, t, J = 8.6 Hz, Ar-H), 7.55-7.59 (1H, m, Ar-H), 7.50 (1H, t, J = 7.48 Hz, Ar-H), 7.26 (2H, dd, J = 0.76 Hz, Ar-H), 5.30 (1H, d, C-H), 4.08-4.12 (2H, q, CH_2), 3.94-3.99 (1H, q, CH_2), 3.86-3.91 (1H, q, CH_2), 3.41 (4H, t, CH_2), 2.53 (4H, t, CH_2), 2.21-2.24 (6H, s, CH_3), 1.22 (3H, s, CH_3), 1.07 (3H, t, CH_3). ^{13}C-NMR ($CDCl_3$, 100 MHz): δ 160.32, 160.24, 158.83, 149.24, 146.64, 146.62, 142.51, 138.74, 138.68, 132.47, 129.70, 127.84, 127.63, 127.49, 125.81, 125.19, 124.62, 123.97, 122.02, 120.99, 112.37, 67.19, 65.56, 63.17, 63.10, 63.06, 62.99, 54.79, 50.74, 45.95, 44.84, 30.31, 29.66, 29.43, 16.54, 16.49, 16.39, 16.33. ^{31}P-NMR ($CDCl_3$, 400 MHz): δ 22.16. Anal. Calc. for $C_{26}H_{35}N_4O_3P$: C, 64.71; H, 7.31; N, 11.61 %. Found: C, 64.73; H, 7.33; N, 11.63 %.

2.4.13. diethyl(((2,5-dimethylphenyl)amino)(2-(4-methylpiperazin-1-yl)quinolin-3 yl)methyl)phosphonate (4m)

Yellow colour solid: FT-IR (KBr): 3320, 3058, 2940, 2842, 2789, 1588, 1426, 1368, 1285, 1243, 1137, 1010, 947, 742, 694, 576, 529 cm^{-1}. ^{1}H-NMR ($CDCl_3$, 400 MHz): δ 8.64 (1H, s, N-H), 8.47 (1H, s, Ar-H), 8.33 (1H, d, J = 2.76 Hz, Ar-H), 7.78 (1H, d, J = 8.44 Hz, Ar-H), 7.72 (1H, d, J = 7.76 Hz, Ar-H), 7.48-7.54 (1H, m, Ar-H), 7.26-7.28 (1H, dd, J = 1.32 Hz, Ar-H), 6.98 (1H, t, J = 6.12 Hz, Ar-H), 6.71-6.78 (1H, m, Ar-H), 5.18-5.26 (1H, dd, J = 9.2 Hz, C-H), 4.53 (1H, t, Ar-H), 4.17 (1H, t, CH_2), 3.94-3.96 (1H, q, CH_2), 3.70-3.73 (1H, m, CH_2), 3.40 (1H, t, CH_2), 2.56 (1H, d, CH_2), 2.26 (3H, t, CH_2), 2.13 (3H, s, CH_2), 2.05 (3H, s, CH_3), 1.26 (3H, t, CH_3), 0.96 (3H, t, CH_3). ^{13}C-NMR ($CDCl_3$, 100 MHz): δ 160.66, 159.94, 156.34, 148.56, 148.02, 146.82, 146.80, 141.72, 141.59, 137.63, 137.21, 137.16, 135.76, 132.23, 131.31, 131.07, 130.55, 129.49, 128.53, 127.89, 127.60, 127.54, 127.48, 127.39, 127.13, 126.03, 125.12, 124.97, 124.55, 123.15, 122.89, 117.27, 111.74, 63.54, 63.48, 63.40, 63.33, 55.42, 55.04, 51.14, 50.85, 50.32, 48.77, 46.29, 46.18, 20.98, 20.26, 17.94, 17.58, 16.61, 16.56, 16.24, 16.18. ^{31}P-NMR ($CDCl_3$, 400 MHz): δ 24.03 TOFMS ES *m/z* (rel. int.): 496.24 $[M]^+$.

Anal. Calc. for $C_{27}H_{37}N_4O_3P$: C, 65.30; H, 7.51; N, 11.28 %. Found: C, 65.32; H, 7.53; N, 11.30 %.

2.4.14. diethyl(((2-methoxyphenyl)amino)(2-(4-methylpiperazin-1-yl)quinolin-3-yl)methyl)phosphonate (4n)

Yellow colour solid: FT-IR (KBr): 3420, 2928, 2833, 2788, 1735, 1583, 1494, 1429, 1373, 1230, 1139, 1026, 955, 740 cm^{-1}. ^{1}H-NMR ($CDCl_3$, 400 MHz): δ 8.76 (1H, s, N-H), 8.65 (1H, s, Ar-H), 7.85 (1H, d, *J* = 8.4 Hz, Ar-H), 7.76 (1H, d, *J* = 8 Hz, Ar-H), 7.57-7.61 (1H, q, *J* = 7.12 Hz, Ar-H), 7.32 (1H, t, *J* = 7.48 Hz, Ar-H), 7.05 (1H, t, *J* = 1.52 Hz, Ar-H), 7.01 (1H, d, *J* = 7.48 Hz, Ar-H), 6.96 (1H, d, *J* = 8.96 Hz, Ar-H), 6.67-6.75 (1H, m, *J* = 1.68 Hz, Ar-H), 5.22 (1H, s, C-H), 4.22-4.26 (2H, q, CH_2), 4.04-4.06 (2H, q, CH_2), 3.87 (3H, s, OCH_3), 3.78 (3H, s, CH_3), 3.50 (4H, s, CH_2), 2..59 (4H, s, CH_2), 1.31-1.42 (3H, s, CH_3), 1.06-1.26 (3H, t, CH_3). ^{13}C-NMR ($CDCl_3$, 100 MHz): δ 160.83, 160.75, 159.85, 158.93, 152.31, 149.30, 148.07, 147.27, 142.39, 141.57, 138.01, 136.22, 132.45, 130.63, 129.25, 128.59, 127.54, 126.93, 125.01, 124.51, 122.92, 121.13, 121.07, 121.69. 118.37, 114.97, 111.66, 110.41, 63.47, 63.40, 63.30, 63.23, 55.85, 55.02, 50.80, 46.15, 29.71, 16.58, 16.52, 16.26, 16.21. ^{31}P-NMR ($CDCl_3$, 400 MHz): δ 23.75 TOFMS ES *m/z* (rel. int.): 521 $[M]^+$. Anal. Calc. for $C_{26}H_{35}N_4O_4P$: C, 62.64; H, 7.08; N, 11.24 %. Found: C, 62.66; H, 7.10; N, 11.26 %.

2.4.15. diethyl(((4-methoxyphenyl)amino)(2-(4-methylpiperazin-1-yl)quinolin-3 yl)methyl)phosphonate (4o)

Yellow colour solid: FT-IR (KBr): 3441, 2926, 2843, 2785, 1745, 1594, 1502, 1420, 1372, 1231, 1148, 1042, 735 cm^{-1}. ^{1}H-NMR ($CDCl_3$, 400 MHz): δ 8.70 (1H, s, N-H), 8.67 (1H, s, Ar-H), 7.87 (1H, d, *J* = 8.48 Hz, Ar-H), 7.78 (1H, d, *J* = 0.68 Hz, Ar-H), 7.61-7.65 (1H, m, Ar-H), 7.35-7.39 (1H, m, Ar-H), 7.29-7.31 (2H, dd, *J* = 2.16 Hz, Ar-H), 6.97-6.99 (2H, dd, *J* = 2.04 Hz, Ar-H), 5.28 (1H, t, C-H), 4.58 (1H, t, CH_2), 4.24-4.26 (2H, q, CH_2), 4.01-4.06 (1H, m, CH_2), 3.85 (3H, s, OCH_3), 3.67 (3H, s, CH_3), 3.49 (4H, t, CH_2), 2.65 (4H, t, CH_2), 1.36 (3H, t, CH_3), 1.06 (3H, t, CH_3). ^{13}C-NMR ($CDCl_3$, 100 MHz): δ 160.66, 159.94, 156.84, 148.56, 148.02, 146.82, 146.80, 141.72, 141.59, 137.63, 137.20, 137.18, 135.75, 132.22, 131.66, 130.55, 129.48, 128.53, 127.89, 127.61, 127.54, 127.49, 127.40, 127.14, 126.04, 125.12, 124.97, 124.56, 123.15, 122.89, 117.27, 111.75, 63.55, 63.48, 63.33, 55.42, 55.05, 51.14, 50.86, 50.32, 48.78, 46.30, 46.19, 20.29, 20.26, 17.94, 17.58, 16.61, 16.56. ^{31}P-NMR ($CDCl_3$, 400 MHz): δ 23.91. Anal. Calc. for $C_{26}H_{35}N_4O_4P$: C, 62.64; H, 7.08; N, 11.24 %. Found: C, 62.66; H, 7.09; N, 11.26 %.

2.4.16. diethyl((2-(4-methylpiperazin-1-yl)quinolin-3-yl)(pyridin-2 ylamino)methyl)phosphonate (4p)

Yellow colour solid: FT-IR (KBr): 3397, 2984, 2937, 2857, 2784, 1748, 1588, 1495, 1424, 1373, 1240, 1190, 1045, 1008, 949, 755, 623 cm^{-1}. ^{1}H-NMR ($CDCl_3$, 400 MHz): δ 8.43 (1H, s, Ar-H), 7.75-7.79 (2H, t, *J* = 6.36 Hz, Ar-H), 7.60 (1H, d, *J* = 7.96 Hz, Ar-H), 7.48 (1H, d, *J* = 7.48 Hz, Ar-H), 7.24-7.28 (2H, q, *J* = 0.92 Hz, Ar-H), 6.40-6.44 (2H, t, *J* = 3.76 Hz, Ar-H), 6.11 (1H, d, *J* = 7.88 Hz, N-H), 5.33 (1H, d, *J* = 12.44 Hz, C-H), 4-4.12 (1H, m, CH_2), 3.98 (1H, d, CH_2), 3.91 (1H, t, CH_2), 3.77-3.81 (1H, q, CH_2), 3.54-3.57 (1H, q, CH_2), 3.37 (1H, t, CH_2), 3.23 (4H, t, CH_2), 2.59 (4H, t, CH_2), 2.26 (3H, s, CH_3), 1.18-1.21 (3H, t, CH_3), 1.06-1.09 (3H, t, CH_3). ^{13}C-NMR ($CDCl_3$, 100 MHz): δ 160.55-160.61, 160.01-160.09, 157.94, 156.73, 146.52, 145.17, 138.92, 138.87, 138.63, 137.32, 129.65, 129.48, 127.68, 127.49, 125.81, 125.79, 125.05, 125, 113.82, 112.98, 109.77, 108.87, 63.06-63.08, 63.13, 63.16, 59.62, 59.58, 54.93, 5.51, 50.15, 45.30, 30.29, 16.54, 16.48, 16.42, 16.36, 16.30. ^{31}P-NMR ($CDCl_3$, 400 MHz): δ 23.49, 22.45. TOFMS ES *m/z* (rel. int.): 470.23 $[M]^+$. Anal. Calc. for $C_{24}H_{32}N_5O_3P$: C, 61.39; H, 6.87; N, 14.92 %. Found: C, 61.41; H, 6.89; N, 14.95 %.

2.4.17. diethyl((2-(4-methylpiperazin-1-yl)quinolin-3-yl)((4-methylpyridin-2 yl)amino)methyl)phosphonate (4q)

Yellow colour solid: FT-IR (KBr): 3288, 2956, 2915, 2842, 2806, 1746, 1615, 1485, 1424, 1367, 1232, 1017, 948, 742, 596, 528 cm^{-1}. ^{1}H-NMR ($CDCl_3$, 400 MHz): δ 8.29 (1H, d, *J* = 2.84 Hz, Ar-H), 7.80 (2H, t, *J* = 4.8 Hz, Ar-H), 7.62 (1H, d, *J* = 7.96 Hz, Ar-H), 7.52 (1H, t, *J* = 7.4 Hz, Ar-H), 7.27-7.31 (1H, q, *J* = 7.24 Hz, Ar-H), 6.37 (1H, s, Ar-H), 6.34 (1H, d, *J* = 5.24 Hz, Ar-H), 5.87 (1H, q, *J* = 9.28 Hz, N-H), 5.50 (1H, t, *J* = 8.6 Hz, C-H), 4.04-4.16 (2H, m, CH_2), 3.83-3.89 (1H, m, CH_2), 3.59-3.65 (1H, m, CH_2), 3.18-3.52 (4H, m, CH_2), 2.49-2.74 (4H, m, CH_2), 2.38 (3H, s, CH_3), 2.11 (3H, s, CH_3), 1.20-1.23 (3H, t, CH_3), 0.93-0.96 (3H, t, CH_3). ^{13}C-NMR ($CDCl_3$, 100 MHz): δ 160.78, 160.71, 157.05, 156.95, 148.51, 147.47, 146.63, 146.62, 137.18, 137.13, 129.43, 127.81, 127.50, 126.35, 125.90, 124.94, 115.66, 108.45, 63.29, 63.22, 63.17, 63.10, 55.24, 55.08, 50.50, 48.15, 46.63, 45.99, 30.32, 29.68, 21.10, 16.47, 16.41, 16.21, 16.15. ^{31}P-NMR ($CDCl_3$, 400 MHz): δ 23.43, 21.88. TOFMS ES *m/z* (rel. int.): 484.24 $[M]^+$. Anal. Calc. for $C_{25}H_{34}N_5O_3P$: C, 62.10; H, 7.09; N, 14.48 %. Found: C, 62.12; H, 7.11; N, 14.46 %.

2.4.18. diethyl((2-(4-methylpiperazin-1-yl)quinolin-3-yl)(naphthalen-1 ylamino)methyl)phosphonate (4r)

Yellow colour solid: FT-IR (KBr): 3457, 3356, 3227, 3046, 2975, 2785, 1748, 1593, 1415, 1369, 1285, 1218, 1142, 1007, 955, 782, 574 cm^{-1}. ^{1}H-NMR ($CDCl_3$, 400 MHz): δ 8.94 (1H, s, N-H), 8.77 (1H, s, Ar-H), 8.47 (1H, t, *J* = 3.32 Hz, Ar-H), 7.88-7.94 (2H, m, *J* = 3.84 Hz, Ar-H), 7.78-7.84 (1H, m, *J* = 4.12 Hz, Ar-H), 7.67-7.72 (1H, m, *J* = 1.24 Hz, Ar-H), 7.57-7.60 (1H, q, *J* = 2.52 Hz, Ar-H), 7.54 (1H, t, *J* = 7.4 Hz, Ar-H), 7.47 (1H, t, *J* = 4.36 Hz, Ar-H), 7.42 (1H, t, *J* = 0.8 Hz, Ar-H), 7.32 (1H, t, *J* = 3.24 Hz, Ar-H), 7.08 (1H, t, *J* = 0.6 Hz Ar-H), 6.80 (1H, d, *J* = 1.6 Hz Ar-H), 4.11-4.17 (4H, m, CH_2), 3.58 (4H, t, CH_2), 2.68 (4H, t, CH_2), 2.39 (1H, s, CH_3), 1.24-1.30 (6H, m, CH_3). ^{13}C-NMR ($CDCl_3$, 100 MHz): δ 160.37, 160.30, 158.91, 149.30, 144.02, 142.50, 135.60, 132.51, 129.25, 127.52, 126.14, 124.66, 124.01, 122.06, 118.77, 116.80, 63.28, 63.21, 63.97, 63, 58.09, 54.88, 51.14, 50.85, 46.03, 29.68, 29.35, 16.59, 16.81, 16.41, 16.36. ^{31}P-NMR ($CDCl_3$, 400 MHz): δ 23.80. TOFMS ES *m/z* (rel. int.): 519.25 $[M]^+$. Anal. Calc. for $C_{29}H_{35}N_4O_3P$: C, 67.17; H, 6.80; N, 10.80 %. Found: C, 67.19; H, 6.83; N, 10.81 %.

2.4.19. diethyl(((9-ethyl-9H-carbazol-3-yl)amino)(2-(4-methylpiperazin-1-yl)quinolin-3 yl)methyl)phosphonate (4s)

Yellow colour solid: FT-IR (KBr): 3320, 2975, 2917, 2853, 2786, 1738, 1598, 1456, 1364, 1232, 1045, 745, 548 cm^{-1}. ^{1}H-NMR ($CDCl_3$, 400 MHz): δ 8.86 (1H, s, Ar-H), 8.80 (1H, s, Ar-H), 8.74 (1H, d, *J* = 2.72 Hz N-H), 8.11-8.17 (1H, dd, *J* = 1.88 Hz, Ar-H), 8.02 (1H, d, *J* = 7.72 Hz, Ar-H), 7.90-7.95 (1H, dd, *J* = 3.96 Hz, Ar-H), 7.87 (1H, t, *J* = 7.2 Hz, Ar-H), 7.74 (1H, d, *J* = 7.64 Hz, Ar-H), 7.55 (1H, t, *J* = 1.92 Hz, Ar-H), 7.36-7.49 (2H, m, *J* = 2.64 Hz, Ar-H), 7.17 (1H, t, *J* = 7.28 Hz, Ar-H), 6.99-7.02 (1H, dd, *J* = 2.16 Hz, Ar-H), 6.91-6.94 (1H, dd, *J* = 2.32 Hz, C-H), 4.40 (1H, q, CH_2), 4.23-4.30 (1H, m, CH_2), 4.14-4.17 (1H, m, CH_2), 3.84 (1H, t, CH_2), 3.58 (4H, t, CH_2), 2.72 (4H, t, CH_2), 2.41 (3H, s, CH_3), 1.40-1.50 (2H, m, CH_2), 1.38 (3H, m, CH_3), 1.29 (3H, t, CH_3), 1.10 (3H, t, CH_3). ^{13}C-NMR ($CDCl_3$, 100 MHz): δ 160.88, 160.80, 159.88, 155.12, 147.91, 143.73, 140.61, 139.05, 137.37, 134.54, 134.47, 130.48, 129.47, 128.53, 127.58, 126.09, 125.44, 124.98, 124.58, 122.46, 120.58, 120.40, 119.76, 119.07, 118.01, 115.57, 115.13, 113.07, 108.99, 108.35, 106.36, 104.65, 63.60, 63.53, 63.35, 63.28, 55.36, 54.97, 50.71, 46.15, 46.07, 37.76, 37.51, 37.44, 29.72, 22.72, 16.63, 16.57, 16.28, 16.22, 13.89, 13.82. ^{31}P-NMR ($CDCl_3$, 400 MHz): δ 24.16. TOFMS ES *m/z* (rel. int.): 608.27

[M] $^{+}$. Anal. Calc. for $C_{33}H_{40}N_5O_3P$: C, 67.67; H, 6.88; N, 11.96 %. Found: C, 67.69; H, 6.70; N, 11.98 %.

2.4.20. diethyl((2-(2-bromoacetamido)benzamido)(2-(4-methylpiperazin-1-yl)quinolin-3 yl)methyl)phosphonate (4t)

Yellow colour solid: FT-IR (KBr): 3404, 3196, 3028, 2944, 2842, 1736, 1677, 1594, 1523, 1364, 1220, 1026, 895, 765 cm^{-1}. ^{1}H-NMR ($CDCl_3$, 400 MHz): δ 11.97 (1H, s, N-H), 10.08 (1H, s, N-H), 8.52 (1H, d, *J* = 8.44 Hz, Ar-H), 8.42 (1H, s, Ar-H), 7.74 (2H, t, *J* = 8.6 Hz, Ar-H), 7.61-7.65 (1H, q, *J* = 1.4 Hz, Ar-H), 7.52-7.54 (1H, dd, *J* = 0.96 Hz, Ar-H), 7.41 (1H, t, *J* = 7.28 Hz, Ar-H), 7.29-7.33 (1H, q, *J* = 0.8 Hz, Ar-H), 7.02-7.06 (1H, q, *J* = 0.68 Hz, Ar-H), 4.94 (1H, d, C-H), 4.08 (4H, s, CH_2), 3.51 (4H, t, CH_2), 2.69 (4H, t, CH_2), 1.35 (3H, s, CH_3), 1.14-1.25 (6H, q, CH_3), 0.82 (2H, t, CH_2). ^{13}C-NMR ($CDCl_3$, 100 MHz): δ 190.14, 176.93, 165.23, 149.23, 143.83, 139.14, 133.20, 132.76, 129.20, 127.61, 124.90, 124.09, 123.61, 121.96, 121.43, 119.40, 54.50, 49.86, 45.40, 43.28, 30.32, 29.69, 29.36, 14.12. ^{31}P-NMR ($CDCl_3$, 400 MHz): δ 21.75. TOFMS ES *m/z* (rel. int.): 570.20 [M] $^{+}$. Anal. Calc. for $C_{28}H_{35}BrN_5O_5P$: C, 53.17; H, 5.58; N, 11.07 %. Found: C, 53.19; H, 5.60; N, 11.10 %.

2.5. Anti-bacterial studies

2.5.1. The preparation of media

The Preparation of Media Fresh Nutrient Agar, Oxoid LTD (Hampshire, England) was prepared according to the manufacturer's instruction as follows:

- 28g of the powder was weighed out into each of three 1L glass bottles
- Made up to the 1L mark with distilled water
- The mixture was shaken until the powder completely dissolved
- Bottles were sterilized by autoclaving at 121°C for 15 minutes
- The agar solution was poured into plates and left to solidify

2.5.2. The preparation of nutrient broth

The Preparation of the Nutrient Broth Fresh Mueller Hinton Broth (Sigma-Aldrich) was made up according to manufacturer's instruction as follows:

- 23g of Nutrient Broth powder was weighed out into a 1L glass bottle
- Made up to the 1L mark with distilled water
- The mixture was shaken until the powder completely dissolved
- The solution was dispensed into bijou bottles
- Bijou bottles were sterilized by autoclaving for at 121°C 15 minutes

2.5.3. Preparation of reagent: Microplate Alamar blue assay (MABA)

To 10mL of autoclaved distilled water, 0.2g of Resazurin powder was added and dissolved. The dye solution was then vortexed vigorously, covered with aluminum foil and kept out of the light as it is sensitive to light [23].

2.5.4. Microbial Cultures

The bacterial strains used in the study were collected from culture collection at the Department of Biotechnology and Food Technology, Durban University of Technology, South Africa.

The bacterial strains include *Bacillus cereus* (DBT*_F), *Staphylococcus aureus* (DBT*_E), *Klebsiella pneumonia* (DBT*_AM) and *Micrococcus luteus* (DBT*_AR); and the three yeast cultures *Candida albicans* (DBT*_AB), *Caraipa utilis* (DBT*_AB) and *Saccharomyces cerevisiae* (DBT*_R).

DBT*: Durban University of Technology, reference based on bacterial culture strain as established at the department of Biotechnology and Food Technology.

The antibacterial activity of synthesized α-APs derivatives (4a-4t) was completed using the agar disc diffusion test [26] by measuring the minimum inhibitory concentration (MIC) of the title compounds.

Minimum inhibitory concentration (MIC) were defined as the lowest concentration of a compound that will inhibit the visible growth of bacteria.

Stock cultures were sub-cultured to check their viability and stored using 50% of glycerol in micro bank vials (Davies Diagnostics, South Africa). For the assay, culture was plated on Nutrient Agar (Biolab) and set aside in an incubator at 37˚C for 24 hours before growth in

Nutrient Broth (Biolab) under the same conditions. A 10^8 cfu/mL amount of MacFarland standard with a 0.5 absorbance was used to standardize the bacterial cell concentration. A suspension (100 µL of 10^8 cfu/mL) of the test bacteria was plated on Mueller Hinton Agar plates (Fluka, Biochemika). The whatman No. 1 filter paper was cut into 5 mm disks then dried in an open sterile petri dish biosafety chamber (LabtecBioflow II, South Africa). The disks were impregnated with 10 µL of each title compound (4a-4t) at the concentration of 3 mg/mL then placed onto the pre-inoculated bacterial agar plates and kept at 37˚C for 24 hours. The assay was carried out in triplicate. Ciprofloxacin (Fluka, Biochemika) (3 mg/mL) was used as the active control and DMSO (100%) as a negative control for the bacterial strains. Amphotericin B (Fluka, Biochemika) was used as the active control and 10 µL DMSO (100%) as negative control for the yeast cultures. The MIC of α-APs derivatives (4a-4t) was determined by the disc diffusion method. Title compounds were tested at final concentrations of 0.09, 0.18, 0.35, 0.75, 1.5 and 3 mg/mL.

2.5.5. Brine Shrimp Assay (toxicity evaluation)

A practical tool for the introductory assessment of toxicity is the brine shrimp lethality assay and was therefore used in this study [28]. Preceding the test, the brine shrimp larvae (Artemia salina) had to be hatched in sea water for 1-24 h. A 5mL volume of sea water and ten brine shrimp were added to separate vials and treated with each of the methyl piperazinyl quinoline α-amionophosphonate derivatives. The analyses were performed in triplicate at the concentration of 10, 100 and 500 µg/mL. Brine shrimp death was observed at 1, 2, 3, 4, 20 and 24 hour intervals.

3. Results and discussion

3.1. Catalyst characterization

The new catalyst Pd-$SrTiO_3$ was prepared by reacting an aqueous mixture of Strontium (II) nitrate and citric acid followed by reflux in an ethanolic solution of Titanium (IV) butoxide. Thereafter, the dried solid was refluxed in a solution of Pd (II) nitrate. The mixture was filtered, calcined and dried. Several techniques were used for the characterization of Pd-$SrTiO_3$.

3.1.1. FT-IR spectrum

The FT-IR spectra of $SrTiO_3$ and Pd-$SrTiO_3$ were compared. In the case of $SrTiO_3$, the absorption at 1641 cm^{-1} is Ti-O stretch, 1465 cm^{-1} is the Sr-Ti-O stretch and Sr-Ti is 555 cm^{-1}

stretch. The spectrum of Pd-$SrTiO_3$ shows the Pd-Sr stretch at 2302 cm^{-1}, the Pd-Sr-Ti stretch at 1745 cm^{-1}, Pd-Sr-Ti-O stretch at 910 cm^{-1}, Sr-Ti-O stretch at 1448 cm^{-1} and Sr-Ti stretch at 574 cm^{-1} (**Fig. 1**).

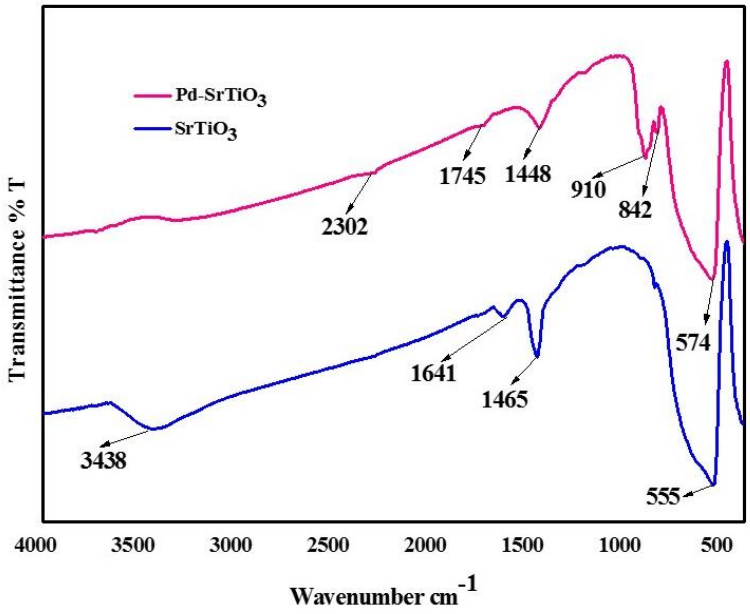

Fig. 1. FT-IR spectrum of $SrTiO_3$ and Pd-$SrTiO_3$

3.1.2. XRD

Figure 2 showed the XRD pattern of the as-prepared samples. It was clearly realized that all diffraction peaks of pure $SrTiO_3$ could be eagerly indexed to a well crystalline phase of $SrTiO_3$ and Pd-SrTiO3. As the Pd doped $SrTiO_3$ powders, it was observed that the diffraction peaks were identical to that of the pure $SrTiO_3$ as shown in (**Fig. 2**).

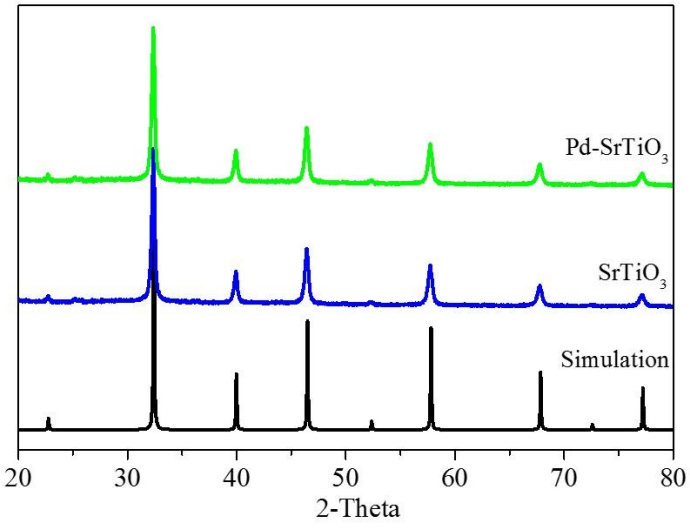

Fig. 2. PXRD pattern of $SrTiO_3$ and Pd-$SrTiO_3$

3.1.3. SEM

Scanning electron microscopy was used to determine the morphology and microstructure of $SrTiO_3$ and Pd-$SrTiO_3$ (**Fig. 3** a, b, and c, d**).** Aggregates of spherically shaped particles were observed. The particles are tightly packed.

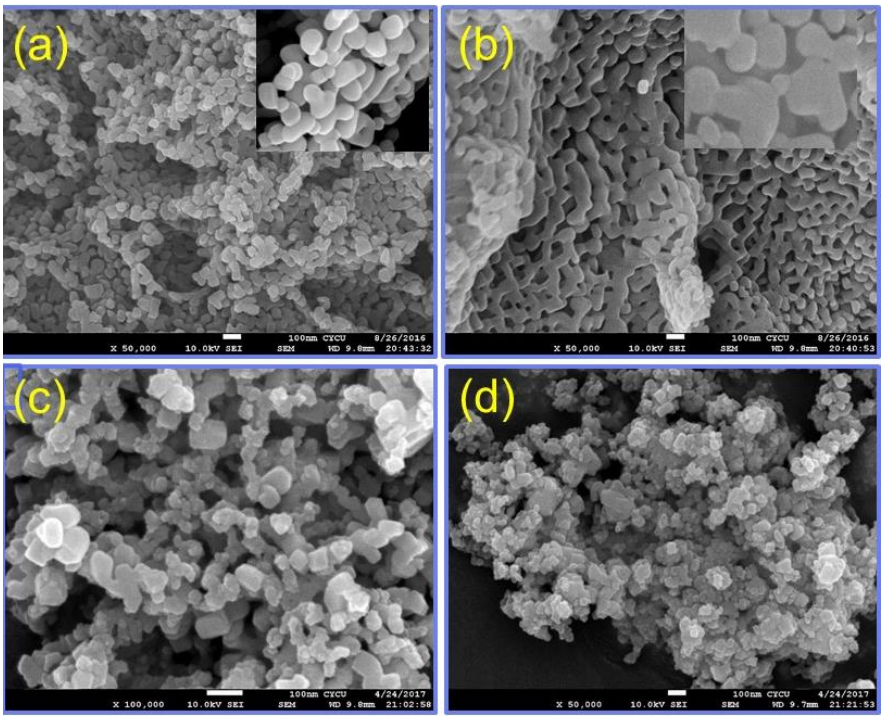

Fig. 3. SEM image of $SrTiO_3$ (a and b) and Pd-$SrTiO_3$ (c and d)

3.1.4. SEM-EDX

The identity of $SrTiO_3$ and Pd-$SrTiO_3$ were confirmed by EDX analysis for C, O, Ti, Sr and Pd (**Fig. 4**). The actual weight (%) in $SrTiO_3$ elements for C, O, Ti and Sr are 17.78, 30.55, 18.49 and 33.17, respectively whilst the atomic (%) were 35.63, 45.96, 9.29 and 9.11, respectively. The carbon content in $SrTiO_3$ may be due to carbon tape that was used. The EDX of Pd-$SrTiO_3$ displayed elements C, O, Ti, Sr and Pd of weight (%) 0, 19.72, 19.84, 28.22 and 32.22, respectively whilst the atomic (%) are 0, 54.26, 18.23, 14.18, and 13.33 respectively (**Table 1**).

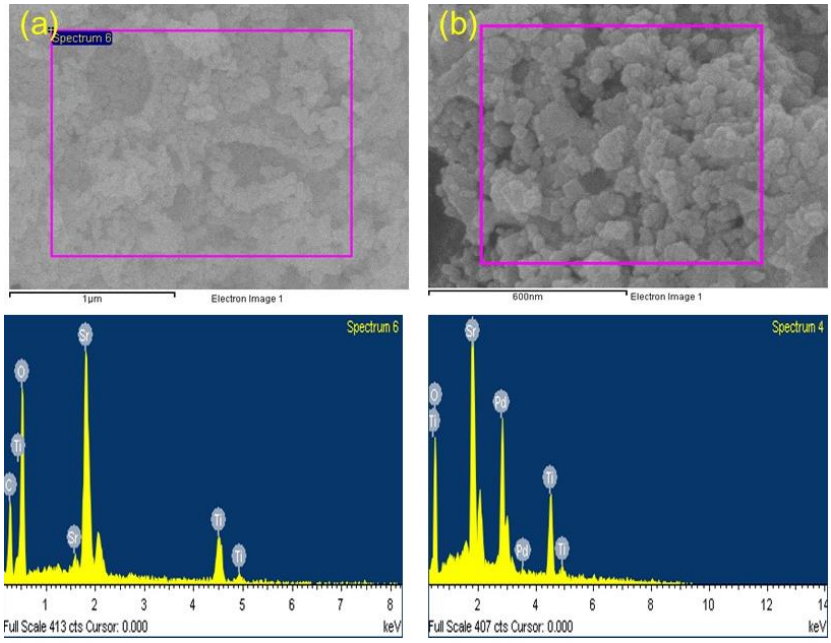

Fig. 4. EDX analysis for $SrTiO_3$ (a) and Pd-$SrTiO_3$ (b)

Table 1 The weight (%) analysis for $SrTiO_3$ and Pd-$SrTiO_3$.

	$SrTiO_3$		Pd-$SrTiO_3$	
Element	Weight (%)	Atomic (%)	Weight (%)	Atomic (%)
C	17.78	35.63	-	-
O	30.55	45.96	19.72	54.26
Ti	18.49	9.29	19.84	18.23
Sr	33.17	9.11	28.22	14.18
Pd	-	-	32.22	13.33

3.1.5. N_2 adsorption and desorption

The porosity of $SrTiO_3$ and Pd-$SrTiO_3$ is shown by N_2 gas adsorption measurements at 273 K (**Fig. 5**). $SrTiO_3$ is a Type-I adsorption isotherm which is characteristic of microporous material and the BET and Langmuir surface area of $SrTiO_3$ were calculated as 89 m^2/g and 158 m^2/g respectively. The N_2 adsorption isotherm of Pd-$SrTiO_3$ also indicates a Type-I adsorption isotherm however the BET and Langmuir surface area were calculated as 127 m^2/g and 214 m^2/g respectively.

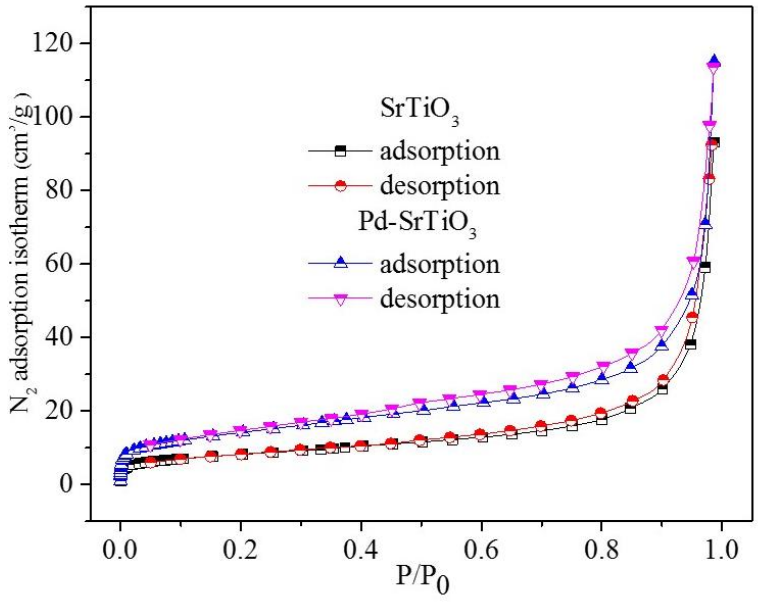

Fig. 5. Adsorption and desorption isotherms of $SrTiO_3$ and Pd-$SrTiO_3$ at 273K.

$SrTiO_3$ BET and Langmuir Surface area = 89 m^2/g and 158 m^2/g

Pd-$SrTiO_3$ BET and Langmuir Surface area = 127 m^2/g and 214 m^2/g

3.1.6. Raman spectrum

The structure of $SrTiO_3$ and Pd-$SrTiO_3$ were also studied by Raman spectroscopy (**Fig. 6**). The adsorption signal of $SrTiO_3$ is at 529 cm^{-1} whilst the absorption signal of Pd-$SrTiO_3$ also occurs at 529 cm^{-1} but the additional signal at 723 cm^{-1} is probably due to Pd.

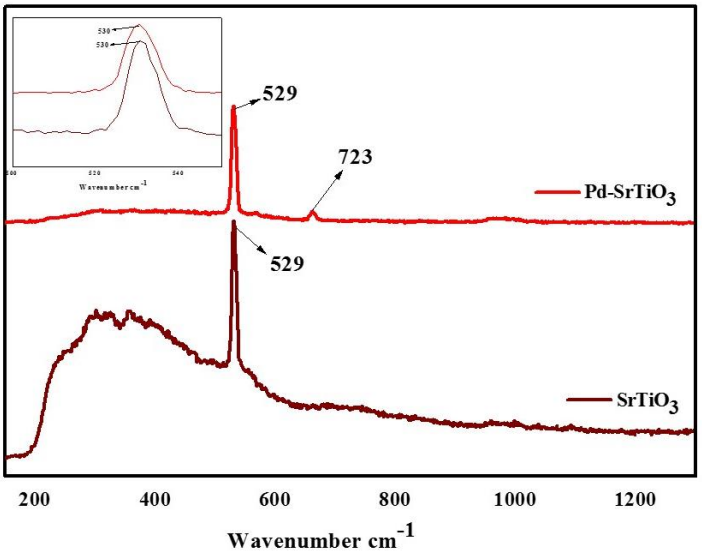

Fig. 6. Raman Shift of $SrTiO_3$ and Pd-$SrTiO_3$

3.2. Synthesis of methyl-piperazinyl quinolinyl α-aminophosphonates derivatives

To synthesize new methyl-piperazinyl quinolinyl (diethyl ((2-(4-methylpiperazin-1-yl)quinolin-3-yl)(phenylamino)methyl)phosphonates (**4a-4t**) with catalytic amounts of Pd-$SrTiO_3$, the substrates **1**, **2** and various amine derivatives (**3a-3t**) were used (**Scheme 1**).

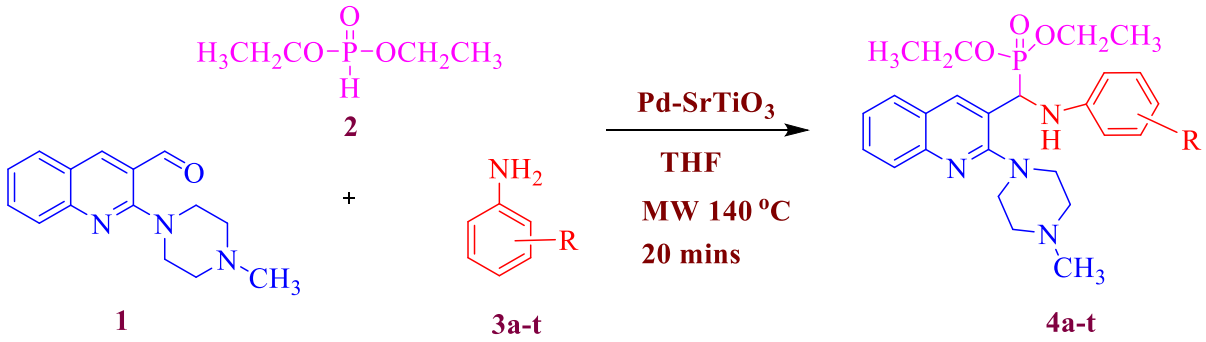

Scheme 1. The synthesis of (diethyl ((2-(4-methylpiperazin-1-yl)quinolin-3 yl)(phenylamino)methyl)phosphonates in the presence of Pd-$SrTiO_3$ catalyst under microwave conditions

In the initial study, **4a** was synthesised using the substrates **1**, **2** and **3a** and this became the model reaction. **4a** was characterised by FT-IR, ^{1}H-NMR, ^{13}C-NMR, 2D-NMR, ^{31}P-NMR, TOF-MS and elemental analysis. In order to determine the optimum amount of Pd-$SrTiO_3$, different amounts of catalyst, viz., 0.03, 0.05, 0.07 g, in THF, under MW conditions for 30 min. The optimum amount was 0, 05 g since an increase to 0, 07 g did not increase the product yield. Thereafter several solvents including ethanol, methanol, acetonitrile, Toluene, DMF and THF were examined. When the reaction was conducted with Pd-$SrTiO_3$, in THF, under MW conditions at 20 min (**Table 2 entries 13**), **4a** was obtained in 96 % yield. Moderate yields were observed when solvents ethanol, methanol, acetonitrile, Toluene, DMF and THF were used at room temperature conditions for 24 h, resulting in % of yield of **4a** as 60, 50, 75, 65, 58 and 70 %, respectively (**Table 2 entries 1-6**). A decrease in product yield and an extended reaction time were requirements for completion of the reaction with the solvents at room temperature conditions. The yield increased slightly when the solvents ethanol, methanol, acetonitrile, Toluene, DMF and THF under reflux conditions were used: the % of yield of **4a** was 65, 53, 78, 60, 62 and 75 %, respectively (**Table 2 entries 7-12**). Also, MW reaction at different time intervals showed 20 min as ideal as the yield of **4a** was 96 %. Shorter reaction

time showed incomplete reaction visualised by TLC whilst higher temperatures gave additional spots on the TLC.

Table 2 Optimization of the synthesis of 4a under MW irradiation system using Pd-$SrTiO_3$

Entry	Catalyst	Solvent	Temp (°C)	Time(h/min)	Isolated Yield (%)
1	Pd-$SrTiO_3$	EtOH	r.t	24	60
2	Pd-$SrTiO_3$	MeOH	r.t	24	50
3	Pd-$SrTiO_3$	CH_3CN	r.t	24	75
4	Pd-$SrTiO_3$	Toluene	r.t	24	65
5	Pd-$SrTiO_3$	DMF	r.t	24	58
6	Pd-$SrTiO_3$	THF	r.t	24	70
7	Pd-$SrTiO_3$	EtOH	Reflux	12	65
8	Pd-$SrTiO_3$	MeOH	Reflux	10	53
9	Pd-$SrTiO_3$	CH_3CN	Reflux	6	78
10	Pd-$SrTiO_3$	Toluene	Reflux	14	60
11	Pd-$SrTiO_3$	DMF	Reflux	24	62
12	Pd-$SrTiO_3$	THF	Reflux	12	75
13	Pd-$SrTiO_3$	THF	MW	20 (mins)	96

After optimising the reaction conditions, all the other products **4a-t** were synthesized using the Pd-$SrTiO_3$ catalyst with THF as solvent and appropriate starting materials **1**, **2** and various amine (**3a-t)** via Kabachnik field's reaction under microwave conditions. The yield of the products (**Table 3**) ranged from 85 to 96 %. The products **4a-t** were characterized by FT-IR, ^{1}H-NMR, ^{13}C-NMR, ^{19}F-NMR, ^{31}P-NMR and MS-TOF whilst **4a** included 2D-NMR, DEPT-90 and DEPT-135 (the Figures showing all characterisation data are presented in supplementary file).

Table 3 The synthesis of methyl piperazinyl-quinolinyl α-Aminophosphonates derivative in the presence of Pd-$SrTiO_3$.

Entry	Substrate (3a-t)	Product (4a-t)	Time (min)	Isolated Yield (%)	M.p. (°C)
1	$C_6H_5NH_2$	4a	20	96	133-135
2	2-$O_2NC_6H_4NH_2$	4b	20	90	114-116
3	3-$O_2NC_6H_4NH_2$	4c	20	88	125-127
4	2-$FC_6H_4NH_2$	4d	20	90	149-151
5	3-$FC_6H_4NH_2$	4e	20	95	128-130
6	4-$FC_6H_4NH_2$	4f	20	88	127-129
7	4-$ClC_6H_4NH_2$	4g	20	91	181-183
8	$Cl_2C_6H_3NH_2$	4h	20	94	188-190
9	4-$BrC_6H_4NH_2$	4i	20	88	194-196
10	o-$CH_3C_6H_4NH_2$	4j	20	92	140-142
11	m-$CH_3C_6H_4NH_2$	4k	20	87	137-139
12	p-$CH_3C_6H_4NH_2$	4l	20	85	150-152
13	$(CH3)_2C_6H_4NH_2$	4m	20	90	147-149
14	o-C_6H_9NO	4n	20	85	130-132
15	p-C_6H_9NO	4o	20	89	119-121
16	$C_6H_6N_2$	4p	20	87	145-147
17	$C_6H_8N_2$	4q	20	90	144-146
18	$C_{10}H_7NH_2$	4r	25	91	131-133
19	$C_{14}H_{14}N_2$	4s	25	93	109-111
20	C_9H_9Br-N_2O_2	4t	25	90	120-122

2-(4-methylpiperazin-1-yl) quinoline-3-carbaldehyde (1mmol), diethyl phosphite (1mmol), and aniline (1mmol), catalyst 0.05g under MW at 140 °C

The possible recyclability of Pd-$SrTiO_3$ was also explored in the model reaction **4a**: briefly the solid catalyst was washed with ethanol, heated at 100 °C then used for succeeding reactions. The outcome indicated that the catalyst may possibly be re-used five times over with only a 4 % loss of catalytic activity. This concluded the catalyst to be satisfactory which makes it applicable for commercial application if required.

4a was chosen as the template structure for unambiguous characterisation. The FT-IR spectrum shows stretching at 1588 and 3320 cm^{-1} for carbonyl and NH groups, respectively. The ^{1}H-NMR spectrum shows two singlets at δ 8.74, and 8.68 for N1″-H and C4-H, respectively. The C1'''-CH proton is assigned to δ 5.29-5.37 as a doublet. The ^{13}C-NMR spectrum shows the presence of two -OCH_2 carbonyl group at δ 63.36-63.49 and ^{31}P-NMR spectrum shows the presence of one phosphorus group at δ 23.76. Accurate mass was confirmed as 469.23 [M] +. The structure was further confirmed on the basis of 2D-NMR spectral studies.

The C, H-COSY (HSQC) correlation at δ 16.16-16.57, 46.10, 48.51, 50.05, 50.79, 54.95, 63.37-63.49, 113.81, 118.54, 122.73, 124.64, 126.40, 127.60, 128.58, 129.36, 137.92, are assigned to C4'", 6'", C5', C2', C7', C6', C3', C3'", 5'", C 3", 7", C5", C7, C4", C5, C8, C6, and C4, respectively. The carbon signal at δ 137.92, is due to the quinolinyl C4-carbon. The H, H COSY spectrum revealed the doublet at δ 5.29-5.37 which confirmed only one nearby hydrogen to C4. The long range HMBC correlation is presented in **Fig. 7** (the COSY, NOESY, HSQC and HMBC all figure in supplementary file).

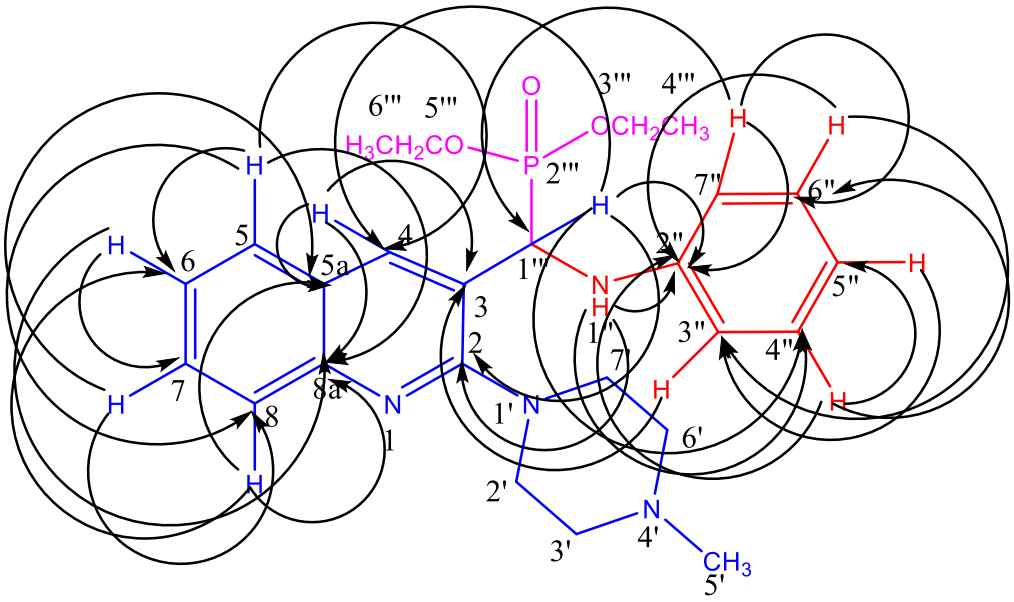

Fig. 7. Selected HMBC correlations of compound **4a**.

The HMBC correlation of **4a,** expressed as δ, is at: C1'"-H proton correlates with quinolinyl and amine carbon C4 at 137.92, C2 at 160.64, C2" at 145.97, C4" at 126.40, whilst the C1"-H (N-H) proton correlates with quinolinyl and amine carbon C2 at 160.64, C2" at 145.97, C4" at 126.40. The C4-H proton correlates with quinolinyl carbon C5a at 151.87, C8a at 148.12, C3

at 121.03, similarly, correlation of C5-H with quinolinyl carbon C6 is at 129.60, C8 at 128.58, C4 at 137.92, C5a at 151.87. The C6-H proton correlates with quinoline carbon C7 at 124.64, C8a at 148.12. The C7-H correlates with quinolinyl carbon C5a at 151.87, C8 at 128.58, whilst C8-H correlates with amine carbon C8a at 148.12, C6 at 129.36, C5a at 151.87. The C3"-H correlates with quinolinyl carbon C3 at 121.03, whilst C4"-H correlates with amine carbon C2" at 145.97, C5" at 118.54, C6" at 122.73. The C5"-H correlates with amine carbon C3" at 113.81, C6"-H correlates with amine carbon C2" at 145.97, C3" at 113.81, and C7"-H correlated with amine and -C-H carbon C2" at 145.97, C1'" at 48.51, C6" at 122.73 (**Fig. 8**).

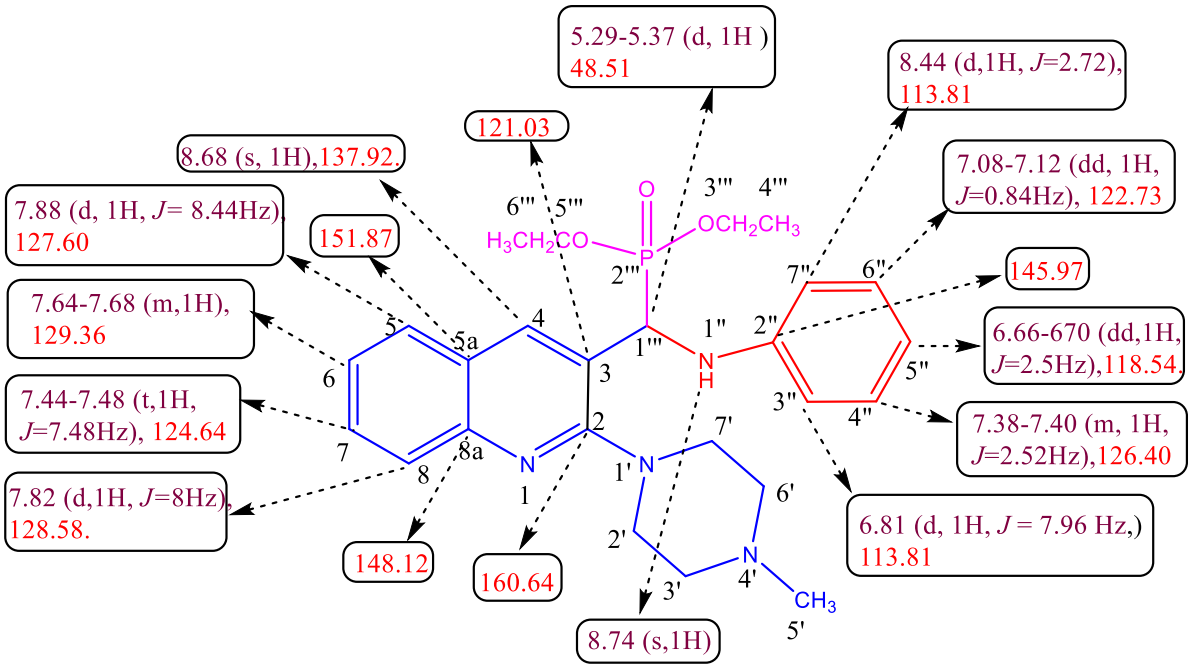

^{1}H-NMR ($CDCl_3$, 400 MHz): δ 8.74 (1H, s, N-H), 8.68 (1H, s, Ar-H), 8.44 (1H, d, J = 2.72 Hz, Ar-H), 7.88 (1H, d, J = 8.44 Hz, Ar-H), 7.82 (1H, d, J = 8 Hz, Ar-H), 7.64-7.68 (1H, m, Ar-H), 7.44-7.48 (1H, t, J = 7.48 Hz, Ar-H), 7.38-7.40 (1H, m, J = 2.52 Hz, Ar-H), 7.08-7.12 (1H, dd, J = 0.84 Hz, Ar-H), 6.81 (1H, d, J = 7.96 Hz, Ar-H), 6.66-6.70 (1H, dd, J = 2.5 Hz, Ar-H), 5.29-5.37 (1H, d, CH), 4.83-4.07 (1H, t, CH_2), 4.24-4.28 (1H, t, CH_2), 4.02-4.06 (1H, m, CH_2), 3.77-3.84 (1H, m, CH_2), 3.51-3.54 (4H, t, CH_2), 2.66-2.69 (4H, t, CH_2), 2.46 (3H, s, CH_3), 1.34-1.38 (3H, t, CH_3), 1.04-1.08 (3H, t, CH_3).

Fig. 8. Selected (^{1}H) NMR and (^{13}C) NMR and HMBC chemical shifts of **4a**.

Selected ^{1}H-NMR and ^{13}C-NMR and HMBC chemical shifts of **4a** are presented in **Table 4**. B TOFMS ES *m/z* (rel. int.) gave 469.23 [M] + as the molecular ion. Elemental analysis gave:

Anal. Calc. for $C_{25}H_{33}N_4O_3P$: C, 64.09; H, 7.10; N, 11.96 %. Found: C, 64.11; H, 7.12; N, 11.98 %, thereby confirming **4a** structure as diethyl ((2-(4-methylpiperazin-1-yl)quinolin-3 yl)(phenylamino)methyl)phosphonate.

Table 4
Selected HMBC correlations of compound 4a

S.NO	Proton	Correlated Carbons
1	$C_{1'''}$-H (d, 1H) at *δ.* 5.29-5.37	C_4 at *δ* (137.92), $C_{2''}$ at *δ* (145.97), $C_{4''}$ at *δ* (126.40), C_2 at *δ* (160.64),
2	$C_{1''}$-H (s, 1H, N-H) at *δ.* 8.74	$C_{2''}$ at *δ* (145.97), C_2 at *δ* (160.64) $C_{4''}$ at *δ* (126.40),
3	C_4-H (s, 1H) at *δ.* 8.68	C_{5a} at *δ* (151.87), C_{8a} at *δ* (148.12), C_3 at *δ* (121.03),
4	C_5-H (d, 1H, *J*= 8.44Hz) at *δ.* 7.88	C_6 at *δ* (129.36), C_8 at *δ* (128.58), C_4 at *δ* (137.92), C_{5a} at *δ* (151.87),
5	C_6-H (m, 1H) at *δ.* 7.64-7.68	C_7 at *δ* (124.64), C_{8a} at *δ* (148.12),
6	C_7-H (t, 1H, *J*= 7.48Hz) at *δ.* 7.44-7.48	C_{5a} at *δ* (151.87), C_8 at *δ* (128.58),
7	C_8-H (d, 1H, *J*= 8Hz) at *δ.* 7.82	C_{8a} at *δ* (148.12), C_6 at *δ* (129.36), C_{5a} at *δ* (151.87),
8	$C_{3''}$-H (d, 1H, *J*= 7.96Hz) at *δ.* 6.81	C_3 at *δ* (121.03),
9	$C_{4''}$-H (m, 1H, *J*= 2.52Hz) at *δ.* 7.38-7.40	$C_{2''}$ at *δ* (145.85), $C_{5''}$ at *δ* (118.54), $C_{6''}$ at *δ* (122.73),
10	$C_{5''}$-H (dd,1H, *J*= 2.5Hz) at *δ.* 6.66-6.70	$C_{3''}$ at *δ* (113.81),
11	$C_{6''}$-H (dd,1H, *J*= 0.84Hz) at *δ.* 7.08-7.12	$C_{2''}$ at *δ* (145.97), $C_{3''}$ at *δ* (113.81),
12	$C_{7''}$-H (d,1H, *J*= 2.72Hz) at *δ.* 8.44	$C_{2''}$ at *δ* (145.97), $C_{1'''}$ at *δ* (48.51), $C_{6''}$ at *δ* (122.73),

3.2.1. Proposed Mechanism

The proposed mechanism is based on the Kabachnik-Fields reaction. Firstly, the condensation of **1** and **3**, with a loss of water molecule, gave the Schiff base intermediate **I.** This is followed by H-bond formation between the P=*O* function of the phosphite **2** and the *H*N unit of the amine to produce intermediate **II**. An intramolecular cyclisation and loss of catalyst finally produced **4a** (**Scheme 2**).

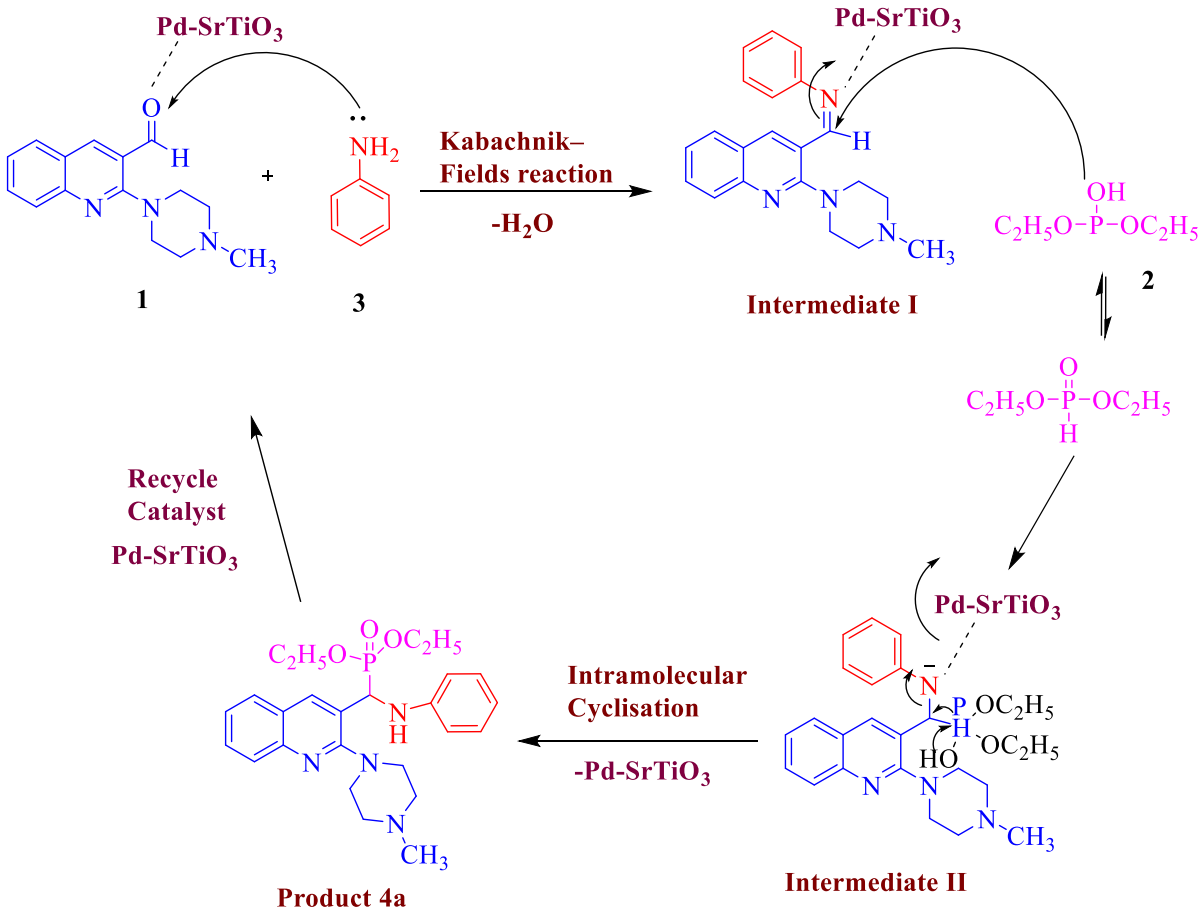

Scheme 2. The proposed mechanism of ((2-(4-methylpiperazin-1-yl)quinolin-3 yl)(phenylamino)methyl)phosphonates **4a-4t**

3.3. Biological Applications

3.3.1. Anti-bacterial studies

The antimicrobial activity of the α-APs derivatives were observed against four bacterial cultures and three yeast strains using the disc diffusion method [25]. The antibacterial activity

of **4a-4t** was assessed by the agar disc diffusion [26] method by measuring the minimum inhibitory concentration (MIC) which is the lowest concentration of a compound that will inhibit the visible growth of bacteria.

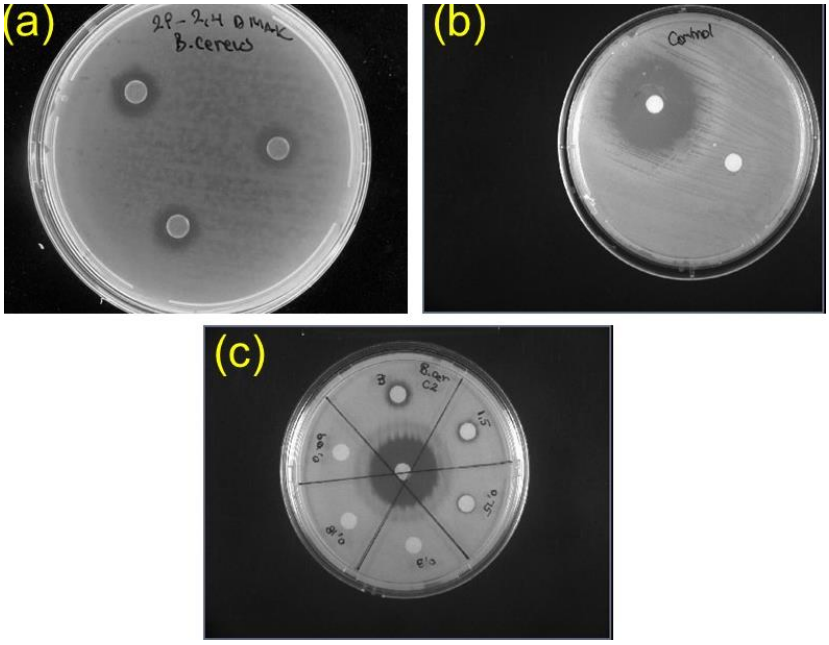

Fig. 9. Antibacterial screening showing zones of inhibition produced by compounds: (a) 4m, (b) Ciprofloxacin (positive control), (c) MIC, against B. cereus

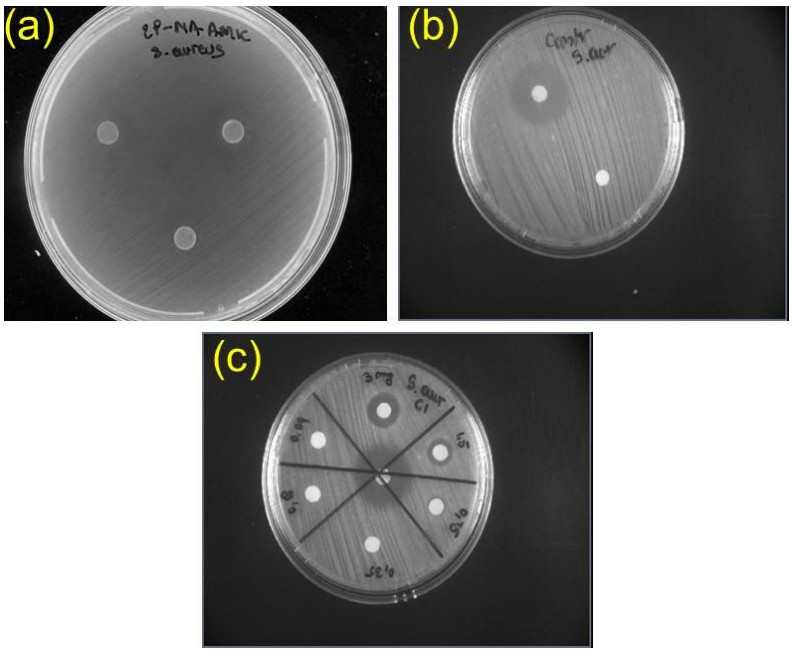

Fig. 10. Antibacterial screening showing zones of inhibition produced by compounds: (a) 4r, (b) Ciprofloxacin (positive control), (c) MIC, against S aureus

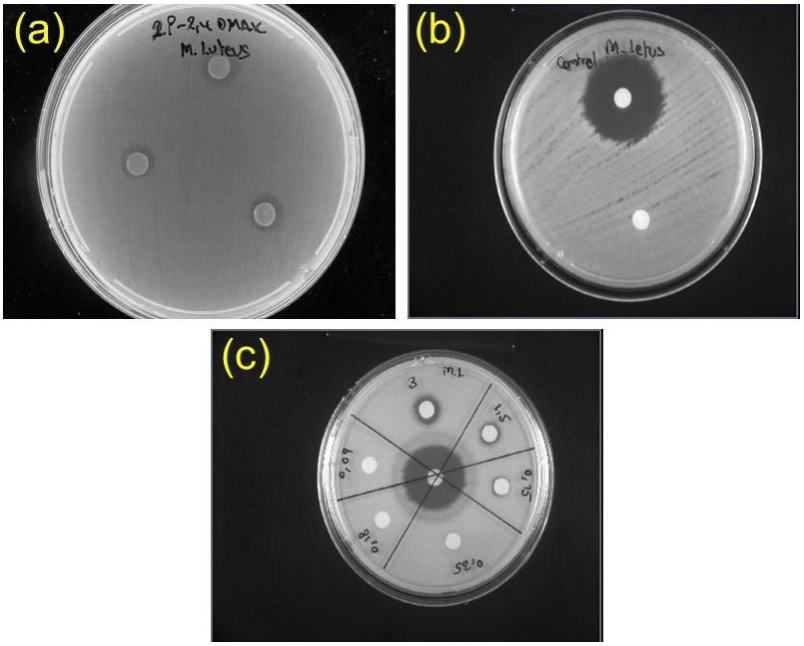

Fig. 11. Antibacterial screening showing zones of inhibition produced by compounds: (a) 4m, (b) Ciprofloxacin (positive control), (c) MIC, against M. Luteus

4a-4t shows antibacterial property against *B. cereus* among the different tested strains (see supportive information shown (**Table S1**). The zones of inhibition were observed as: (a) 4m, (b) Ciprofloxacin (positive control), (c) MIC, against *B. cereus* (**Fig. 9**). Antibacterial screening showing zones of inhibition produced by compounds: (a) 4r, (b) Ciprofloxacin (positive control), (c) MIC, against *S aureus* shows clear zone against *B. cereus* (**Fig. 10**). Antibacterial screening showing zones of inhibition produced by compounds: (a) 4m, (b) Ciprofloxacin (positive control), (c) MIC, against *M. Luteus* (**Fig. 11**). In addition, the MICs shows clear zone against *B. cereus* by using broth dilution methods (supplementary file **Table S1**).

3.3.2. Anti-Oxidant Studies

The free radical scavenging activity of methyl piperazinyl quinoline based α-amionophosphonates was measured in reaction with the stable free radical scavenger 2, 2 diphenyl-2-picryl hydrate (DPPH•) according to the decolouration protocol earlier reported by [27]. When in solution, DPPH• forms a stable molecule on accepting an electron or a hydrogen atom from a donor compound resulting in the non-radical form of DPPH. This change from a radical to non-radical form is observed by the colour change of the solution from violet to

residual pale yellow. The process was monitored by absorbance measurements at λ max = 517 nm.

All stock solutions of the compounds were diluted with methanol to the final concentrations of 1, 20, 40, 60, 80, 100, 250, 500, and 1000 µg/mL. A comparison of the results was attained with an effective anti-oxidant, Qeucertin-3-rutinoside.

The radical scavenging was calculated as the decolourization percentage of the test sample using the formula below:

$$\text{Scavenging capacity (\%)} = 100 - \frac{\text{absorbance of negative} - \text{absorbance of sample}}{\text{Absorbance of negative control}} \text{ X } 100$$

4f and 4r were found to be effective DPPH scavenging agents as shown by results of an antioxidant study (**Fig. 12**). Additionally, α-APs shows positive antioxidant activities at different concentrations. Rutin hydrate was used as a control to determine the radical-scavenging inhibitory concentration. The experiment was carried out in triplicate and all results obtained is shown in supportive information **(**supplementary file **Table S2).**

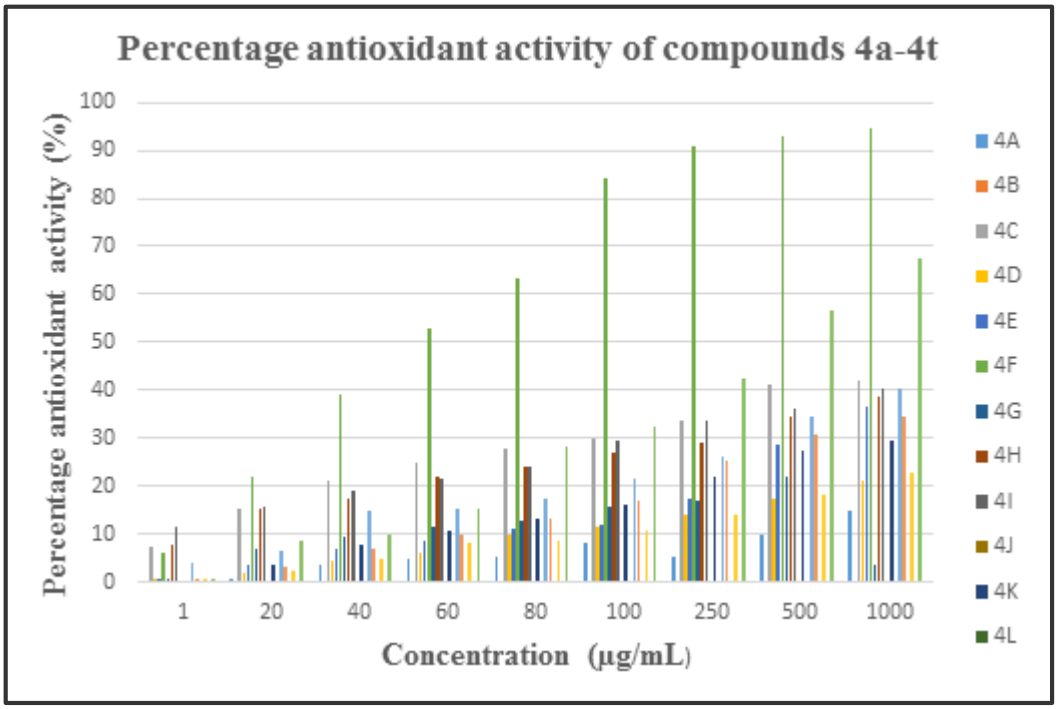

Fig. 12. The percentage antioxidant activity of compound 4a-4t

3.*3.3. Brine Shrimp Assay (toxicity evaluation)*

The toxic effect of **4a-4t** is presented in supplementary file **Table S3**, with results expressed as mean (±SD). The binding interactions between 4d, 4e, 4f, 4m, 4q, 4r and 4s indicates less toxicity against *Artemia salina* (supportive information **Table S3**) at the regular hourly intervals mentioned above. The results demonstrated the brine shrimp mortality rate of lower than 50% is applicable for 4d, 4e, 4f, 4m, 4q, 4r and 4s when treated with 10, 100 and 500 μg/mL. These results indicates that the amino phosphonates are safe for biological applications.

4. Conclusion

An efficient synthetic method for methyl piperazinyl-quinolinyl amionophosphonates was developed and optimised using catalytic amounts of Pd-$SrTiO_3$ under microwave irradiation conditions. The method is comparably quick, safe and ecological while offering high yields.

All the compounds were evaluated for antimicrobial and antioxidant activities: compounds **4m** and **4r** shows positive results for antimicrobial and **4m**, **4r**, **4f** shows positive results for antioxidant. Furthermore, low toxicity of these compounds suggests other biological activity elucidation is possible.

Acknowledgements

The authors acknowledge the financial support of the Durban University of Technology (DUT).

Supporting information

Full experimental detail, ^{1}H and ^{13}C-NMR spectra can be found via the "Supplementary content" section of this article's webpage.

References

[1] Menor-Salván, C. Marín-Yaseli M. R. Chem. Soc. Rev. 16, (2012) 5404-5415.

[2] Quin, L. D. Tyrell, J. A. John Wiley & Sons, 2010.

[3] Pozharski, A.F. Soldatenkov, A.T. Katritzky, A.R. 2011.

[4] Onita, N. Sisu, I. Penescu, M. Purcarea, V. L. Kurunczi, L. Synthesis, 2010.

[5] Allen, M. C. Fuhrer, W. Tuck, B. Wade, R. Wood, J. M. J. Med. Chem. 7, (1989) 1652-1661.

[6] Peyman, A. Stahl, W. Wagner, K. Ruppert, D. Budt, K. H. Bioorg. & Med. Chem. Lett. 21, (1994) 2601-2604.

[7] Atherton, F. R. Hassall, C. H. Lambert, R. W. J. Med. Chem. 1 (1986**)** 29-40.

[8] Krishnaa, A. Bala, M. Veera Narayana Reddya, G. Chandra Shekar Reddya, B. S. Krishnaa, S. K. Nayakb, and C. Suresh Reddy. The International Journal of Applied Biology and Pharmaceutical Technology3 (2010) 873-882.

[9] Z. Rezuei, S. Khabnadideh, K. Zomordian, K. Pakshir, S. Nadali, N. Mohtashami, Int J. Med. Chem, 2011.

[10] Abdelkader, H. Salah, C. Nadjib, C. J. Sci. and Eng. Research, 6, (2015) 1622-1627.

[11] Ramana, K. V. Rasheed, S. Sekhar, K. C. Adam, S. Raj, C. N. Der Pharmacia Letter. 30, (2012) 456-463

[12] Keglevich, G. Bálint, E. Molecules 11, (2012) 12821-31285.

[13] Kabachnik, M. M. Zobnina, E. V. Beletskaya, I. P. Russian J. Org. Chem. 4, (2005) 505-507.

[14] Dindulkar, S. D. Reddy, M. V. Jeong, Y. T. Catalysis Comm. 17, (2012) 114-117.

[15] Yadav, J. S. Reddy, B. V. Raj, K. S. Reddy, K. B. Prasad, A. R. Synth. 15, (2001) 2277-2280.

[16] Ghosh. R. Maiti, S. Chakraborty, A. Maiti, D. K. J. Molecular Catalysis A: Chemical. 1-2, (2004) 53-57.

[17] Chandrasekhar, S. Prakash, S. J. Jagadeshwar, V. Narsihmulu, C. Tetrahedron Lett. 32, (2001) 5561-5563.

[18] Karki, B. S. Verma, S. Agrwal, A. Kasana, V. IJCS. 2, (2017) 280-290.

[19] Yadav, J. S. Reddy, B. V. Mada, C. Synlett. 7, (2001) 1131-1133.

[20] Murugesan, A. Gengan, R. M. Krishnan, A. Materials Chemistry and Physics 15, (2017) 188:154-167.

[21] Murugesan, A. Gengan, R. M. Rajamanikandan, R. Ilanchelian, M. J. Molecular Structure 1149, (2017) 439-451.

[22] Murugesan, A. Gengan, R. M. Rajamanikandan, R. Ilanchelian, M. Lin, C.H. *Synth. Comm*. 20, (2017) 1884-1904.

[23] Fothergill, A. W. Rinaldi, M. G. J. Clin. Microbiol. 33, (1995) 2660-2665.

[24] Beyth, N. Houri-Haddad, Y. Domb, A. Khan, W. Hazan, R. 2015.

[25] Balouiri, M. Sadiki, M. Ibnsouda, S. K. J. Pharm. Anal. 6, (2016) 71–79.

[26] Cos, P. Vlietinck, A. J. Berghe, D. V. Maes, L. 106, (2006) 290-302.

[27] Choi, C. W. Kim, S. C. Hwang, S. S. Choi, B. K. Ahn, H. J. Lee, M. Y. Park, S. H. Kim, S. K.. Plant Sci. 163, (2002) 1161-1168.

[28] Carballo, J. L. Hernández-Inda, Z. L. Pérez, P. García-Grávalos, P. BMC Biotechnol. 2, (2002) 17–22.